

Blue Blood on Ice

Cephalopod haemocyanin function and evolution in a
latitudinal cline

Dissertation
Zur Erlangung des akademischen Grades
-Dr. rer. nat. –

dem Fachbereich 2 Biologie / Chemie
der Universität Bremen
vorgelegt von

Michael Oellermann
Diplom-Biologe

Bremen 2014

Cover photo: Courtesy of Armin Rose

Research is like painting pictures. The product hardly ever turns out quite as well as one might have hoped; it can be maddeningly frustrating; and one spends a lot of time simply cleaning up the equipment. But once in a long while everything goes really well, and that is euphoric. And even in the bad times one is adding something, however slight, to the sum of human knowledge. Some poor people work just as hard and all they make is money.

- Martin J. Wells, Civilization and the Limpet -

This thesis is dedicated to all those who have affected me and my work positively and supported me along this long yet fulfilling experience.

For their continuous support, love and care, I would like to dedicate the work to my family, my wife Saumya, my son Yuva Lalit and of course to the little addition on my last stretch Neel Vayu born few days before submission of my first draft.

Gutachter

Prof. Dr. Hans-Otto Pörtner
Alfred-Wegener-Institut für Polar und Meeresforschung
Sektion Integrative Ökophysiologie
Am Handelshafen 12
27570 Bremerhaven, Germany

Prof. Dr. Bernhard Lieb
Institut für Zoologie
Johannes Gutenberg-Universität Mainz
Müllerweg 6
55099 Mainz, Germany

Prüfer

Prof. Dr. Juliane Filser
Universität Bremen
UFT Zentrum für Umweltforschung und -Technologie
Abt. 10 - Allgemeine und Theoretische Ökologie
Leobener Str., 28359 Bremen, Germany

Dr. Felix C. Mark
Alfred-Wegener-Institut für Polar und Meeresforschung
Sektion Integrative Ökophysiologie
Am Handelshafen 12
27570 Bremerhaven, Germany

Datum des Dissertationskolloquiums 04.02.2015

Table of Contents

ABBREVIATIONS	VIII
LIST OF FIGURES	IX
SUMMARY.....	XI
ZUSAMMENFASSUNG.....	XIII
1 INTRODUCTION.....	1
1.1. LIFE IN THE COLD	1
1.1.1. <i>The Southern Ocean</i>	1
1.1.2. <i>Cold adaptation and oxygen supply</i>	2
1.1.3. <i>Antarctic octopods</i>	4
1.2. THE BLUE BLOOD OF CEPHALOPODS	8
1.2.1. <i>Evolution</i>	8
1.2.2. <i>Function</i>	9
1.2.3. <i>Structure</i>	11
1.3. OXYGEN BINDING MEASUREMENTS IN NON-MODEL ORGANISMS.....	13
1.4. SCOPE OF THE THESIS	15
2 MATERIAL AND METHODS	17
2.1. ANIMALS.....	17
2.1.1. <i>Collection</i>	17
2.1.2. <i>Culture and sampling</i>	18
2.1.3. <i>Ethics approval</i>	19
2.2. ANALYSIS OF BLOOD OXYGEN TRANSPORT	20
2.2.1. <i>Technical modifications</i>	20
2.2.2. <i>Experimental procedures</i>	20
2.2.3. <i>Oxygen carrying capacity</i>	22
2.2.4. <i>Alpha-stat pattern of haemolymph pH</i>	23
2.2.5. <i>Protein and ion concentration</i>	23
2.3. MOLECULAR AND STRUCTURAL ANALYSIS OF HAEMOCYANIN.....	24
2.3.1. <i>PCR, cloning and sequencing</i>	24
2.3.2. <i>Phylogenetic analysis</i>	25
2.3.3. <i>Natural selection</i>	26
2.3.4. <i>Analysis of polar surface residues</i>	28
2.3.5. <i>Native page gel electrophoresis</i>	28
2.4. DATA ANALYSIS.....	29
3 PUBLICATIONS	31
3.1. PUBLICATION I.....	33
3.2. PUBLICATION II	49
3.3. PUBLICATION III	85
4 DISCUSSION	129
4.1. HIGH RESOLUTION MEASUREMENTS IN BLOOD FROM NON-MODEL ORGANISMS.....	129
4.1.1. <i>Advances in blood gas analysis</i>	130
4.1.2. <i>Instrumental shortcomings</i>	131
4.1.3. <i>Future improvements</i>	132
4.2. FUNCTIONAL COLD-ADAPTATION OF OCTOPOD HAEMOCYANIN.....	133
4.2.1. <i>Reliance on haemocyanin functioning in an oxygen rich ocean.</i>	133
4.2.2. <i>Cold compensation of haemocyanin function</i>	137
4.3. MOLECULAR BASIS OF FUNCTIONAL COLD-ADAPTATION	141
4.3.1. <i>High pH and surface charge</i>	142
4.3.2. <i>Alternative modulators of haemocyanin function</i>	145
4.4. CONCLUDING EVOLUTIONARY PERSPECTIVE	149
4.5. RESEARCH PERSPECTIVES	154
5 REFERENCES.....	155
6 APPENDIX.....	171
6.1. PATENT.....	171
6.2. RELATIVE HEART MASSES OF CEPHALOPODS	191
6.3. SPONSORING AND SUPPORTING ORGANISATIONS.....	192
6.4. MEDIA RELEASES.....	193
7 ACKNOWLEDGEMENTS	195
ERKLÄRUNG GEMÄß § 6 (5) DER PROMO DER UNIVERSITÄT BREMEN	197

Abbreviations

OEC	Oxygen equilibrium curve
PO_2	Oxygen partial pressure
PCO_2	Carbon dioxide partial pressure
P_{50}	Oxygen affinity
n_{50}	Hill coefficient
ATP	Adenosine triphosphate
c(Hc)	Haemocyanin concentration
CO_2	Carbon dioxide
C_{O_2}	Oxygen carrying capacity
MO_2	oxygen consumption rates of <i>Pareledone charcoti</i> (MO_2)
MW	Molecular weight
NIST	National Institute of Standards and Technology
OEC	Oxygen equilibrium curve
PCO_2	Carbon dioxide partial pressure
PO_2	Oxygen partial pressure
FU	Functional unit
COI	Cytochrome c oxidase subunit I
COIII	Cytochrome c oxidase subunit III
JSD	Jensen-Shannon Divergence
dN	Rate of non-synonymous codon substitutions
dS	Rate of synonymous codon substitutions
PCR	Polymerase chain reaction
GARD	Genetic algorithm for recombination detection
SLAC	Single Likelihood Ancestral Counting
FEL	Fixed Effects Likelihood
MEME	Mixed Effects Model of Evolution
FUBAR	Fast Unconstrained Bayesian AppRoximation
EF	Evolutionary Fingerprinting
PRIME	PRoperty Informed Models of Evolution

List of Figures

Figure 1: Some Antarctic benthic incirrate octopods analysed in this study.	5
Figure 2: Haemocyanin structure.	12
Figure 3: Climatic origins of octopod samples used in this study.	18
Figure 4: Native page gel electrophoresis of purified cephalopod haemocyanins.	136
Figure 5: Relative heart masses of cephalopods.	140
Figure 6: Amino acid differences between Antarctic and temperate haemocyanins.	143
Figure 7: Isoelectric points of octopod haemocyanins.	147

Summary

The Southern Ocean hosts a rich and diverse fauna that required specialist adaptations to colonize and persist at temperatures close to freezing. While much has been revealed about key adaptations in Antarctic fishes little is known about evolutionary strategies of other Antarctic ectotherms, particularly the abundant benthic invertebrate octopods. Their oxygen demand is largely fuelled by the blue oxygen transporter haemocyanin that however, due to its increasing functional failure towards colder temperatures, poses a prime target for cold-adaptive adjustment. While haemocyanin structure has been well understood it remains unclear which molecular features and evolutionary trajectories explain functional properties of octopod haemocyanin. This thesis thus aimed to unravel cold-adaptive features of octopod haemocyanin and the underlying molecular features that evolved to sustain oxygen supply at sub-zero temperatures.

Haemocyanin function is best assessed by oxygen binding experiments, which however was challenged due to the minute haemolymph volumes non-model organisms like Antarctic octopods, yield. I thus upgraded an oxygen diffusion chamber with a broad range fibre optic spectrophotometer and a micro-pH optode and tested the setup for *Octopus vulgaris*, the Antarctic eelpout and a Baikal amphipod. This technical advancement enabled simultaneous recordings of pH and oxygen dependent pigment absorbance in only 15 μ l of sample. Results were highly reproducible and accurate and provided detailed insight to the complex and dynamic spectral features of three diverse blood-types.

To identify cold-adaptive functional traits of blood oxygen transport this study compared haemocyanin oxygen binding properties, oxygen carrying capacities and haemolymph protein and ion composition between the Antarctic octopod *Pareledone charcoti*, the temperate *Octopus pallidus* and the subtropical *Eledone moschata*. Compared to octopods from warmer climates, *Pareledone charcoti* showed incomplete but significantly reduced oxygen affinity, which together with increased haemocyanin concentrations and high physically dissolved oxygen levels supported oxygen supply at 0°C. Therefore, unlike many Antarctic fishes *Pareledone charcoti* continued to rely on an oxygen transporting pigment. High temperature sensitivity of oxygen binding enabled *Pareledone charcoti* to utilise most of the oxygen bound by haemocyanin at 10°C. The

concomitant relief for the circulatory system at warmer temperatures promotes warm tolerance and thus eurythermy in *Pareledone charcoti*.

Underlying molecular mechanisms were studied by comparing 239 partial haemocyanin sequences of the functional unit f and g of 28 octopods species of polar, temperate, subtropical and tropical origin. Despite high conservation of these haemocyanin regions several sites were positively selected for their charge properties at the molecule's surface. Net surface charges were generally elevated in polar octopods suggesting that charge-charge interactions raise intrinsic pK values to stabilise quaternary structure against higher ambient pH present in cold waters. The presence of at least two haemocyanin isoforms and high allelic variation in polar octopods indicate sustained genetic diversity of haemocyanin and thus the genetic potential to regulate blood oxygen transport in the cold. Further, amino acid variability located within a potential metal binding site suggests regulation of blood oxygen transport in octopods via altered intrinsic sensitivity to allosteric ligands

In conclusion, this study revealed significant adaptations of octopod haemocyanin at the functional and molecular level that support oxygen supply at near freezing temperatures. However, 'imperfect' functional adaptation and ensuing reliance on high haemocyanin levels in *Pareledone charcoti* seems to add to the various design constraints of octopods compared to fishes. Hence, at second glance functional oxygen reserves indicate a higher capacity to sustain oxygen transport at warmer temperatures and together with a potential ability to regulate and reverse cold-adaptive molecular traits may be key to determine future winners and losers in an ecosystem facing radical environmental change.

Zusammenfassung

Der Antarktische Ozean beherbergt eine reiche Vielfalt an Meerestieren, die durch einzigartige Anpassungen in der Lage waren bei Temperaturen nahe dem Gefrierpunkt zu überleben. Trotz der umfangreichen Kenntnisse über Schlüsselanpassungen bei antarktischen Fischen ist nur wenig über andere antarktische ektotherme Tiere und deren Anpassungsstrategien bekannt. Dies trifft besonders auf benthische incirrate Kraken zu, die in der Antarktis divers und weit verbreitet sind. Der Sauerstoffbedarf ihres Stoffwechsels wird hauptsächlich von dem bläulichen Sauerstofftransporter Haemocyanin bedient, der allerdings mit sinkenden Temperaturen zunehmend an Funktionalität einbüßt. Anpassungen an die Kälte sind deshalb sehr wahrscheinlich mit funktionellen Veränderungen von Haemocyanin verbunden. Obwohl die molekulare Struktur von Cephalopoden-Haemocyanin detailreich entschlüsselt wurde ist es weiterhin unklar welche genauen molekularen und evolutionären Merkmale Anpassungen auf funktioneller Ebene verursachen. Ziel dieser Studie war es deshalb funktionelle und die damit verbundenen molekularen Anpassungen von Haemocyanin an die Kälte zu identifizieren, die eine nachhaltige Sauerstoffversorgung bei eiskalten Temperaturen unterstützen.

Die Funktion von Blutpigmenten wie Haemocyanin wird mit Hilfe von Sauerstoffbindungskurven untersucht, was jedoch technisch schwierig ist, da man kleinen Organismen wie den antarktischen Kraken, nur geringe Mengen Hämolymphe entnehmen kann. Aus diesem Grund habe ich eine Sauerstoffdiffusionskammer mit einem faseroptischen Breitband-Spektral-photometer und einer pH Mikrooptode aufgerüstet und den Aufbau mit Hämolymphe bzw. Blut von *Octopus vulgaris*, der antarktischen Aalmutter und einem Amphipoden vom Baikalsee getestet. Die technischen Neuerungen erlaubten die simultane Messung von pH und sauerstoffabhängiger Absorption in nicht mehr als 15 µl Probenvolumen. Die Ergebnisse waren reproduzierbar und akkurat und ermöglichten detailreiche Einsichten in die komplexen und dynamischen spektralen Eigenschaften der drei sehr unterschiedlichen Bluttypen.

Im zweiten Teil der Studie wurde anhand vergleichender Messungen von Sauerstoffbindungseigenschaften, maximaler Sauerstoffbindungskapazität sowie Protein- und Ionenzusammensetzung zwischen dem Antarktischen Kraken *Pareledone charcoti*, dem temperaten *Octopus pallidus* und dem subtropischen

Eledone moschata, funktionelle Anpassungen des Sauerstofftransportes an die Kälte identifiziert. Im Vergleich zu Kraken aus wärmeren Gefilden, wies *Pareledone charcoti* eine unvollständig aber signifikant reduzierte Sauerstoffaffinität auf, die zusammen mit erhöhten Haemocyaninkonzentrationen und einem hohem Gehalt an physikalisch gelöstem Sauerstoff, die Sauerstoffversorgung bei 0°C unterstützten. Im Gegensatz zu antarktischen Fischen ist *Pareledone charcoti* deshalb weiterhin auf ein Sauerstofftransportprotein im Blut angewiesen. Eine hohe Temperatursensitivität der Sauerstoffbindung ermöglichte allerdings auch, dass *Pareledone charcoti* einen großen Teil den bei 0°C fest gebundenen Sauerstoffes bei 10°C nutzen kann. Die damit verbundene Entlastung des Blutzirkulationssystems fördert die Toleranz wärmerer Temperaturen und deutet auf die Anpassung an ein breites Temperaturspektrum (Eurythermie) von *Pareledone charcoti* hin.

Im letzten Teil der Studie, wurden 239 partielle Haemocyaninsequenzen der funktionellen Einheiten f und g von 28 Krakenarten aus polaren, temperaten, subtropischen und tropischen Regionen analysiert, um Anpassungen auf molekularer Ebene zu identifizieren. Trotz hoher Konserviertheit der untersuchten Haemocyaninabschnitte unterlagen die Ladungseigenschaften mehrerer Sequenzpositionen an der Moleküloberfläche positiver Selektion. Polare Kraken zeigten eine erhöhte Nettoladung der Moleküloberfläche, was darauf hinweist, dass durch elektrostatische Wechselwirkungen intrinsische pK Werte angehoben wurden um einer De-Stabilisierung der Quartärstruktur bei erhöhtem Hämolymphe pH in kaltem Wasser entgegenzuwirken. Die Präsenz von mindestens zwei Haemocyaninisoformen und hohe allelische Variation in polaren Kraken, zeigt das die genetische Diversität und damit das genetische Potential zur Regulation des Sauerstofftransportes auch in der Kälte fortbesteht. Aminosäureaustausche inmitten einer potentiellen Bindungsstelle für Metallionen, weisen zudem darauf hin, dass Sauerstofftransport in Kraken zusätzlich durch veränderte intrinsische Sensitivität zu allosterischen Liganden reguliert wird.

Insgesamt wies diese Studie signifikante Anpassungen des Haemocyanins von Kraken auf funktioneller und molekularer Ebene nach, die eine nachhaltige Sauerstoffversorgung bei Temperaturen nahe dem Gefrierpunkt unterstützen. Allerdings scheint die unvollständige funktionelle Anpassung an die polare Kälte und die anhaltende starke Abhängigkeit von Haemocyanin in *Pareledone charcoti* eine weitere Designlimitierung im Vergleich zu Fischen darzustellen. Auf den zweiten Blick jedoch wird offenbar, dass die funktionelle Sauerstoffreserve die Sauerstoffversorgung

bei wärmeren Temperaturen verbessert und zusammen mit einer anhaltenden potentiellen Fähigkeit zur Regulation und erleichterten Umkehrbarkeit kalt-angepasster molekularer Eigenschaften von Haemocyanin der Schlüssel sein könnten, in einem sich rapide verändernden Ökosystem zu bestehen.

1 Introduction

The recent decade of research underlined that a detailed understanding of key physiological mechanisms considerably advances insight into past evolutionary processes or biogeographic patterns and lays a solid foundation to predict animals' ability to persist or adapt to changing environments, particularly in the light of accelerated climate change (Pörtner, 2002a; Pörtner and Farrell, 2008; Helmuth, 2009; Chown et al., 2010). The diverse fish fauna of the Southern Ocean evolved remarkable adaptations to the extreme cold (e.g. Ruud, 1954; DeVries, 1988). However, cold-adaptations of ectotherms other than fish are poorly understood, particularly of the abundant octopods. Octopods consume much oxygen and thus highly depend on their oxygen transport protein haemocyanin. Yet, despite apparent detrimental effects of cold temperatures on the function of cephalopod haemocyanin (Zielinski et al., 2001; Melzner et al., 2007a) it is unclear whether haemocyanins of octopods underwent evolutionary adjustments to sustain blood oxygen transport in polar waters. In this study, I thus aimed to unravel the adaptive traits of the respiratory pigment haemocyanin in order to understand its impact on the successful persistence of Antarctic octopods at temperatures close to freezing.

The following introduction will outline conditions and the role of oxygen transport for life in ice-cold waters and how octopods' blue blood may have played a key role for their persistence in the Southern Ocean, followed by a review of current knowledge on cephalopod haemocyanin and methodological limitations that hamper functional analysis of haemocyanin.

1.1. Life in the cold

1.1.1. The Southern Ocean

The Southern Ocean is one of the coldest habitats on earth with temperatures ranging between -1.8 to 2°C all year round (e.g. Jacobs et al., 1970; Klinck et al., 2004). This has not always been the case. In fact, some 55 million years ago, Southern Ocean surface temperatures peaked at about 16°C and afterwards meandered downwards, until glacial conditions were reached ca. 34 million years ago (Clarke et al., 1992; Zachos et al., 2001). Cooling to current Antarctic conditions (<2°C) set in about four

million years ago (Clarke et al., 1992). The opening of the Drake Passage and the formation of the circumpolar current ca. 30 million years ago, isolated the ice-cold Southern Ocean from adjacent warmer waters until today (Barker and Burrell, 1977; Livermore et al., 2005). Despite such low temperatures and months of darkness and low productivity, life is abundant and diverse with more than 8200 known species, largely dominated by benthic organisms like sponges, polychaetes, gastropods or amphipods (Arntz et al., 1997; Clarke and Johnston, 2003; Clarke et al., 2004; Griffiths, 2010). The origin of marine animals in the Southern Ocean comprises three major pathways: 1) an *in situ* origin from the Southern Ocean itself, 2) migration from adjacent deep-waters and 3) migrations from the shallow South-American shelf via the Scotia Arc island bridge (Knox and Lowry, 1977; Strugnell et al., 2008; Strugnell et al., 2011). Irrespective of the type of origin, species were required to permanently tolerate or adjust to close to freezing conditions and overcome major physiological challenges (Clarke, 1991).

1.1.2. Cold adaptation and oxygen supply

Apart from birds and mammals, Antarctic Ocean fauna is dominated by ectothermic animals, which are unable to regulate their body temperatures and thus experience the same body temperatures as the surrounding ice-cold water. This poses a major challenge as cold temperatures slow down body functions, of which most (e.g. metabolism, muscle contraction, oxygen or substrate diffusion), require to operate at rates sustaining whole animal activity and consequently the ability to feed, escape or reproduce. The long-standing investigation of cold-adaptation has brought much light to the adaptive strategies animals employed to overcome these challenges (e.g. Scholander et al., 1950; Clarke, 1991; Fields and Somero, 1998; Pörtner, 2006). Among them are key innovations, such as anti-freeze proteins that protect cells from ice crystal damage, and thus allowed wide spread radiation of the Notothenioid fishes across the Southern Ocean (Cheng, 1998; Matschiner et al., 2011). Other adaptations to the cold include the adjustment of function and expression of proteins or enzymes, to improve e.g. neuronal signalling (Garrett and Rosenthal, 2012) and aerobic or anaerobic capacity (Johnston et al., 1998; Kawall et al., 2002) as well as increased membrane fluidity (Logue et al., 2000) or reduced blood viscosity (Egginton, 1996).

Interestingly, numerous adaptations concern the relaxation but also the facilitation of oxygen transport. Antarctic waters are rich in oxygen due to rigorous

mixing across the water column and high levels of dissolved oxygen, which dissolves better in the cold (Sidell and O'Brien, 2006). Levels of dissolved oxygen in seawater are 1.55 times higher at 0°C than at 20°C [$358.4 \mu\text{mol L}^{-1}$ at 0°C vs. $230.9 \mu\text{mol L}^{-1}$ at 20°C at 35 psu, (Ramsing and Gundersen)]. Paired with low oxygen consumption rates commonly found among Antarctic ectotherms (Ahn and Shim, 1998; Clarke and Johnston, 1999; Daly and Peck, 2000), oxygen supply does not appear limiting in the cold. For example, haemolymph oxygen levels were in excess in the Antarctic bivalve *Laternula elliptica* between 0-6°C due to low oxygen consumption rates and sustained functionality of the oxygen supply system (Peck et al., 2002). Similarly, haemolymph oxygen levels were high in the sub-Antarctic stone crab *Paralomis granulosa* between -1°C - 1°C [venous $PO_2 \sim 10$ kPa, arterial $PO_2 \sim 15$ kPa, (Wittmann et al., 2012)] as well as in the sub-Arctic spider crab *Hyas araneus* between 0°C - 4°C [~ 12 kPa, (Walther et al., 2009)]. The surplus of oxygen in polar waters enabled Antarctic notothenioid fishes to relax oxygen supply characterised by largely reduced concentrations and isoform diversity of their blood oxygen carrier haemoglobin and in the case of the Antarctic icefishes (Channichthyidae) even the complete loss of haemoglobin and partly of intracellular myoglobin (Ruud, 1954; Sidell and O'Brien, 2006). However, while reduced globin content may lower metabolic costs for globin synthesis and decrease cardiac workload due to lowered blood viscosity, the complete loss of oxygen carrying globins required compensation such as increased blood volumes, heart size or vascularization and came at the expense of limited warm tolerance (Sidell and O'Brien, 2006; Garofalo et al., 2009; Beers and Sidell, 2011; Buckley et al., 2014). On the other hand, cold temperatures also impair oxygen supply by slowing the diffusion of oxygen across tissue and cellular boundaries, impair blood flow due to increased blood viscosity (Sidell, 1998) and decrease the ability of oxygen transport proteins to release oxygen to tissues (Zielinski et al., 2001; Weber and Campbell, 2011). Antarctic fishes responded to the impaired oxygen supply by increased mitochondrial and membrane densities to increase the lipid content and thus cellular oxygen diffusion (Sidell, 1998) and a decreased affinity of haemoglobin for oxygen to facilitate venous oxygen release (Qvist et al., 1977; D'Avino and Di Prisco, 1989; Tamburrini et al., 1992). Eventually, excess oxygen and low oxygen demand enabled cost-saving adaptations in Antarctic ectotherms such as reduced globin expression (Pörtner et al., 2013) that may outweigh expenses caused by concurrent detrimental effects of cold temperatures. While most of the knowledge on cold-adaptation builds on Antarctic fishes it needs to be assessed

whether other widespread Antarctic ectotherms employed similar strategies to cope with temperatures close to freezing, particularly one of the prime competitors of Antarctic fish, the highly oxygen dependent cephalopods.

1.1.3. Antarctic octopods

Cephalopods are found all across the Southern Ocean from pelagic to benthic regions and from the shallow intertidal down to deep sea basins (Collins and Rodhouse, 2006). Among them are benthic incirrate octopods, the most abundant and species-rich Antarctic cephalopod group that form an important part of the benthic megafauna as both prey and predators (Daly, 1996; Allcock et al., 2001; Piatkowski et al., 2003; Collins et al., 2004; Collins and Rodhouse, 2006). Unlike the highly mobile pelagic oegopsid squids, Antarctic octopods are rather local with limited dispersal abilities due to their bottom dwelling crawling life style and lacking pelagic larval stages (Collins and Rodhouse, 2006; Barratt et al., 2008; Laptikhovskiy et al., 2014). Similar to notothenioid fishes, benthic Antarctic octopods are highly endemic and probably colonized the Southern Ocean after the formation of the Southern Ocean ca. 25-28 million year ago (Allcock and Piertney, 2002; Allcock, 2005; Collins and Rodhouse, 2006). The two Antarctic benthic octopod families include the Enteroctopodidae and the Megaleledonidae, with the latter containing the most speciose genus *Pareledone* that underwent extensive radiation in shallow Antarctic waters (<400m) leading to many cryptic and geographically distinct species [(Allcock, 2005; Allcock et al., 2007; Allcock et al., 2011; Strugnell et al., 2014), Figure 1]. Antarctic benthic octopods are most suitable to study cold-adaptation owing to i) the enhanced adaptive pressure faced by species with low capacity to escape from challenging environmental conditions due to non-pelagic larval stages (Barratt et al., 2008; Laptikhovskiy et al., 2014) and slow crawling adults (Allcock, 1997); ii) short generation times in comparison to other Antarctic ectotherms, despite reduced growth rates and breeding periods between 1-4.4 years (Nesis, 1999; Robison et al., 2014) and little overlap and genetic mixing between parent and offspring generation due to a 'breed once and die' life style (Laptikhovskiy, 2013); iii) the possibility to compare traits with an abundant number of species from warmer climates with similar life styles and thus comparable metabolic rates [i.e. after accounting for temperature and mass, (Daly and Peck, 2000; Seibel and Childress, 2000; Seibel, 2007) and iv) lastly the most advanced and complex physiology among invertebrates (Pörtner et al., 1994).

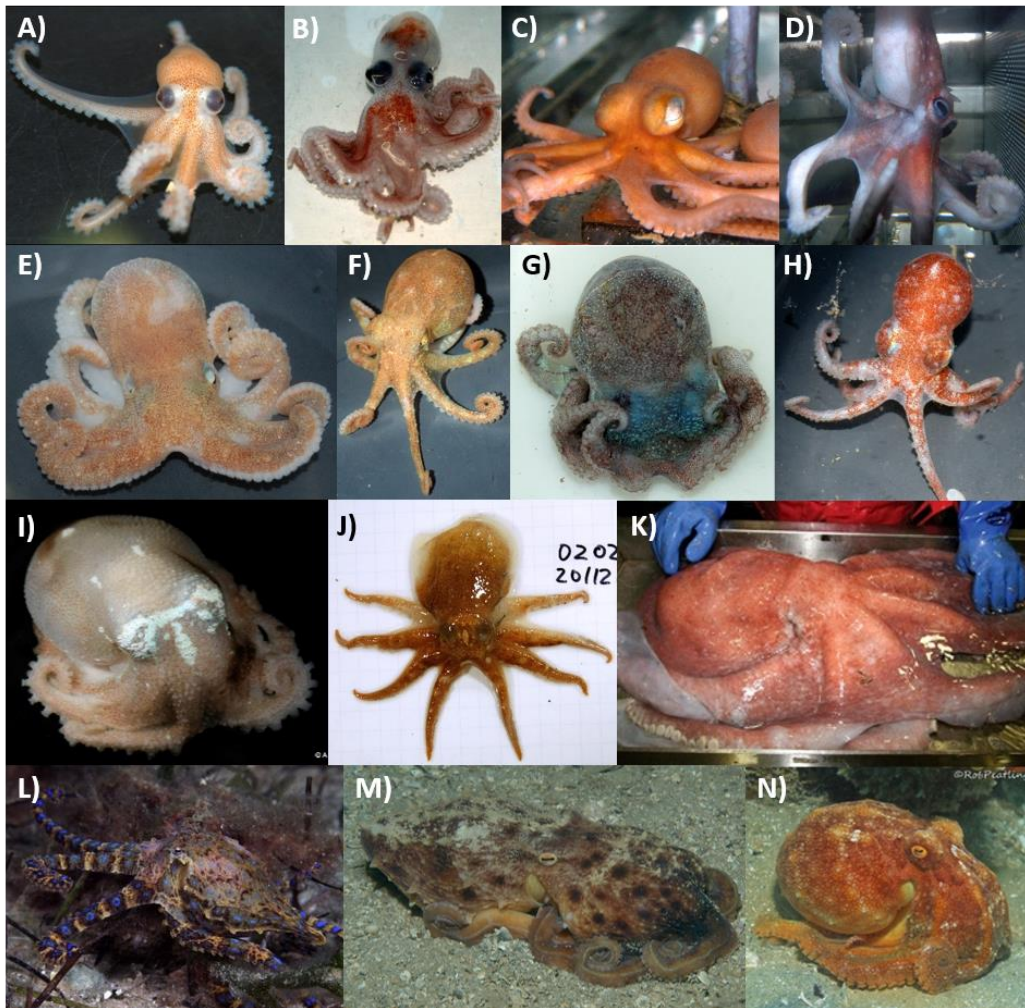


Figure 1: Some benthic incirrate octopods analysed in this study.

A) *Benthoctopus cf. rigbyae*, B) *Benthoctopus sp.*, C) *Benthoctopus cf. longibrachus*, D) *Graneledone yamana*, E) *Adelleledone polymorpha*, F) *Pareledone prydzensis*, G) *Pareledone panchroma*, H) *Pareledone turqueti*, I) *Pareledone cornuta* (foto by: Armin Rose), J) *Pareledone charcoti*, K) *Megaleledone setebos* (foto by: Robin Beaman), L) *Hapalochlaena maculosa* (foto by: Julian Finn), M) *Eledone moschata* (foto by: Anne Frijsinger) N) *Octopus pallidus* (foto by: Rob Peatling). The Antarctic species A-C comprise members of the family Enteroctopodidae and D-K of Megaleledonidae.

Like all modern cephalopods, benthic octopods exhibit an advanced oxygen supply system characterized by: i) the relative closure of the blood circulation system to allow higher blood pressures and faster blood circulation rates [e.g. 2.0-4.2 kPa and 30-40 sec in *Octopus vulgaris* (O'dor and Wells, 1984; Schipp, 1987)]; ii) the separation of arterial and venous blood distributed via an extensive network of arteries, capillary-like vessels and even coronary veins (Houlihan et al., 1987; Schipp, 1987; Reiber and McGaw, 2009); iii) for invertebrates standards high blood volumes and oxygen carrying capacity [e.g. 3.3-3.9% in *O. vulgaris* and 1.86 mmol O₂ L⁻¹ in *Megaleledone setebos* (O'dor and Wells, 1984; Zielinski et al., 2001)]; iv) enhanced blood flow driven by one powerful systemic heart, two accessory branchial hearts, contractile veins and

coordinated mantle pressure movements (Schipf, 1987; Wells, 1992; Melzner et al., 2007b); v) substantial oxygen uptake via a thin shell-less skin surface [between 13-21% of oxygen uptake in *Enteroctopus dofleini* (Pörtner, 1994) and up to 41% in resting *O. vulgaris* (Madan, J. J. and Wells, J., 1996; Pörtner, 2002b)]; vi) an efficient ventilatory oxygen extraction via highly diffusive gills (Madan, J. J. and Wells, M. J., 1996; Melzner et al., 2006b) and vii) importantly, high concentrations of a very cooperative and pH sensitive type of haemocyanin as their prime oxygen transporter (Bridges, 1994).

However, given the multiplicity of components driving oxygen supply in octopods, it is unlikely that each component or their sum changes at the same rate with temperature as whole animal oxygen consumption rate. If temperatures decrease, and the performance of single or multiple components decreases faster than the demand for oxygen, aerobic activity may no longer be sustained in the cold (Pörtner et al., 2007). Therefore, it is intriguing to know, whether components of the octopod's highly sophisticated oxygen supply system required adjustments to sustain functionality at sub-zero temperatures. At high temperatures, circulatory support by ventilatory pressure oscillations as well as heart performance fail to fuel increasing oxygen demand in the cephalopod *Sepia officinalis* (Fiedler, 1992; Melzner et al., 2007a). In contrast, at low temperatures, *Sepia officinalis* may suffer from limited oxygen supply due to the decreasing ability of its respiratory pigment haemocyanin to release sufficient oxygen to tissues (Zielinski et al., 2001; Melzner et al., 2007a). At the lower temperature margin of *Sepia officinalis* (10°) haemocyanin releases only 20% of its bound oxygen (at 1.7kPa O₂ and pH 7.4) and less than 10% if one accounts for the increase of haemolymph pH towards colder temperatures (Reeves, 1972; Howell and Gilbert, 1976; Zielinski et al., 2001; Melzner et al., 2007a). However, while haemocyanin may contribute to failing oxygen supply at the lower temperature margin of temperate cephalopods such as *Sepia*, polar species may not experience oxygen limitation at temperatures close to zero (Pörtner et al., 2013). Despite poor venous oxygen release of haemocyanin of the Antarctic octopus *Megaleledone setebos* at 0°C [only ~10% of bound oxygen at 1.7kPa O₂ and pH 7.43 and ~40% at 1.0kPa O₂ (Zielinski et al., 2001)], oxygen supply may be unconstrained in Antarctic octopods due to the high levels of dissolved oxygen and low oxygen consumption rates [*Pareledone charcoti* 0.319 mmol O₂ kg⁻¹ (wet mass) h⁻¹ at 0°C vs. *Octopus vulgaris* 2.672 mmol O₂ kg⁻¹ at 21°C (Wells et al., 1983; Daly and Peck, 2000)]. Yet, concentrations of haemocyanin were high in *Megaleledone setebos* [93 mg ml⁻¹, (Zielinski et al., 2001)] in contrast to reduced or absent haemoglobin content in

Antarctic fishes (Ruud, 1954; Sidell and O'Brien, 2006). Therefore, the questions arise whether Antarctic octopods continued to rely on haemocyanin despite relaxation of oxygen supply and in this case whether haemocyanin underwent adaptive modifications to remain functional at polar temperatures.

Unfortunately, little is known about cold-adaptive modifications in Antarctic benthic octopods. The few available studies report accelerated kinetics of potassium channels to sustain neuronal signalling (Galarza-Muñoz et al., 2011; Garrett and Rosenthal, 2012) in *Pareledone* sp. as well as enhanced activity of alkaline phosphatase in four Antarctic octopod species, which seems to sustain toxicity of octopus venom at 0°C (Undheim et al., 2010). Cadmium levels were further enhanced in *Graneledone* sp. and *Benthoctopus thiele*, yet without knowing the causes (Bustamante et al., 1998). Only two studies addressed oxygen supply and reported low and uncompensated oxygen consumption rates in *Pareledone charcoti* (Daly and Peck, 2000) and high but temperature insensitive oxygen affinity of haemocyanin in *Megaleledone setebos* (P_{50} of 0.98 kPa at 0°C and pH 7.2, Q_{10} of 1.12 between 0°C - 10°C), indicating poor oxygen unloading at 0°C and failing oxygen supply at higher temperatures (Zielinski et al., 2001). Further cooperativity was low (Hill coefficient n_{50} of 1.4 at pH 7.43) and Bohr coefficients moderate at 0°C [$\Delta \log P_{50} / \Delta \text{pH}$ ca. -0.9 (Zielinski et al., 2001)]. However, comparisons of blood oxygen transport features with those in warm adapted octopod species are required using comparable methodology. It thus remains unresolved whether Antarctic octopods rely on haemocyanin to sustain oxygen supply and if this involved functional modifications to sustain sufficient functioning of haemocyanin in the cold. It is further unclear whether oxygen binding in *Megaleledone setebos*, which is rather large in size and more common in deeper waters (Allcock et al., 2003), differs from that in the much smaller shallow water octopods of the genus *Pareledone* (Allcock, 2005).

1.2. The blue blood of cephalopods

1.2.1. Evolution

Haemocyanins are one of the major oxygen carriers in the animal kingdom next to hemoglobin and are found among molluscs, arthropods and urochordates (Terwilliger, 1998; Aguilera et al., 2013). Instead of iron, haemocyanins utilize two copper atoms to bind oxygen, giving the protein a blue appearance upon oxygenation (van Holde et al., 2001). Deoxygenated haemocyanins appear colourless. Three histidine residues keep each copper atom in place and form the active oxygen binding site, a structure which is also present in the common oxidizing phenol oxidases, comprised of tyrosinase and catecholoxidase. It was thus concluded that haemocyanins originated from ancestral tyrosinase-like proteins (van Holde and Miller, 1995; Decker et al., 2007). Recent analysis of type-3 bi-nuclear copper proteins showed that this ancestral tyrosinase existed before the emergence of eukaryotes and from then diversified into three major subclasses (α , β , γ) via various gene duplications and losses (Aguilera et al., 2013; Martín-Durán et al., 2013). This is why molluscan and arthropod haemocyanins share very similar copper binding active sites. Their secondary, tertiary and quaternary structure however differ vastly (van Holde et al., 2001), as mollusc haemocyanin evolved independently from an α -subclass tyrosinase some 740 million years ago (Lieb et al., 2000; Lieb and Markl, 2004) and arthropod haemocyanin from a β -subclass tyrosinase approximately 600 million years ago (Burmester, 2002; Aguilera et al., 2013). Based on haemocyanin phylogenetic analysis, cephalopods diverged from gastropods in the Cambrian ca. 520 million years ago (Lieb and Markl, 2004). Modern coleoid cephalopods, (e.g. octopods, squids and sepiids) then separated from the ancient and sluggish nautiloids ca. 420 million years back (Lieb and Markl, 2004) and ever since have advanced their oxygen carrier haemocyanin to match the increased metabolic demands, particularly within the athletic squids facing tight competition with the faster moving fishes (Packard, 1972; O'Dor and Webber, 1986; O'Dor and Webber, 1991).

1.2.2. Function

The transport of oxygen from the breathing organs to the tissue forms the foremost task of haemocyanin, which is particularly essential to the highly oxygen dependent cephalopods. It is generally held that cephalopods show the highest oxygen consumption rates found in invertebrates that even resemble that of pelagic fishes or mammals if one corrects for mass and temperature (O'Dor and Webber, 1991; Seibel, 2007). To fuel such high oxygen demand, cephalopods require an efficient oxygen transport protein. In comparison to their sluggish gastropod relatives (Mangum, 1980; Lieb et al., 2010), cephalopods advanced the oxygen transport capacity of their haemocyanins, characterized by largely increased cooperativity, high pH sensitivity, low oxygen affinities and probably the highest haemocyanin concentrations and thus oxygen carrying capacities found among molluscs (Mangum, 1980; Brix et al., 1989; Mangum, 1990; Bridges, 1994). However, there are two major drawbacks compared to haemoglobin carrying organisms. Unlike cellular haemoglobin, haemocyanin freely dissolves in haemolymph without a cellular containment and therefore directly affects colloidal osmotic pressure and viscosity (O'Dor and Webber, 1986; Mangum, 1990). As high viscosities overburden the circulatory system, haemocyanin and thus oxygen levels are limited in cephalopods. Second, haemolymph containing haemocyanin is only able to carry less than half the amount of oxygen than blood containing intracellular haemoglobin (O'Dor and Webber, 1986). Haemolymph of the European squid *Loligo vulgaris* for instance, has the highest oxygen carrying capacity [3.38 mmol L⁻¹ O₂, calculated from Brix et al. (1989)] reported for cephalopods at a haemocyanin concentration of 169 mg ml⁻¹. In contrast, the blue fin tuna, carries up to 8.1 mmol L⁻¹ O₂ at a haemoglobin concentration of 153 mg ml⁻¹ [calculated from Clark et al. (2008)]. This is due to the far more extensive protein structure around the copper binding centre of haemocyanin with an average molecular mass of ca. 48,600 Da per dioxygen molecule bound. Fish haemoglobins, in comparison, only require 16,500 Da to bind one dioxygen molecule in terms of protein mass and thus bind oxygen three times more economically. As a result, the limited ability of cephalopods to increase haemocyanin concentrations combined with their lower capacity to bind oxygen poses a substantial disadvantage to haemoglobin carrying fishes, their prime contestants.

As an extracellular protein, haemocyanin is directly exposed to ambient conditions prevailing in the surrounding haemolymph. Temperature, oxygen concentration and pH are the most important factors that determine oxygen loading and

unloading. It is thus not surprising that the physiological properties of haemocyanin vary widely among cephalopods, given their broad range of habitats and latitudinal or vertical distribution in the water column (Brix et al., 1994). Lower temperatures increase the oxygen affinity of haemocyanin due to the endothermic nature of oxygen release, an effect that seems universal among blood pigments, although the extent of this response may vary strongly depending on life style and habitat conditions (Brix et al., 1989; Seibel, 2012). Further, small changes of pH affect oxygen affinity in cephalopods far more than in many other species (Pörtner, 1990; Bridges, 1994), indicating a higher intolerance to blood pH disturbances and changing ambient CO₂ levels (Pörtner, 2004). However, at least some cephalopods, like *Sepia officinalis*, are able to buffer blood-pH changes via e.g. active bicarbonate accumulation or lowered pH sensitivity of their haemocyanin (Gutowska et al., 2010). Also, although low oxygen affinities generally found in cephalopods improve oxygen unloading in the tissue, this may be detrimental at low ambient oxygen levels due to poor oxygen loading at the gills. The jumbo squid *Dosidicus gigas* faces such hypoxic conditions (ambient PO₂ <5 kPa) during its diel migration but sustains oxygen supply by adjusting the affinity of its haemocyanin for oxygen via increased temperature and pH sensitivity (Seibel, 2012). Moreover, sensitivity of haemocyanin to allosteric effectors, particularly magnesium, was reported to affect oxygen affinity *in vitro* (Miller, 1985; Mangum, 1990), which however does not seem to be a major regulative tool as magnesium concentrations remain largely unchanged in cephalopods compared to sea water (Robertson, 1953; Oellermann et al., 2015). Overall, cephalopods often respond to the tight coupling between environment and oxygen transport via concerted adjustments of the intrinsic properties of their respiratory pigment haemocyanin and also, but seemingly to a lesser extent, via adjustment of its surrounding medium, the haemolymph.

Due to its phenol oxidase origin, mollusc haemocyanin also retained functions other than oxygen transport, including a tyrosinase activity to hydrolyse monophenol into *o*-diphenols, and a catechol oxidase activity to oxidize *o*-diphenols, which initiates an immune response upon bacterial infections (Decker and Jaenicke, 2004; Jiang et al., 2007). Most interestingly, haemocyanin plays a major role in the symbiotic relationship between the bobtail squid *Euprymna scolopes* and the bioluminescent bacterium *Vibrio fischeri*, as it not only delivers oxygen to the bacteria for the light producing reaction, but also supports selective harvesting of *Vibrio fischeri* from the water column (Kremer et al., 2014).

1.2.3. Structure

Cephalopod haemocyanins are among the largest and most complex respiratory pigments reaching a molecular size between ~3.5-4.0 MDa (Markl, 2013). Its basic structure is a cylinder, 35 nm in diameter and 18 nm in height, formed by ten identical 350 to 400 kDa sized subunits (isomers), each of which comprises a 'pearl chain' of globular paralogous functional units [FU, (Miller et al., 1998; Gatsogiannis et al., 2007; Markl, 2013), Figure 2A-B]. The FUs originated from various events of gene duplications and losses and therefore share ~45% of their gene sequence and vary only slightly in size [e.g. 45.7-49.6 kDa, 394-420 amino acids in *Enteroctopus dofleini*, (Miller et al., 1998; Markl, 2013)]. Cephalopods lost the ancestral FU h and in the case of octopods and nautiloids contain only seven FUs, termed as FU a, b, c, d, e, f, g. Squids and Sepiids contain eight FUs due to a duplication of FU d and are termed as FU a, b, c, d (d*), e, f, g (Miller et al., 1998; Gatsogiannis et al., 2007; Markl, 2013). In octopods and nautiloids, FU a-f form the conserved wall structure of the haemocyanin cylinder and FU g a collar-like structure at the inside of the cylinder [(Gatsogiannis et al., 2007; Markl, 2013), Figure 2A-B]. FUs themselves comprise two domains, one domain rich in β -strands and an α -helices enriched domain, which contains two copper atoms in its center [(Cuff et al., 1998), Figure 2C]. Six histidines coordinate this pair of copper atoms that reversibly bind one dioxygen molecule and thus enable a single octopus haemocyanin molecule to bind up to 70 oxygen molecules [i.e. seven FUs times ten, (Cuff et al., 1998), Figure 2D]. FUs do not assemble arbitrarily to the decameric holoenzyme but in a well-defined order via 15 different types of intra- or inter-subunit interfaces, linked non-covalently via salt bridges or hydrophobic interactions (Gatsogiannis et al., 2007). However, it remains to be defined how these interfaces connect in detail and how their interactions affect oxygen binding of cephalopod haemocyanins (Markl, 2013).

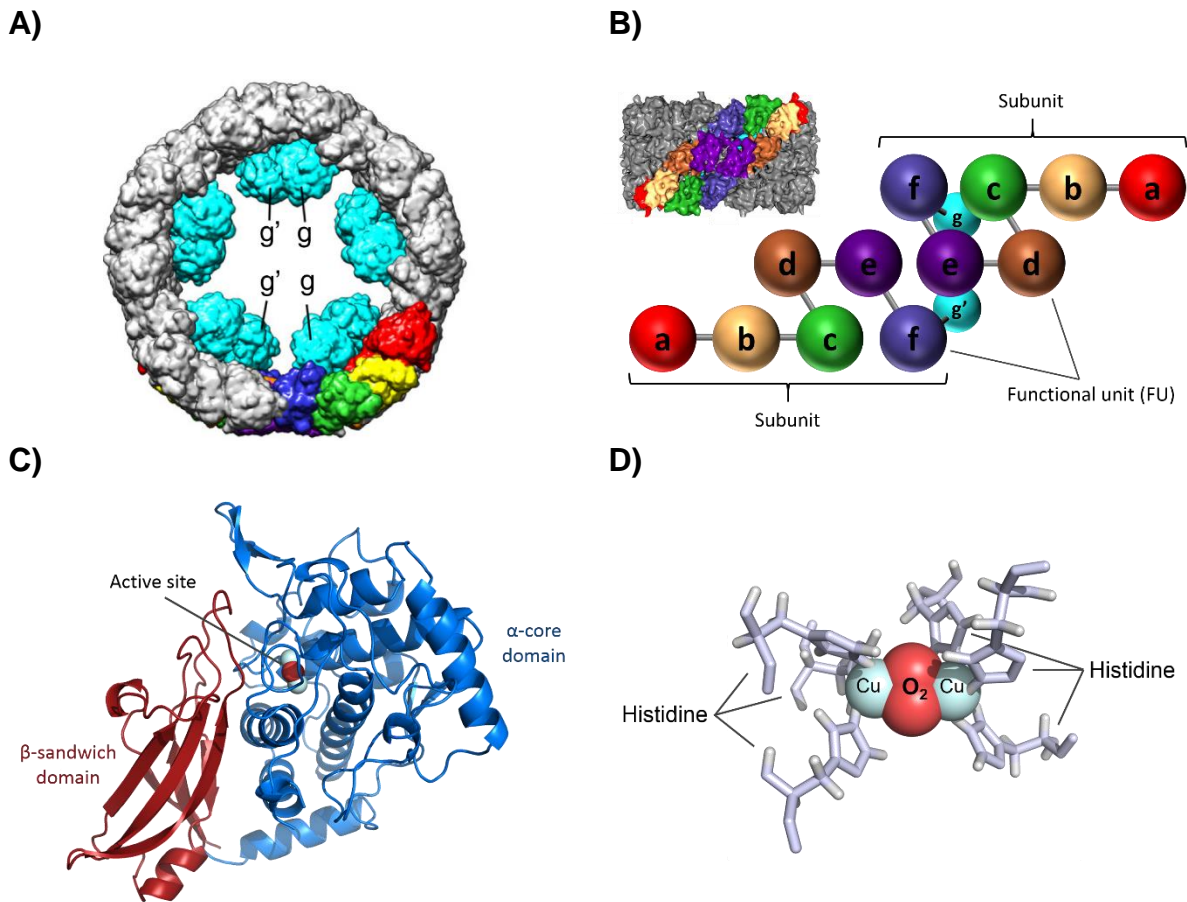


Figure 2: Haemocyanin structure.

A) Top-down view of the decameric haemocyanin of *Nautilus pompilius* with functional units a-f forming the wall structure and functional unit g the internal collar [EMDB-ID 1434, taken from (Markl, 2013)]. **B)** Side view of the cryo-EM structure of the haemocyanin molecule [taken from (Gatsogiannis et al., 2007)] and the schematic arrangement of functional units a-g [after (Gatsogiannis et al., 2007; Markl, 2013)]. **C)** Structure of the functional unit g and its two domains (PDB ID 1JS8A). **D)** The haemocyanin active site which reversibly binds one di-oxygen molecule via a central pair of copper atoms each coordinated by three histidines.

This overview illustrates that ‘cephalopod haemocyanins are among the best understood molluscan respiratory proteins’ since more than 20 years (Miller, 1995) in terms of structure and for more than 88 years in terms of function [since Redfield et al. (1926)]! It is thus astonishing that there has been no progress in understanding the mechanisms that link structure and function in cephalopod haemocyanin. The large size of haemocyanin with more than 2800 amino acids, certainly complicated sequencing efforts and prevented attempts to perform mutational experiments to infer structure-function relationships. To date, only few candidate mechanisms have been proposed. Gatsoganni et al. (2007) suggested several FU interfaces to communicate cooperatively, particularly via the protonation of histidine-rich motifs. Functional studies identified an allosteric unit with seven sites in octopus haemocyanin (Miller, 1985; Zolla

et al., 1985; Miller et al., 1988; Connelly et al., 1989), which however could not be allocated to specific interfaces (Gatsogiannis et al., 2007). Further, several isoforms of cephalopod haemocyanins exist, with at least two isoforms in octopus (Miller et al., 1998) and even three in *Sepia officinalis* (Thonig et al., 2014). Such isoforms were found to differ in sequence and their inferred physico-chemical properties such as the isoelectric point (Melzner et al., 2007a). Differential expression of isoforms that differ in their content of protonable histidines was thus suggested to modulate oxygen binding properties in response to changing environmental conditions in *Sepia officinalis* (Melzner et al., 2007a), however which later on was ascribed to ontogeny only (Strobel et al., 2012; Thonig et al., 2014). Yet, isoform expression in response to environmental cues remains to be tested for other cephalopods. Further, detailed mechanistic evidence is missing due to the current lack of functional studies on isolated isoforms.

1.3. Oxygen binding measurements in non-model organisms

To understand functional modifications of haemocyanin from Antarctic octopods one needs to assess oxygen binding by haemocyanin under various combinations of oxygen concentration, pH or temperatures as they may occur *in vivo*. This is achieved by oxygen binding experiments that mimic such conditions while recording the absorbance change of the blood or haemolymph at a particular wavelength, which reflects oxygenation changes of the respiratory pigment. However, most of the available devices (e.g. CO-Oximeter, HEMOX-Analyser) have been designed to analyse mammalian, and particularly human or rodent blood and consequently do not provide the experimental flexibility required for the analysis of non-model organism blood (Oellermann et al., 2014), which may limit and even prevent experimentation. First, accurate recording of oxygen affinity requires detailed knowledge of temperature, carbon dioxide or pH. However, during oxygenation changes, pH changes occur as well due to the release or uptake of protons by the respiratory pigment [Haldane effect, (Haldane and Priestley, 1935)]. Therefore, pH needs to be recorded at different oxygenation levels (Pörtner, 1990; Zielinski et al., 2001) or fixed with buffers to prevent intrinsic pH variation (e.g. Weber et al., 2008). Yet, such pH fixation does not reflect oxygen binding as it occurs *in vivo* and also disturbs the temperature sensitivity of oxygen binding (Brix et al., 1994). On the other hand, monitoring of pH with conventional pH electrodes requires relatively large sample volumes to immerse the sensor and its reference electrode. Even most recent cuvette based setups employing microelectrodes

to measure pH and absorbance simultaneously in the same sample require at least 400 μl sample volume (Zielinski et al., 2001). Such large sample volumes are often limited in small non-model organisms particularly in marine fish and invertebrates from remote regions with limited access (such as the shallow water Antarctic octopods) and if one plans multiple and replicated measurements. Second, blood of non-model organisms may have very complex spectra with absorbance peaks not captured by single wavelength filters designed for mammalian bloods. Third, the analysis of blood from marine ectotherms requires measurements at temperatures ranging from -1.8 to more than 30°C , very different from the human 'standard' temperature of 37°C . In this regard, conventional pH electrodes may fail to provide accurate and rapid recordings at temperatures close to zero due to increasing membrane resistance (Barron et al., 2006). At the beginning of this study no device was available that could successfully meet all these challenges at once, posing the foremost initial obstacle for the analysis of blood from Antarctic octopods.

1.4. Scope of the thesis

This study aims to unravel cold-adaptive traits of the respiratory pigment haemocyanin at the functional and molecular level and how the mechanistic interplay between both supported the adaptive radiation of octopods into cold Antarctic waters. In three major sections this thesis will advance existing technology and assess functional and genetic traits of Antarctic octopods in comparison to octopods from warmer climates.

Which technical advancements enable close to *in vivo* oxygen binding experiments for small non-model organisms?

This part of the study laid the foundation for the analysis of haemocyanin function and included the patented upgrade of a modified diffusion chamber with a fibre optic micro pH sensor and a broad-range miniature spectrophotometer to simultaneously measure pH and pigment absorbance in only 15 µl sample volume.

Are there functional traits of octopus haemocyanin that reflect cold-adaptation?

Cold adaptation of haemocyanin was assessed by comparing properties of haemolymph oxygen transport between the Antarctic octopus *Pareledone charcoti*, the temperate *Octopus pallidus* and the subtropical *Eledone moschata*.

Has natural selection acted on the evolution of haemocyanin and does this link to functional cold-adaptation?

Natural selection acting on haemocyanin was assessed by comparing 239 partial sequences of the haemocyanin functional unit f and g of 28 octopod species of polar, temperate, subtropical and tropical origin using phylogenetic analysis as well as analysis based non-synonymous codon substitutions. Subsequent examination of the quaternary structure and surface charge properties explored links to adaptive properties.

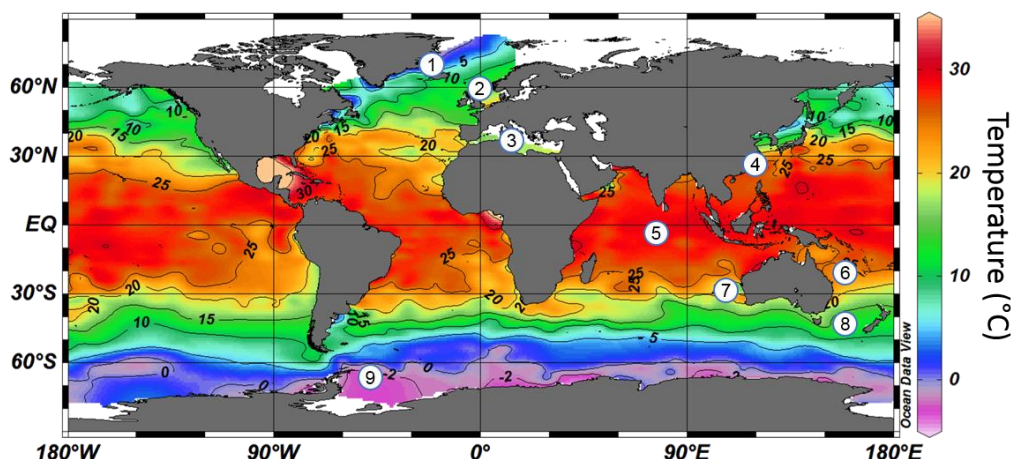
2 Material and Methods

This section mirrors and summarises the material and methods of publication I, II and III if not stated otherwise.

2.1. Animals

2.1.1. Collection

For publication I three non-model organisms were chosen to test the experimental setup. These comprised the common octopus *Octopus vulgaris* (Lamarck, 1798), hand-caught by snorkelling at Banuyls sur Mer, France; the Antarctic eelpout *Pachycara brachycephalum*, caught on RV Polarstern cruise ANTXXV/4 near Maxwell Bay at King George Island, Antarctica in May 2009 using fish traps, and the amphipod *Eulimnogammarus verrucosus* (Gerstfeld, 1858), collected in Bolshie Koty, Lake Baikal, Russia during summer 2012 using a spoon net. For publication II three benthic incirrate octopods were used: *Pareledone charcoti* collected on the RV Polarstern cruise ANTXXVIII/4 in March 2012 using bottom trawls, at depths between 90-470 m around Elephant Island [61°S, 56°W, cruise details (EXPEDITION, 2012)], where temperatures ranged between 0.1-1.6°C and salinities between 34.3-34.6 psu; *Octopus pallidus* caught by fishermen (T.O.P. Fish Pty Ltd.) in July 2012 using plastic octopus pots at 40-50 m depth in the western Bass Strait near Stanley, Australia (41°S, 145°E), where habitat temperatures range between 12-18°C from winter to summer (Leporati et al., 2006; André et al., 2009); and *Eledone moschata* collected in November 2008 using bottom trawls at 20-40 m depth in the northern Adriatic Sea near Chioggia, Italy, where habitat temperatures vary largely, both by depth and seasonally, between approximately 10-23°C (Artegiani et al., 1997). For publication III samples of 28 benthic incirrate octopod species were provided by collaborators or purchased from traders except for Antarctic octopods, which were collected during Polarstern cruises ANTXXV-3, ANTXXVII-3 and ANTXXIII-8 using bottom and Agassiz trawls (see expedition.awi.de for cruise- and supplementary material S1 of publication III for sample details). Climatic origins of all samples are illustrated in Figure 3.



- | | |
|-------------------------|-------------------------------|
| 1. Barents Sea | 6. Coral Sea |
| 2. North Atlantic Ocean | 7. South-Eastern Indian Ocean |
| 3. Mediterranean Sea | 8. Tasman Sea |
| 4. South China Sea | 9. Southern Ocean |
| 5. Indian Ocean | |

Figure 3: Climatic origins of octopod samples used in this study.

Colours refer to the annual average sea temperatures between 0-200m depth in 2009 [modelled from data of the World Ocean Atlas 2009 (Locarnini et al., 2009) using Ocean Data Viewer (Schlitzer, 2002)]. Lines indicate isotherms.

2.1.2. Culture and sampling

Specimens of *Pareledone charcoti* and *Pachycara brachycephalum* collected on RV Polarstern cruise ANTXXVIII/4 and ANTXXV/4 respectively, were transported to the Alfred Wegener Institute, Bremerhaven, Germany and kept in aerated tanks connected to a re-circulating aquaculture system at 0°C until sampling. Living specimens of *Octopus pallidus* purchased in Stanley, Australia, were transported and kept overnight in large tanks connected to a flow-through seawater system at the Institute for Marine and Antarctic Studies, Hobart and sampled the day thereafter. *Eulimnogammarus verrucosus* collected at Lake Baikal, Russia were transported to Irkutsk, Russia and kept in aerated 2.5 l tanks at 6°C until sampling. The Mediterranean *Eledone moschata* and *Octopus vulgaris* as well as Antarctic octopods obtained from the RV Polarstern cruises ANT XV-3, ANTXXVII-3 and ANTXXIII-8 were killed and sampled immediately upon catch.

All octopods obtained alive were anaesthetised in 3% EtOH (as in Oosthuizen and Smale, 2003; Ikeda et al., 2009; Mähnger et al., 2012) until non responsive and killed by a cut through the brain. Although seemingly more effective (Andrews et al.,

2013), I could not employ magnesium chloride as sedative due to its confounding effects as allosteric ligand on oxygen binding. Animals were opened ventrally to withdraw haemolymph from the cephalic vein, the afferent branchial vessels and the systemic heart and to excise gill glands, gills, hepatopancreas, funnel and mantle muscle. Haemolymph samples were spun down at 15.000 g for 15 min at 0°C to pellet cell debris and supernatants were stored at -20°C. Tissue samples were immediately frozen in liquid nitrogen or preserved in RNAlater (QIAGEN, Germany) and stored at -80°C. *Pachycara brachycephalum* were anaesthetised with 0.3 g L⁻¹ tricaine methanesulphonate (MS222) until non responsive and blood withdrawn using a heparinised syringe and finally killed by a spinal cut. The fish blood was used freshly and kept on ice till the beginning of the measurement. Haemolymph of *Eulimnogammarus verrucosus* was withdrawn using a dorsally inserted capillary and then centrifuged at 15.000 g for 15 min at 0°C to remove cell debris and stored at -20°C.

2.1.3. Ethics approval

Any handling and sampling of octopods complied to common ethical and experimental procedures for cephalopods (Sykes et al., 2012) and, according to § 8 animal welfare act (18.05.2006; 8081. I p. 1207), was communicated to the veterinary inspection office, Bremen, Germany. At the time of sampling German and EU regulations did not require ethical approval for cephalopod sampling and experimentation (Smith et al., 2013). Collection of Antarctic octopods complied with the general guidelines under §1 Umweltschutzprotokoll zum Antarktisvertrag (AUG). Collection, culture and sampling of *Octopus pallidus* was approved by the ethics committee at La Trobe University, Bundoora, Australia (Animal ethics approval no. AEC12-43, valid from June 25th, 2012 until November 31st 2012). *Octopus pallidus* specimens were purchased from registered fishermen (T.O.P. Fish Pty Ltd., Stanley, TAS, Australia) and thus did not require a collection permit. I further declared not to use any samples obtained in Australia for commercial purposes on March 14th 2012 (roll of Deeds No, 68/2012 K, Notary Burkhard Klüver, Bremen, Germany). Handling and sampling of *Pachycara brachycephalum* was approved by the veterinary inspection office, Bremen, Germany (Animal research permit no. 522-27-11/02-00(93)) on January 15th, 2008 (permit valid until February 21th, 2016).

2.2. Analysis of blood oxygen transport

2.2.1. Technical modifications

A gas diffusion chamber (Eschweiler Co., Kiel, Germany) designed and described in detail by (Niesel and Thews, 1961; Sick and Gersonde, 1969, 1972) has been used to determine OECs by recording absorbance of a thin layer of a haemoglobin or haemocyanin bearing solution during continuous or stepwise changes of PO_2 (Wells and Weber, 1989). To overcome shortcomings in oxygen transport analysis outlined in section 0, I further modified the diffusion chamber as follows. (1) A broad range (200 to 1100 nm) fibre optic spectrophotometer (USB2000+, Ocean Optics, USA) was connected via two fibre optic cables fitted to the central cylinder of the diffusion chamber to direct the light beam via collimating lenses from the deuterium halogen light source (DT-Mini-2-GS, Ocean Optics, USA) through the sample glass plate back to the 2048-element CCD-array detector of the spectrophotometer (Publication I). (2) The plastic slide that holds the sample glass plate in the light tunnel was modified to fit a fibre optic micro-pH optode (NTH-HP5-L5-NS*25/0.8-OIW, PreSens, Germany), housed in a syringe and connected to a phase detection device (μ PDD 3470, PreSens, Germany, Publication I). The needle of the syringe was then inserted through a silicone ring to prevent the leakage of gas (Publication I).

2.2.2. Experimental procedures

The modified gas diffusion chamber was first tested for its accuracy using three non-model organisms (*Octopus vulgaris*, *Pachycara brachycephalum* and *Eulimnogammarus verrucosus*, Publication I) and subsequently employed for broad-scale functional measurements on octopod haemocyanin of the Antarctic *Pareledone charcoti*, the temperate *Octopus pallidus* and the subtropical *Eledone moschata*, Publication II). For both approaches experiments were performed at approximate habitat temperatures of each species (*Octopus vulgaris* at 15°C, *Pachycara brachycephalum* at 0°C, *Eulimnogammarus verrucosus* at 6°C, *Pareledone charcoti* at 0°C and 5°C, *Octopus pallidus* at 10°C, 15°C and 20°C, *Eledone moschata* at 10°C, 15°C and 20°C). For *Pareledone charcoti* additional measurements were performed at 10°C to allow functional comparisons with haemocyanin with *Octopus pallidus* and *Eledone moschata*. The temperature was monitored and controlled via a temperature

sensor (PreSens, Germany) and a connected water bath with a thermostat (LAUDA Ecoline Staredition RE 104, Germany), filled with an anti-freeze solution (20% ethylene glycol, AppliChem, Germany). Prior to measurements, aliquots of 18 μl thawed haemolymph (octopus/amphipod) were spun down to collect all liquid at the bottom of a 1.5 ml microcentrifuge tube (5 sec at 1000 g), preconditioned with pure oxygen gas to deplete dissolved carbon dioxide (CO_2) and 0.6-0.9 μl of 0.2 mmol L^{-1} NaOH (8-12 $\mu\text{mol L}^{-1}$ final concentration) added to raise blood pH above 8.0 to ensure full pigment oxygenation. To avoid haemolysis and the formation of methaemoglobin by freezing, I used freshly sampled whole blood from *Pachycara brachycephalum* and diluted the sample with one volume of blood plasma to improve light transmission during the measurement and preconditioned the sample with pure oxygen gas prior to measurements as well. Each measurement was performed with 15 μl of preconditioned haemolymph/whole blood. The pH of haemolymph/whole blood was not stabilized with extrinsic buffers such as Tris or HEPES as they disturb the effects by ligands and temperature on pigment oxygenation (Brix et al., 1994).

Prior to each experiment, the pH optode was calibrated in MOPS-buffered (40 mmol L^{-1} , 3-(N-Morpholino)propanesulfonic acid), filtered artificial seawater (35 psu) equilibrated to the respective experimental temperature at six pH ranging from 6.7 to 8.1. The pH of buffers was checked with a pH glass electrode (InLab Routine Pt1100, Mettler Toledo, Germany) and a pH meter (pH 330i, WTW, Germany), calibrated with low ionic strength NIST pH standards (AppliChem, Germany, DIN19266) and corrected to Free Scale pH with Tris-buffered seawater standard [Dickson, CO_2 QCLab, batch 4 2010, USA, (Dickson, 2010)] equilibrated at the same temperature. The pH signal was corrected for instrumental drift and for effects of auto-fluorescence intrinsic to haemolymph (Publication I) and is presented here on the free hydrogen ion scale (Dickson, 1984). The spectrophotometer was set to 15 milliseconds integration time, 100 scans to average and 30 seconds measurement intervals and calibrated by recording light and dark spectra without sample.

To account for the pronounced pH sensitivity of cephalopod pigments (Pörtner, 1990), changes of pH and absorbance were recorded at 347 nm in 15 μl haemolymph, at continuously decreasing $P\text{CO}_2$ / pH (0-10 kPa / \sim pH 8.1-6.8) and four constant $P\text{O}_2$ levels [21, 13, 4, 1 kPa, after Pörtner (1990)], with gas mixtures being supplied by gas mixing pumps (Wösthoff, Germany). To test the accuracy of the diffusion chamber I further employed conventional methodology for haemolymph of *Octopus vulgaris*,

characterized by stepwise changes of discrete PO_2 (1, 2, 4, 9, 13, 17, 21 kPa) and a PCO_2 kept constant [Publication I, (e.g. Wells and Weber, 1989)]. The exemplary analysis of whole blood of *Pachycara brachycephalum* was performed from 21-0 kPa PO_2 and pH 8.2-7.1 and of thawed haemolymph of *Eulimnogammarus verrucosus* at a constant PO_2 of 21 kPa and pH 7.7-6.9.

Each experiment involved the calibration with pure oxygen or nitrogen to obtain maximum and minimum oxygenation signals. Correct pigment saturation was calculated by continuous readjustments of the maximum oxygenation signal to account for its linear drift observed during the course of an experiment [(Wells and Weber, 1989), Publication I]. While the maximum oxygenation signal did not change within the range of temperatures employed for each species, the minimum oxygenation signal increased towards colder temperatures due to incomplete oxygen unloading, even under pure nitrogen and low pH (< 6.6). For such experiments I predicted minimum absorbance from a reference wavelength of the first recorded spectrum with an uncertainty of 5%, based on a linear regression model applied to 20 experiments with fully deoxygenated pigments (Publication II).

2.2.3. Oxygen carrying capacity

In publication II the total oxygen bound to octopod haemocyanin was determined (i.e. oxygen carrying capacity). For this 10 μ l of thawed haemolymph were equilibrated with pure oxygen gas in a microcentrifuge tube on ice for 10 min and transferred with a gas tight Hamilton syringe to a gas sealed chamber containing 2 ml of a 32°C warm cyanide solution [6 g L⁻¹ potassium cyanide, 3 g L⁻¹ saponin, (Bridges et al., 1979)]. Two high-resolution Oxygraph-2k respirometers (OROBOROS Instruments, Innsbruck, Austria) and DatLab analysis software (version 5.1.0.20) recorded the liberated oxygen (nmol ml⁻¹), corrected for air pressure, temperature and background oxygen flux. For each experiment, the respirometers were calibrated with air at the beginning and sodium dithionite added at the end for a zero calibration. The contribution of dissolved oxygen was experimentally determined by the addition of ice-cold, oxygen saturated, filtered seawater (35 psu). The observed change of oxygen concentration was then subtracted from the haemolymph measurements to obtain the final oxygen carrying capacity of haemocyanin.

2.2.4. Alpha-stat pattern of haemolymph pH

In publication II it was assessed whether the pH of octopod haemolymph follows an alpha-stat pattern (Reeves, 1972) or remains constant across temperatures (i.e. pH stat pattern). Replicated measurements on 20 µl thawed haemolymph of *Octopus pallidus* at 0°C, 10°C and 20°C, using a micro pH electrode (InLab Ultra-Micro, Mettler Toledo, Germany), showed that pH decreases linearly with temperature ($b = -0.0153$ pH units / °C, $t_{31} = -9.71$, $P < 0.001$, $R^2 = 0.75$, Publication II), analogous to an imidazole buffered system [-0.0162 pH units / °C, (Reeves, 1972)]. pH analysis of freshly sampled blood from other species confirmed that octopod haemolymph follows this linear pH-temperature relationship *in vivo* (Publication II) and therefore exhibits an alpha-stat pattern as also demonstrated for squid (Howell and Gilbert, 1976). Hence, venous and arterial pH were determined on this basis for various temperatures.

2.2.5. Protein and ion concentration

In publication II protein content of octopod haemolymph was determined according to Bradford (1976). For this thawed haemolymph was diluted tenfold (v:v) with stabilising buffer (in mmol l⁻¹, 50 Tris-HCl, 5 CaCl₂ 6 H₂O, 5 MgCl₂ 6 H₂O, 150 NaCl, pH 7.47 at 22°C) and 5 µl mixed with 250 µl Bradford reagent (Bio-Rad, Germany). Following 10 min incubation at room temperature, absorbance was recorded at 595 nm using a microplate spectrophotometer (PowerWave HT, BioTek, U.S.A.). Bovine albumin serum served as protein standard to calculate total protein concentrations.

Concentrations of functional haemocyanin [$c(Hc)$] in haemolymph were derived from the oxygen carrying capacity (C_{O_2}), the molecular weight (MW) of octopod haemocyanin (3.5 MDa) and its 70 oxygen binding sites [$n(HcO_2)$, (Miller et al., 1998), Equation 1].

$$c(Hc) = \frac{C_{O_2}}{n(HcO_2)} MW \quad \text{Equation 1}$$

Results from preceding tests with thawed haemolymph of *Octopus vulgaris* (mean ± S.D., 54.3 ± 6.9 g L⁻¹) agreed well with data obtained from freshly observed haemolymph via atomic absorption spectroscopy [55.9 ± 7.4 g L⁻¹, (Senozan et al., 1988)], which not only confirmed the accuracy of our approach but also that storage at -20°C does not affect the oxygen binding capacity of cephalopod haemolymph (Mangum, 1990).

Although inorganic ions such as Mg^{2+} or Na^+ can affect oxygen affinity in octopods (Miller, 1985), they seem to be insignificant regulators of oxygen binding in most cephalopods (Mangum, 1990). I re-assessed this for the three octopod species analysed in publication II. Haemolymph was 400-fold diluted with deionised water and determined cation concentrations by ion chromatography (ICS-2000, Dionex, Germany) following cation separation by an IonPac CS 16 column (Dionex, Germany) with methane sulfonic acid (MSA, 30 mmol L⁻¹) as an eluent at 0.36 ml min⁻¹ flow rate and 40°C. Ion concentrations were derived from the peaks corresponding to the Dionex Combined Six Cation Standard-II.

2.3. Molecular and structural analysis of haemocyanin

All methodology described in this section refers to publication III if not stated otherwise.

2.3.1. PCR, cloning and sequencing

Genomic DNA was extracted from either gill glands, mantle tissue or arm tips of each of the 28 benthic incirrate octopod species analysed in publication III, using the QIAGEN DNeasy Blood and tissue kit following the manufactures instructions. To construct a species phylogeny for the sampled octopods, I amplified partial sequences of cytochrome c oxidase subunit I (COI) and cytochrome c oxidase subunit III (COIII) using polymerase chain reaction (PCR) and the primers detailed in (Folmer et al., 1994; Simon et al., 1994; Allcock et al., 2008). COI and COIII were amplified in 25 µl PCR mix containing final concentrations of 0.5 µmol L⁻¹ dNTPs, 0.05 units µl⁻¹ Taq DNA Polymerase, 1 x Taq buffer (5 Prime, Germany) and 1 µmol L⁻¹ of each Primer. The PCR reaction comprised an initial denaturation at 94°C for 4 mins, followed by 35 cycles at 94°C for 40 s, 50°C (COI) or 42°C (COIII) respectively for 40 s, 68°C for 90 s and a final extension step at 68°C for 10 min.

Regions of the haemocyanin gene were amplified using two pairs of degenerate primers, which bind to conserved sites present across all seven functional units [i.e. amino acid sequence PYWDW and WAIWQ, (Lieb et al., 2001)]. Template specificity was enhanced via Touchdown-PCR in 25 µl reaction volume containing final concentrations of 0.2 µmol L⁻¹ dNTPs, 0.05 units µl⁻¹ DreamTaq DNA Polymerase (Thermo Scientific, Germany), 1 x DreamTaq Green buffer (Thermo Scientific,

Germany) and $1 \mu\text{mol L}^{-1}$ of each Primer. The PCR reaction comprised an initial denaturation at 94°C for 4 mins, 12 cycles at 94°C for 45 s, $60 \rightarrow 48^{\circ}\text{C}$ for 60 s ($-1^{\circ}\text{C}/\text{cycle}$), 72°C for 90 s followed by 35 cycles at 94°C for 45 s, 52°C for 60 s, 72°C for 90 s and a final extension at 72°C for 8 min. PCR products were separated on 1.3% Agarose gel with GelRed (Biotium, U.S.A.) and distinct bands excised and purified using the QIAQuick Gel Extraction Kit (QIAGEN, Germany). Purified PCR fragments were then cloned using the pGEM-T Easy vector system (Promega, Germany) due to the potential binding of the primer pairs at each of the seven FUs, the presence of isoforms as well as alleles. Plasmids of positive clones were purified using the QIAprep Spin Miniprep Kit (QIAGEN, Germany), tested for successful insertion via a EcoRI (Life Technologies, Germany) restriction digest and send for sanger sequencing (Eurofins MWG Operon or GATC Biotech AG, Germany). Amplicons were most frequent for the regions FU f-g and FU g comprising fragments of 370 bp or 1090 bp length (Publication III). Amplicons of other regions were not represented across all sampled species and were thus not included in subsequent analysis.

In addition, full sequencing of the haemocyanin gene for *Pareledone charcoti* was performed but included in neither of the publications. First, RNA was extracted from gill glands using the QIAGEN RNeasy Mini Kit and transcribed to cDNA using SuperScript III Reverse Transcriptase (Invitrogen, Germany) and a custom 3'-end T-rich primer to enrich haemocyanin transcripts. By means of degenerate primers, binding to regions PYWDW and WAIWQ (Lieb et al., 2001) initial sequences were obtained using the protocol described above and subsequently sequence gaps closed by primer walking. 5' and 3' ends were sequenced using the First Choice RLM-RACE Kit (Ambion, Germany) according to the manufactures instructions. Following agarose gel electrophoresis target fragments were excised, purified using the QIAQuick Gel Extraction Kit (QIAGEN, Germany) and submitted for Sanger sequencing (Eurofins MWG Operon or GATC Biotech AG, Germany). Sequence editing and assembly was performed using Geneious 7.1.5 (Biomatters, New Zealand).

2.3.2. Phylogenetic analysis

Obtained sequences were assembled and verified by means of their chromatograms and primer sequences trimmed using Geneious 7.1.5 (Biomatters, New Zealand). Published sequences further supplemented the COI (*Enteroctopus dofleini* [GenBank: GU802397], *Nautilus pompilius* [GenBank: AF120628]), the COIII

(*Enteroctopus dofleini* [GenBank: X83103]) and the haemocyanin data sets (*Enteroctopus dofleini* [GenBank: AF338426 & AF020548]). COI and COIII were concatenated and multiple sequence alignments obtained using the MUSCLE plugin of Geneious (Edgar, 2004). The two amplified haemocyanin regions FU f-g and FU g were not concatenated as the presence of multiple isoforms as well as allelic variation did not allow reliable sequence matching. Thus, multiple sequence alignments and subsequent analysis were performed separately for each of the two regions. The intron region between the FU f and FU g was identified by means of the *Enteroctopus dofleini* haemocyanin sequence and trimmed from the alignment. For haemocyanin alignments 3' and 5' ends were trimmed to obtain a consistent reading frame as well as gap free 3' and 5' ends, which otherwise would produce false results in the selection analysis. Translated sequences containing stop codons were removed. The quality of the COI/COII and haemocyanin alignments were tested using GBlocks 0.91b (Castresana, 2000; Talavera and Castresana, 2007) tolerating gap positions within final blocks, which retained between 98-100% of the original alignment. Based on the Akaike Information Criteria (Akaike, 1974), JModeltest 2.1.5 (Darriba et al., 2012) identified the GTR+I+G model for the COI-COIII data set and the HKY85 model for the two haemocyanin regions as the best available substitution models.

Based on the COI-COIII and haemocyanin alignments phylogenetic relationships were inferred using Bayesian and maximum likelihood methods. Bayesian trees were constructed using MrBayes (Huelsenbeck and Ronquist, 2001) as implemented in Geneious (v. 2.0.3) running at least two independent Monte Carlo Markov Chain (MCMC) analysis with 10,000,000 generations sampled every 10,000 generation. The appropriate burnin was chosen based on the resulting traces, which showed a stationary distribution before 10% of the MCMC chain. Maximum likelihood trees were constructed using the PhyML (Guindon and Gascuel, 2003) plugin of Geneious and bootstrap values calculated from 1000 replicates. *Nautilus pompilius* and *Vampyroreuthis infernalis* were used as outgroups for the COI-COIII phylogeny.

2.3.3. Natural selection

Prior to selection analysis, I screened both partial haemocyanin regions for conserved and variable sites using the Jensen-Shannon Divergence (Capra and Singh, 2007), which identifies conserved sites as deviations of a probability distribution from

the overall amino acid distribution of the respective BLOSUM62 alignment as background and also accounts for conservation in neighbouring sites.

To assess whether natural selection affected the evolution of octopod haemocyanin I employed codon-based Bayesian and maximum likelihood approaches to estimate rates of non-synonymous (dN) to synonymous substitutions (dS). Ratios ≤ 1 denote purifying or negative selection and ratios > 1 diversifying or positive selection. The unrooted haemocyanin phylogenies, without outgroup (Publication III) were uploaded to the Datamonkey webserver (Pond and Frost, 2005; Delpont et al., 2010) and selection inferred via the following methods. Prior to performing selection tests, alignments were tested for recombination using Genetic Algorithms for Recombination Detection analysis (GARD) implemented in Datamonkey. Single sites under selection were identified using Single Likelihood Ancestral Counting (SLAC), Fixed Effects Likelihood (FEL), Mixed Effects Model of Evolution (MEME), Fast Unconstrained Bayesian AppRoximation (FUBAR), Evolutionary Fingerprinting (EF) as well as PProperty Informed Models of Evolution (PRIME). SLAC estimates and compares normalized expected and observed numbers of synonymous and non-synonymous substitutions at each codon position based on a single ancestral sequence reconstruction (Kosakovsky Pond and Frost, 2005). FEL estimates and compares dN and dS independently for each site (Kosakovsky Pond and Frost, 2005). MEME assesses whether single sites undergo positive as well as episodic diversifying selection along particular branches (Murrell et al., 2012). FUBAR enables larger numbers of site classes and efficiently identifies positively selected sites using a hierarchical Bayesian MCMC routine (Murrell et al., 2013). EF compares 'evolutionary fingerprints' between homologous as well as non-homologous sequences obtained from a posterior sample of a bivariate distribution of dN and dS at each site (Kosakovsky Pond et al., 2010). PRIME resembles FEL or MEME but additionally links an amino acid property category (Atchley et al., 2005; Conant et al., 2007) to the non-synonymous substitution rate. Significance thresholds for selection tests were: $P \leq 0.10$ for SLAC, FEL and MEME; $P \leq 0.05$ for PRIME; posterior probability ≥ 0.90 for FUBAR and Bayes factor ≥ 0.50 for EF.

I further employed the software TreeSAAP 3.2 [Selection on Amino Acid Properties using phylogenetic trees, (Woolley et al., 2003)] to analyse which out of 31 amino acid properties are under positive selection. TreeSAAP categorizes these physico-chemical properties into eight magnitudes with low magnitudes being more

conservative and high magnitudes being more radical and assesses codon by codon whether the distribution of observed changes of amino acid properties differs from an expected uniform distribution. I considered changes of amino acid properties of codons with magnitudes ≥ 6 and z-scores ≤ 0.001 to be positively selected. Sites were considered positively selected if at least three tests yielded significant results.

Amino acid sites under selection were illustrated with PhyMol 1.3 (Schrodinger, 2010) using the crystal structure of the functional unit G based and the protein sequence of *Enteroctopus dofleini* [PDB ID: 1JS8, (Cuff et al., 1998; Miller et al., 1998)]. The homologous partial haemocyanin region of FU f was aligned with the FU g PDB sequence to match and display positively selected FU f residues on the 3D protein structure.

2.3.4. Analysis of polar surface residues

Polar surface residues were assessed for differences between octopods originating from different climates. Surface residues of the FU g crystal structure were identified via the GETAREA webserver (Fraczkiewicz and Braun, 1998), setting the radius of the water probe to 1.4. This yielded 65 surface residues for the partial haemocyanin fragment FU f-g and 19 surface residues for the partial haemocyanin fragment FU g. Numbers of each type of polar surface residues as well as net charge (at pH 7.27) were determined and analysed via principal component analysis to assess correlation patterns and the impact of climatic origin.

2.3.5. Native page gel electrophoresis

Additional protein analysis of haemocyanin was performed, (not included in publication III), using native page gel electrophoresis for several cephalopods, collected on RV Polarstern cruise ANTXXVIII/4 as well as *Octopus pallidus*, *Octopus vulgaris* and *Megaleledone setebos*. Fresh haemolymph samples were spun down at 12,000 g at 4°C for 20 min to remove cellular debris and 200 μ l clean supernatant transferred into micro-centrifugation tubes (PE 5x20mm Beckmann, Germany) and haemocyanin pelleted in a micro-ultracentrifuge (Airfuge, Beckmann, Germany) for 120 min at 130,000 g at 4°C. Supernatants were then removed and pellets resuspended in equal volumes of stabilization buffer (in mmol L⁻¹, 50 Tris Base, 150 NaCl, 5 MgCl₂, 5 CaCl₂, pH 7.4). Protein content was determined at 280 nm using a Nanodrop2000 spectrophotometer (Thermo Fisher Scientific, USA) and a protein standard, to dilute

haemocyanin solutions with dissociation buffer (Glycine 133 mmol L⁻¹, pH 9.6) to a concentration of 4-9 µg µl⁻¹. 20 µl of diluted sample was mixed with 7.5 µl loading buffer (4% Stabilising buffer, 4% glycerine (v/v), Bromphenol Blue), of which 5 µl were run on a 3.9% polyacrylamide gel (running buffer in mmol L⁻¹, 23 Tris Base, 190 Glycine, 5 MgCl₂, 5 CaCl₂, pH 8.3) for 4.5 hours at 20 mA, followed by staining for 30 min (staining solution 40% methanol, 10% acetic acid (v/v), 2.5 mg ml⁻¹ Coomassie Blue G, 1 mg ml⁻¹ Trichloroacetic acid) and destaining overnight [de-staining solution 20% methanol and 10% acetic acid (v/v)] to visualize protein bands.

2.4. Data analysis

Processing of data and statistical analysis was performed using the ‘R’ statistical language (R Core Team, 2014) if not mentioned otherwise.

For the analysis of oxygen equilibrium curves recordings of pH and pigment oxygenation were time-matched and analysed in pH/saturation diagrams, most suitable for pH sensitive pigments like cephalopod haemocyanin (Pörtner, 1990). An empirical five parameter logistic model was applied [Equation 2, ‘drc’ add-on package, (Ritz and Streibig, 2005)] to fit sigmoidal curves to the pH/saturation data (Publication I). Resulting OECs display the change of pigment oxygenation with pH at constant *PO*₂. Affinity of haemocyanin to oxygen, expressed as *P*₅₀, denotes the log₁₀ of the *PO*₂ corresponding to an OEC and the intersecting pH at half saturation [pH₅₀, (Pörtner, 1990)]. Δlog₁₀*P*₅₀ was then plotted versus ΔpH₅₀ to obtain the Bohr coefficient from the resulting linear regression slope. Cooperativity was expressed as the pH dependent rate of oxygen release by haemocyanin [Δmmol L⁻¹ / ΔpH, (Pörtner, 1990)] and derived from the maximum slope of a fitted OEC. Differences between *Pareledone charcoti*, *Octopus pallidus* and *Eledone moschata* and experimental temperatures were tested to be significant (*P* < 0.05) using analysis of variance (ANOVA) followed by Tukey’s *post hoc* test. Normality and homogeneity of variance were assessed by Kolmogorov–Smirnov and Levene’s tests, respectively. Results were expressed as means and their 95% confidence interval range if not stated otherwise.

$$f(x, (b, c, d, e, f)) = c + \frac{(d-c)}{(1+\exp\{b(\log(\frac{x}{e}))\})^f} \quad \text{Equation 2}$$

The parameters *c* and *d* of this empirical five parameter logistic model denote the upper and lower asymptotes and *f* the asymmetry of the curve. The parameters *b* and

e correspond to the slope and inflection point of a four parameter logistic model if the parameter f equals 1. Note that this equation represents an empirical curve fit that does not describe the functional properties of the haemocyanin sub-units according to mechanistic insight.

For the processing, statistical analysis and graphical display of polar surface residues (Publication III) I employed the R packages 'seqinr' (Charif and Lobry, 2007), 'ape' (Paradis et al., 2004) and 'ade4' (Dray and Dufour, 2007).

3 Publications

List of publications and declaration of my contribution towards them.

Publication I

Oellermann, M., Pörtner, H.-O. and Mark, F. C. (2014). Simultaneous high-resolution pH and spectrophotometric recordings of oxygen binding in blood microvolumes. *J. Exp. Biol.* 217, 1430-1436. ([doi: 10.1242/jeb.092726](https://doi.org/10.1242/jeb.092726))

I and FCM conceived and developed the technical modifications. I performed the experiments and analysis and wrote the first draft of the manuscript, which was revised by FCM and HOP.

Publication II

Oellermann, M., Lieb, B., Pörtner H.-O., Semmens J. M. and Mark, F. C. (2015). Blue blood on ice: modulated blood oxygen transport facilitates cold compensation and eurythermy in an Antarctic octopod. *Frontiers in Zoology* 2015, 12, 6. ([doi:10.1186/s12983-015-0097-x](https://doi.org/10.1186/s12983-015-0097-x))

I and FCM developed the study design and acquired samples. I performed the experiments and analysis and wrote the first draft of the manuscript, which was revised by FCM, HOP, BL and JMS. JMS supported the sample acquisition and blood sampling of *Octopus pallidus*. FCM and HOP contributed to data interpretation.

Publication III

Oellermann, M., Strugnell, J., Lieb, B. and Mark, F. C. (2015). Positive selection in octopus haemocyanin reveals functional links to temperature adaptation. (in revision for *BMC Evolutionary Biology*)

I, FCM and BL developed the study design. I, FCM and JS acquired samples. I and FCM performed PCRs and cloning. I analysed the data and performed phylogenetic analysis with JS. I compiled the first draft of the manuscript, which was revised by FCM, JS and BL.

Patent (Appendix)

Oellermann, M., Mark, F. and Dunker, E. (2014). Diffusionskammer zur Ermittlung unterschiedlicher Parameter einer wässrigen Substanz, Patentnummer: DE 10 2013 011 343 B3 2014.07.10 (ed. D. P. u. Markenamt), pp. 16. Germany.

I and FCM conceived and developed the technical modifications. I performed the experiments and analysis and revised the patent draft compiled by the contracted patent engineer Nicola Cochu.

3.1. Publication I

Simultaneous high-resolution pH and spectrophotometric recordings of
oxygen binding in blood microvolumes

M Oellermann, HO Pörtner, FC Mark

2014

Journal of Experimental Biology

217, 1430-1436.

([doi: 10.1242/jeb.092726](https://doi.org/10.1242/jeb.092726))

METHODS & TECHNIQUES

Simultaneous high-resolution pH and spectrophotometric recordings of oxygen binding in blood microvolumes

Michael Oellermann, Hans-O. Pörtner and Felix C. Mark*

ABSTRACT

Oxygen equilibrium curves have been widely used to understand oxygen transport in numerous organisms. A major challenge has been to monitor oxygen binding characteristics and concomitant pH changes as they occur *in vivo*, in limited sample volumes. Here we report a technique allowing highly resolved and simultaneous monitoring of pH and blood pigment saturation in minute blood volumes. We equipped a gas diffusion chamber with a broad-range fibre-optic spectrophotometer and a micro-pH optode and recorded changes of pigment oxygenation along oxygen partial pressure (P_{O_2}) and pH gradients to test the setup. Oxygen binding parameters derived from measurements in only 15 μ l of haemolymph from the cephalopod *Octopus vulgaris* showed low instrumental error (0.93%) and good agreement with published data. Broad-range spectra, each resolving 2048 data points, provided detailed insight into the complex absorbance characteristics of diverse blood types. After consideration of photobleaching and intrinsic fluorescence, pH optodes yielded accurate recordings and resolved a sigmoidal shift of 0.03 pH units in response to changing P_{O_2} from 0 to 21 kPa. Highly resolved continuous recordings along pH gradients conformed to stepwise measurements at low rates of pH changes. In this study we showed that a diffusion chamber upgraded with a broad-range spectrophotometer and an optical pH sensor accurately characterizes oxygen binding with minimal sample consumption and manipulation. We conclude that the modified diffusion chamber is highly suitable for experimental biologists who demand high flexibility, detailed insight into oxygen binding as well as experimental and biological accuracy combined in a single setup.

KEY WORDS: Diffusion chamber, Oxygen equilibrium curve, Hemocyanin, Haemocyanin, Haemoglobin, pH optode, Octopus, Amphipod, Antarctic fish

INTRODUCTION

Since the first oxygen binding experiments by Paul Bert (Bert, 1878) and Carl Gustav von Hüfner (Hüfner, 1890) and the pioneering work by Bohr, Hasselbalch and Krogh (Bohr et al., 1904) dating back more than a century, oxygen binding experiments have served to understand human blood physiology and diseases (e.g. Chanutin and Curnish, 1967; Festa and Asakura, 1979) or the environmental adaptation of various organisms (e.g. Brix, 1983; Herbert et al., 2006; Meir et al., 2009; Scott, 2011), and have even resolved crime (Olson et al., 2010). Ever since, researchers have developed and refined techniques to comprehend the complex physiology of oxygen transport, leading to a variety of currently employed methods (supplementary material Table S1).

Alfred Wegener Institute for Polar and Marine Research, 27570 Bremerhaven, Germany.

*Author for correspondence (FMark@awi.de)

Received 18 June 2013; Accepted 9 January 2014

1430

Such analysis commonly involves the determination of oxygen affinity (P_{50}). Accurate determination of P_{50} requires the control or monitoring of extrinsic factors such as temperature, carbon dioxide and particularly pH. Assessing the effects of pH and the variation of pH during transition from the oxygenated to the deoxygenated state, due to the oxygenation-dependent release or uptake of protons by the pigment (Haldane effect), requires knowledge of pH at different levels of saturation for the analysis of oxygen equilibrium curves (OECs). Conventionally, experimenters control pH by added buffers [e.g. Tris, HEPES (Brix et al., 1994)] or determine pH from sub-samples or separately conditioned samples (e.g. Seibel et al., 1999; Weber et al., 2008) and rarely directly in the original sample (Pörtner, 1990; Zielinski et al., 2001). While added buffers prevent pH changes and may help to address specific functional characteristics of the pigment [e.g. effects of inorganic ions (Mangum and Lykkeboe, 1979)], they disturb the fine tuning of oxygen binding (Brix et al., 1994) and block pH changes relevant as part of the oxygen transport process, which need to be included for a comprehensive picture of oxygen transport *in vivo*. A major challenge in monitoring pH has been the relatively large sample volume required to immerse a pH electrode and its reference electrode. Particularly, analysis in highly limited sample volumes or devices that employ thin blood films (e.g. diffusion chamber, HemOscan, Pwee 50; supplementary material Table S1) suffer from this constraint.

Further, while many commercially available devices have been designed for mammalian (including human) blood analysis (e.g. CO-Oximeter, HEMOX-Analyser), only few provide the flexibility needed for the analysis of non-model organism blood, characterized by small sample volumes, unusual spectra, extreme *in vitro* temperatures or high pH sensitivity.

Here we report a major step forward in the respective methodology, allowing the simultaneous analyses of pH and pigment absorbance in microvolumes of blood. The challenges successfully met by our technique comprise: (1) the parallel measurement of oxygenation, paired with the simultaneous monitoring of pH depending on oxygenation level; (2) the use of minimal sample volumes of 15 μ l; and (3) high-resolution recordings, facilitated by continuous recordings of broad-range spectra and pH.

We upgraded a gas diffusion chamber (Niesel and Thews, 1961; Sick and Gersonde, 1969; Sick and Gersonde, 1972; Bridges et al., 1984; Morris and Oliver, 1999; Weber et al., 2010) with an integrated fibre-optic micro-pH optode and a miniature broad-range fibre-optic spectrophotometer. The experimental setup offers high flexibility to produce accurate OECs and pH recordings from only minute volumes of sample.

RESULTS AND DISCUSSION**Spectrophotometric measurements**

Using the modified diffusion chamber, we successfully performed measurements on haemolymph from *Octopus vulgaris* and

List of symbols and abbreviations	
n_{50}	Hill coefficient
OEC	oxygen equilibrium curve
P_{50}	oxygen affinity
P_{CO_2}	carbon dioxide partial pressure
P_{O_2}	oxygen partial pressure

Eulimnogammarus verrucosus and whole blood of *Pachycara brachycephalum* at various oxygen and carbon dioxide partial pressures (P_{O_2} and P_{CO_2} , respectively) and temperatures. The integrated broad-range spectrophotometer resolved 2048 data points per spectrum from 200 to 1100 nm and yielded characteristic absorbance spectra for haemolymph containing haemocyanin with an oxygenation-dependent peak at 347 nm (*O. vulgaris*; Fig. 1A), and multiple responsive peaks at 540, 575, 412 and 335 nm for oxygenated haemoglobin-bearing blood and at 553, 427 and 366 nm for deoxygenated haemoglobin-bearing blood (*P. brachycephalum*; Fig. 1B). In addition, to the haemocyanin peak at 336 nm, haemolymph from *E. verrucosus* showed absorbance features above 400 nm that explain its green coloration (Fig. 1C). The detailed broad-range spectra strongly facilitate and enhance the analysis of solutions with complex absorbance spectra. Studies that gather only snapshots of the spectrum by means of single wavelength filters (e.g. Morris et al., 1985; Rasmussen et al., 2009) limit their experimental setup to a particular pigment type and may miss further relevant features.

The modified diffusion chamber yielded reproducible and accurate results employing both conventional stepwise measurements along an oxygen partial pressure (P_{O_2}) gradient (Fig. 2) as well as measurements along a pH gradient (Fig. 3), designed for pH-sensitive pigments such as cephalopod haemocyanins (Pörtner, 1990). OECs of *O. vulgaris* haemolymph constructed from five replicated experiments with discrete oxygenation steps at constant P_{CO_2} (1 kPa) showed low variability among OECs and the derived parameters (Fig. 2, Table 1; supplementary material Fig. S1), with a relative error of 0.93% for P_{50} and 2.74% for the Hill coefficient, n_{50} . This low instrumental error and the good agreement of P_{50} and n_{50} with published data on *O. vulgaris* haemolymph recorded at the same temperature and pH (Table 1, Fig. 4) underline the accuracy of the setup. The Bohr coefficient recorded at 15°C was higher than that reported in Brix et al. (Brix et al., 1989), but closely matched values reported for *O. vulgaris* by Houlihan et al. (Houlihan et al., 1982) and Bridges (Bridges, 1995) *Octopus dofleini* [-1.7; pH 7.0–8.3 (Miller, 1985)] or *Octopus*

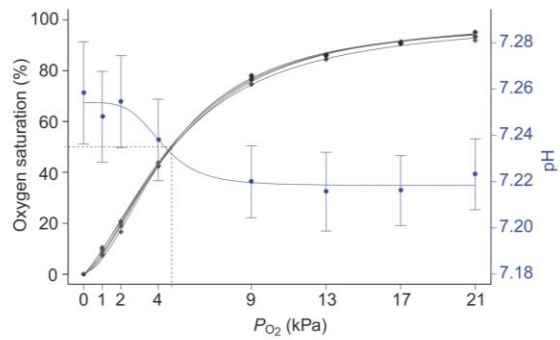


Fig. 2. Replicated ($n=5$) oxygen equilibrium curves of haemolymph from one *Octopus vulgaris* specimen obtained by stepwise changes to discrete P_{O_2} at constant P_{CO_2} (1 kPa). Five parameter logistic curves were fitted and individually plotted for each measurement to illustrate instrumental variability. Haemolymph pH (means \pm s.e.m., blue), recorded by an optical pH microsensor immersed in the same sample droplet, changed sigmoidal and reverse directional to pigment saturation (black). The pH at half saturation (mean \pm s.e.m. = 7.23 ± 0.018) can be derived from the intersection between P_{50} (dashed line) and the fitted pH line.

macropus [-1.99; pH 7.3–7.5 (Lykkeboe and Johansen, 1982)] (Fig. 4, Table 1). The difference in Bohr coefficients with those in the study by Brix et al. (Brix et al., 1989) relates to the pH ranges used to determine the Bohr coefficient. In octopods, P_{50} increases linearly with pH and levels off at lower pH (~7.0; Fig. 4) (Miller, 1985) as oxygen binding becomes pH insensitive (see 13 kPa OEC, Fig. 3). Brix et al. (Brix et al., 1989) included pH values below 7.0 (6.85–7.40), which consequently led to reduced regression slopes and underestimated Bohr coefficients. Thus, agreement with studies using pH ranges above 7.0 confirms the accuracy of Bohr coefficients determined with the modified diffusion chamber.

Both pigment absorbance and haemolymph pH responded to changes in gas composition within 30 s (Fig. 5). The recording of one OEC, including calibration at 100% and 0% oxygen saturation, lasted on average 3.5 ± 0.23 h for measurements ($n=5$) with eight discrete oxygenation steps and 5.2 ± 0.21 h for measurements ($n=4$) with eight discrete pH steps. While the maximum absorbance signal at 347 nm (haemocyanin oxygenation peak) drifted by $-3.5 \pm 0.6\%$ per hour ($n=5$), minimal absorbance remained nearly constant ($0.27 \pm 0.21\%$, $n=5$). The protein peak drifted less and varied more

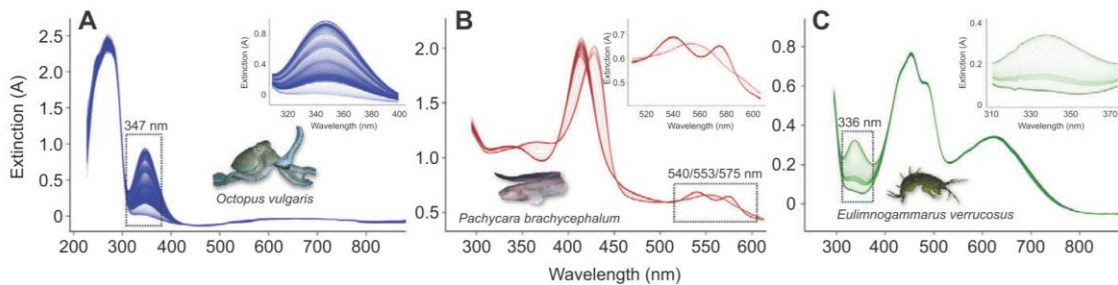


Fig. 1. Highly resolved spectral changes of several non-model organisms. (A) Broad-range spectra of haemolymph from *Octopus vulgaris* (15°C), measured at 4 kPa P_{O_2} from high to low pH (ca. 8.2–6.8). Exemplary, broad-range spectral recordings of whole blood from (B) the Antarctic eelpout *Pachycara brachycephalum* (0°C) and (C) of haemolymph from the Lake Baikal amphipod *Eulimnogammarus verrucosus* (6°C) reveal complex absorbance features. Spectral zones responding to oxygenation are marked by boxes and magnifications are shown in the insets. Spectra were coloured according to the visual appearance of the respective haemolymph/blood type. (Animal photos reprinted with permission by: Vladimír Motyčka, Christoph Held and Lena Jakob.)

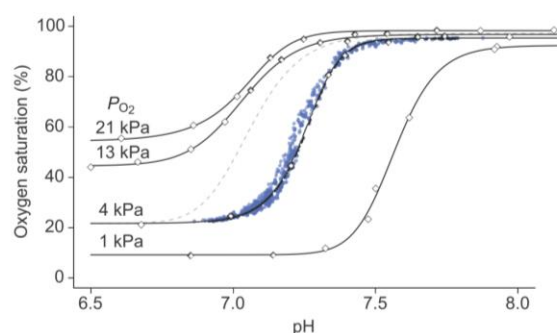


Fig. 3. Stepwise oxygen equilibrium curves (OECs) along a pH gradient (Pörtner, 1990), each derived from 15 μ l *Octopus vulgaris* haemolymph and measured by means of the modified diffusion chamber at 15°C and decreasing pH and various constant P_{O_2} (1, 4, 13 and 21 kPa). The continuous OEC recorded at slow rates of P_{CO_2} changes (0.015 kPa min⁻¹, blue points) was highly resolved and closely matched the stepwise curves, while at faster rates the OEC shifted left (dashed grey curve).

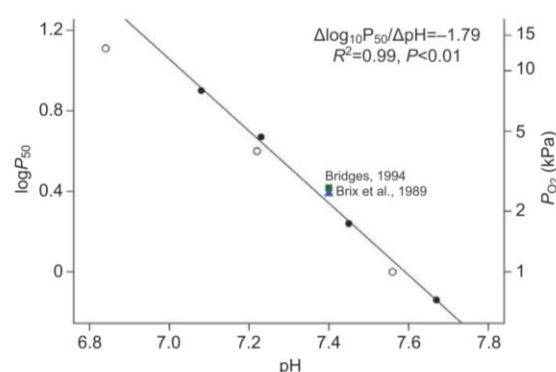


Fig. 4. Bohr plot illustrating the pH dependence of oxygen affinity (P_{50}) of *Octopus vulgaris* haemolymph measured at 15°C. P_{50} from experiments with stepwise changes of P_{O_2} (filled circles) and pH (open circles) agreed with literature data [blue triangle (Brix et al., 1989); green square (Bridges, 1995)]. The data point at 13 kPa was excluded from the linear regression fit as P_{50} leveled off at low pH (~7.0).

among experiments ($2.3 \pm 2.7\%$, $n=5$; Fig. 5B). Negative drift observed for the maximum oxygenation signal was reported previously and explained by autoxidation of the blood pigment (Wells and Weber, 1989). Consequently, each measurement needs to comprise calibration steps with pure oxygen at the beginning and end to determine and include the apparent and constant drift in the calculation of pigment oxygenation by readjusting maximum absorbance at each consecutive oxygenation step (Wells and Weber, 1989). The less pronounced positive drift of the protein peak (Fig. 5B) indicates a low degree of sample drying and no apparent dilution by condensation or denaturation of the haemolymph sample.

Interestingly, the height of the protein peak did not remain stable, but increased/decreased upon oxygenation/deoxygenation (Fig. 5; supplementary material Fig. S2). This unexpected response of the protein peak to oxygenation/deoxygenation of the pigment (Fig. 5; supplementary material Fig. S2) cannot be ascribed to irreversible protein denaturation as the protein absorbance increased again upon re-oxygenation. Consequently, oxygenation status may affect protein absorbance spectra and thus measurements of protein concentration

in haemolymph or blood. Conformational changes depending on the degree of oxygenation may affect the absorbance features of the aromatic tryptophan, tyrosine and phenylalanine residues that account for the absorbance at 270–295 nm (Alexander and Ingram, 1980). Although the protein peak may not always vary with oxygen content (Bolton et al., 2009), it would be advisable to test a given blood type for such oxygenation dependency.

pH recordings in blood microvolumes

Simultaneous monitoring of pH, using a pH micro-optode in the same 15 μ l sample, yielded stable recordings within the calibrated range between pH 6.5 and 8.2. In response to changing P_{O_2} (0–21 kPa), these recordings were sufficiently precise to resolve a sigmoidal shift by 0.03 pH units, running in reverse to the OEC (Fig. 2). This shift denotes the oxygenation-dependent, lowered affinity of the pigment for protons (Haldane effect) and agrees well with other studies [e.g. *Carcinus maenas* Δ pH=0.02 (Truchot, 1976)]. A sigmoidal rather than linear change of pH (Lapennas et al., 1981) may correspond to the linked sigmoidal trajectory of

Table 1. Comparison of blood physiological parameters of *Octopus vulgaris* haemolymph with literature data

Source	P_{50} (kPa)	n_{50}	Bohr coefficient	pH	Temperature (°C)
Present study	0.72	1.56	-1.79 (pH 7.1–7.7)	7.68	15
	1.72	1.59		7.45	
	4.72 (0.07)	1.75 (0.07)		7.23 (0.046)	
	7.94	1.61		7.08	
	2.20^a	–		7.4	
Brix et al., 1989	2.45	1.5	-1.34 (pH 6.85–7.4)	7.4	15
	4.41	1.6		-1.10 (pH 6.85–7.4)	7.4
Houlihan et al., 1982	3.20	2.6 ^b	-1.58/-1.73 (pH 7.2–7.6/7.3–7.7)	7.588	22
	4.09	2.9 ^b		7.520	
	4.80	3.5 ^b		7.415	
	6.76	2.9 ^b		7.327	
Bridges, 1995	1.91	–	-1.86	7.4	10
	2.61	–		-1.83	7.4

P_{50} , oxygen affinity; n_{50} Hill coefficient. Bold values denote parameters recorded under the same conditions. Values in parentheses for P_{50} , n_{50} and pH represent $\pm 95\%$ confidence intervals.

^a P_{50} extrapolated from linear regression line of Bohr plot at pH 7.4 (Fig. 4).

^bHill coefficients were recalculated from Houlihan et al. (Houlihan et al., 1982).

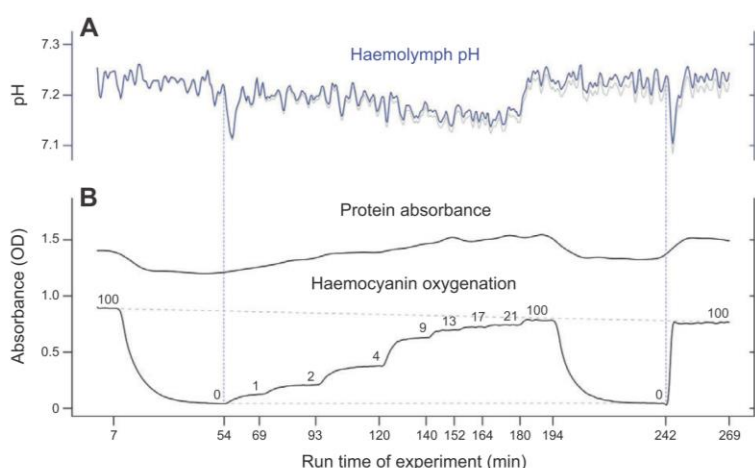


Fig. 5. Change of haemolymph pH and wavelength-specific absorbance during an oxygen equilibrium measurement. Response of (A) pH (uncorrected, grey trace; corrected by instrumental pH drift, blue trace) and (B) absorbance of the oxygenation-dependent peak (347 nm) and the protein peak of *Octopus vulgaris* haemolymph to stepwise changes of P_{O_2} recorded at 15°C. Numbers above the absorbance trace indicate P_{O_2} (kPa) of each oxygenation step. Horizontal dashed lines indicate the change of maximal and minimum absorbance (at 347 nm) over time, and vertical dashed lines the sudden but reversible pH changes upon initial oxygenation.

oxygen binding. The continuous recording of pH further revealed pronounced but reversible decreases of ~0.1 pH units upon initial oxygenation, which indicates a high affinity state for protons in fully deoxygenated haemocyanins (Fig. 5).

P_{50} derived from OECs recorded along pH gradients matched those recorded along P_{O_2} gradients and together showed a linear interdependence of pH and P_{50} in the pH range between 7.1 and 7.7 (Fig. 4). The OEC recorded by a continuous decrease of pH was highly resolved (~500 data points; Fig. 6) and fully equilibrated at slow P_{CO_2} changes of $0.015 \text{ kPa min}^{-1}$, as confirmed by the close match with the stepwise OEC (Fig. 3). This further underlines the validity of this alternative methodology, designed for pH-sensitive pigments. Simultaneous pH recordings, as in the present study, allow construction of highly resolved, continuous OECs from which blood parameters may be directly derived without curve modelling (Fig. 3). At faster rates ($0.045 \text{ kPa min}^{-1}$), the OEC shifted left as saturation required longer to stabilize than pH (Fig. 3). A shift of continuous OEC at higher rates of change of P_{CO_2} or P_{O_2} has been explained by dislike equilibration rates with the surrounding gas between the sensor and the sample, due to differences in their physical properties or their relative position [‘dynamic error’ (Lapennas et al., 1981)]. However, as the pH optode was immersed in the sample, gas diffusion rates between the sample and the sensor

were likely similar, suggesting some delay in oxygenation of octopus haemocyanin in response to pH changes.

The signal of the pH optode drifted by $-0.016 \text{ pH units per } 100 \text{ recordings}$ (± 0.004) and was corrected accordingly (Fig. 5A). This drift was higher than stated by the manufacturer ($-0.0035 \text{ pH units per } 100 \text{ recordings}$) (PreSens, 2004; PreSens, 2012), probably because of incomplete protection from the light beam of the UV-VIS light source and resulting photobleaching of the optode’s fluorescent dyes. Thus, pH optodes may be re-calibrated prior to each measurement and the pH signal corrected for instrumental signal drift. Light exposure and therefore pH signal drift can be reduced by a software-controlled shutter in the light path that opens only during measurements or by using optically isolated sensor tips. The pH signal was also corrected for autofluorescence emitted by the sample, which decreased the pH signal in haemolymph by 0.06 units. Optical isolation but also calibration in the analysed medium can reduce or prevent the effects by intrinsic fluorescence between 530 and 660 nm, caused by, for example, porphyrine structures, which affect phase and amplitude of the pH raw signal (PreSens, C. Krause, personal communication).

Advantages and disadvantages

The modified diffusion chamber benefits the analysis of oxygen binding in several ways. Simultaneous recording of pigment oxygenation and pH allows characterization of oxygen binding and intrinsic pH responses under conditions mimicking *in vivo* conditions. Minute sample volumes facilitate the analysis of blood from small organisms or less invasive and repeated sampling from the same individual. Small sample volumes reduce the need to pool blood, facilitate replicate measurements and shorten measurement time because of accelerated gas equilibration. Highly resolved broad-range spectra capture detailed spectral properties of the pigment and promote the analysis of diverse blood types. Thin optical microsensors (for pH or P_{O_2}) deliver stable and rapid recordings down to 0°C (M.O., unpublished observation) and allow recording of continuous and highly resolved OECs (Fig. 3). The gain of detail improves the accuracy of biophysical oxygen binding models, particularly if OECs do not follow a simple sigmoidal shape (Wells and Weber, 1989). The additional flexibility to operate at a large range of experimental temperatures and gas compositions makes this device not only highly suitable for standard applications

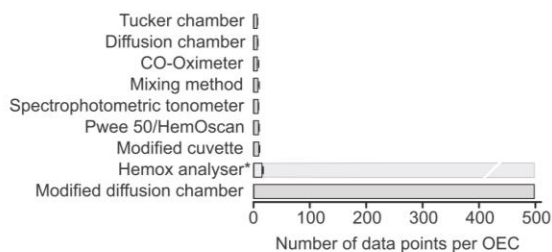


Fig. 6. Number of data points (means $\pm 95\% \text{ CI}$) for single oxygen equilibrium curves (OECs) compared between different methods (for references, see supplementary material Table S2). The modified diffusion chamber method refers to continuous OEC measurements along a pH gradient. *While some studies record fewer data points, recording intervals may be maximized to 1 s^{-1} .

but particularly for the functional analysis of blood from non-model organisms.

The use of optical microsensors and thin layers of blood also require specific care. The fluorescent dyes of the pH optodes are prone to photobleaching, which can be overcome by optical isolation or determination and correction for signal drift. Effects of intrinsic fluorescence of the sample are resolved by optical isolation, calibration in the same type of sample or by an initial cross-validation of pH with a pH electrode. The non-linear dynamic range of pH optodes restricts accurate recordings to pH values between 5.5 and 8.5, which, however, suffices in most of the blood-physiological experiments. Optical pH sensors that cover the extreme and even the full pH range may soon remove this limitation (Safavi and Bagheri, 2003). Further, the 150 μm sensor tip breaks easily and requires careful handling. Like pH electrodes, pH optodes require calibration with buffers of similar ionic strength as the sample analysed and at the same experimental temperature (PreSens, 2004). Some blood types may clog on the sensor tip, which can be avoided by bathing the pH optode in a heparin solution (1000 units ml^{-1}). Lastly, thin layers of blood are at higher risk of desiccation (Reeves, 1980), particularly at higher temperatures. Measures to avoid desiccation include decreased gas flow or covering of the blood sample with a gas permeable Teflon membrane (Reeves, 1980; Lapennas and Lutz, 1982; Clark et al., 2008).

Conclusions

In this study we showed that a diffusion chamber upgraded with a broad-range spectrophotometer and a fibre-optical pH sensor allows for parallel measurement of pH and pigment saturation in microvolumes of blood samples. The setup yields reproducible and accurate results and offers high flexibility regarding the type of samples and experimental setting. The availability of optical P_{O_2} or P_{CO_2} probes and the rapid development of other optical sensor types (e.g. nitrogen oxide) suggest a broad array of future implementations that will help to address novel biological questions.

MATERIALS AND METHODS

Experimental setup and modifications

A gas diffusion chamber (Eschweiler Co., Kiel, Germany) designed and described in detail previously (Niesel and Thews, 1961; Sick and Gersonde, 1969; Sick and Gersonde, 1972) has been used to determine OECs by recording absorbance of a thin layer of a haemoglobin- or haemocyanin-bearing solution during continuous or stepwise changes of P_{O_2} (Wells and Weber, 1989). The original principle, characterized by full pigment deoxygenation with nitrogen gas followed by the time-dependent diffusion of oxygenated gas into the chamber (Niesel and Thews, 1961; Sick and Gersonde, 1969), was essentially abolished in subsequent studies that continuously perfused the chamber with defined gas mixtures (e.g. Bridges et al., 1984; Morris and Oliver, 1999; Weber et al., 2010). We adopted this amendment and further modified the diffusion chamber as follows. (1) A broad-range (200 to 1100 nm) fibre-optic spectrophotometer (USB2000+, Ocean Optics, USA) was connected via two fibre-optic cables fitted to the central cylinder of the diffusion chamber to direct the light beam via collimating lenses from the deuterium halogen light source (DT-Mini-2-GS, Ocean Optics) through the sample glass plate back to the 2048-element CCD-array detector of the spectrophotometer (Fig. 7; supplementary material Table S3). (2) The plastic slide that holds the sample glass plate in the light tunnel was modified to fit a fibre-optic micro-pH optode (NTH-HP5-L5-NS*25/0.8-OIW, PreSens, Germany), housed in a syringe and connected to a phase detection device (μPDD 3470, PreSens; Figs 7, 8). The needle of the syringe was then inserted through a silicone ring to prevent the leakage of gas (Fig. 8). In contrast to pH electrodes, pH optodes exhibit very small sensor tips ($<150 \mu\text{m}$) and determine pH from the intensity ratio between two pH-sensitive fluorescent dyes (PreSens, 2004). The modified diffusion chamber has been registered under patent number 10 2013 011 343 at the Deutsches Patent- und Markenamt, Germany.

The water reservoir of the diffusion chamber was filled with a 20% ethylene glycol solution (anti-freeze agent, AppliChem, Germany) and the temperature was monitored and controlled by means of a supplied temperature sensor (PreSens, Germany) and a connected circulating thermostatted water bath (LAUDA Ecoline Staredition RE 104, Germany). A gas mixing pump (Wösthoff, Germany) supplied an adjustable mixture of nitrogen, oxygen and carbon dioxide gas, humidified by an integrated scrubber to prevent desiccation of the sample (Fig. 8).

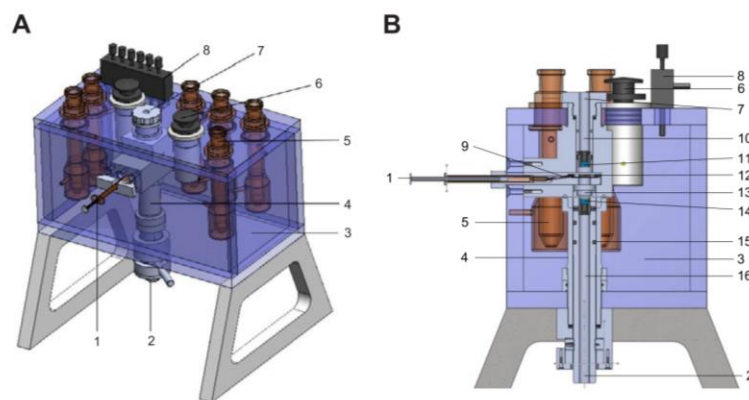


Fig. 7. Illustration of the modified diffusion chamber. (A) 3D model of the modified diffusion chamber and (B) a detailed cross-section through the central cylinder of the gas diffusion chamber illustrating the embedded fibre-optic micro-pH optode and an upper and lower custom-made tube containing collimating lenses and fittings for incoming and outgoing fibre-optic cables of the light source and the broad-range spectrophotometer. 1, Syringe housing for the pH micro optode; 2, fibre-optic cable exit to the spectrophotometer; 3, temperature-controlled water reservoir; 4, central cylinder containing optical devices; 5, gas-washing flask; 6, control wheel for gas distribution; 7, fibre-optic cable inlet from the light source; 8, control panel for gas inflow; 9, needle housing for the fibre-optic sensor tip; 10, upper custom-made tube, housing a collimating lens and the fibre-optic cable from the light source; 11, upper collimating lens; 12, blood sample spread on a glass plate; 13, spacer to keep 10 mm minimal distance between collimating lens and sample; 14, lower collimating lens; 15, rubber stop lower tubing; 16, lower custom-made tube, housing a collimating lens and the fibre-optic cable leading to the spectrophotometer. Illustrations were drawn with 3D CAD software (SolidWorks, version 12.0; files available at <http://doi.pangaea.de/10.1594/PANGAEA.831205>).

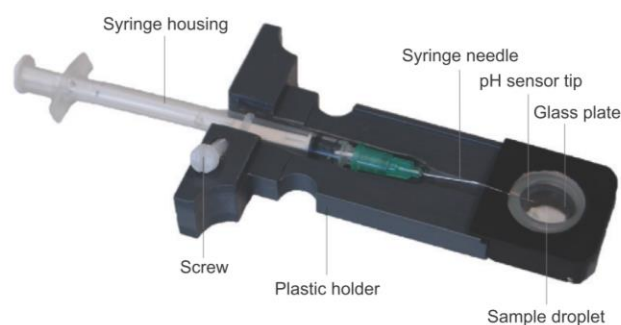


Fig. 8. Detailed illustration of the pH optode housed in a syringe, mounted with a screw and fitted to a plastic holder, which is moved into the gas-tight compartment centered in the diffusion chamber. The bended syringe needle is inserted through a silicon ring, which prevents gas leakage, and the sensor tip moved into the edge of the sample droplet located on a silica glass plate.

Prior to each experiment, we performed a six-point calibration (pH 6.7, 7.0, 7.2, 7.4, 7.7 and 8.1) of the pH optode, in MOPS-buffered [40 mmol l⁻¹, 3-(*N*-morpholino)-propanesulfonic acid], filtered artificial seawater (35 PSU) at the corresponding experimental temperature. pH of buffers was checked with a pH glass electrode (InLab Routine Pt1100, Mettler Toledo, Germany) and a pH meter (pH 330i, WTW, Germany), calibrated with low ionic strength pH standards (AppliChem, Germany, DIN19266) and corrected to the free scale pH with Tris-buffered seawater standard (CO₂ QCLab, batch 4 2010, Dickson, USA) (Dickson, 2010) equilibrated at the same temperature. Aliquots of 18 µl of haemolymph (octopus or amphipod) were thawed on ice, shortly spun down to collect content (5 s at 1000 g), and 0.35 µl of 0.2 mmol l⁻¹ NaOH (4.6 µmol l⁻¹ final concentration) was added to raise haemolymph pH above 8.0 to ensure full pigment oxygenation. To avoid haemolysis and the formation of methaemoglobin by freezing, we used freshly sampled whole blood from *P. brachycephalum* and diluted the sample with one volume of blood plasma to improve light transmission during the measurement. The pH of haemolymph or whole blood was not stabilized with extrinsic buffers such as Tris or HEPES as they disturb the effects by ligands and temperature on pigment oxygenation (Brix et al., 1995). We then spread out 15 µl of haemolymph or whole blood on the glass plate without contacting the sealing ring. The pH optode needle was inserted through the sealing ring and the sensor tip moved into the edge of the droplet to reduce bleaching of the dye by the light beam passing through the centre of the glass plate (Fig. 8). Both the glass plate holder and the fitted pH optode were then inserted and fixed in the diffusion chamber (Fig. 7). The spectrophotometer required the recording of light and dark spectra without blood sample before each measurement and was set to 15 ms integration time, averaging 100 scans per recording and 30 s measurement intervals. pH drift of the pH optode was evaluated by measuring the pH difference of a MOPS-buffered seawater pH standard (pH 7.2) at 15°C before and after each experiment. Effects of intrinsic fluorescence were assessed by comparing pH recordings of the pH optode and the pH electrode in octopus haemolymph at 15°C.

Using *O. vulgaris* haemolymph, we tested the setup via two previously employed methodologies. OECs were obtained (1) by stepwise changes of discrete P_{O_2} (1, 2, 4, 9, 13, 17 and 21 kPa) at constant P_{CO_2} (e.g. Wells and Weber, 1989) or (2) by stepwise as well as continuous decreases of pH by means of increasing CO₂ concentrations (0–20 kPa) and constant P_{O_2} (e.g. Pörtner, 1990). While stepwise measurements allow the sample to fully equilibrate at several successive but discrete P_{O_2} or pH steps (Lapennas et al., 1981; Pörtner, 1990), continuous measurements characterize a constant change and monitoring of P_{O_2} or pH (Wells and Weber, 1989). Each experiment involved calibration with pure nitrogen as well as pure oxygen at the beginning and at the end to determine the drift of the maximum absorbance signal. The exemplary analysis of whole blood of *P. brachycephalum* was performed from 21 to 0 kPa P_{O_2} and pH 8.2–7.1 at 0°C and of thawed haemolymph of *E. verrucosus* at a constant P_{O_2} of 21 kPa and pH 7.7–6.9 at 6°C.

Animals

One major incentive to advance this method was to enhance the investigation of non-model organisms, which often suffer from instrumental restrictions (e.g. sample volume, wavelength filters, temperature setting) by devices optimised for human or rodent blood. We thus chose three non-model organisms with diverse experimental demands to test the flexibility and

accuracy of the modified diffusion chamber. The cephalopod *Octopus vulgaris* Cuvier 1797 lives between 11 and 18°C and has evolved a closed circulatory system containing blue haemolymph with high concentrations [54.3±6.9 g l⁻¹ (Wells and Smith, 1987; Brix et al., 1989)] of the extracellular, pH-sensitive respiratory pigment haemocyanin, which evolved independently from arthropod haemocyanin (van Holde et al., 2001). Published data on *O. vulgaris* blood physiology allowed us to test the accuracy of the modified diffusion chamber. The Antarctic eelpout *Pachycara brachycephalum* (Pappenheim 1912) lives at freezing temperatures, yields only little blood and circulates intracellular haemoglobin at – for teleosts – low concentrations (37.4 g l⁻¹) in a closed system. The Baikal amphipod *Eulimnogammarus verrucosus* (Gerstfeldt 1858) lives at 5–6°C and yields small amounts of green haemolymph that transports oxygen via extracellular haemocyanin (45.3±7.9 g l⁻¹) in an open vascular system (Wirkner and Richter, 2013).

Octopus vulgaris specimens were hand-caught by snorkelling at Banuyls sur Mer, France, at 16°C. Animals were anaesthetized in 3% EtOH (Ikeda et al., 2009), and after withdrawing haemolymph from the cephalic vein, were finally killed by a cut through the brain following sampling. *Pachycara brachycephalum* was caught on the Polarstern cruise ANTXXXV/4 near Maxwell Bay at King George Island, Antarctica, in May 2009 using fish traps, transported to the Alfred Wegener Institute, Bremerhaven, Germany, and kept in aerated tanks connected to a re-circulating aquaculture system at 0°C. The animal was anaesthetised with 0.3 g l⁻¹ tricaine methanesulphonate, blood was withdrawn using a heparinized syringe and the animal was finally killed by a spinal cut [animal research permit no. 522-27-11/02-00(93), Freie Hansestadt Bremen, Germany]. *Eulimnogammarus verrucosus* was collected in Bolshie Koty, Lake Baikal, Russia, during summer 2012, transported to Irkutsk, Russia, and kept in aerated 2.5 l tanks at 6°C. Haemolymph was withdrawn using a dorsally inserted capillary. All haemolymph samples were centrifuged at 15,000 g for 15 min at 0°C to remove cell debris and stored at –20°C.

Data analysis

The processing, time-matching and analysis of data from both the spectrophotometer and the pH meter were performed using the R statistical language (R Development Core Team, 2013) (for R scripts, see <http://doi.pangaea.de/10.1594/PANGAEA.831205>).

An integrated five-parameter logistic model [Eqn 1; R ‘drc’ add-on package (Ritz and Streibig, 2005)] was applied to fit sigmoidal curves to stepwise OECs:

$$f[x, (b, c, d, e, f)] = c + \frac{(d - c)}{\left(1 + \exp\left\{b \left[\log\left(\frac{x}{e}\right)\right]\right\}\right)} \quad (1)$$

The parameters c and d denote the upper and lower asymptotes, respectively, and f the asymmetry of the curve. The parameters b and e correspond to the slope and inflection point, respectively, of a four-parameter logistic model if the parameter f equals 1. Note that this equation represents an empirical curve fit that does not describe the functional properties of the haemocyanin sub-units according to mechanistic insight.

Oxygen affinity (P_{50}) was interpolated from fitted OECs at half saturation and cooperativity (Hill's coefficient, n_{50}) was determined via Hill plots by regressing $\log_{10}[Y/(1-Y)]$ versus $\log_{10}P_{O_2}$ in the linear mid-range (–20–80%

saturation), with Y denoting the fractional saturation. The Bohr coefficient was calculated from the regression slope ($\Delta \log_{10} P_{50}$ versus ΔpH) between pH 7.1 and 7.7. In pH/saturation diagrams, P_{50} denotes the \log_{10} of the oxygen isobar and the pH of the isobar at half saturation [pH₅₀ (Pörtner, 1990)]. Data were expressed as means \pm 95% confidence intervals if not stated otherwise.

Acknowledgements

We thank Dr Jan Strügnell (La Trobe University, Bundoora) for providing lab space and her extensive support; Michael Imsic and all other staff and technicians of the La Trobe University for their kind support during the initial tests of the modified diffusion chamber; Erich Dunker, Matthias Littmann and Dirk Wethje (scientific workshop, Alfred Wegener Institute, Bremerhaven) for the technical modifications and drawings of the diffusion chamber; Lena Jakob for providing haemolymph samples from *Eulimnogammarus verrucosus*; Marian Y Hu for his help catching *Octopus vulgaris*; the logistics department of the Alfred Wegener Institute; and last of all Saumya Pant and little Yuva Lalit Pant for their enriching company. We further thank Roy Weber for his kind advice and the two anonymous reviewers for their many helpful remarks and suggestions on an earlier version of this manuscript. We dedicate this article to the memory of Steve Morris and express our special thanks to Maria Morris and Elizabeth Morgan (University of Bristol), who saved and donated the diffusion chamber to our department.

Competing interests

The authors declare no competing financial interests.

Author contributions

M.O. and F.C.M. conceived and developed the technical modifications, compiled the manuscript and interpreted results. M.O. performed the experiments and analysis. H.-O.P. initiated the discussion and contributed to data interpretation and manuscript editing.

Funding

This study was supported by a *Journal of Experimental Biology* travelling fellowship, a PhD scholarship by the German Academic Exchange Service (DAAD, D/11/43882) to M.O., the Deutsche Forschungsgemeinschaft (MA4271/1-2 to F.C.M.) and the Alfred Wegener Institute for Polar and Marine Research.

Supplementary material

Supplementary material available online at <http://jeb.biologists.org/lookup/suppl/doi:10.1242/jeb.092726/-/DC1>

References

- Alexander, J. B. and Ingram, G. A. (1980). A comparison of five of the methods commonly used to measure protein concentrations in fish sera. *J. Fish Biol.* **16**, 115-122.
- Bert, P. (1878). *La Pression Barométrique: Recherches de Physiologie Expérimentale*. Paris: G. Masson.
- Bohr, C., Hasselbalch, K. and Krogh, A. (1904). Über einen in biologischer Beziehung wichtigen Einfluss, den die Kohlensäurespannung des Blutes auf dessen Sauerstoffbindung übt. *Skand. Arch. Physiol.* **16**, 402-412.
- Bolton, J. C., Collins, S., Smith, R., Perkins, B., Bushway, R., Bayer, R. and Vetelino, J. (2009). Spectroscopic analysis of hemolymph from the American lobster (*Homarus americanus*). *J. Shellfish Res.* **28**, 905-912.
- Bridges, C. R. (1995). Bohr and root effects in cephalopod haemocyanins – paradox or pressure in *Sepia officinalis*? *Mar. Freshw. Behav. Physiol.* **25**, 121-130.
- Bridges, C. R., Morris, S. and Grieshaber, M. K. (1984). Modulation of haemocyanin oxygen affinity in the intertidal prawn *Palaemon elegans* (Rathke). *Respir. Physiol.* **57**, 189-200.
- Brix, O. (1983). Giant squids may die when exposed to warm water currents. *Nature* **303**, 422-423.
- Brix, O., Bårdgard, A., Cau, A., Colosimo, A., Condo, S. and Giardina, B. (1989). Oxygen-binding properties of cephalopod blood with special reference to environmental temperatures and ecological distribution. *J. Exp. Zool.* **252**, 34-42.
- Brix, O., Colosimo, A. and Giardina, B. (1995). Temperature dependence of oxygen binding to cephalopod haemocyanins: ecological implications. *Mar. Freshw. Behav. Physiol.* **25**, 149-162.
- Chanutin, A. and Curnish, R. R. (1967). Effect of organic and inorganic phosphates on the oxygen equilibrium of human erythrocytes. *Arch. Biochem. Biophys.* **121**, 96-102.
- Clark, T. D., Seymour, R. S., Wells, R. M. G. and Frappell, P. B. (2008). Thermal effects on the blood respiratory properties of southern bluefin tuna, *Thunnus maccoyii*. *Comp. Biochem. Physiol.* **150A**, 239-246.
- Dickson, A. (2010). The carbon dioxide system in seawater: equilibrium chemistry and measurements. In *Guide to Best Practices for Ocean Acidification Research and Data Reporting* (ed. U. Riebesell, V. J. Fabry, L. Hansson and J.-P. Gattuso). Luxembourg: Publications Office of the European Union.
- Festa, R. S. and Asakura, T. (1979). Oxygen dissociation curves in children with anemia and malignant disease. *Am. J. Hematol.* **7**, 233-244.
- Herbert, N. A., Skov, P. V., Wells, R. M. G. and Steffensen, J. F. (2006). Whole blood-oxygen binding properties of four cold-temperate marine fishes: blood affinity

is independent of pH-dependent binding, routine swimming performance, and environmental hypoxia. *Physiol. Biochem. Zool.* **79**, 909-918.

- Houlihan, D., Innes, A., Wells, M. and Wells, J. (1982). Oxygen consumption and blood gases of *Octopus vulgaris* in hypoxic conditions. *J. Comp. Physiol. B* **148**, 35-40.
- Hüfner, G. (1890). Über das gesetz der dissociation des oxyhaemoglobins und über einige daran sich knüpfende wichtige fragen aus der biologie. *Arch. Anat. Physiol.* **1**, 1-27.
- Ikeda, Y., Sugimoto, C., Yonamine, H. and Oshima, Y. (2009). Method of ethanol anaesthesia and individual marking for oval squid (*Sepioteuthis lessoniana* Ferrussac, 1831 in Lesson 1830-1831). *Aquac. Res.* **41**, 157-160.
- Lapennas, G. N. and Lutz, P. L. (1982). Oxygen affinity of sea turtle blood. *Respir. Physiol.* **48**, 59-74.
- Lapennas, G. N., Colacino, J. M. and Bonaventura, J. (1981). Thin-layer methods for determination of oxygen binding curves of hemoglobin solutions and blood. In *Methods in Enzymology*, Vol. 76 (ed. E. Chianconi, L. Rossi-Bernardi and E. Antonini), pp. 449-470. London: Academic Press.
- Lykkeboe, G. and Johansen, K. (1982). A cephalopod approach to rethinking about the importance of the bohr and haldane effects. *Pac. Sci.* **36**, 305-313.
- Mangum, C. P. and Lykkeboe, G. (1979). The influence of inorganic ions and pH on oxygenation properties of the blood in the gastropod mollusc *Lyscaea canalicularum*. *J. Exp. Zool.* **207**, 417-430.
- Meir, J. U., Champagne, C. D., Costa, D. P., Williams, C. L. and Ponganis, P. J. (2009). Extreme hypoxic tolerance and blood oxygen depletion in diving elephant seals. *Am. J. Physiol.* **297**, R927-R939.
- Miller, K. I. (1985). Oxygen equilibria of *Octopus doffeini* hemocyanin. *Biochemistry* **24**, 4582-4586.
- Morris, S. and Oliver, S. (1999). Respiratory gas transport, haemocyanin function and acid-base balance in *Janus edwardsii* during emersion and chilling: simulation studies of commercial shipping methods. *Comp. Biochem. Physiol.* **122A**, 309-321.
- Morris, S., Taylor, A. C., Bridges, C. R. and Grieshaber, M. K. (1985). Respiratory properties of the haemolymph of the intertidal prawn *Palaemon elegans* (Rathke). *J. Exp. Zool.* **233**, 175-186.
- Niesel, W. and Thews, G. (1961). Ein neues verfahren zur schnellen und genauen aufnahme der sauerstoffbindungskurve des blutes und konzentrierter hämoproteidlösungen. *Pflügers Arch.* **273**, 380-395.
- Olson, K. N., Hillyer, M. A., Kloss, J. S., Geiselhart, R. J. and Apple, F. S. (2010). Accident or arson: is CO-oximetry reliable for carboxyhemoglobin measurement postmortem? *Clin. Chem.* **56**, 515-519.
- Pörtner, H. O. (1990). An analysis of the effects of pH on oxygen binding by squid (*Illex illecebrosus*, *Loligo pealeii*) haemocyanin. *J. Exp. Biol.* **150**, 407-424.
- PreSens (2004). *Instruction Manual pH-4 mini*. Regensburg, Germany: Precision Sensing GmbH.
- PreSens (2012). *Product Sheet for pH Microsensors*. Regensburg, Germany: Precision Sensing GmbH.
- R Development Core Team (2013). *R: A Language and Environment for Statistical Computing*. Vienna, Austria: R Foundation for Statistical Computing.
- Rasmussen, J. R., Wells, R. M. G., Henty, K., Clark, T. D. and Brittain, T. (2009). Characterization of the hemoglobins of the Australian lungfish *Neoceratodus forsteri* (Kreffl). *Comp. Biochem. Physiol.* **152A**, 162-167.
- Reeves, R. B. (1980). A rapid micro method for obtaining oxygen equilibrium curves on whole blood. *Respir. Physiol.* **42**, 299-315.
- Ritz, C. and Streibig, J. C. (2005). Bioassay analysis using R. *J. Stat. Softw.* **12**, 1-22.
- Safavi, A. and Bagheri, M. (2003). Novel optical pH sensor for high and low pH values. *Sens. Actuators B Chem.* **90**, 143-150.
- Scott, G. R. (2011). Elevated performance: the unique physiology of birds that fly at high altitudes. *J. Exp. Biol.* **214**, 2455-2462.
- Seibel, B., Chausson, F., Lallier, F., Zal, F. and Childress, J. (1999). Vampire blood: respiratory physiology of the vampire squid (Cephalopoda: Vampyromorpha) in relation to the oxygen minimum layer. *Exp. Biol. Online* **4**, 1-10.
- Sick, H. and Gersonde, K. (1969). Method for continuous registration of O₂-binding curves of hemoproteins by means of a diffusion chamber. *Anal. Biochem.* **32**, 362-376.
- Sick, H. and Gersonde, K. (1972). Theory and application of the diffusion technique for measurement and analysis of O₂-binding properties of very autoxidizable hemoproteins. *Anal. Biochem.* **47**, 46-56.
- Truchot, J. P. (1976). Carbon dioxide combining properties of the blood of the shore crab, *Carcinus maenas* (L.): CO₂-dissociation curves and Haldane effect. *J. Comp. Physiol.* **112**, 283-293.
- van Holde, K. E., Miller, K. I. and Decker, H. (2001). Hemocyanins and invertebrate evolution. *J. Biol. Chem.* **276**, 15563-15566.
- Weber, R. E., Behrens, J. W., Malte, H. and Fago, A. (2008). Thermodynamics of oxygenation-linked proton and lactate binding govern the temperature sensitivity of O₂ binding in crustacean (*Carcinus maenas*) hemocyanin. *J. Exp. Biol.* **211**, 1057-1062.
- Weber, R. E., Campbell, K. L., Fago, A., Malte, H. and Jensen, F. B. (2010). ATP-induced temperature independence of hemoglobin-O₂ affinity in heterothermic billfish. *J. Exp. Biol.* **213**, 1579-1585.
- Wells, M. and Smith, P. (1987). The performance of the octopus circulatory system: a triumph of engineering over design. *Experientia* **43**, 487-499.
- Wells, R. M. G. and Weber, R. E. (1989). The measurement of oxygen affinity in blood and haemoglobin solutions. In *Techniques in Comparative Respiratory Physiology: An Experimental Approach* (ed. C. R. Bridges and P. J. Butler), pp. 279-303. Cambridge: Cambridge University Press.
- Wirkner, C. S. and Richter, S. (2013). Circulatory system and respiration. *The Natural History of the Crustacea* **1**, 376-412.
- Zielinski, S., Sartoris, F. J. and Pörtner, H. O. (2001). Temperature effects on hemocyanin oxygen binding in an antarctic cephalopod. *Biol. Bull.* **200**, 67-76.

Supplementary material of publication I

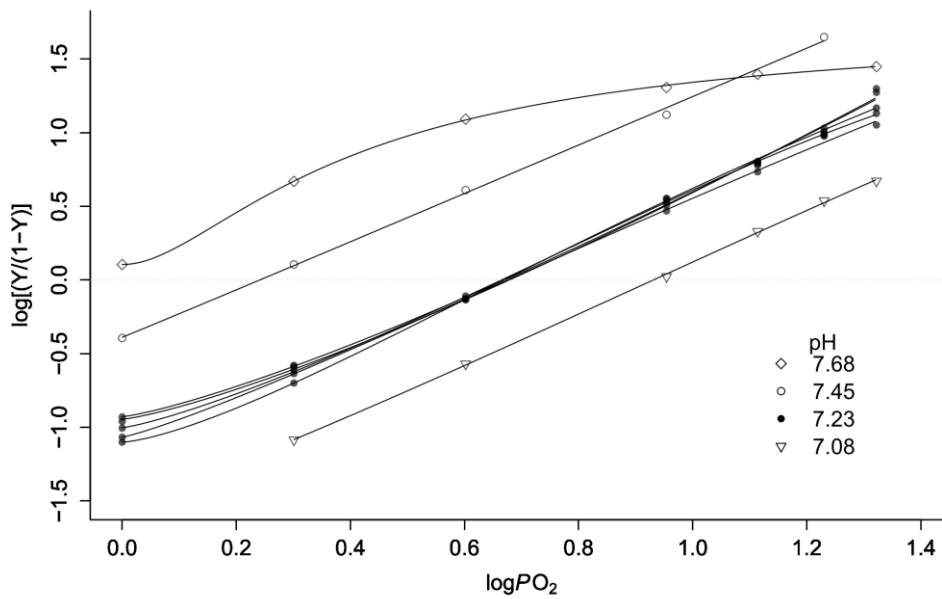


Fig. S1: Hill plot of *Octopus vulgaris* haemolymph measured at 15°C and four different pH. The five replicated measurements at pH 7.23 illustrate low instrumental variability. Lines were fitted using a five parameter logistic model.

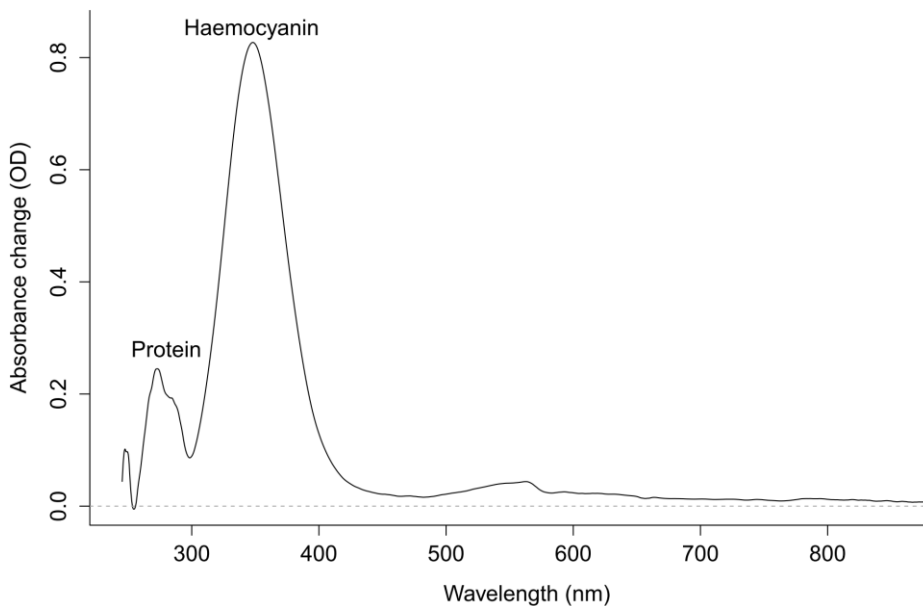


Fig. S2: Subtractive spectrum (absorbance change) of *Octopus vulgaris* haemolymph between the fully deoxygenated (pure nitrogen) and the fully oxygenated state (pure oxygen) determined with 15 μ l sample volume at 15°C. Note that pronounced spectral changes not only occur at the haemocyanin peak at 347 nm but also at the protein peak at 280 nm.

Publications

Table S1. Currently employed methods to construct oxygen equilibrium curves (OEC).

Method	Characteristics of method	Means to record saturation	Type of temperature control	Range of sample volume	pH determination	PO ₂ determination	Blood treatment	Time per ODC	Pros	Cons	Example applications
Diffusion chamber	Photospectrometric measurement in chamber equilibrated with gas via diffusion capillaries	Monochromatic / continuous spectrum photospectrometry	Thermostated water bath	3 – 15µl	Measurement with pH capillary electrode (BMS radiometer) in separate sub-sample	Injection of known gas mixture via gas mixing pumps	buffered	10-30 min	Small sample volumes	pH measurements in separate blood sample Low data density	(Weber et al., 1976; Morris et al., 1985; Menze et al., 2005; Harnois et al., 2009; Storz et al., 2009; Campbell et al., 2010)
HEMOX-Analyser	Photospectrometric measurement combined with oxygen sensor	Dual wavelength photospectrometry	Cooling loop connect to thermostated water bath	2 – 50µl	none	Clarke electrode	buffered	30 min	Small samples volumes Very accurate High data density	No pH measurement Recording of only few wavelengths	(Guarnone et al., 1995; Stawski et al., 2006; Biolo et al., 2009; Rasmussen et al., 2009; Cook et al., 2012)
Tonometer	Gas equilibration in glass chamber and external measurement of oxygen tension	Measurement of total O ₂ content	Submersion in thermostated water bath	~3ml	Measurement of subsample with pH capillary electrode (Radiometer)	Measurement with Clark type electrode	Unbuffered	> 2 hours	Use of native/unbuffered blood	pH measurements in separate blood sample Large sample volumes Low data density	(Pörtner, 1990; Brill et al., 2008)
Thunberg tube / Photometric tonometer	Photospectrometric measurement in cuvette fused with gas equilibrated glass chamber	Monochromatic / continuous spectrum photospectrometry	Immersed into thermostated water bath	~3ml	None or in separate blood samples via pH electrodes	Injection of known gas mixture via e.g. gas flow controllers	buffered	> 2 hours	-	No pH measurement or measurement in separate blood sample Large sample volumes Low data density Long equilibration times	(Hill and Wolvenkamp, 1936; Olanas et al., 2009; Bonaventura et al., 2010; Seibel, 2012)
Modified cuvette	Photospectrometric measurement in modified cuvette	Continuous spectrum photospectrometry	Temperature controlled cuvette holder	~400 µl	Simultaneously in same blood sample via immersed micro pH electrode	Injection of known gas mixture via gas mixing pumps	Un-buffered blood	> 4 hours	Direct measurement of pH in same sample Use of native/unbuffered blood	Large sample volume Long lasting measurements	(Zelinski et al., 2001)
Pwee 50 / HemOscan	Photospectrometric measurement of thin blood films enclosed by Teflon-membranes	Dual wavelength photospectrometry	Temperature controlled chamber (Peltier controller)	1-2µl	Estimated via defined PCO ₂ and literature or measurement of subsamples with pH capillary electrode (Radiometer)	Injection of known gas mixture via gas mixing pumps or gas flow controller	unbuffered	30-40 min	Small sample volumes	Indirect pH measurement or measurement in separate blood sample Low data density Recording of only few wavelengths	(Clark et al., 2008; Henriksson et al., 2008; Verhille and Farrell, 2012)
CO-Oximeter	Photospectrometric measurement with modified cuvette	3-6 wavelength photospectrometry	none	35-50µl	None or measurement of subsamples with pH capillary electrode (Radiometer)	None / tonometric equilibration with known gas mixtures	unbuffered	20-60 sec per data point	Measures multiple haemoglobin forms	No pH measurement or measurement in separate blood sample Restricted to haemoglobin Low data density Recording of only few wavelengths	(Jahr et al., 2001)
Mixing method	Volumetric mixing of known amounts of fully oxygenated and de-oxygenated blood followed by PO ₂ measurement	Setting of O ₂ saturation by mixing of defined proportions of oxygenated and de-oxygenated blood samples	Immersed into thermostated water bath	Max. 0.8 ml per data point	Measurement with pH capillary electrode (BMS radiometer) or blood gas analyser	Polarographic oxygen electrode via Radiometer (E5046) or Tucker chamber	unbuffered	>50 min per data point	Setting of a desired mixtures allows targeted measurement of e.g. P50 with only a single measurement	Low data density Laborious procedure Time consuming measurement	(Scheid and Meyer, 1978; Meir and Pongonis, 2009; Soegaard et al., 2012)
Tucker chamber	Deoxygenation of blood sample with ferricyanide to release and measure total bound oxygen	Measurement of total bound oxygen	Thermostatically controlled chamber	15-300µl	Measurement with capillary electrode (BMS 2 or PHM 71/73 radiometer)	Polarographic oxygen electrode (Radiometer)	Diluted with saline or unbuffered	>60min	Measurement of total bound oxygen	pH measurements in separate blood sample Low data density	(Tucker, 1967; Herbert et al., 2006; Brill et al., 2008; Petersen and Gamperl, 2011; Leon et al., 2012)

References

- Biolo, A., Greferath, R., Siwik, D. A., Qin, F., Valsky, E., Fylaktakidou, K. C., Pothukanuri, S., Duarte, C. D., Schwarz, R. P., Lehn, J.-M. et al.** (2009). Enhanced exercise capacity in mice with severe heart failure treated with an allosteric effector of hemoglobin, myo-inositol trispyrophosphate. *Proc. Natl. Acad. Sci. USA* **106**, 1926-1929.
- Bonaventura, C., Henkens, R., De Jesus-Bonilla, W., Lopez-Garriga, J., Jia, Y., Alayash, A. I., Siburt, C. J. P. and Crumbliss, A. L.** (2010). Extreme differences between hemoglobins I and II of the clam *Lucina pectinalis* in their reactions with nitrite. *BBA-Proteins Proteom.* **1804**, 1988-1995.
- Brill, R., Bushnell, P., Schroff, S., Seifert, R. and Galvin, M.** (2008). Effects of anaerobic exercise accompanying catch-and-release fishing on blood-oxygen affinity of the sandbar shark (*Carcharhinus plumbeus*, Nardo). *J. Exp. Mar. Biol. Ecol.* **354**, 132-143.
- Campbell, K. L., Roberts, J. E., Watson, L. N., Stetefeld, J., Sloan, A. M., Signore, A. V., Howatt, J. W., Tame, J. R., Rohland, N., Shen, T. J. et al.** (2010). Substitutions in woolly mammoth hemoglobin confer biochemical properties adaptive for cold tolerance. *Nat. Genet.* **42**, 536-540.
- Clark, T. D., Seymour, R. S., Wells, R. M. G. and Frappell, P. B.** (2008). Thermal effects on the blood respiratory properties of southern bluefin tuna, *Thunnus maccoyii*. *Comp. Biochem. Physiol. Part A Mol. Integr. Physiol.* **150**, 239-246.
- Cook, D. G., Iftikar, F. I., Baker, D. W., Hickey, A. J. R. and Herbert, N. A.** (2012). Low O₂ acclimation shifts the hypoxia avoidance behaviour of snapper (*Pagrus auratus*) with only subtle changes in aerobic and anaerobic function. *J. Exp. Biol.*
- Guarnone, R., Centenara, E. and Barosi, G.** (1995). Performance characteristics of HemoX-Analyzer for assessment of the hemoglobin dissociation curve. *Haematologica* **80**, 426-430.
- Harnois, T., Rouselot, M., Rogniaux, H. and Zal, F.** (2009). High-level production of recombinant *Arenicola marina* globin chains in *Escherichia coli*: A new generation of blood substitute. *Artif. Cells Blood Substit. Biotechnol.* **37**, 106-116.

- Henriksson, P., Mandic, M. and Richards, J. G.** (2008). The osmorepiratory compromise in sculpins: impaired gas exchange is associated with freshwater tolerance. *Physiol. Biochem. Zool.* **81**, 310-319.
- Herbert, Neill A., Skov, Peter V., Wells, Rufus M. G. and Steffensen, John F.** (2006). Whole blood-oxygen binding properties of four cold-temperate marine fishes: Blood affinity is independent of pH-dependent binding, routine swimming performance, and environmental hypoxia. *Physiol. Biochem. Zool.* **79**, 909-918.
- Hill, R. and Wolvekamp, H. P.** (1936). The oxygen dissociation curve of haemoglobin in dilute solution. *Proc. R. Soc. Lond. B Biol. Sci.* **120**, 484-495.
- Jahr, J. S., Driessen, B., Lurie, F., Tang, Z., Louie, R. F. and Kost, G.** (2001). Oxygen saturation measurements in canine blood containing hemoglobin glutamer-200 (bovine): In vitro validation of the NOVA CO-Oximeter. *Vet. Clin. Pathol.* **30**, 39-45.
- Leon, K., Pichavant-Rafini, K., Quemener, E., Sebert, P., Egreteau, P. Y., Ollivier, H., Carre, J. L. and L'Her, E.** (2012). Oxygen blood transport during experimental sepsis: effect of hypothermia*. *Crit Care Med* **40**, 912-918.
- Meir, J. U. and Ponganis, P. J.** (2009). High-affinity hemoglobin and blood oxygen saturation in diving emperor penguins. *J. Exp. Biol.* **212**, 3330-3338.
- Menze, M. A., Hellmann, N., Decker, H. and Grieshaber, M. K.** (2005). Allosteric models for multimeric proteins: Oxygen-linked effector binding in hemocyanin†. *Biochemistry* **44**, 10328-10338.
- Morris, S., Taylor, A. C., Bridges, C. R. and Grieshaber, M. K.** (1985). Respiratory properties of the haemolymph of the intertidal prawn *Palaemon elegans* (Rathke). *J. Exp. Zool.* **233**, 175-186.
- Olianas, A., Manconi, B., Masia, D., Sanna, M. T., Castagnola, M., Salvadori, S., Messina, I., Giardina, B. and Pellegrini, M.** (2009). The oxygen-binding modulation of hemocyanin from the Southern spiny lobster *Palinurus gilchristi*. *J. Comp. Physiol. B* **179**, 193-203.
- Petersen, L. H. and Gamperl, A. K.** (2011). Cod (*Gadus morhua*) cardiorespiratory physiology and hypoxia tolerance following acclimation to low-oxygen conditions. *Physiol. Biochem. Zool.* **84**, 18-31.
- Pörtner, H. O.** (1990). An analysis of the effects of pH on oxygen binding by squid (*Illex illecebrosus*, *Loligo pealei*) haemocyanin. *J. Exp. Biol.* **150**, 407.
- Rasmussen, J. R., Wells, R. M. G., Henty, K., Clark, T. D. and Brittain, T.** (2009). Characterization of the hemoglobins of the Australian lungfish *Neoceratodus forsteri* (Kreffl). *Comp. Biochem. Physiol., A: Comp. Physiol.* **152**, 162-167.
- Scheid, P. and Meyer, M.** (1978). Mixing technique for study of oxygen-hemoglobin equilibrium: a critical evaluation. *J. Appl. Physiol.* **45**, 818-822.
- Seibel, B. A.** (2012). The jumbo squid, *Dosidicus gigas* (Ommastrephidae), living in oxygen minimum zones II: Blood-oxygen binding. *Deep-Sea Res. Pt. II*.
- Soegaard, L. B., Hansen, M. N., van Elk, C., Brahm, J. and Jensen, F. B.** (2012). Respiratory properties of blood in the harbor porpoise, *Phocoena phocoena*. *J. Exp. Biol.* **215**, 1938-1943.
- Stawski, C. Y., Grigg, G. C., Booth, D. T. and Beard, L. A.** (2006). Temperature and the respiratory properties of whole blood in two reptiles, *Pogona barbata* and *Emydura signata*. *Comp. Biochem. Physiol. Part A Mol. Integr. Physiol.* **143**, 173-183.
- Storz, J. F., Runck, A. M., Sabatino, S. J., Kelly, J. K., Ferrand, N., Moriyama, H., Weber, R. E. and Fago, A.** (2009). Evolutionary and functional insights into the mechanism underlying high-altitude adaptation of deer mouse hemoglobin. *Proc. Natl. Acad. Sci. USA* **106**, 14450-14455.
- Tucker, V. A.** (1967). Method for oxygen content and dissociation curves on microliter blood samples. *J. Appl. Physiol.* **23**, 410-414.
- Verhille, C. and Farrell, A. P.** (2012). The in vitro blood-O₂ affinity of triploid rainbow trout *Oncorhynchus mykiss* at different temperatures and CO₂ tensions. *J. Fish Biol.* **81**, 1124-1132.
- Weber, R. E., Lykkeboe, G. and Johansen, K.** (1976). Physiological properties of eel haemoglobin: hypoxic acclimation, phosphate effects and multiplicity. *J. Exp. Biol.* **64**, 75-88.
- Zielinski, S., Sartoris, F. J. and Pörtner, H. O.** (2001). Temperature effects on hemocyanin oxygen binding in an Antarctic cephalopod. *Biol. Bull. (Woods Hole)* **200**, 67-76.

Table S2: Detailed description of diffusion chamber components

#	Component	Description
1	Collimating lenses	The collimating lenses form a straight light beam penetrating the sample droplet.
2	Control panel for gas inflow	The control panel contains multiple gas inlets to connect up to six types of gases (e.g. N ₂ , O ₂ , CO ₂). In this study only one inlet was used and connected to a Wösthoff gas mixing pump, which supplied the desired gas mixture. Each inlet has one adjustable valve to regulate the incoming gas pressure.
3	Control wheel for gas distribution	Control wheel that directs the gas flow via a copper tube from a particular gas washing flask/gas (19) inlet to the sample chamber
4	Upper lens holder	The custom made upper plastic lens holder positions a collimating lens (1) connected to a fiber optic cable on top of the sample droplet.
5	Central metal block	The metal block contains the sample chamber and holds the sample holder (16) with the sample droplet and the pH optode (9). The metal block is ventrally penetrated by the central cylinder (14) to allow the passage of light through the sample. The metal itself allows fast temperature equilibration between the samples chamber and the surrounding medium.
6	Pressure balance tube	Tube that releases excess gas supplied by gas mixing pumps to avoid overpressure in the sample chamber.
7	Water disperser	The water disperser is connected to an external thermostatted water bath and assures rigorous mixing of water.
8	Gas dispersing membrane	Sponge-type membrane that disperses inflowing dry gas into temperature equilibrated water on top of the membrane.
9	pH optode	Micro pH optode that fitted onto the sample holder (16) to measure pH of the sample droplet
10	Lens spacer	The lens spacer is screwed on top of the lower lens holder (11) to assure a minimum distance of 10mm to the sample glass plate. The spacer also presses against the sample slide if the lower lens holder (11) is moved upwards, which seals the sample chamber from the surrounding gas atmosphere.
11	Lower lens holder	The custom made lower plastic lens holder positions a collimating lens (1) connected to a fiber optic cable below the sample droplet.
12	Locking bushing	Ring that moves the lower lens holder (11) upwards upon turning to fix the sample holder (16).
13	Sealing rings	The rubber sealing rings prevent gas leakage from the surrounding atmosphere into the sample chamber.
14	Central cylinder	The central hollow metal cylinder forms the light channel for the absorbance measurement and houses the upper (4) and lower (11) lens holders.
15	Water reservoir	Can be connected to a thermostatted water bath via insulated hoses, which circulates water or water mixed

Publications

		with anti-freeze agent to equilibrate all diffusion chamber components to the experimental temperature.
16	Sample holder	Plastic samples holder that carries the sample glass plate with the sample droplet at its end as well as the pH optode (9). The sample holder is moved into the central metal block (5) to position the sample droplet into the light beam in the center of the diffusion chamber.
17	Tygon® tubings	Gas tight tubings (CM Scientific Ltd., Silsden, U.K.) that connect the gas inlets with the gas-washing flasks (19) and the gas distributor (3).
18	Diffusion chamber housing	The housing of the diffusion chamber is made of acrylic glass and fixed with regular spaced metal screws. The inner sides are sealed with aquarium sealing.
19	Gas-washing flask	The gas-washing flasks are composed of glass humidify the incoming gas to prevent drying and temperature changes of the sample droplet.
20	Thermostat connectors	To connect the water bath to an external circulating thermostated water bath.
21	Temperature sensor	External temperature sensor connected to the pH recorder to monitor the temperature of the diffusion chamber during measurements.
22	Fiber optic cable	Fiber optic cable from the UV-VIS light source fixed to the collimating lens (1) and housed in the upper lens holder (4).

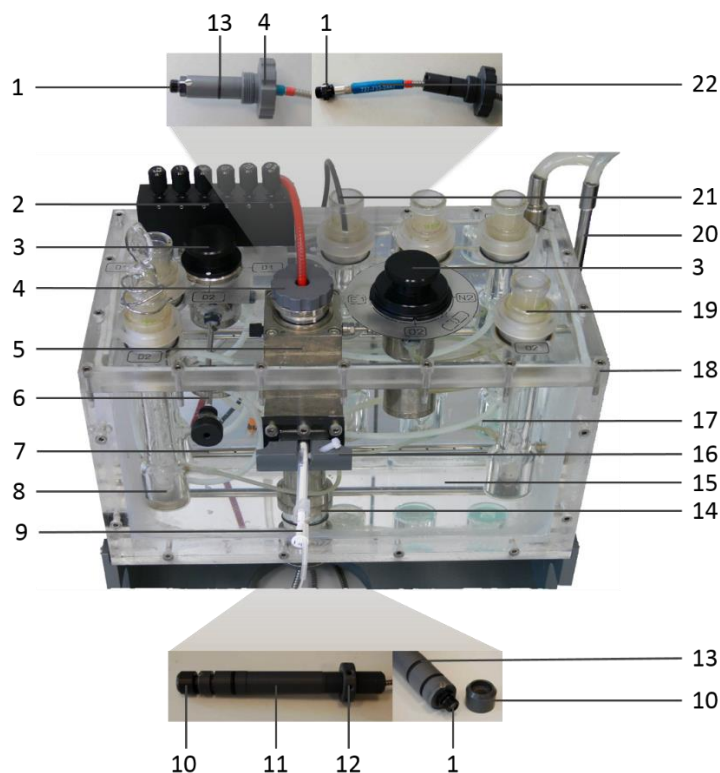


Table S2: References used to analyse data density of oxygen dissociation curves from various methods

Method	References
Modified diffusion chamber	This study
HEMOX-analyser	(Stawski et al., 2006; Cabrales et al., 2008; Biolo et al., 2009; Liu et al., 2009; Liu et al., 2010)
Modified cuvette	(Zielinski et al., 2001)
Pwee 50 / HemOscan	(Clark et al., 2008; Bianchini, 2012; Verhille and Farrell, 2012)
Thunberg tube / Spectrophotometric tonometer	(Hill and Wolvekamp, 1936; Nakagawa et al., 2005; Olianias et al., 2009; Bonaventura et al., 2010; Seibel, 2012)
Mixing method	(Scheid and Meyer, 1978; Boutilier et al., 2000; Soncini and Glass, 2000; de Salvo Souza et al., 2001; Meir and Ponganis, 2009)
CO-Oximeter	(Bunn et al., 1972; Lokich et al., 1973; Elbaum et al., 1974; Harms et al., 1998; Jahr et al., 2001)
Diffusion chamber	(Morris et al., 1985; Menze et al., 2005; Broekman et al., 2006; Rutjes et al., 2007; Sugumar and Munuswamy, 2007; Storz et al., 2009)
Tucker chamber	(Bridges et al., 1979; Airaksinen and Nikinmaa, 1995; Gollock et al., 2006; Brill et al., 2008; Petersen and Gamperl, 2011; Leon et al., 2012)

References

- Airaksinen, S. and Nikinmaa, M.** (1995). Effect of haemoglobin concentration on the oxygen affinity of intact lamprey erythrocytes. *J. Exp. Biol.* **198**, 2393-2396.
- Bianchini, K.** (2012). The ontogeny of blood oxygen transport and the hypoxia response in early life stages of the rainbow trout, *Oncorhynchus mykiss*. In *Department of Integrative Biology*, vol. Master of Science, pp. 103. Guelph, Ontario, Canada: University of Guelph.
- Biolo, A., Greferath, R., Siwik, D. A., Qin, F., Valsky, E., Fylaktakidou, K. C., Pothukanuri, S., Duarte, C. D., Schwarz, R. P., Lehn, J.-M. et al.** (2009). Enhanced exercise capacity in mice with severe heart failure treated with an allosteric effector of hemoglobin, myo-inositol trispyrophosphate. *Proc. Natl. Acad. Sci. USA* **106**, 1926-1929.
- Bonaventura, C., Henkens, R., De Jesus-Bonilla, W., Lopez-Garriga, J., Jia, Y., Alayash, A. I., Siburt, C. J. P. and Crumbliss, A. L.** (2010). Extreme differences between hemoglobins I and II of the clam *Lucina pectinalis* in their reactions with nitrite. *BBA-Proteins Proteom.* **1804**, 1988-1995.
- Boutilier, R. G., West, T. G., Webber, D. M., Pogson, G. H., Mesa, K. A., Wells, J. and Wells, M. J.** (2000). The protective effects of hypoxia-induced hypometabolism in the *Nautilus*. *J. Comp. Physiol. B* **170**, 261-268.
- Bridges, C., Bicudo, J. and Lykkeboe, G.** (1979). Oxygen content measurement in blood containing haemocyanin. *Comp. Biochem. Physiol. A Physiol.* **62**, 457-461.
- Brill, R., Bushnell, P., Schroff, S., Seifert, R. and Galvin, M.** (2008). Effects of anaerobic exercise accompanying catch-and-release fishing on blood-oxygen affinity of the sandbar shark (*Carcharhinus plumbeus*, Nardo). *J. Exp. Mar. Biol. Ecol.* **354**, 132-143.
- Broekman, M. S., Bennett, N. C., Jackson, C. R. and Weber, R. E.** (2006). Does altitudinal difference modulate the respiratory properties in subterranean rodents' (*Cryptomys hottentotus mahali*) blood? *Physiol. Behav.* **88**, 77-81.
- Bunn, H. F., Meriwether, W. D., Balcerzak, S. P. and Rucknagel, D. L.** (1972). Oxygen equilibrium of hemoglobin E. *J. Clin. Investig.* **51**, 2984.
- Cabrales, P., Tsai, A. G. and Intaglietta, M.** (2008). Modulation of perfusion and oxygenation by red blood cell oxygen affinity during acute anemia. *Am. J. Respir. Cell Mol. Biol.* **38**, 354.
- Clark, T. D., Seymour, R. S., Wells, R. M. G. and Frappell, P. B.** (2008). Thermal effects on the blood respiratory properties of southern bluefin tuna, *Thunnus maccoyii*. *Comp. Biochem. Physiol. Part A Mol. Integr. Physiol.* **150**, 239-246.
- de Salvo Souza, R., Soncini, R., Glass, M., Sanches, J. and Rantin, F.** (2001). Ventilation, gill perfusion and blood gases in dourado, *Salminus maxillosus* Valenciennes (Teleostei, Characidae), exposed to graded hypoxia. *J. Comp. Physiol. B* **171**, 483-489.

- Elbaum, D., Nagel, R. L., Bookchin, R. M. and Herskovits, T. T. (1974). Effect of alkylureas on the polymerization of hemoglobins. *Proc. Natl. Acad. Sci. USA* **71**, 4718-4722.
- Gollock, M. J., Currie, S., Petersen, L. H. and Gamperl, A. K. (2006). Cardiovascular and haematological responses of Atlantic cod (*Gadus morhua*) to acute temperature increase. *J. Exp. Biol.* **209**, 2961-2970.
- Harms, C. A., McClaran, S. R., Nickele, G. A., Pegelow, D. F., Nelson, W. B. and Dempsey, J. A. (1998). Exercise-induced arterial hypoxaemia in healthy young women. *J. Physiol.* **507**, 619-628.
- Hill, R. and Wolvekamp, H. P. (1936). The oxygen dissociation curve of haemoglobin in dilute solution. *Proc. R. Soc. Lond. B Biol. Sci.* **120**, 484-495.
- Jahr, J. S., Driessen, B., Lurie, F., Tang, Z., Louie, R. F. and Kost, G. (2001). Oxygen saturation measurements in canine blood containing hemoglobin glutamer-200 (bovine): In vitro validation of the NOVA CO-Oximeter. *Vet. Clin. Pathol.* **30**, 39-45.
- Leon, K., Pichavant-Rafini, K., Quemener, E., Sebert, P., Egreteau, P. Y., Ollivier, H., Carre, J. L. and L'Her, E. (2012). Oxygen blood transport during experimental sepsis: effect of hypothermia*. *Crit Care Med* **40**, 912-918.
- Liu, C., Zhang, L. F., Song, M. L., Bao, H. G., Zhao, C. J. and Li, N. (2009). Highly efficient dissociation of oxygen from hemoglobin in Tibetan chicken embryos compared with lowland chicken embryos incubated in hypoxia. *Poult. Sci.* **88**, 2689-2694.
- Liu, Y.-x., Yue, W., Ji, L., Nan, X. and Pei, X.-t. (2010). Production of erythroid cells from human embryonic stem cells by fetal liver cell extract treatment. *BMC Dev. Biol.* **10**, 85.
- Lokich, J. J., Moloney, W. C., Bunn, H. F., Bruckheimer, S. M. and Ranney, H. M. (1973). Hemoglobin brigham (alpha2Abeta2100 Pro-->Leu). Hemoglobin variant associated with familial erythrocytosis. *J. Clin. Invest.* **52**, 2060-2067.
- Meir, J. U. and Ponganis, P. J. (2009). High-affinity hemoglobin and blood oxygen saturation in diving emperor penguins. *J. Exp. Biol.* **212**, 3330-3338.
- Menze, M. A., Hellmann, N., Decker, H. and Grieshaber, M. K. (2005). Allosteric models for multimeric proteins: Oxygen-linked effector binding in hemocyanin†. *Biochemistry* **44**, 10328-10338.
- Morris, S., Taylor, A. C., Bridges, C. R. and Grieshaber, M. K. (1985). Respiratory properties of the haemolymph of the intertidal prawn *Palaemon elegans* (Rathke). *J. Exp. Zool.* **233**, 175-186.
- Nakagawa, T., Onoda, S., Kanemori, M., Sasayama, Y. and Fukumori, Y. (2005). Purification, characterization and sequence analyses of the extracellular giant hemoglobin from *Oligobranchia mashikoi*. *Zool Sci* **22**, 283-291.
- Olianas, A., Manconi, B., Masia, D., Sanna, M. T., Castagnola, M., Salvadori, S., Messina, I., Giardina, B. and Pellegrini, M. (2009). The oxygen-binding modulation of hemocyanin from the Southern spiny lobster *Palinurus gilchristi*. *J. Comp. Physiol. B* **179**, 193-203.
- Petersen, L. H. and Gamperl, A. K. (2011). Cod (*Gadus morhua*) cardiorespiratory physiology and hypoxia tolerance following acclimation to low-oxygen conditions. *Physiol. Biochem. Zool.* **84**, 18-31.
- Rutjes, H. A., Nieveen, M. C., Weber, R. E., Witte, F. and Van den Thillart, G. E. E. J. M. (2007). Multiple strategies of Lake Victoria cichlids to cope with lifelong hypoxia include hemoglobin switching. *Am. J. Physiol. Regul. Integr. Comp. Physiol.* **293**, R1376-R1383.
- Scheid, P. and Meyer, M. (1978). Mixing technique for study of oxygen-hemoglobin equilibrium: a critical evaluation. *J. Appl. Physiol.* **45**, 818-822.
- Seibel, B. A. (2012). The jumbo squid, *Dosidicus gigas* (Ommastrephidae), living in oxygen minimum zones II: Blood-oxygen binding. *Deep-Sea Res. Pt. II*.
- Soncini, R. and Glass, M. L. (2000). Oxygen and acid-base status related drives to gill ventilation in carp. *J. Fish Biol.* **56**, 528-541.
- Stawski, C. Y., Grigg, G. C., Booth, D. T. and Beard, L. A. (2006). Temperature and the respiratory properties of whole blood in two reptiles, *Pogona barbata* and *Emydura signata*. *Comp. Biochem. Physiol. Part A Mol. Integr. Physiol.* **143**, 173-183.
- Storz, J. F., Runck, A. M., Sabatino, S. J., Kelly, J. K., Ferrand, N., Moriyama, H., Weber, R. E. and Fago, A. (2009). Evolutionary and functional insights into the mechanism underlying high-altitude adaptation of deer mouse hemoglobin. *Proc. Natl. Acad. Sci. USA* **106**, 14450-14455.
- Sugumar, V. and Munuswamy, N. (2007). Physical, biochemical and functional characterization of haemoglobin from three strains of *Artemia*. *Comp. Biochem. Physiol. Part A Mol. Integr. Physiol.* **146**, 291-298.
- Verhille, C. and Farrell, A. P. (2012). The in vitro blood-O₂ affinity of triploid rainbow trout *Oncorhynchus mykiss* at different temperatures and CO₂ tensions. *J. Fish Biol.* **81**, 1124-1132.
- Zielinski, S., Sartoris, F. J. and Pörtner, H. O. (2001). Temperature effects on hemocyanin oxygen binding in an Antarctic cephalopod. *Biol. Bull. (Woods Hole)* **200**, 67-76.

3.2. Publication II

Blue blood on ice: Modulated blood oxygen transport facilitates cold compensation and eurythermy in an Antarctic octopod.

M Oellermann, B Lieb, HO Pörtner, JM Semmens, FC Mark

2015

Frontiers in Zoology

12, 6.

(doi:10.1186/s12983-015-0097-x)

Blue blood on ice: Modulated blood oxygen transport facilitates cold compensation and eurythermy in an Antarctic octopod.

Michael Oellermann^{1, §}, Bernhard Lieb², Hans-O. Pörtner¹, Jayson M. Semmens³, Felix C. Mark¹

¹Alfred-Wegener-Institute Helmholtz Centre for Polar and Marine Research, Am Handelshafen 12, 27570 Bremerhaven, Germany

²Institute of Zoology, Johannes Gutenberg-Universität, Müllerweg 6, 55099 Mainz, Germany

³Fisheries, Aquaculture and Coasts Centre, Institute for Marine and Antarctic Studies (IMAS), University of Tasmania, Hobart, Tasmania 7001, Australia

§Corresponding author

Email addresses:

MO: oellermann.m@gmail.com

BL: lieb@uni-mainz.de

HOP: Hans.Poertner@awi.de

JMS: Jayson.Semmens@utas.edu.au

FCM: Felix.Christopher.Mark@awi.de

Keywords: Oxygen equilibrium curve, haemocyanin, hemocyanin, cephalopod, oxygen affinity, oxygen carrying capacity, diffusion chamber, *Pareledone charcoti*, *Octopus pallidus*, *Eledone moschata*

Abstract

Introduction

The Antarctic Ocean hosts a rich and diverse fauna despite inhospitable temperatures close to freezing, which require specialist adaptations to sustain animal activity and various underlying body functions. While oxygen transport plays a key role in setting thermal tolerance in warmer climates, this constraint is relaxed in Antarctic fishes and crustaceans, due to high levels of dissolved oxygen. Less is known about how other Antarctic ectotherms cope with temperatures near zero, particularly the more active invertebrates like the abundant octopods. A continued reliance on the highly specialised blood oxygen transport system of cephalopods may concur with functional constraints at cold temperatures. We therefore analysed the octopod's central oxygen transport component, the blue blood pigment haemocyanin, to unravel strategies that sustain oxygen supply and thus survival at cold temperatures.

Results

To identify cold induced adaptations of blood oxygen transport in octopods, we compared haemocyanin oxygen binding properties, oxygen carrying capacities as well as haemolymph protein and ion composition between the Antarctic octopod *Pareledone charcoti*, the South-east Australian *Octopus pallidus* and the Mediterranean *Eledone moschata*. The warm adapted octopods likely suffer from reduced oxygen availability at colder temperatures. Among them, *Octopus pallidus* minimizes the increase in oxygen affinity below 15°C and is thereby more cold-tolerant than *Eledone moschata*. In the Antarctic *Pareledone charcoti* at 0°C, high levels of dissolved oxygen and poor oxygen unloading reflect a lower reliance on haemocyanin, but reduced oxygen affinity and increased oxygen carrying capacity compared to warmer water octopods still point to its significant contribution to oxygen transport. At warmer temperatures haemocyanin releases most of the bound oxygen, supporting oxygen supply and thus thermal tolerance at 10°C.

Conclusions

Adjustments of haemocyanin physiological function and expression levels but also high dissolved oxygen concentrations support oxygen supply in the Antarctic octopus *Pareledone charcoti* at near freezing temperatures. Enhanced haemocyanin oxygen transport at warmer temperatures extends warm tolerance thus making

Pareledone charcoti more eurythermal. Extended haemocyanin function towards colder temperatures in Antarctic and warm adapted octopods highlights the general role of haemocyanin oxygen transport at both warm and cold habitat temperatures and in setting limits to cold tolerance in octopods.

Introduction

The Antarctic Ocean forms an extreme habitat with temperatures ranging between -1.8 to 2°C all year round [e.g. 1, 2]. Most marine animals living under these conditions are unable to regulate their body temperature (ectotherms) and are thus required to sustain body functions at near freezing temperatures, via numerous adjustments at the molecular, cellular or systemic level [3]. Yet, Antarctic waters are rich in oxygen due to increased solubility of oxygen and rigorous mixing across the water column [4]. Paired with low metabolic rates, commonly found among Antarctic ectotherms [5-7], oxygen supply seems less challenging in the cold, as demonstrated by the ability of Antarctic notothenioid fishes to sustain life with low levels of haemoglobin [8] and in case of the Antarctic icefishes (Channichthyidae), even with the complete absence of oxygen transport proteins in the cold [4, 9]. Conversely, cold temperatures may hamper oxygen supply by lowered diffusion across tissue and cellular boundaries, increased viscosity [10] and decreased ability of blood pigments to release oxygen to tissues as the pigment's affinity for oxygen increases [11]. Antarctic fishes cope with these challenges by increased mitochondrial and membrane densities supporting diffusion [10], loss of blood cells reducing blood viscosity [12] or lowered oxygen affinity sustaining oxygen transport by their haemoglobins [13-15]. Little is known whether Antarctic ectotherms other than fish evolved comparable physiological adaptations to sustain oxygen supply in the cold.

Among those other ectotherms are numerous species of Antarctic octopods, which occur exclusively in the Antarctic Ocean and form an important part of the benthic megafauna as both prey and predators [16-20]. Colonisation of the Antarctic Ocean by octopods may have occurred via the deep-sea [21] or prior to the cooling of Antarctica and the associated opening of sea passages between 29-32 million years ago [22]. To become successful members of the Antarctic fauna as they are today, octopods were eventually required to adjust to temperatures as low as -1.9°C.

Survival at such cold temperatures is supported by physiological adjustments that sustain metabolism and motor activity [23, 24]. Unlike fishes, which are hypo-osmotic to seawater [25], octopods do not need to fear freezing, as their body fluids are

nearly isosmotic to seawater [26] and freeze at about the same temperature of -1.9°C . A major challenge, however, may involve retaining the functionality of the advanced oxygen supply system of coleoid cephalopods. Their closed circulatory system comprises three hearts and contractile veins that pump haemolymph, which is highly enriched with the blue coloured oxygen transport protein haemocyanin (93 mg ml^{-1} in *Megaleledone setebos* [27] or up to $>160\text{ mg ml}^{-1}$ in *Loligo vulgaris* [28-30]), at blood pressures which are high for invertebrates (e.g. *Enteroctopus dofleini* $5.3\text{-}9.3\text{ kPa}$, [31-33]). Evidence suggests that circulatory support by ventilatory pressure oscillations as well as heart performance may fail at high temperatures and decrease oxygen supply in cephalopods [34, 35]. At low temperatures, haemocyanin may cause systemic oxygen shortage due to its decreasing ability to release sufficient oxygen to tissues [27, 36].

To date only few studies have investigated cold adaptation features in Antarctic octopods. Garrett and Rosenthal [37] reported accelerated kinetics of potassium channels to enhance nervous signal transduction in the Antarctic octopus *Pareledone* sp.. Daly and Peck [7] observed oxygen consumption rates that were low and uncompensated in *Pareledone charcoti* compared to temperate octopus. Zielinski et al. [27] studied haemocyanin oxygen binding in the large *Megaleledone setebos* (former *Megaleledone senoi*, [38]) and observed oxygen affinity to be high and irresponsive to temperature, implying poor oxygen unloading and very limited temperature tolerance. However, comparisons of these features with those in warm adapted octopod species are required. It therefore remains unclear whether oxygen supply in Antarctic octopods features adjustments to the cold or simply lacks compensation. It further remains open whether the findings in *Megaleledone setebos* also apply to the much smaller and more common Antarctic octopods of the genus *Pareledone*, and to what extent oxygen supply via haemocyanin differs between the cold water species and octopods that face much higher and more variable temperatures.

Therefore, in this study, we aimed to assess

Whether oxygen transport via haemocyanin features modifications that facilitate oxygen supply and thus survival of Antarctic octopods at close to freezing temperatures.

Whether oxygen transport properties and related stenothermy of *Megaleledone setebos* are species specific or universal to Antarctic octopods.

Whether octopods adapted to warmer and broader temperature windows employ diverging strategies to sustain haemocyanin mediated oxygen supply across various temperatures

To address these objectives, we compared oxygen binding properties, total oxygen carrying capacities as well as protein and ion composition of haemolymph of the abundant Antarctic octopod species *Pareledone charcoti* with two octopod species adapted to warmer waters, the South-east Australian *Octopus pallidus* and the Mediterranean *Eledone moschata*.

Here we report cold-specific adjustments of oxygen transport in the Antarctic octopod *Pareledone charcoti*, which include reduced oxygen affinities and high oxygen carrying capacities, but also a high, thermally sensitive venous reserve that enhances eurythermy in *Pareledone charcoti*. We emphasize the general role of haemocyanin in supporting cold tolerance in both cold- and warm-water octopods.

Results

Temperature dependent oxygen binding *in vitro*

In vitro changes in oxygen binding by the respiratory pigment haemocyanin were assessed by pH saturation analysis (see Materials and Methods). At a common temperature of 10°C the haemocyanin of the Antarctic octopod *Pareledone charcoti* displayed a lower affinity for oxygen than haemocyanin of the South-east Australian *Octopus pallidus* and the Mediterranean *Eledone moschata*, reflected in a 1.4- or 4.2-fold higher P_{50} (PO_2 at which haemocyanin reaches half-maximum saturation with oxygen (50%)), respectively (Figure 1A, Table 1). Temperature changes affected oxygen binding in all three octopod species, indicated by increased oxygen affinities and diminished pH dependent oxygen release towards colder temperatures (Table 1, Figure 2, 3). In *Pareledone charcoti* and *Eledone moschata* oxygen affinities increased more steadily, in *Octopus pallidus* however, oxygen affinities remained nearly unchanged between 10-15°C but decreased considerably above 15°C (Table 1, Figure 3). According to the changes in oxygen affinity, oxygen saturation decreased with increasing temperatures. However, this drop mostly occurred in the range of low, i.e. venous PO_2 between 4 and 1 kPa (Figure 3A). At a PO_2 of 13 kPa, oxygen saturation remained virtually unchanged in *Pareledone charcoti* and *Eledone moschata* and decreased only slightly but significantly by 9.7% in *Octopus pallidus* above 15°C (ANOVA_{1-way}, $F_{2, 15} = 5.40$, $P = 0.017$, Figure 3A). pH sensitivity of oxygen affinity

expressed as the Bohr coefficient ($\Delta \log P_{50} / \Delta \text{pH}$) remained unaffected by experimental temperatures (ANOVA_{2-way}, $F_{1, 16} = 0.36$, $P = 0.555$). Among species the lowest Bohr coefficients were found in *Pareledone charcoti* (Table 1). The maximum rate of pH dependent oxygen release by haemocyanin (i.e. the slope of the oxygen equilibrium curve (OEC), $\Delta \text{mmol O}_2 \text{ L}^{-1} / \Delta \text{pH}$) decreased significantly at lower temperatures in all three species (ANOVA_{3-way}, $F_{4, 119} = 20.91$, $P < 0.001$, Table 1).

The analysis of inorganic cations in the haemolymph showed no differences between *Pareledone charcoti*, *Octopus pallidus* and *Eledone moschata* (Table 1). Interestingly, haemocyanin content did not co-vary with or equal total haemolymph protein but differed significantly between species (ANOVA_{1-way}, $F_{2, 29} = 8.98$, $P < 0.001$, Figure 4). The highest concentrations of haemocyanin were found in the Antarctic octopod *Pareledone charcoti* (78.9 mg ml⁻¹, 95% confidence interval (CI) from 69.2-88.6 mg ml⁻¹, Figure 4).

Implications for blood oxygen transport in vivo

In this section, the in vitro results are described in terms of their implications for the putative in vivo patterns of oxygen binding. At 0°C haemocyanin of *Pareledone charcoti* would release only 16.3% of its bound oxygen during an arterial-venous transition from 13 to 1 kPa PO_2 (Figure 2A, Figure 3), considering an alpha-stat shift to a venous pH of 7.42 and an arterial pH of 7.53. Even at low pH (<6.4) and low oxygen tensions (1kPa PO_2), 33.6% (28.4-38.8) of the oxygen would remain bound to the Antarctic haemocyanin. For comparison, within the range of their habitat temperature from 10 to 20°C, haemocyanins of *Octopus pallidus* and *Eledone moschata* would release between 33.0-60.0% and 29.8-70.0% oxygen, respectively (Figure 2D-I, Figure 3).

Haemocyanin of *Pareledone charcoti* showed the lowest venous oxygen saturation at a common temperature of 10°C, given an arterial-venous transition from 13 to 1 kPa PO_2 and an arterial-venous pH gradient from 7.38 to 7.27 (Figure 1B). At 10°C the Antarctic haemocyanin thus has the potential to release far more oxygen (on average 76.7%, 95% CI 68.6% to 84.8%) upon each cycle than the warm-water octopods *Octopus pallidus* (33.0%, 5.0-60.9) and *Eledone moschata* (29.8%, 9.9-49.7, Figure 2C, D, G, Figure 3A). This is mostly due to an increased pH dependent rate of oxygen release in *Pareledone charcoti* (Figure 2C, D, G), with maximum rates occurring 0.16 or 0.25 pH values above those of *Octopus pallidus* or *Eledone moschata* respectively (Figure 5).

Surprisingly, the Antarctic *Pareledone charcoti* has a larger capacity to carry oxygen in its haemolymph than *Octopus pallidus* or *Eledone moschata* (ANOVA_{1-way}, $F_{2, 31} = 12.57$, $P < 0.001$, Table 2), due to the highest haemocyanin content of all three species (Figure 4). This increased capacity for oxygen transport in *Pareledone charcoti* is further enhanced by high levels of dissolved oxygen at 0°C (359.5 $\mu\text{mol L}^{-1}$, 35 psu, Figure 3B) accounting for 18.5% of the total haemolymph oxygen content and up to 42% of the oxygen released to the tissue (i.e. from 13-1 kPa PO_2) in *Pareledone charcoti*. The contribution of dissolved oxygen is also significant in the warm-water octopods *Octopus pallidus* and *Eledone moschata*, within the range of their habitat temperatures between 10-20°C, amounting to between 17-20% or 18-21%, respectively, of total haemolymph oxygen content and 30-16% or 34-15%, respectively, of the oxygen eventually released to tissues (from 13-1 kPa PO_2 , Figure 3B).

Discussion

Comparing the haemocyanins of the Antarctic octopod *Pareledone charcoti* with those of the warmer-water octopods *Octopus pallidus* and *Eledone moschata* reveals modifications and properties of the respiratory pigment that enhance oxygen supply at close to freezing temperatures but also support an extended range of thermal tolerance in the Antarctic species. Haemocyanin functional properties in *Eledone moschata* reflect limited cold tolerance due to progressively impaired oxygen supply in the cold. In *Octopus pallidus*, however, oxygen affinities decrease strongly above 15°C but stabilise at 10°C, suggesting a dual strategy to improve oxygen supply at both its upper and lower temperature margins.

Cold adaptation of blood oxygen transport

Due to the exothermic nature of oxygen binding, oxygen affinity increases towards colder temperatures [11] and may severely hamper oxygen release to tissues at the sub-zero temperatures [39] prevailing in the Antarctic Ocean. Our results show that *Pareledone charcoti* attenuates this detrimental effect by means of lowered oxygen affinity of the haemocyanin (Figure 1A, B, Table 1). Such lowered, cold-compensated oxygen affinities are not unique to *Pareledone charcoti* and the respiratory pigment haemocyanin, but were also observed in red-blooded Antarctic fishes such as *Dissostichus mawsoni* (P_{50} of 1.93 kPa at pH 8.16 and -1.9°C, [15]) or *Pagothenia borchgrevinki* (2.8 kPa at pH 8.1 and -1.5°C), whose oxygen affinities were much lower than those of temperate fish extrapolated to the same temperatures [40].

Allosteric effectors (e.g. ATP) may strongly contribute to decreased oxygen affinities of the haemoglobins of Antarctic fishes [15]. *Pareledone charcoti* however, relies on modifying the intrinsic properties and the pH sensitivity of its haemocyanin. The only known allosteric effectors in octopod blood, inorganic ions, particularly magnesium [41, 42], are not regulated and found at levels similar to those in sea water (54.2 mmol L⁻¹ at 35 psu, [43] and similar to those in blood of other octopods (i.e. *Octopus pallidus*, *Eledone moschata*, Table 1; *Eledone cirrhosa*, 54.6 mmol L⁻¹ [26]). This confirms the general perception that cephalopods poorly exploit the effectiveness of magnesium to modulate oxygen binding. Instead, *Pareledone charcoti* enhances oxygen release via an increased rate of pH dependent oxygen release and by shifting the pH sensitive range of oxygen binding towards higher pH values than seen in the warm water octopods (Figure 2C, D, G, Figure 5) and thereby aligning with the cold-induced alpha-stat shift of venous pH (Figure 6). Altered isoelectric and thus proton binding properties of haemocyanin may have accounted for this type of affinity modulation, as reported for fish, where adjustment of oxygen affinity and pH sensitivity to particular temperatures relate to specific isoelectric properties of the respective haemoglobins [44-46].

Compensation for incomplete cold adaptation

Although *Pareledone charcoti* has experienced a decrease in oxygen affinity of its haemocyanin to enhance oxygen release at 0°C, adaptation is far from being complete as more than 77% of the oxygen remains bound to haemocyanin under venous conditions (Figure 2A, 3A). The major factors contributing to the projected incomplete oxygen unloading at 0°C are the i) cold-induced increase of affinity of haemocyanin for oxygen, ii) reduced rate of pH dependent oxygen release and iii) alpha-stat shift of haemolymph pH towards higher pH (Figure 2A, 6). In fact, increased oxygen affinity and reduced rates of oxygen release at colder temperatures are consistently reported for octopods [30, 47 for review] and explained by a more rigid structure of the haemocyanin molecule [42]. The alpha-stat pattern of haemolymph pH changes observed for octopods (Figure 6) has also been reported for squids [48], suggesting that temperature dependent changes of haemolymph pH affect oxygen supply in most if not all cephalopods. Melzner et al. [34] illustrated that the interplay of these factors lead to a venous oxygen release of less than 10% in *Sepia officinalis* at 10°C and 1.7 kPa PO₂, and accordingly, to only ~22% or ~5% oxygen release at 0°C and 1.0 or 1.7 kPa PO₂, respectively, in the Antarctic octopod *Megaleledone setebos* [27]. Although PO₂ values

below 1 kPa may further improve oxygen unloading, it is questionable whether the remaining oxygen gradient to mitochondria would be steep enough to maintain oxygen flux [34]. Therefore, poor oxygen unloading in *Pareledone charcoti* at 0°C due to high oxygen affinity, lowered rate of oxygen release and high venous pH are well in line with previous notions describing these factors to be crucial in defining limits of oxygen supply in the cold [34, 39, 47].

Most surprisingly, *Pareledone charcoti* compensates for poor oxygen unloading by considerably increasing haemocyanin concentrations. It thereby carries 40% or 46% more haemocyanin-bound oxygen in its haemolymph than *Octopus pallidus* or *Eledone moschata*, respectively (Figure 4). Overall, oxygen carrying capacities of the Antarctic octopods *Pareledone charcoti* and *Megaleledone setebos* rank among the highest reported for octopods and resemble those of red-blooded Antarctic fishes (Table 2). This and the presence of deeply blue-colored haemolymph in many other Antarctic octopods (*Adelieledone polymorpha*, *Pareledone* spp., *Benthoctopus* sp., M. Oellermann, pers. obs.) not only underlines the dependence of cold adapted octopods on high haemocyanin concentrations but also contrasts the general finding of reduced erythrocyte and blood pigment concentrations in red-blooded Antarctic fishes [8] or Antarctic crustaceans [49]. It appears that red-blooded Antarctic fishes depend less on their oxygen transport protein than Antarctic octopods, despite higher rates of oxygen consumption (e.g. *Trematomus hansonii* 0.700 mmol O₂ kg⁻¹ (wet mass) h⁻¹ [50] vs. *Pareledone charcoti* 0.319 mmol O₂ kg⁻¹ (wet mass) h⁻¹ [7]). This may reflect a lower degree of capillarisation in the cephalopods [51]. However, we can presently not exclude that haemocyanin protein concentrations serve other cold compensated processes as well.

The reduction of haemoglobin content in red-blooded Antarctic fishes has been interpreted to balance the increase in blood viscosity at low temperatures [52, 53]. One therefore wonders why Antarctic octopods evolved to maximize the concentration of an extracellular protein, which enhances viscosity even further? This may be best explained by either one or all of the following reasons, i) an increase in the fraction of haemocyanin in extracellular protein without causing higher levels of haemolymph proteins (Figure 4), ii) the non-existence of anti-freeze proteins that can largely contribute to blood protein levels in Antarctic fishes (e.g. 32 mg ml⁻¹ or ~35% of total blood protein concentration in *Dissostichus mawsoni*, [8, 25]) and increase blood viscosity [54] and iii) haemocyanin concentrations well below viscosity limits. Squids

were reported to have haemocyanin in excess of 160 mg ml^{-1} [*Loligo spp.*, 30, 42, 55], whereas maximum haemocyanin levels of *Pareledone charcoti* seen in the present study were 106.8 mg ml^{-1} . We conclude that as a tradeoff, enhanced oxygen supply occurs at the expense of enhanced viscosity. The ability to maximize haemocyanin levels at sub-zero temperatures supports *Pareledone charcoti* in compensating for the poor oxygen unloading by the haemocyanin.

Oxygen supply is further enhanced by high levels of physically dissolved oxygen, as oxygen solubility increases with decreasing temperatures (e.g. by 40% from 15°C to 0°C , [56]). Consequently, dissolved oxygen contributes 18.5% to total haemolymph oxygen content. Given the small degree of putative venous oxygen unloading in *Pareledone charcoti* (below 20%), even at very low PO_2 (1 kPa), physically dissolved oxygen contributes a large fraction (42% from 13 to 1kPa, Figure 3B) of the actual oxygen supplied to tissues. Red-blooded Antarctic fishes also benefit from high ambient oxygen levels in the cold [57] and combined with low metabolic rates [5, 50], this may be the key to the reduction in haemoglobin levels [58]. For *Pareledone charcoti* it rather seemed inevitable to increase haemocyanin concentrations, despite high dissolved oxygen levels, reduced oxygen affinity and metabolic rates lower than in fish [7]. Sustaining high haemocyanin levels may be energetically costly but may alleviate the pressure to evolve functional changes enabling complete oxygen unloading at 0°C . Such adjustments may not be possible considering the enormous size (3.5 MDa) and multimeric complexity of the haemocyanin molecule [59]. Although *Octopus pallidus* and *Eledone moschata* live at higher temperatures and lower dissolved oxygen levels, dissolved oxygen still contributes significantly to oxygen transport, especially towards colder temperatures when their haemocyanin increasingly fails to supply oxygen to tissues (Figure 3B).

Temperature sensitivity of oxygen transport

The increase in oxygen affinity and decrease of pH dependent oxygen release rates towards colder temperatures (Table 1, Figure 2) results in progressively reduced capacities to unload oxygen in all three octopod species. The change of oxygen affinity with temperature in *Pareledone charcoti* and *Eledone moschata* (Table 1) conforms well with findings in other octopod species (in ΔP_{50} (kPa) / $^\circ\text{C}$: 0.24, *Enteroctopus dofleini*; 0.20, *Octopus vulgaris* [30]; 0.10, *Eledone cirrhosa*; 0.14, *Octopus vulgaris* [60]), which underlines the crucial role of increased oxygen affinity in limiting oxygen supply in the cold among octopods.

However, some species deviate from this pattern, such as the Antarctic octopod *Megaleledone setebos*. The response of its haemocyanin oxygen affinity to temperature changes ($0.01 \text{ kPa } \Delta P_{50} / ^\circ\text{C}$, [27]), was 8-32 times less than that in any other octopod studied and 12 times less than the respective change in *Pareledone charcoti*. Despite similarities in oxygen affinity and oxygen carrying capacity between these two Antarctic octopods, this difference is striking. Thus, in addition to enhanced oxygen carrying capacities, two alternating strategies emerge to compensate for excessively high oxygen affinities in the cold: 1) A general decrease in oxygen affinity at all temperatures but with high sensitivity to temperature maintained as in *Pareledone charcoti* or 2) a considerable decrease of temperature sensitivity leading to reduced oxygen affinity at low temperatures only, as in *Megaleledone setebos*. Interestingly, *Octopus pallidus* seems to take advantage of both strategies as oxygen affinity barely changes between 10 and 15°C but strongly decreases between 15 and 20°C (Table 1, Figure 3). As a consequence, oxygen supply is sustained at temperatures below 10°C but also improves rapidly at higher temperatures (>15°C) when metabolic demand for oxygen increases. *Eledone moschata*, on the other hand, faces a constant increase of oxygen affinity and thus insufficient oxygen supply below 10°C (Table 1, Figure 3), which would contribute to cold-death at around 6°C (F. C. Mark, pers. obs.). Thus with respect to haemocyanin-mediated oxygen supply, *Octopus pallidus* seems to tolerate cold temperatures better than *Eledone moschata*.

Within the studied temperature ranges, warming hardly compromises the capacity for oxygen loading at the gills but does compromise oxygen release to tissues in all three octopods (Figure 3A). Only *Octopus pallidus* will experience reduced arterial oxygen loading above 15°C, which however is paralleled by enhanced venous oxygen unloading (Figure 3). This conforms with findings in other cephalopods and indicates that temperature changes affect venous unloading more than arterial oxygen loading (*Megaleledone setebos*, *Sepia officinalis*, [27], *Dosidicus gigas*, [61], *Todarodes sagittatus*, [30]). Only few species like the giant squid *Architeuthis monachus* experience significantly reduced arterial saturation at higher temperatures (Brix 1983). Thus, in octopods, oxygen loading at the gills is largely safeguarded at habitat temperatures and normoxic conditions and may only be compromised at low ambient oxygen levels.

The pH sensitivity of oxygen binding expressed as the Bohr coefficient remained unaffected by temperature changes in all three octopods, unlike in *Megaleledone*

setebos or *Sepia officinalis*, whose Bohr coefficients decreased with falling temperatures [27]. Octopods may benefit from low Bohr coefficients in the cold, equivalent to a switch from pH dependent to PO_2 dependent oxygen release. This may preserve the venous oxygen reserve when metabolic rate is low and largely covered by elevated physically dissolved oxygen levels. The lower Bohr coefficient of cold-adapted *Pareledone charcoti*, may also reflect its low activity mode of life in cold Antarctic waters where rapid pH dependent mobilization of the venous reserve is not required. Conversely, the strong increase in the Bohr coefficient of *Megaleledone setebos* haemocyanin during warming to 10°C (-2.33) may indicate a disadaptation as it challenges effective oxygen release outside of the animal's usual thermal range [27]. In contrast to the findings in the cold adapted species, the maintenance of high Bohr coefficients in cold exposed temperate *Octopus pallidus* and *Eledone moschata* may reflect suboptimal or even impaired oxygen supply at their lower temperature margins.

Haemocyanin supports eurythermy

Pareledone charcoti benefits from its thermally sensitive oxygen binding during warming, as much of the bound oxygen is liberated then (Figure 3A). Consequently, the increased demand for oxygen at 10°C requires only a minimal increase in circulatory performance, by 5.2% compared to the 110.4% required without the additional oxygen release by haemocyanin (Figure 7). Therefore, haemocyanin in *Pareledone charcoti* plays a major role in buffering oxygen demand when temperature increases and drastically reduces the workload for other circulatory components, particularly the hearts, which often limit ectotherm performance at high temperatures [35, 62-64]. Haemocyanin function extends the range of warm tolerance of *Pareledone charcoti*, which may cope far better with higher temperatures than *Megaleledone setebos*, whose haemocyanin, due to its low temperature sensitivity and extreme Bohr coefficient, barely supports oxygen supply at higher temperatures [27]. In fact, *Pareledone charcoti* sustains fully aerobic metabolism up to 8-10°C and thus tolerates elevated temperatures well [65]. Although both species are closely related and likely originate from shallow Southern Ocean waters (i.e. possess ink sac [66]), this may in part reflect the different geographic and vertical distribution of the two species. *Megaleledone setebos* is a circum-Antarctic species found between 30-850 m and most frequently below 100 m [38] where temperatures remain close to freezing all year round [67]. *Pareledone charcoti* inhabits the waters around the Northern Antarctic Peninsula mostly from less than 120 m [68] to very shallow waters (intertidal < 3 m, F. C. Mark, pers.

obs.), where water temperatures vary (e.g. from -0.5°C to 10.7°C in tidal water pools during summer [67, 69]). Our data provide first evidence that haemocyanin supports eurythermy in an Antarctic invertebrate ectotherm and conform to analogous findings in the temperate, eurythermic crab *Carcinus maenas* [70]. Considering the strong warming trend at the Antarctic Peninsula [71], *Pareledone charcoti* may eventually benefit from its physiological capacity to adjust to more variable temperatures than more stenothermal species.

Conclusions

This study highlights the importance of the oxygen transport pigment haemocyanin in octopods with regard to temperature adaptation. In comparison to findings in the south east Australian *Octopus pallidus* and the Mediterranean *Eledone moschata*, the analysis of blood oxygen binding in the Antarctic octopod *Pareledone charcoti* revealed adjustments of its blood pigment haemocyanin that support oxygen supply in the cold but at the same time maintain haemocyanin function in the warmth. Significant but incomplete reductions of oxygen affinity in *Pareledone charcoti* resulted in sustained but poor oxygen unloading at 0°C, which however, was compensated for by high levels of dissolved oxygen as well as elevated haemocyanin concentrations and thus oxygen carrying capacities. In contrast to the stenothermic Antarctic octopod *Megaleledone setebos*, *Pareledone charcoti* benefits from a thermally sensitive haemocyanin that supports extended warm tolerance and thus eurythermy by maintaining suitable oxygen transport characteristics at warmer temperatures. Compromised oxygen release from haemocyanin in the cold underlines the crucial role of the pigment for defining cold tolerance not only in Antarctic but also in warmer water octopods. While some warmer water octopods succeed to extend cold tolerance by e.g. reduced temperature sensitivity of oxygen binding in the cold others fail to do so. However, for a complete picture of thermal tolerance in *Pareledone charcoti* and the other octopods much more information is needed regarding the role of cardiac and circulatory performance, aerobic scope and growth rates across various temperatures as well as acclimation capacities. Only then may one predict the future role of this abundant group of ectotherms in a rapidly warming ecosystem.

Methods

Study design

To assess whether blood oxygen transport in cold-adapted octopods features modifications that enhance oxygen supply in the cold, we compared oxygen binding properties, total oxygen carrying capacities as well as protein and ion composition of haemolymph of the Antarctic octopod *Pareledone charcoti* with two octopods adapted to warmer waters - *Octopus pallidus* and *Eledone moschata*. Comparisons were performed at habitat temperatures and at a common temperature of 10°C, assuming that all haemocyanin types remained functional at these temperatures. To evaluate if earlier observations for *Megaleledone setebos* haemocyanin are specific or universal to Antarctic octopods, we chose *Pareledone charcoti* as a representative of the most abundant and more typically sized genus *Pareledone* [18, 68]. Temperature sensitivity of oxygen binding was analysed in all three species to assess the role of octopod haemocyanin in thermal tolerance.

Animals and sampling

The cold adapted octopod *Pareledone charcoti* inhabits the shallow shelf area around the Antarctic Peninsula [68] with temperatures varying between -1.9-2°C [72]. Using bottom trawls, specimens were collected on the RV Polarstern cruise ANTXXVIII/4 in March 2012, at depths between 90-470 m around Elephant Island (61°S, 56°W, cruise details [73]), where temperatures ranged between 0.1-1.6°C and salinities between 34.3-34.6 psu. *Octopus pallidus* inhabits the well mixed waters in South East Australia with habitat temperatures ranging from 12-18°C from winter to summer [74, 75]. Specimens were caught in July 2012, between 40-50 m depth, in the western Bass Strait near Stanley (41°S, 145°E) by fishermen (T.O.P. Fish Pty Ltd.) using plastic octopus pots and then transported and kept overnight in large tanks connected to a flow-through seawater system at the Institute for Marine and Antarctic Studies, Hobart. *Eledone moschata* occurs all over the Mediterranean Sea mainly at depths between 0-200 m [76, 77]. Specimens were fished in November 2008, between 20-40 m depth using bottom trawls, in the northern Adriatic Sea near Chioggia, where habitat temperatures vary largely, both by depth and seasonally, between approximately 10-23°C [78]. All animals were anaesthetised in 3% ethanol [79] until non responsive, then ventrally opened to withdraw haemolymph from the cephalic vein, the afferent branchial vessels and the systemic heart and finally killed by a final cut through

the brain (Animal research permit no. 522-27-11/02-00(93), Freie Hansestadt Bremen, Germany and animal ethics approval no. AEC12-43, La Trobe University, Bundoora, Australia). Blood samples were spun down at 15.000 g for 15 min at 0°C to pellet cell debris and supernatants were stored at -20°C.

Blood characteristics

Oxygen binding properties

Oxygen binding of octopod haemocyanin was characterised using a modified diffusion chamber [for details see 80], which simultaneously measures pigment oxygenation and pH in a 15 µl sample. Experiments were performed at common habitat temperatures of each species (0°C *Pareledone charcoti*, ~10-20°C *Octopus pallidus*, ~10-20°C *Eledone moschata*) and at a comparative temperature of 10°C. The temperature was monitored and controlled via a temperature sensor (PreSens, Germany) and a connected water bath with a thermostat (LAUDA Ecoline Staredition RE 104, Germany), filled with an anti-freeze solution (20% ethylene glycol, AppliChem, Germany). Prior to measurements, aliquots of 18 µl thawed haemolymph were spun down to collect all liquid at the bottom of a 1.5 ml microcentrifuge tube (5 sec at 1000 g), preconditioned with pure oxygen gas to deplete dissolved carbon dioxide (CO₂) and 0.6-0.9 µl of 0.2 mmol L⁻¹ NaOH (8-12 µmol L⁻¹ final concentration) added to raise blood pH above 8.0 to ensure full oxygenation. To account for the pronounced pH sensitivity of cephalopod pigments [81], changes of pH and absorbance were recorded at 347 nm in 15 µl haemolymph, at continuously decreasing *P*CO₂ / pH (0-10 kPa / ~ pH 8.1-6.8) and four constant *P*O₂ levels (21, 13, 4, 1 kPa, after Pörtner (1990)), with gas mixtures being supplied by gas mixing pumps (Wösthoff, Germany). The spectrophotometer (USB2000+, Ocean Optics, USA) was set to 15 milliseconds integration time, 100 scans to average and 30 seconds measurement intervals and calibrated by recording light and dark spectra without sample. Prior to each experiment, the pH optode was calibrated in MOPS-buffered (40 mmol L⁻¹, 3-(N-Morpholino)propanesulfonic acid), filtered artificial seawater (35 psu) equilibrated to the respective experimental temperature at six pHs ranging from 6.7 to 8.1. The pH of buffers was checked with a pH glass electrode (InLab Routine Pt1100, Mettler Toledo, Germany) and a pH meter (pH 330i, WTW, Germany), calibrated with low ionic strength NIST pH standards (AppliChem, Germany, DIN19266) and corrected to Free Scale pH with Tris-buffered seawater standard (Dickson, CO₂ QCLab, batch 4 2010, USA, [82]) equilibrated at the same temperature. The pH signal

was corrected for instrumental drift and for effects of auto-fluorescence intrinsic to haemolymph [80] and is presented here on the free hydrogen ion scale [83].

Each experiment involved the calibration with pure oxygen or nitrogen to obtain maximum and minimum oxygenation signals. Correct pigment saturation was calculated by continuous readjustments of the maximum oxygenation signal to account for its linear drift observed during the course of an experiment [80, 84]. While the maximum oxygenation signal did not change within the range of temperatures employed for each species, the minimum oxygenation signal increased towards colder temperatures due to incomplete oxygen unloading, even under pure nitrogen and low pH (< 6.6). For such experiments we predicted minimum absorbance from a reference wavelength of the first recorded spectrum with an uncertainty of 5%, based on a linear regression model applied to 20 experiments with fully deoxygenated pigments (Supplementary Figure S1).

To determine the total oxygen bound to octopod haemocyanin (i.e. oxygen carrying capacity) 10 μ l of thawed haemolymph were equilibrated with pure oxygen gas in a microcentrifuge tube on ice for 10 min and transferred with a gas tight Hamilton syringe to a gas sealed chamber containing 2 ml of a 32°C warm cyanide solution (6 g L⁻¹ potassium cyanide, 3 g L⁻¹ saponin, [85]). Two high-resolution Oxygraph-2k respirometers (OROBOROS Instruments, Innsbruck, Austria) and DatLab analysis software (version 5.1.0.20) recorded the liberated oxygen (nmol ml⁻¹), corrected for air pressure, temperature and background oxygen flux. For each experiment, the respirometers were calibrated with air at the beginning and sodium dithionite added at the end for a zero calibration. The contribution of dissolved oxygen was experimentally determined by the addition of ice-cold, oxygen saturated, filtered seawater (35 psu). The observed change of oxygen concentration was then subtracted from the haemolymph measurements to obtain the final oxygen carrying capacity of haemocyanin.

Alpha-stat pattern of haemolymph pH

To be able to analyse oxygen binding parameters at various temperatures, we assessed whether the pH of octopod haemolymph follows an alpha-stat pattern [86] or remains constant across temperatures (i.e. pH stat pattern). Replicated measurements on 20 μ l thawed haemolymph of *Octopus pallidus* at 0°C, 10°C and 20°C, using a micro pH electrode (InLab Ultra-Micro, Mettler Toledo, Germany), showed that pH decreases linearly with temperature ($b = -0.0153$ pH units / °C, $t_{31} = -9.71$, $P < 0.001$, $R^2 = 0.75$, Figure 6), analogous to an imidazole buffered system (-0.0162 pH units / °C, [86]). pH

analysis of freshly sampled blood from other species confirmed that octopod haemolymph follows this linear pH-temperature relationship *in vivo* (Figure 6) and therefore exhibits an alpha-stat pattern as also demonstrated for squid [48]. Hence, venous and arterial pH were determined on this basis for various temperatures.

Protein and ion concentration

Protein content of octopod haemolymph was determined according to Bradford [87]. Thawed haemolymph was diluted tenfold (v:v) with stabilising buffer (in mmol l⁻¹, 50 Tris-HCl, 5 CaCl₂ 6 H₂O, 5 MgCl₂ 6 H₂O, 150 NaCl, pH 7.47 at 22°C) and 5 µl mixed with 250 µl Bradford reagent (Bio-Rad, Germany). Following 10 min incubation at room temperature, absorbance was recorded at 595 nm using a microplate spectrophotometer (PowerWave HT, BioTek, U.S.A.). Bovine albumin serum served as protein standard to calculate total protein concentrations.

Concentrations of functional haemocyanin (c(Hc)) in haemolymph were derived from the oxygen carrying capacity (C_{O_2}), the molecular weight (MW) of octopod haemocyanin (3.5 MDa) and its 70 oxygen binding sites ($n(HcO_2)$), [59], Equation 1).

$$c(Hc) = \frac{C_{O_2}}{n(HcO_2)} MW \quad \text{Equation 3}$$

Results from tests with thawed haemolymph of *Octopus vulgaris* (mean ± S.D., 54.3 ± 6.9 g L⁻¹) agreed well with data obtained from freshly observed haemolymph via atomic absorption spectroscopy (55.9 ± 7.4 g L⁻¹, [29]), which not only confirmed the accuracy of our approach but also that storage at -20°C does not affect the oxygen binding capacity of cephalopod haemolymph [42].

Although inorganic ions such as Mg²⁺ or Na⁺ can affect oxygen affinity in octopods [41], they seem to be insignificant regulators of oxygen binding in most cephalopods [42]. To verify this for the observed species, we diluted haemolymph 400-fold with deionised water and determined cation concentrations by ion chromatography (ICS-2000, Dionex, Germany) following cation separation by an IonPac CS 16 column (Dionex, Germany) with methane sulfonic acid (MSA, 30 mmol L⁻¹) as an eluent at 0.36 ml min⁻¹ flow rate and 40°C. Ion concentrations were derived from the peaks corresponding to the Dionex Combined Six Cation Standard-II.

Data analysis

Processing of raw data and statistical analysis was performed using the 'R' statistical language [R Core 88]. Recordings of pH and pigment oxygenation were time-matched and analysed in pH/saturation diagrams, most suitable for pH sensitive pigments like cephalopod haemocyanin [81]. An empirical five parameter logistic model was applied ('drc' add-on package, [89]) to fit sigmoidal curves to the pH/saturation data [80]. Resulting OECs display the change of pigment oxygenation with pH at constant PO_2 . Affinity of haemocyanin to oxygen, expressed as P_{50} , denotes the \log_{10} of the PO_2 corresponding to an OEC and the intersecting pH at half saturation (pH_{50} , [81]). $\Delta \log_{10} P_{50}$ was then plotted versus ΔpH_{50} to obtain the Bohr coefficient from the resulting linear regression slope. Cooperativity was expressed as the pH dependent rate of oxygen release by haemocyanin ($\Delta \text{mmol L}^{-1} / \Delta \text{pH}$, (Pörtner, 1990)) and derived from the maximum slope of a fitted OEC. Differences between species and experimental temperatures were tested to be significant ($P < 0.05$) using analysis of variance (ANOVA) followed by Tukey's *post hoc* test. Normality and homogeneity of variance were assessed by Kolmogorov–Smirnov and Levene's tests, respectively. Results were expressed as means and their 95% confidence interval range if not stated otherwise.

Abbreviations

ATP	Adenosine triphosphate
c(Hc)	Haemocyanin concentration
CO ₂	Carbon dioxide
C_{O_2}	Oxygen carrying capacity
MO ₂	oxygen consumption rates of <i>Pareledone charcoti</i> (MO ₂)
MW	Molecular weight
NIST	National Institute of Standards and Technology
OEC	Oxygen equilibrium curve
PCO ₂	Carbon dioxide partial pressure
PO ₂	Oxygen partial pressure
P ₅₀	PO ₂ at which the pigment is half saturated
pH ₅₀	pH of haemolymph/blood at which the pigment is half saturated
Q ₁₀	Temperature coefficient

Acknowledgements

We wish to thank all colleagues and technical staff of the Alfred Wegener Institute including Lena Jakob for performing ion chromatography, Fredy Véliz Moraleda and Nils Koschnick for acquisition and care of *Pareledone charcoti*, Timo Hirse, and Guido Krieten for technical assistance and Anneli Strobel for providing haemolymph pH data of *Eledone moschata*. We would like to express our special thanks to Jan Strugnell (La Trobe University, Bundoora) for providing lab space and her extensive practical and theoretical support, Michael Imsic and all other staff and technicians of the La Trobe University for their kind support and the fishermen of T.O.P. Fish Pty Ltd for catching *Octopus pallidus*. This study was supported by a Journal of Experimental Biology travelling fellowship, a PhD scholarship by the German Academic Exchange Service (DAAD, D/11/43882) to MO, the Deutsche Forschungsgemeinschaft DFG (MA4271/1-2 to FCM) and the Alfred Wegener Institute for Polar and Marine Research.

References

1. Klinck JM, Hofmann EE, Beardsley RC, Salihoglu B, Howard S: **Water-mass properties and circulation on the west Antarctic Peninsula Continental Shelf in Austral Fall and Winter 2001.** *Deep-Sea Res Pt II* 2004, **51**:1925-1946.
2. Jacobs SS, Amos AF, Bruchhausen PM: **Ross sea oceanography and antarctic bottom water formation.** *Deep-Sea Res Oceanogr Abstr* 1970, **17**:935-962.
3. Pörtner HO, Peck L, Somero G: **Thermal limits and adaptation in marine Antarctic ectotherms: an integrative view.** *Philos Trans R Soc Lond B Biol Sci* 2007, **362**:2233-2258.
4. Sidell BD, O'Brien KM: **When bad things happen to good fish: the loss of hemoglobin and myoglobin expression in Antarctic icefishes.** *J Exp Biol* 2006, **209**:1791-1802.
5. Clarke A, Johnston NM: **Scaling of metabolic rate with body mass and temperature in teleost fish.** *J Anim Ecol* 1999, **68**:893-905.
6. Ahn I-Y, Shim JH: **Summer metabolism of the Antarctic clam, *Laternula elliptica* (King and Broderip) in Maxwell Bay, King George Island and its implications.** *J Exp Mar Biol Ecol* 1998, **224**:253-264.
7. Daly H, Peck L: **Energy balance and cold adaptation in the octopus *Pareledone charcoti*.** *J Exp Mar Biol Ecol* 2000, **245**:197-214.
8. Wells RMG, Ashby MD, Duncan SJ, Macdonald JA: **Comparative study of the erythrocytes and haemoglobins in nototheniid fishes from Antarctica.** *J Fish Biol* 1980, **17**:517-527.
9. Ruud JT: **Vertebrates without erythrocytes and blood pigment.** *Nature* 1954, **173**:848-850.
10. Sidell BD: **Intracellular oxygen diffusion: the roles of myoglobin and lipid at cold body temperature.** *J Exp Biol* 1998, **201**:1119-1128.
11. Weber RE, Campbell KL: **Temperature dependence of haemoglobin-oxygen affinity in heterothermic vertebrates: mechanisms and biological significance.** *Acta Physiol (Oxf)* 2011, **202**:549-562.
12. Macdonald JA, Wells RMG: **Viscosity of body fluids from Antarctic nototheniid fish.** In *Biology of Antarctic Fish*. Edited by Prisco G, Maresca B, Tota B: Springer Berlin Heidelberg; 1991: 163-178
13. D'Avino R, Di Prisco G: **Hemoglobin from the Antarctic fish *Notothenia coriiceps neglecta*.** *Eur J Biochem* 1989, **179**:699-705.
14. Tamburrini M, Brancaccio A, Ippoliti R, Di Prisco G: **The amino acid sequence and oxygen-binding properties of the single hemoglobin of the cold-adapted Antarctic teleost *Gymnodraco acuticeps*.** *Arch Biochem Biophys* 1992, **292**:295-302.
15. Qvist J, Weber RE, DeVries AL, Zapol WM: **pH and haemoglobin oxygen affinity in blood from the Antarctic cod *Dissostichus mawsoni*.** *J Exp Biol* 1977, **67**:77-88.
16. Collins MA, Rodhouse PGK: **Southern Ocean Cephalopods.** In *Adv Mar Biol. Volume* Volume 50. Edited by Alan J. Southward CMY, Lee AF: Academic Press; 2006: 191-265
17. Collins MA, Allcock AL, Belchier M: **Cephalopods of the South Georgia slope.** *J Mar Biol Assoc U K* 2004, **84**:415-419.

18. Allcock AL, Piatkowski U, Rodhouse PGK, Thorpe JP: **A study on octopodids from the eastern Weddell Sea, Antarctica.** *Polar Biol* 2001, **24**:832-838.
19. Piatkowski U, Allcock L, Vecchione M: **Cephalopod diversity and ecology.** *Ber Polarforsch* 2003, **470**:32-38.
20. Daly HI: **Ecology of the Antarctic octopus Pareledone from the Scotia Sea.** University of Aberdeen, 1996.
21. Strugnell J, Cherel Y, Cooke I, Gleadall I, Hochberg F, Ibanez C, Jorgensen E, Laptikhovskiy V: **The Southern Ocean: Source and sink?** *Deep-Sea Res Pt II* 2011, **58**:196-204.
22. Zachos J, Pagani M, Sloan L, Thomas E, Billups K: **Trends, rhythms, and aberrations in global climate 65 ma to present.** *Science* 2001, **292**:686-693.
23. Clarke A: **Costs and consequences of evolutionary temperature adaptation.** *Trends Ecol Evol* 2003, **18**:573-581.
24. Clarke A: **What is cold adaptation and how should we measure it?** *Integr Comp Biol* 1991, **31**:81.
25. Ahlgren JA, Cheng CC, Schrag JD, DeVries AL: **Freezing avoidance and the distribution of antifreeze glycopeptides in body fluids and tissues of Antarctic fish.** *J Exp Biol* 1988, **137**:549-563.
26. Robertson JD: **Further Studies on Ionic Regulation in Marine Invertebrates.** *J Exp Biol* 1953, **30**:277-296.
27. Zielinski S, Sartoris FJ, Pörtner HO: **Temperature effects on hemocyanin oxygen binding in an Antarctic cephalopod.** *Biol Bull (Woods Hole)* 2001, **200**:67-76.
28. Wells M, Smith P: **The performance of the octopus circulatory system: a triumph of engineering over design.** *Cell Mol Life Sci* 1987, **43**:487-499.
29. Senozan N, Avinc A, Unver Z: **Hemocyanin levels in *Octopus vulgaris* and the cuttlefish *Sepia officinalis* from the Aegean sea.** *Comp Biochem Physiol A Physiol* 1988, **91**:581-585.
30. Brix O, Bårdgard A, Cau A, Colosimo A, Condo S, Giardina B: **Oxygen-binding properties of cephalopod blood with special reference to environmental temperatures and ecological distribution.** *J Exp Zool* 1989, **252**:34-42.
31. Bourne GB, Redmond JR, Jorgensen DD: **Dynamics of the Molluscan Circulatory System: Open versus Closed.** *Physiol Zool* 1990, **63**:140-166.
32. Schipp R: **General morphological and functional characteristics of the cephalopod circulatory system. An introduction.** *Cell Mol Life Sci* 1987, **43**:474-477.
33. Johansen K, Martin AW: **Circulation in the cephalopod, *Octopus dofleini*.** *Comp Biochem Physiol* 1962, **5**:161-176.
34. Melzner F, Mark FC, Pörtner HO: **Role of blood-oxygen transport in thermal tolerance of the cuttlefish, *Sepia officinalis*.** *Integr Comp Biol* 2007, **47**:645-655.
35. Fiedler A: **Die Rolle des venösen Füllungsdrucks bei der Autoregulation der Kiemenherzen von *Sepia officinalis* L.(Cephalopoda).** *Zoologische Jahrbücher Abteilung für allgemeine Zoologie und Physiologie der Tiere* 1992, **96**:265-278.
36. Melzner F, Bock C, Pörtner H-O: **Allometry of thermal limitation in the cephalopod *Sepia officinalis*.** *Comp Biochem Physiol Part A Mol Integr Physiol* 2007, **146**:149-154.

37. Garrett S, Rosenthal JJ: **RNA editing underlies temperature adaptation in K⁺ channels from polar octopuses.** *Science* 2012, **335**:848-851.
38. Allcock AL, Hochberg FG, Stranks TN: **Re-evaluation of *Graneledone setebos* (Cephalopoda : Octopodidae) and allocation to the genus Megaleledone.** *J Mar Biol Assoc U K* 2003, **83**:319-328.
39. Decker H, van Holde KE: **Facilitated Oxygen Transport.** In *Oxygen and the Evolution of Life*. Springer Berlin Heidelberg; 2011: 79-105
40. Tetens V, Wells RMG, DeVries AL: **Antarctic fish blood: respiratory properties and the effects of thermal acclimation.** *J Exp Biol* 1984, **109**:265.
41. Miller KI: **Oxygen equilibria of *Octopus dofleini* hemocyanin.** *Biochemistry* 1985, **24**:4582-4586.
42. Mangum CP: **Gas transport in the blood.** In *Squid as experimental animals*. Edited by Gilbert DL, Adelman Jr WJ, Arnold JM. New York: Plenum Publishing Corporation; 1990: 443-468
43. Wittmann A, Held C, Pörtner H, Sartoris F: **Ion regulatory capacity and the biogeography of Crustacea at high southern latitudes.** *Polar Biol* 2010, **33**:919-928.
44. Weber RE, Wood SC, Lomholt JP: **Temperature acclimation and oxygen-binding properties of blood and multiple haemoglobins of rainbow trout.** *J Exp Biol* 1976, **65**:333-345.
45. Brix O, Clements KD, Wells RMG: **An ecophysiological interpretation of hemoglobin multiplicity in three herbivorous marine teleost species from New Zealand.** *Comp Biochem Physiol Part A Mol Integr Physiol* 1998, **121**:189-195.
46. Brix O, Clements KD, Wells RMG: **Haemoglobin components and oxygen transport in relation to habitat distribution in triplefin fishes [Tripterygiidae].** *J Comp Physiol B* 1999, **169**:329-334.
47. Brix O, Colosimo A, Giardina B: **Temperature dependence of oxygen binding to cephalopod haemocyanins: ecological implications.** *Mar Freshw Behav Physiol* 1994, **25**:149-162.
48. Howell BJ, Gilbert DL: **pH-temperature dependence of the hemolymph of the squid, *Loligo pealei*.** *Comp Biochem Physiol A Physiol* 1976, **55**:287-289.
49. Whiteley NM, Taylor EW, Clarke A, Haj AJE: **Haemolymph oxygen transport and acid-base status in *Glyptonotus antarcticus* Eights.** *Polar Biol* 1997, **18**:10-15.
50. Steffensen JF: **Metabolic cold adaptation of polar fish based on measurements of aerobic oxygen consumption: fact or artefact? Artefact!** *Comp Biochem Physiol Part A Mol Integr Physiol* 2002, **132**:789-795.
51. Bone Q, Pulsford A, Chubb AD: **Squid Mantle Muscle.** *J Mar Biol Assoc U K* 1981, **61**:327-342.
52. Egginton S: **Blood rheology of Antarctic fishes: viscosity adaptations at very low temperatures.** *J Fish Biol* 1996, **48**:513-521.
53. Wells RMG, Macdonald JA, DiPrisco G: **Thin-blooded Antarctic fishes: a rheological comparison of the haemoglobin-free icefishes *Chionodraco kathleenae* and *Cryodraco antarcticus* with a red-blooded nototheniid, *Pagothenia bernacchii*.** *J Fish Biol* 1990, **36**:595-609.
54. Eto TK, Rubinsky B: **Antifreeze glycoproteins increase solution viscosity.** *Biochem Biophys Res Commun* 1993, **197**:927-931.

55. Redfield AC, Ingalls EN: **The oxygen dissociation curves of some bloods containing hemocyanin.** *J Cell Comp Physiol* 1933, **3**:169-202.
56. Boutilier RG, Heming TA, Iwama GK: **Appendix: physicochemical parameters for use in fish respiratory physiology.** *Fish Physiol* 1984, **10**:403-430.
57. Prisco G, Macdonald JA, Brunori M: **Antarctic fishes survive exposure to carbon monoxide.** *Experientia* 1992, **48**:473-475.
58. Di Prisco G, Eastman JT, Giordano D, Parisi E, Verde C: **Biogeography and adaptation of Notothenioid fish: Hemoglobin function and globin-gene evolution.** *Gene* 2007, **398**:143-155.
59. Miller K, Cuff M, Lang W, Varga-Weisz P, Field K, van Holde K: **Sequence of the *Octopus dofleini* hemocyanin subunit: structural and evolutionary implications¹.** *J Mol Biol* 1998, **278**:827-842.
60. Bridges CR: **Bohr and root effects in cephalopod haemocyanins - paradox or pressure in *Sepia officinalis*?** *Mar Freshw Behav Physiol* 1994, **25**:121-130.
61. Seibel BA: **The jumbo squid, *Dosidicus gigas* (Ommastrephidae), living in oxygen minimum zones II: Blood-oxygen binding.** *Deep-Sea Res Pt II* 2012.
62. Iftikar FI, Hickey AJR: **Do mitochondria limit hot fish hearts? Understanding the role of mitochondrial function with heat stress in *Notolabrus celidotus*.** *Plos One* 2013, **8**:e64120.
63. Pörtner HO: **Climate variations and the physiological basis of temperature dependent biogeography: systemic to molecular hierarchy of thermal tolerance in animals.** *Comp Biochem Physiol Part A Mol Integr Physiol* 2002, **132**:739-761.
64. Farrell AP: **Cardiorespiratory performance in salmonids during exercise at high temperature: insights into cardiovascular design limitations in fishes.** *Comp Biochem Physiol Part A Mol Integr Physiol* 2002, **132**:797-810.
65. Pörtner HO, Zielinski S: **Environmental constraints and the physiology of performance in squids.** *S Afr J Mar Sci* 1998, **20**:207-221.
66. Strugnell J, Norman M, Vecchione M, Guzik M, Allcock AL: **The ink sac clouds octopod evolutionary history.** *Hydrobiologia* 2014, **725**:215-235.
67. Barnes DKA, Fuentes V, Clarke A, Schloss IR, Wallace MI: **Spatial and temporal variation in shallow seawater temperatures around Antarctica.** *Deep-Sea Res Pt II* 2006, **53**:853-865.
68. Allcock AL: **On the confusion surrounding *Pareledone charcoti* (Joubin, 1905) (Cephalopoda : Octopodidae): endemic radiation in the Southern Ocean.** *Zool J Linn Soc* 2005, **143**:75-108.
69. Barnes DKA, Rothery P, Clarke A: **Colonisation and development in encrusting communities from the Antarctic intertidal and sublittoral.** *J Exp Mar Biol Ecol* 1996, **196**:251-265.
70. Giomi F, Pörtner H-O: **A role for haemolymph oxygen capacity in heat tolerance of eurythermal crabs.** *Front Physiol* 2013, **4**.
71. Meredith MP, King JC: **Rapid climate change in the ocean west of the Antarctic Peninsula during the second half of the 20th century.** *Geophys Res Lett* 2005, **32**:L19604.
72. Dinniman MS, Klinck JM, Smith Jr WO: **A model study of Circumpolar Deep Water on the West Antarctic Peninsula and Ross Sea continental shelves.** *Deep-Sea Res Pt II* 2011, **58**:1508-1523.

73. **An information portal for research platforms of the Alfred Wegener Institute Helmholtz Centre for Polar and Marine Research** [<http://expedition.awi.de/expedition?id=226#events>]
74. Leporati SC, Pecl GT, Semmens JM: **Cephalopod hatchling growth: the effects of initial size and seasonal temperatures.** *Mar Biol* 2006, **151**:1375-1383.
75. André J, Pecl GT, Grist EPM, Semmens JM, Haddon M, Leporati SC: **Modelling size-at-age in wild immature female octopus: a bioenergetics approach.** *Mar Ecol Prog Ser* 2009, **384**:159-174.
76. Belcari P, Tserpes G, González M, Lefkaditou E, Marceta B, Manfrin GP, Souplet A: *Distribution and abundance of Eledone cirrhosa (Lamarck, 1798) and Eledone moschata (Lamarck, 1798) (Cephalopoda: Octopoda) in the Mediterranean Sea.* 2002.
77. González M, Sánchez P: *Cephalopod assemblages caught by trawling along the Iberian Peninsula mediterranean coast.* 2002.
78. Artegiani A, Paschini E, Russo A, Bregant D, Raicich F, Pinardi N: **The Adriatic Sea general circulation. Part I: Air-sea interactions and water mass structure.** *J Phys Oceanogr* 1997, **27**:1492-1514.
79. Ikeda Y, Sugimoto C, Yonamine H, Oshima Y: **Method of ethanol anaesthesia and individual marking for oval squid (*Sepioteuthis lessoniana* Férussac, 1831 in Lesson 1830–1831).** *Aquac Res* 2009, **41**:157-160.
80. Oellermann M, Pörtner H-O, Mark FC: **Simultaneous high-resolution pH and spectrophotometric recordings of oxygen binding in blood microvolumes.** *J Exp Biol* 2014, **217**:1430-1436.
81. Pörtner HO: **An analysis of the effects of pH on oxygen binding by squid (*Illex illecebrosus*, *Loligo pealei*) haemocyanin.** *J Exp Biol* 1990, **150**:407.
82. Dickson A: **The carbon dioxide system in seawater: equilibrium chemistry and measurements.** In *Guide to best practices for ocean acidification research and data reporting.* Edited by Riebesell U, Fabry VJ, Hansson L, Gattuso J-P. Luxembourg: Publications Office of the European Union; 2010
83. Dickson AG: **pH scales and proton-transfer reactions in saline media such as sea water.** *Geochimica et Cosmochimica Acta* 1984, **48**:2299-2308.
84. Wells RMG, Weber RE: **The measurement of oxygen affinity in blood and haemoglobin solutions.** *Techniques in comparative respiratory physiology: an experimental approach* Cambridge University Press, Cambridge 1989:279-303.
85. Bridges C, Bicudo J, Lykkeboe G: **Oxygen content measurement in blood containing haemocyanin.** *Comp Biochem Physiol A Physiol* 1979, **62**:457-461.
86. Reeves RB: **An imidazole alaphastat hypothesis for vertebrate acid-base regulation: Tissue carbon dioxide content and body temperature in bullfrogs.** *Resp Physiol* 1972, **14**:219-236.
87. Bradford M: **A rapid and sensitive method for the quantitation of microgram quantities of protein utilizing the principle of protein-dye binding.** *Anal Biochem* 1976, **72**:248-254.
88. Team RC: **R: A language and environment for statistical computing.** Vienna, Austria: R Foundation for Statistical Computing; 2014.
89. Ritz C, Streibig JC: **Bioassay analysis using R.** *J Stat Softw* 2005, **12**:1-22.
90. Houlihan D, Innes A, Wells M, Wells J: **Oxygen consumption and blood gases of *Octopus vulgaris* in hypoxic conditions.** *J Comp Physiol B Biochem Syst Environ Physiol* 1982, **148**:35-40.

91. Houlihan DF, Duthie G, Smith PJ, Wells MJ, Wells J: **Ventilation and circulation during exercise in *Octopus vulgaris***. *J Comp Physiol B* 1986, **156**:683-689.
92. Wells M, O Dor R, Mangold K, Wells J: **Diurnal changes in activity and metabolic rate in *Octopus vulgaris***. *Mar Freshw Behav Physiol* 1983, **9**:275-287.
93. Borer KT, Lane CE: **Oxygen requirements of *Octopus briareus* Robson at different temperatures and oxygen concentrations**. *J Exp Mar Biol Ecol* 1971, **7**:263-269.
94. Katsanevakis S, Stephanopoulou S, Miliou H, Moraitou-Apostolopoulou M, Verriopoulos G: **Oxygen consumption and ammonia excretion of *Octopus vulgaris* (Cephalopoda) in relation to body mass and temperature**. *Mar Biol* 2004, **146**:725-732.
95. Martin A, Harrison F, Huston M, Stewart D: **The blood volumes of some representative molluscs**. *J Exp Biol* 1958, **35**:260-279.
96. O'dor RK, Wells MJ: **Circulation time, blood reserves and extracellular space in a cephalopod**. *J Exp Biol* 1984, **113**:461-464.
97. D'Avino R, Di Prisco G: **Antarctic fish hemoglobin: an outline of the molecular structure and oxygen binding properties—I. Molecular structure**. *Comp Biochem Physiol, B: Comp Biochem* 1988, **90**:579-584.
98. Lykkeboe G, Johansen K: **A cephalopod approach to rethinking about the importance of the Bohr and Haldane effects**. *Pac Sci* 1982, **36**:305-313.
99. Lenfant C, Johansen K: **Gas transport by hemocyanin-containing blood of the Cephalopod *Octopus dofleini***. *American Journal of Physiology -- Legacy Content* 1965, **209**:991-998.

Figures

Figure 1

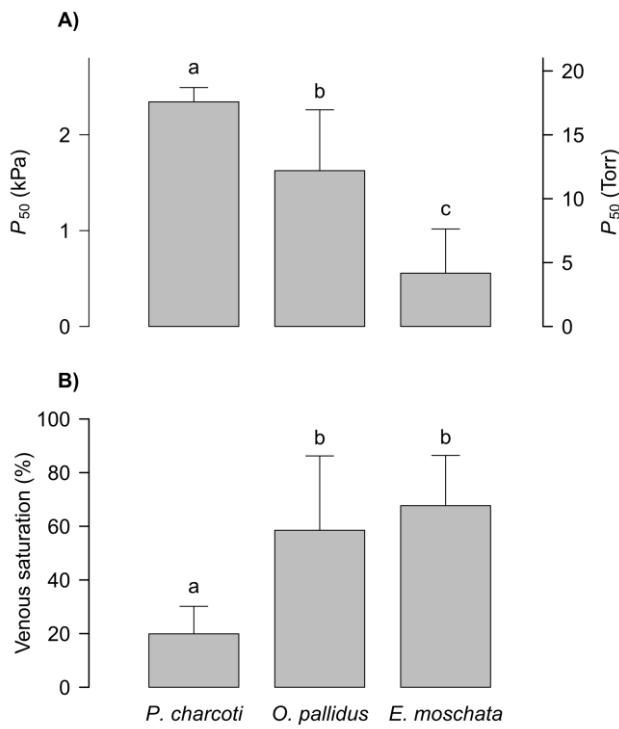


Figure 2

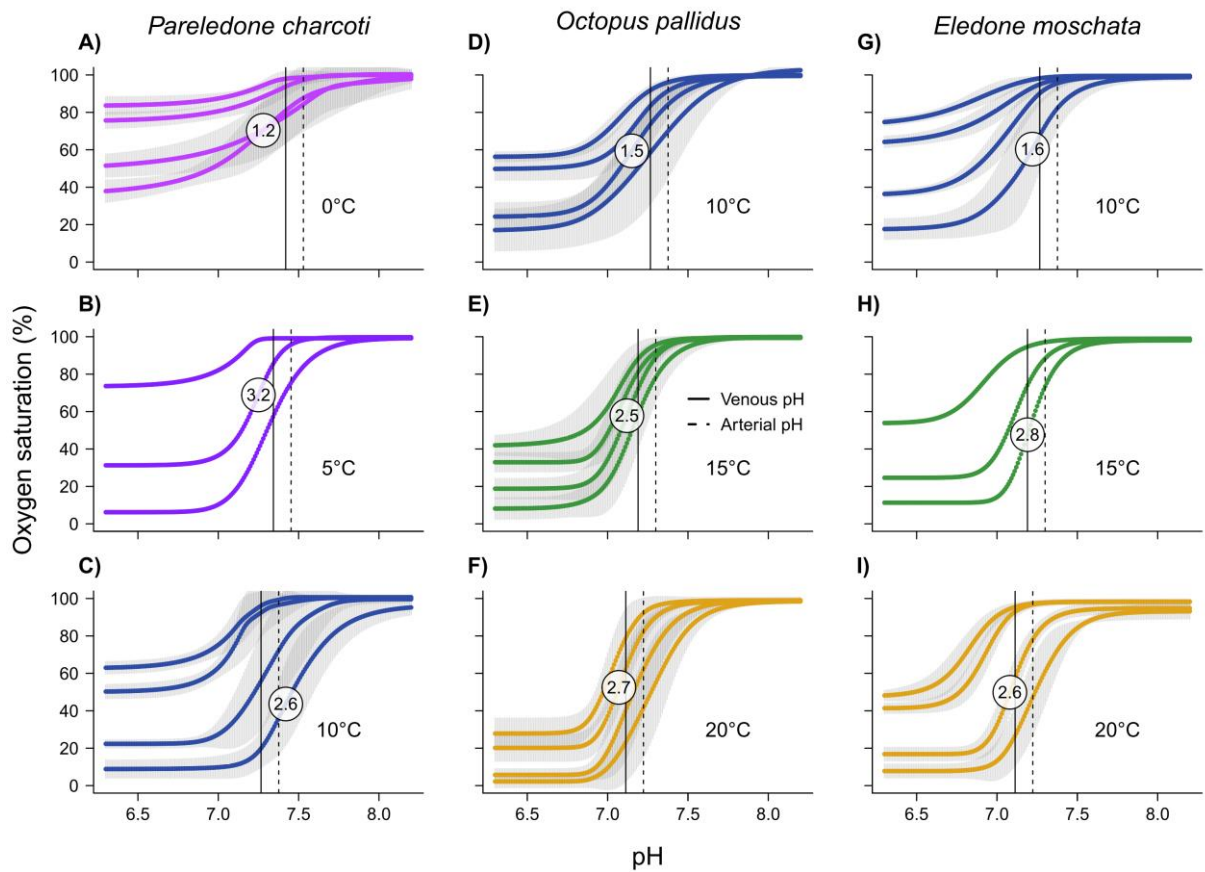


Figure 3

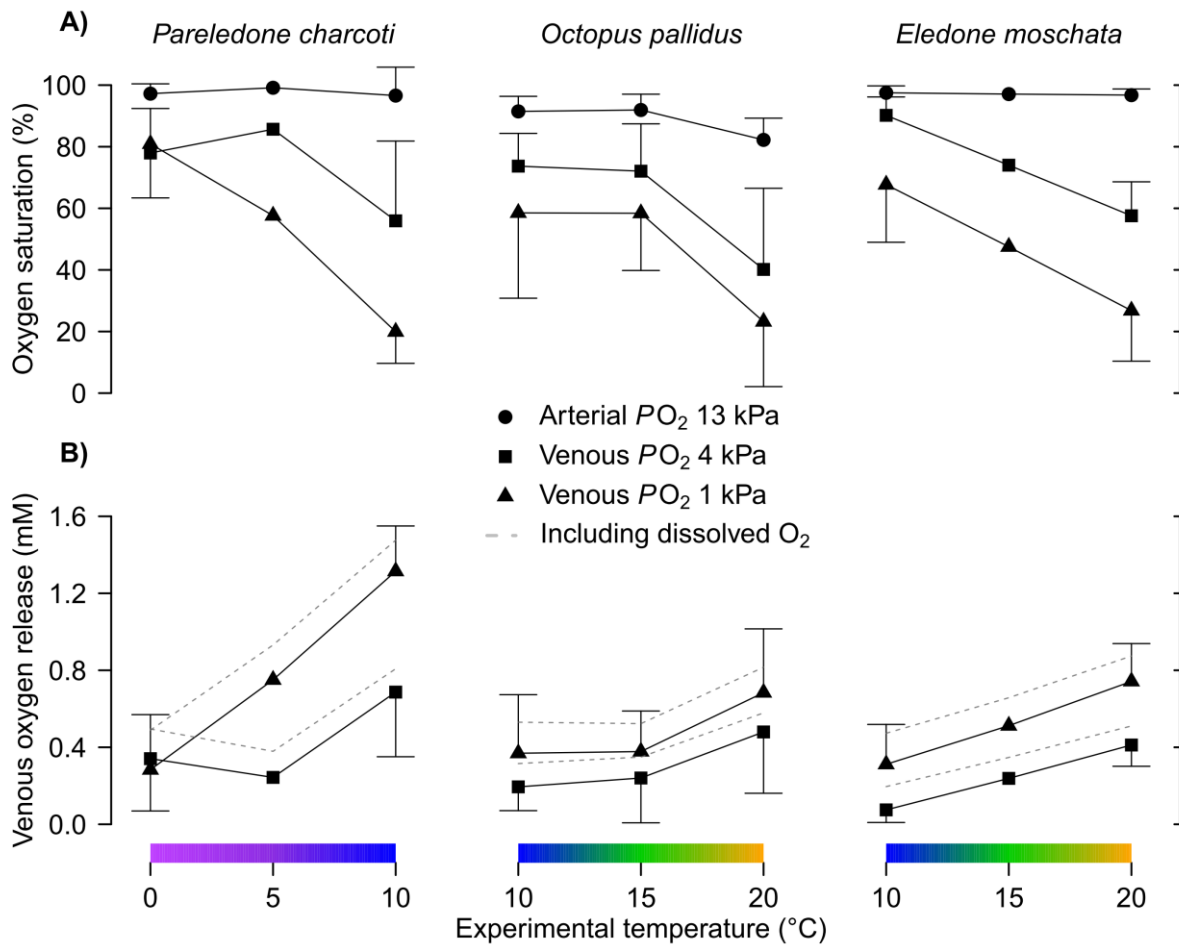


Figure 4

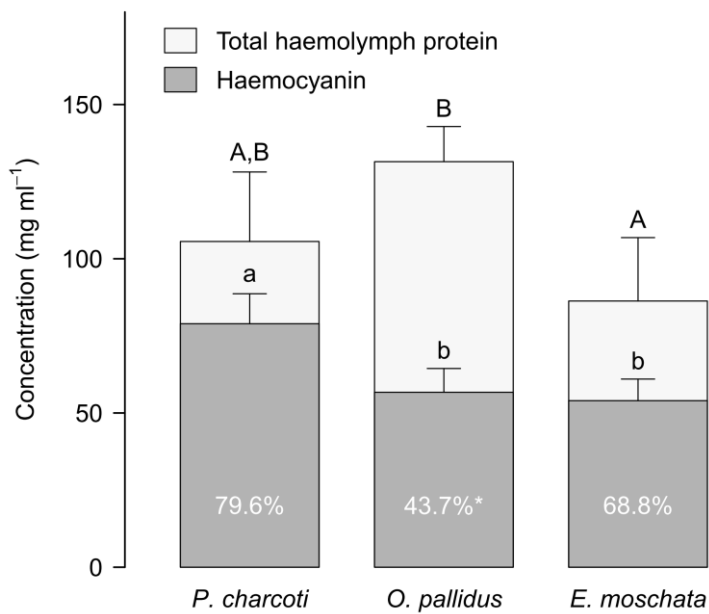


Figure 5

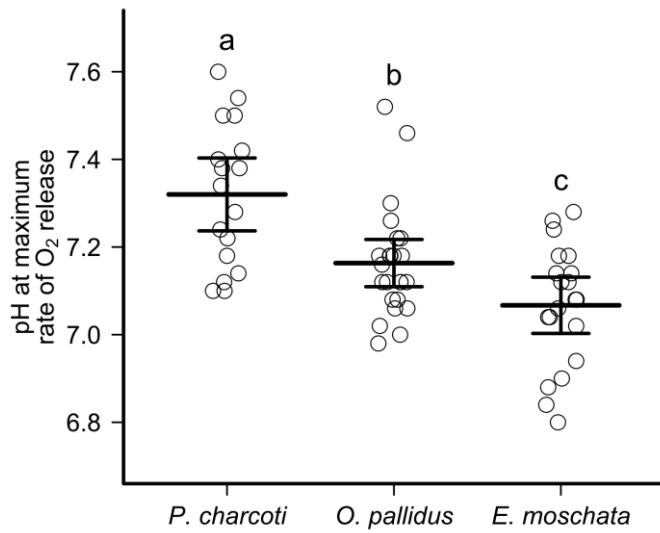


Figure 6

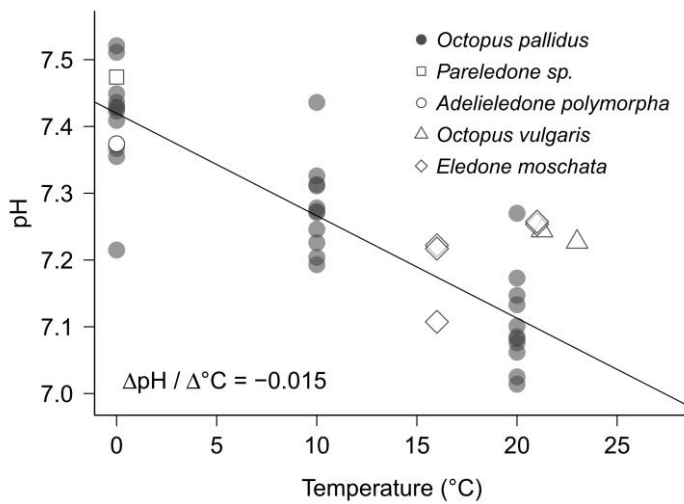
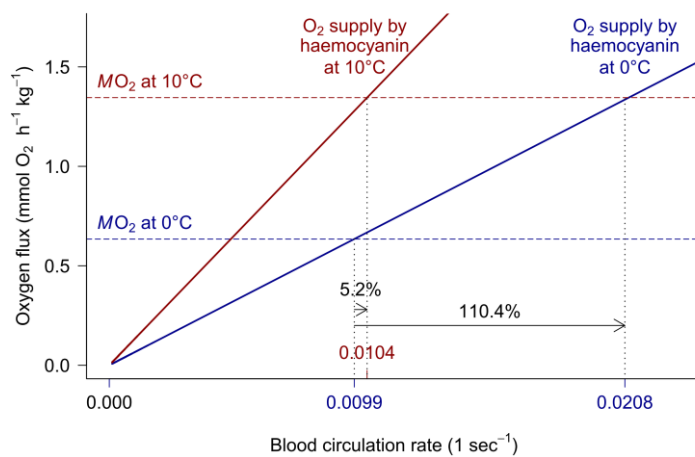


Figure 7



Tables

Table 1

Temperature (°C)	P_{50} (kPa)	Bohr coefficient* (pH range 6.7-7.5) ($\Delta \log P_{50} / \Delta \text{pH}$)	ΔP_{50} (kPa) / °C [#]		Cation concentration (mmol L ⁻¹)				
				Mg ²⁺	Na ⁺	K ⁺	NH ⁴⁺	Ca ²⁺	
<i>Pareledone charcoti</i>									
0	0.41 (NA, pH 7.42)								
5	0.7 (NA, pH 7.34)	-1.22 (-1.67 - -0.78)	0.15 (NA)	52.6 (39.8 - 65.5)	385.5 (348.4 - 422.6)	8.5 (6.7 - 10.2)	6.1 (1.6 - 10.5)	8.8 (7.3 - 10.2)	
10	2.34 (2.19-2.49, pH 7.27)								
<i>Octopus pallidus</i>									
10	1.63 (0.99-2.26, pH 7.27)								
15	1.81 (1.46-2.15, pH 7.19)	-1.97 (-2.50 - -1.44)	0.39 (0.05 - 0.72)	45.6 (41.6 - 49.6)	372.0 (356.2 - 387.8)	10.0 (7.7 - 12.3)	8.6 (3.2 - 13.9)	7.5 (6.7 - 8.2)	
20	6.07 (3.74-8.40, pH 7.11)								
<i>Eledone moschata</i>									
10	0.56 (0.1-1.02 pH 7.27)								
15	1.11 (NA, pH 7.19)	-1.88 (-2.26 - -1.50)	0.21 (0.11 - 0.30)	49.9 (42.2 - 57.6)	386.8 (334.0 - 439.5)	8.8 (6.2 - 11.4)	3.0 (-3.8 - 9.8)	7.3 (5.7 - 8.9)	
20	2.62 (2.00-3.24, pH 7.11)								
ANOVA [†]		$F_{2,16} = 3.71$ $P = 0.048$	$F_{2,7} = 1.58$ $P = 0.271$	$F_{2,17} = 0.78$ $P = 0.475$	$F_{2,17} = 0.31$ $P = 0.739$	$F_{2,17} = 0.85$ $P = 0.446$	$F_{2,17} = 1.35$ $P = 0.285$	$F_{2,17} = 2.28$ $P = 0.133$	

Numbers in brackets indicate the range of 95% confidence intervals

*Data were pooled for temperatures

[#]Based on alpha-stat shifted venous pH and a 10°C temperature interval

[†]ANOVA results for between species comparison

Table 2

Species	Oxygen carrying capacity (mmol L ⁻¹)	Source
<i>Megaleledone setebos</i>	1.86	[27]
<i>Octopus macropus</i>	1.60	[98]
<i>Pareledone charcoti</i>	1.58 (1.38-1.77, 14)	This study
<i>Enteroctopus dofleini</i>	1.36	[99]
<i>Octopus pallidus</i>	1.13 (0.98-1.29, 10)	This study
<i>Eledone moschata</i>	1.08 (0.94-1.22, 10)	This study
<i>Octopus vulgaris</i>	0.61	[30]
Red blooded Antarctic fishes	1.77 (1.44-2.09, 11)	[8]

Figure legends

Figure 1. Lowered affinity of haemocyanin for oxygen in the Antarctic *Pareledone charcoti*.

(A) Oxygen affinity, expressed as the PO_2 of haemocyanin half-saturation, (P_{50}), and (B) venous oxygen saturation of *Pareledone charcoti* were compared to two octopods adapted to warmer waters, *Octopus pallidus* and *Eledone moschata*, at a comparative experimental temperature of 10°C. Calculations refer to an alpha-stat corrected venous pH of 7.27 at 10°C and a venous PO_2 of 1 kPa. Differing letters indicate significant differences ($P < 0.05$) between species.

Figure 2. Oxygen equilibrium curves (OEC) of haemolymph from Antarctic (A-C), South-east Australian (D-F) and Mediterranean (G-I) octopods analysed at various temperatures.

OECs denote the change of oxygen saturation of haemocyanin from high to low pH at constant PO_2 (21, 13, 4, 1 kPa from left to right, [after 81]). For replicated measurements ($n = 5-6$), means and 95% confidence intervals (shaded area) of fitted OECs are displayed. Vertical lines indicate the alpha-stat corrected arterial (dashed) and venous pH (solid). The maximum rate of oxygen release by haemocyanin (i.e. maximum slope of an OEC, $\Delta\text{mmol l}^{-1} / \Delta\text{pH}$, [81]) and its position is indicated by numbers in white circles. The ten degree temperature windows cover habitat temperatures for each species except for *Pareledone charcoti*.

Figure 3. A) Change of arterial and venous oxygen saturation and B) venous oxygen release by octopod haemocyanin with temperature.

Data refer to an arterial PO_2 of 13 kPa and to venous PO_2 for a resting (4 kPa) and exercised (1 kPa) octopus [90, 91]. Venous pH values were alpha-stat corrected for each temperature and arterial pH assumed to be 0.11 pH units higher than venous pH [90]. Venous oxygen release including the contribution by dissolved oxygen is indicated by dashed lines. The ten degree temperature windows cover habitat temperatures for each species except for *Pareledone charcoti*.

Figure 4. Total protein and haemocyanin concentrations in haemolymph of cold and warm adapted octopods.

Haemocyanin concentrations were calculated from the haemolymph oxygen carrying capacity, based on a molecular weight of 3.5 MDa and 70 oxygen binding sites stated

for octopod haemocyanin [59]. Total protein concentration was determined according to Bradford [87]. Bars depict means + 95% C.I., $n = 9-13$. Differing letters indicate significant differences ($P < 0.05$) between octopod species for total haemolymph protein (upper case) or haemocyanin concentrations (lower case). White values on bars indicate the fraction of haemocyanin relative to total haemolymph protein and asterisks significant differences between species.

Figure 5: pH at which the rate of pH-dependent oxygen release becomes maximal.

Comparison between the Antarctic *Pareledone charcoti*, the South-east Australian *Octopus pallidus* and the Mediterranean *Eledone moschata* at an experimental temperature of 10°C. Calculations include OECs from all analysed PO₂. Letters indicate significant differences ($P < 0.05$) between species. Data from different PO₂ were pooled due to similar effects by PO₂ among species.

Figure 6. Observed alpha-stat pH pattern for octopus haemolymph.

The temperature dependent change of pH was determined for thawed *Octopus pallidus* haemolymph at 0°C, 10°C, and 20°C. Venous pH of the other species refer to freshly sampled and analysed haemolymph. pH were corrected to the free hydrogen ion scale by subtracting an experimentally determined offset of -0.136 (0.130-0.142, $n = 87$) pH units to account for the high ionic strength of cephalopod blood [42]. Sources: *Octopus pallidus*, *Pareledone sp.*, *Adelieledone polymorpha* (Strobel and Oellermann 2011, unpublished); *Eledone moschata* (Strobel and Mark 2010, unpublished); *Octopus vulgaris* [90, 91].

Figure 7. Additional release of oxygen by haemocyanin relieves the circulation system of the Antarctic octopod *Pareledone charcoti* at 10°C.

Oxygen that remained bound to haemocyanin at 0°C (blue) was largely liberated at 10°C (red), and thereby reduces the need for increased blood circulation (i.e. expressed as number of times to circulate the whole blood volume per second, 5.2% vs. 110.4% increase in circulation) to match an increased oxygen demand at 10°C. Oxygen supply rates (O₂ release from haemocyanin between 13 and 4 kPa PO₂, solid lines) match oxygen consumption rates of *Pareledone charcoti* (mean MO₂ ± SD, 0.63 mmol O₂ kg⁻¹ (wet mass) h⁻¹ ± 0.12, at 0°C, vertical dashed lines, taken from [7]) at the intersections of both rates at 0°C or 10°C (values indicated on x axis). Oxygen supply comprises the oxygen transported by haemocyanin only without dissolved oxygen or oxygen absorbed via the skin. The MO₂ at 10°C was interpolated assuming a Q₁₀ of 2.12 (average Q₁₀ for

Octopoda taken from [92-94]. The blood volume was assumed to be 5.2% (v/w) based on average literature values from *Octopus vulgaris* and *Enteroctopus dofleini* [95, 96].

Table 1. Comparison of oxygen binding parameters and cation composition of haemolymph between *Pareledone charcoti*, *Octopus pallidus* and *Eledone moschata*.

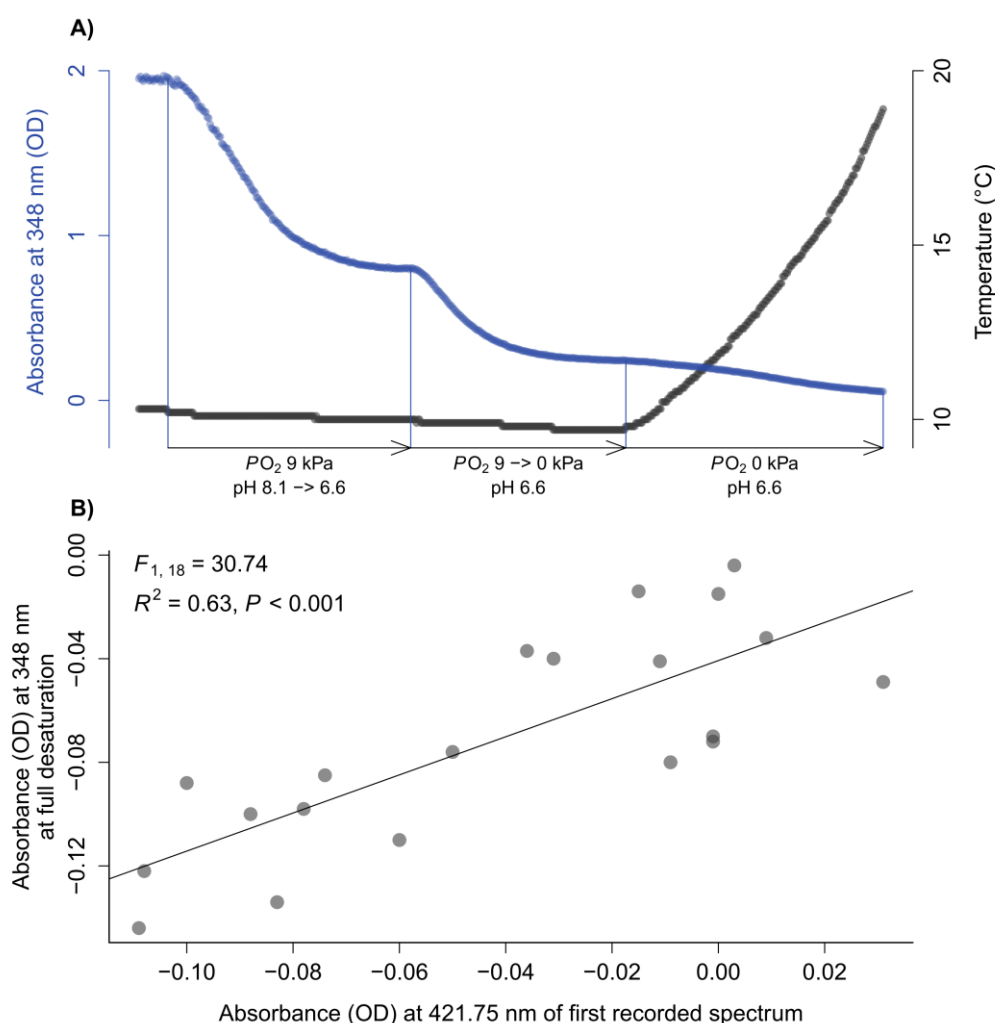
Table 2. Comparison of oxygen carrying capacities.

Values are listed in descending order. Numbers in brackets indicate 95% confidence intervals and samples size n , when available. Oxygen carrying capacities of red blooded Antarctic fishes were calculated from their haemoglobin content, based on a molecular weight of 66 kDa [97], and averaged for 11 species.

Supplementary Material

Supplementary Figure S1. Incomplete desaturation of octopus haemocyanin at low temperatures requires correct identification of the zero calibration point.

(A) At 10°C, haemocyanin of e.g. *Octopus pallidus* fails to fully deoxygenate under pure nitrogen gas and very low pH. Deoxygenation only completes when temperatures increase above 10°C, which complicates the determination of the zero calibration point at low temperature measurement. **(B)** A linear regression between the absorbance at a reference wavelength (421.75 nm) of the first recorded spectrum and the absorbance peak at 348 nm of fully deoxygenated octopus haemocyanin helped to predict the true zero calibration point at low temperatures for low temperature measurements. The reference absorbance signal at 421.75 nm was selected, as the sum of squares of the differences between the predicted and measured zero calibration point across 20 experiments, were lowest at this wavelength.



3.3. Publication III

Positive selection in octopus haemocyanin reveals functional links to
temperature adaptation

M Oellermann, J Strugnell, B Lieb, FC Mark

2015

BMC Evolutionary Biology
(in revision)

Positive selection in octopus haemocyanin reveals functional links to temperature adaptation.

Michael Oellermann¹ §, Jan M. Strugnell², Bernhard Lieb³, Felix C. Mark¹

¹Alfred-Wegener-Institute Helmholtz Centre for Polar and Marine Research, Am Handelshafen 12, 27570 Bremerhaven, Germany

²Department of Genetics, La Trobe Institute for Molecular Sciences, La Trobe University, Bundoora, VIC 3086, Australia

³Institute of Zoology, Johannes Gutenberg-Universität, Müllerweg 6, 55099 Mainz, Germany

§Corresponding author

Email addresses:

MO: oellermann.m@gmail.com

JMS: J.Strugnell@latrobe.edu.au

BL: lieb@uni-mainz.de

FCM: Felix.Christopher.Mark@awi.de

Keywords: cephalopoda, oxygen binding, net surface charge, cold tolerance

Abstract

Background

Octopods have successfully colonised the world's oceans from the tropics to the poles. Yet, successful persistence at these habitats has required adaptations of their advanced physiological apparatus to compensate impaired oxygen supply. Their oxygen transporter haemocyanin plays a major role in cold tolerance and accordingly has undergone functional modifications to sustain oxygen release at sub-zero temperatures. However, it remains unknown how molecular properties evolved to explain the observed functional adaptations. We thus aimed to assess whether natural selection affected molecular and structural properties of haemocyanin that explains temperature adaptation in octopods.

Results

Analysis of 239 partial haemocyanin sequences of the functional unit f and g of 28 octopods species of polar, temperate, subtropical and tropical origin revealed natural selection acting primarily on charge properties of surface residues. Polar octopods contained haemocyanins with more positive net surface charge due to decreased glutamic acid content and higher numbers of basic amino acids. Within the analysed partial sequences, positive selection was present at site 2545, positioned between the active copper binding centre and the protein's surface. At this site methionine was the dominant amino acid in polar octopods and leucine was dominant in tropical octopods. Sites directly involved in oxygen binding or quaternary interactions were highly conserved within the analysed sequence.

Conclusions

This study has provided the first insights into molecular and structural mechanisms that have enabled octopods to sustain oxygen supply from polar to tropical conditions. Our findings imply modulation of oxygen binding via charge-charge interaction at the protein surface, which stabilize quaternary interactions among functional units to reduce detrimental effects of high pH on venous oxygen release. Of the observed partial haemocyanin sequence, residue 2545 formed a close link between the protein surface and the active centre, suggesting a role as allosteric binding site, potentially present in other functional units too. The prevalence of methionine at this site in polar octopods, implies regulation of oxygen affinity via increased sensitivity to allosteric metal binding.

High sequence conservation of sites directly involved in oxygen binding indicates that functional modifications of octopod haemocyanin rather occur via more subtle mechanisms as observed in this study.

Background

For over 400 million years (Lieb and Markl, 2004; Strugnell et al., 2006; Warnke et al., 2011), cephalopods have been vital members of ecosystems spanning tropical to polar regions (Collins and Rodhouse, 2006; Boyle and Rodhouse, 2008). Cephalopods play an important role as both consumers and prey and there are about 800 known extant species (Allcock et al., 2014; Jereb et al., 2014). Despite the fact they are molluscs, cephalopods often directly compete with fishes (Packard, 1972; O'Dor and Webber, 1986). This is facilitated not only by the possession of a highly developed nervous system but particularly due to their advanced oxygen supply system. The cephalopod oxygen supply system is powered by three hearts which pushes blood containing the oxygen carrier haemocyanin around their closed circulatory system (Wells and Smith, 1987; O'Dor and Webber, 1991; Pörtner and Zielinski, 1998).

As ectotherms, cephalopods are required to sustain metabolic performance and thus body functions at their respective habitat temperature. This task seems challenging considering the large temperature variation in temperate climates or the sub-zero temperatures prevailing in polar waters. Temperature has been reported to affect oxygen supply in marine ectotherms and even to cause failure of oxygen supply at the margins of an animal's thermal niche (Pörtner, 2002; Pörtner and Knust, 2007). This has also been confirmed in cephalopods. In the common cuttlefish, *Sepia officinalis*, blood perfusion failed to fuel the increased metabolic demand for oxygen at higher temperatures (Melzner et al., 2007). At lower temperatures however, recent evidence ascribes haemocyanin a major role in limiting cold tolerance (Melzner et al., 2007; Oellermann et al., 2015). This is because the affinity of haemocyanin for oxygen increases as temperature decreases, an effect which decreases oxygen release to the tissues in *Sepia officinalis* and octopods at lower temperatures. However, the Antarctic octopod, *Pareledone charcoti*, was shown to mitigate this detrimental effect by an increased expression of a haemocyanin with lowered affinity for oxygen, and an increased rate of pH dependent oxygen release. This allows haemocyanin of *Pareledone charcoti* to release oxygen at higher pH than haemocyanins from warm water octopods (Oellermann et al., 2015).

While much progress has been made in understanding the underlying molecular and evolutionary mechanisms that explain adaptations of blood oxygen transport in polar fishes (Giordano et al., 2010; Verde et al., 2011), such mechanisms remain unknown in polar ectotherms, which use haemocyanin as blood oxygen carrier. This is surprising, as cephalopod haemocyanins have been considered among the best understood of molluscan respiratory proteins' for over 20 years (Miller, 1995; Bergmann et al., 2006; Gatsogiannis et al., 2007). Between ~3.5-4.0 MDa in size, cephalopod haemocyanins are one of the largest known respiratory pigments (Markl, 2013). They form a single cylinder built from 10 subunits, each composed of a 'chain' of eight (in decapods such as squids and cuttlefish) or seven (in octopods and *Nautilus spp.*) paralogous functional units (FU) termed as FU a, b, c, d (d*), e, f, g (Miller et al., 1998; Gatsogiannis et al., 2007; Markl, 2013). In octopods and *Nautilus*, subunits are 350 kDa in size, with FU a-f forming the wall structure and FU g a collar like structure at the inside of the cylinder (Gatsogiannis et al., 2007; Markl, 2013). Every FU binds one dioxygen molecule to a central pair of copper atoms each coordinated by three histidines, enabling each octopus haemocyanin to carry up to 70 oxygen molecules (Cuff et al., 1998). Recurring duplication events of one subunit coding gene has led to the presence of two or even three haemocyanin isoforms in cephalopods (Miller et al., 1998; Thonig et al., 2014).

Despite the well-established structural details it remains unknown how molecular and structural features evolved to enable haemocyanin mediated oxygen supply in cephalopods at temperatures as low as -1.9°C. We therefore aimed to 1) assess whether natural selection affected the haemocyanin gene and if so, 2) how selection on particular sites or regions may have affected haemocyanin function and 3) lastly if this explains mechanisms of cold adaptation previously observed in octopods (Pörtner and Zielinski, 1998; Zielinski et al., 2001; Oellermann et al., 2015).

In this study we analysed two partial regions of the haemocyanin gene, spanning both, wall- and collar-type functional units and compared them among 28 species of polar, temperate, subtropical and tropical benthic octopods. In this sequence of 396 amino acids, we found 13 sites under positive selection (3.3%) predominantly at the protein's surface suggesting functional modifications via indirect charge-charge interactions that stabilize quaternary interaction among FUs in cold adapted octopods. The presence of a potential allosteric site may further support oxygen release in the cold.

Results

Phylogenetic analysis.

In this study we analysed 59 individuals of 28 benthic octopods species. New sequences obtained in this study included 57 sequences of cytochrome c oxidase subunit I (COI), 57 sequences of cytochrome c oxidase subunit III (COIII) as well as 239 partial haemocyanin sequences (for GenBank ID see Supplementary Figure S1). COI and COIII have been frequently employed to resolve species relationships among cephalopods elsewhere (e.g Bonnaud et al., 1997; Strugnell and Nishiguchi, 2007; Strugnell et al., 2014) and were thus used as a 'phylogenetic standard' in comparison to the haemocyanin phylogeny to identify cues of natural selection. Phylogenetic relationships resulting from Bayesian and maximum likelihood (ML) analyses of COI and COIII sequence data conformed to the most recent classification of octopod families [Figure 5 in (Strugnell et al., 2014)]. The analysed Antarctic octopods included two families; 11 species of the Megaleledonidae sampled in sub-Antarctic and Antarctic waters as well as three species of the Enteroctopodidae exclusively sampled in sub-Antarctic waters (for sample details see Supplementary material S2). Arctic octopods comprised two species of the Bathypolypodidae. Non-polar octopods comprised 12 species; five temperate species represented in the Enteroctopodidae, Eledonidae and the Octopodidae, three subtropical species represented in the Eledonidae and the Octopodidae and four tropical species found in the Octopodidae only (Figure 1).

Two separate phylogenies of the haemocyanin gene based on a 1) 858 bp long region spanning FU f to FU g and a 2) 330 bp long region within the FU g (Figure 2) had some important topological differences to the recent octopod classification (Strugnell et al 2014). For the haemocyanin region FU f-g, all octopod families identified with COI and COIII formed distinct clades as well, yet with the Eledonidae being a well-supported sister group to the Antarctic Megaleledonidae (Figure 3A), which was not the case in the COI/COIII phylogeny (Figure 1). For the haemocyanin region FU g, neither the Antarctic Megaleledonidae nor the Arctic Bathypolypodidae formed monophyletic groups, rather species within these two families were mixed together within a single clade (Figure 3B), despite being distinct families in the COI-COIII phylogeny (Figure 1). Octopodidae species also did not form a well-supported monophyletic group (Figure 3B). The Eledonidae and Enteroctopodidae remained distinct, with the latter forming a

well-supported sister group with the polar Megaleledonidae and Bathypolypodidae (Figure 3B). However, within the COI-COIII phylogeny such relationship was unresolved with these three clades forming a polytomy (Figure 1).

The analysis retrieved at least two isoforms for most families that however were often not easily discernible from allelic variation. Most apparently, in the partial haemocyanin region FU g two distinct isoforms were present, contained in both octopods from warm and cold climates that caused a major split of the phylogeny (Figure 3B). This was at least partly due to the lack of a five amino acid long region (i.e. DPEKG indel) at positions 2638-2643 (positions refer to the full haemocyanin sequence of *Enteroctopus dofleini*, GenBank: O61363) in the FU g isoform 1, which was most frequent in the Bathypolypodidae and the Antarctic Enteroctopodidae (Figure 3B, Supplementary Figure S3).

Natural selection in octopus haemocyanin

The analysed partial haemocyanin regions of FU f-g and FU g spanning the amino acid positions 2306-2708 were highly conserved, as indicated by the Jensen-Shannon Divergence measure [JSD, (Capra and Singh, 2007)] being 0.80 on average (95% C.I. 0.790-0.801, $n = 396$) and larger than 0.73 for more than 90% of positions (Figure 4A). Particularly sites known to be involved in oxygen binding or protein stability such as the copper binding histidines (JSD 0.82-0.89), disulfide or thioether bridge forming cysteines (JSD 0.83-0.89), or other residues within a 7 Å radius of the active site [Figure 4A, (Cuff et al., 1998)]. Pronounced sequence variation was found within the peptide linking the FU f and FU g (positions 2495-2504) as well as at the region flanked by the alpha helix $\alpha 6$ and $\alpha 7$ (positions 2638-2644) located within a structural FU domain rich in α helices (Figure 4A). Variation in the latter was mostly explained by the DPEKG indel at this position (Figure 4A, Supplementary Figure S3).

Analysis of the partial haemocyanin regions revealed both negative as well as positive selection. While negative selection removes alleles that are detrimental to protein function for example and thus 'purifies' genes from sequence variability, positive selection increases the frequency of advantageous alleles. Negative selection prevailed within the analysed haemocyanin regions as indicated 1) by the high conservation of the haemocyanin genes (mean JSD 0.80), 2) predominant negative differences of non-synonymous and synonymous codon substitutions (65% of sites with $dN-dS < 0$ vs. 23% of sites with $dN-dS > 0$) inferred from Single Likelihood Ancestral Counting (SLAC, Figure 4B) as well as 3) by codon based maximum likelihood and Bayesian analysis,

which identified 26% of sites being under significant negative selection (i.e. sites were considered significantly selected if at least three out of seven selection tests were significant at a site, Figure 4C). In contrast, only 13 sites of the analysed 396 codons (3.3%) were identified to be positively selected (Table 1, Figure 4C). Amino acid properties being affected at these positively selected sites included the isoelectric point identified by both, PRIME and TreeSAAP analysis, as well as chemical composition (PRIME only), equilibrium constant (ionization of COOH), alpha helical tendencies and the power to be at the C-terminal (TreeSAAP only, Table 1).

Structural links to protein function

Eleven out of the 13 positively selected sites could be mapped onto the published crystal structure of the haemocyanin FU g (PDB ID: 1JS8, Figure 5). Seven of these sites were located at the protein's surface and only three sites at the inside, despite a surface to buried residue ratio of 0.4 for the whole analysed partial sequence. One site, located in FU g at position 2585, was embedded into a small surface pocket and therefore was neither defined as buried or exposed (Figure 5).

The seven positively selected surface residues as well as the residue at position 2585, were largely characterized by changes of their side chain charge with either substitutions among polar amino acids as the case for most sequences at positions 2602 and 2610, 2409 and 2585 (Table 1) or substitutions between polar and hydrophobic amino acids as the case for most sequences at positions 2383, 2410, 2469 (Supplementary Figure S3). The site at position 2503 was located in the linker region between FU f and FU g and showed the by far highest number of substitution events; 18 non-synonymous substitutions, involving alanine, valine, threonine, or serine (Supplementary Figure S3). Polar changes also affected the residue at position 2496 located at the end of FU f, however this residue could not be mapped onto the published haemocyanin crystal structure.

The buried residues at position 2545 and 2575 were only two or four residues adjacent to the copper binding histidines His2543 or His2571, respectively (Figure 5, Supplementary Figure S3). Position 2545 was characterized by its proximity to both the copper binding His2543 and the protein surface. It was embedded in a surface pocket surrounded by highly conserved neighbours, comprising the hydrophobic Pro2546, Leu2547, Tyr2691 and the hydrophilic His2690 and His2834 as well as the variable residue 2622, which included valine in the FU g isoform 2 and polar serine and threonine in the FU g isoform 1 (Figure 3B). At site 2545, three exclusively hydrophobic amino

acids were present, methionine, isoleucine or leucine, whose side chains were $> 7 \text{ \AA}$ distant from the closest copper binding histidine (His2543) (distances calculated from the haemocyanin FU g model, PDB ID: 1JS8). At position 2575 three different amino acids were present across the alignment; threonine, alanine and valine (Supplementary Figure S3), of which only threonine was able to form polar interaction. The analysis of the structural environment using PhyMol showed that the only polar neighbour in proximity of the polar -OH group was the terminal amino group of His2571 (2.8 \AA), which however, is involved in a peptide bond with Arg2572. The amino groups of the histidine side chains were too distant for any polar interaction [$\geq 5.6 \text{ \AA}$, weak hydrogen bonding and salt bridge formation begins at $\leq 4.0 \text{ \AA}$ (Jeffrey and Jeffrey, 1997; Kumar and Nussinov, 2002)]. The third buried residue 2442 was located within the alpha helix $\alpha 16$ and comprised exclusively aliphatic residues, methionine, isoleucine, leucine or valine (Supplementary Figure S3).

Correlates of temperature adaptation

Based on the predominant positive selection on charge properties of haemocyanin surface residues, we assessed the effect of climate origin of octopods on polar surface residues for each of the two haemocyanin regions. Principal component analysis, based on total counts of each polar amino acid type, showed a distinct separation of species from cold and warm climates, with tropical octopods being most distant from Antarctic and Arctic octopods. Temperate and subtropical octopods overlapped one another and occurred between polar and tropical octopods in the PCA plots with respect to their composition of charged amino acids (Figure 6). The Antarctic Enteroctopodidae, however, did not group with the Antarctic Megaleledonidae but rather with octopods from warmer climates in (FU f-g, Figure 6A) or within a distinct cluster formed by the isoform 1 present in FU g (Figure 6B).

The frequency of glutamic acid increased in both haemocyanin regions towards octopods from warmer climates, except for the Antarctic Enteroctopodidae, and correlated negatively with numbers of positively charged amino acids (His and Arg in FU f-g and Lys in FU g, Figure 6), which accordingly increased by frequency in octopods from polar climates. Numbers of cysteine and tyrosine did not help to explain the divisions between climate origins in both FU regions. The observed pattern persisted also independent of evolutionary relationships. For example temperate octopods from three distinct families grouped closely together (Figure 6B). Similarly Arctic octopods grouped within the Antarctic Megaleledonidae despite these being well understood to

be distinct families (Figure 6A). Due to the climate dependent trend of acidic or basic surface residues, the net charge of surface residues was highly correlated with climate in FU f-g ($P_{\text{Kendall's rank}} < 0.001$, tau -0.386), however not in FU g ($P_{\text{Kendall's rank}} = 0.203$, tau -0.097). The lack of correlation in FU g was due to the differing surface charge properties between the two distinct isoforms present in FU g (Figure 3B). When analysed separately isoform 2 conformed to the high correlation between climate origin and net charge ($P_{\text{Kendall's rank}} < 0.001$, tau -0.494), yet not isoform 1, which showed a slightly positive trend between climate origin and net charge ($P_{\text{Kendall's rank}} = 0.040$, tau 0.34). Separation between the two isoforms in FU g was mostly determined by a higher histidine and lower arginine content in isoform 1 (Figure 6B). Moreover, residue 2545 varied between the three hydrophobic amino acids, of which methionine prevailed in polar and leucine in tropical octopods. Of the 73 haemocyanin sequences from polar octopods 88% contained methionine, 12% isoleucine and 0% leucine. In contrast, of the 13 haemocyanin sequences from tropical octopods, 23% contained methionine (only *H. lunulata*), 0% isoleucine and 77% leucine (three species). Subtropical and temperate octopods showed a mixed pattern for these amino acids (Supplementary Material S3). Lastly, although residue 2503 was highly positively selected there was no correlation with climatic origin ($P_{\text{Kendall's rank}} = 0.179$, tau -0.115).

Discussion

Natural selection in octopus haemocyanin

Mollusc haemocyanin evolved from an α -subclass tyrosinase some 740 million years ago (Lieb et al., 2000; Lieb and Markl, 2004) and has evolved independently of arthropod haemocyanin since this time (van Holde et al., 2001; Aguilera et al., 2013). Cephalopod haemocyanin emerged about 520 million years ago (Lieb and Markl, 2004) with modern coleoid cephalopods (e.g. octopods, squids and sepiids) separating from the ancient and sluggish nautiloids around 420 million years ago (Lieb and Markl, 2004). Since this time, the haemocyanin of coleoid cephalopods has evolved to keep pace with the increased metabolic demands imposed by rising competition with the faster moving fishes (Packard, 1972; O'Dor and Webber, 1986; O'Dor and Webber, 1991). Given the several hundreds of millions of years of evolutionary history, it is thus not surprising that the cephalopod haemocyanin gene underwent extensive purifying selection (Figure 4) leading to widespread sequence conservation as has been confirmed for *Enteroctopus dofleini* (Miller et al., 1998). High conservation of sites being directly involved in oxygen

binding such as the copper binding centre indicate rather indirect mechanisms modulating oxygen binding in octopods.

Nevertheless, comparisons of two partial haemocyanin regions among octopods from various climates revealed evidence for natural selection acting on the *Octopus* haemocyanin gene. This is indicated by phylogenetic deviations between the mitochondrial genes and the two haemocyanin regions (Figure 1, 3) and also by the presence of variable sites within otherwise highly conserved regions (Figure 4A), and lastly pinpointed by sites with increased rates of non-synonymous substitutions confirmed by various selection tests (Figure 4B,C, Table 1). Unfortunately, studies assessing positive selection in mollusc haemocyanins are lacking and at least scarce in other groups. Positive selection was reported for lobster haemocyanins due to high non-synonymous substitution rates estimated for whole sequence regions in some species (Kusche et al., 2003; Padhi et al., 2007), however analysis of single codon sites failed to confirm these findings (Padhi et al., 2007). This first report of positive selection in cephalopod haemocyanin indicates the presence of sites potentially involved in functional adaptation of haemocyanin.

Structural links to protein function

Although *Octopus* haemocyanin contains sites identified to be positively selected one needs to assess their functional relevance. We thus analysed all 13 selected sites for their structural properties to deduce potential functional effects.

Our analyses showed that selection prevailed on residues located at the protein surface, mostly affecting polar/charged properties (Figure 5, Table 1), suggesting functional relevance for tertiary or quaternary interactions. Polar and particularly charged surface residues play a major role in stabilizing contacts among functional units of cephalopod haemocyanin via salt bridges (Gatsogiannis et al., 2007). Further, cooperativity, often found to be pronounced in cephalopods (Brix et al., 1994), has been proposed to operate via various interfaces among all seven FU types (Gatsogiannis et al., 2007). The partial regions analysed in this study are part of FU f and FU g, which interact with other FU via various surface interfaces. These comprise the closely spaced morphological unit interface FU c↔f, the horizontal tier interface FU e↔f and the arc wall interface FU g1/g2↔d as well as the more distant major groove interface FU a↔f and the arc morphological unit interface FU g1↔g2 characterized by weaker interactions (Gatsogiannis et al., 2007). Based on the detailed interface models of *Nautilus* haemocyanin (Gatsogiannis et al., 2007), contact residues for the

morphological unit interface FU c↔f were identified as F2393, 2428WHFDRT2433 and P2479 for the octopods analysed in this study (corresponds to H2401, 2437WKYDRL2442 and H2488 in *Nautilus*). Interestingly, this region did not contain any of the variable and positively selected sites, and in fact, was highly conserved across all 113 sequences (Figure 4A, Supplementary Figure S3). Therefore, the morphological unit interface FU c↔f seems a less likely target for direct functional regulation, although significant sequence differences of haemocyanins between octopods and *Nautilus* suggest further or different contact regions at this interface than proposed for *Nautilus* haemocyanin only. Contact residues for the alternative interfaces FU e↔f, FU g1/g2↔d, FU a↔f and FU g1↔g2 were located outside the analysed sequence region and remain to be assessed in subsequent studies.

Only three buried residues were identified to be positively selected, out of which residue 2545 has high potential to be an allosteric site. This is due to its linking position between the copper binding histidine (His2543) and the nearby protein surface as well as its immediate neighbourhood composed of hydrophobic and hydrophilic amino acids. These create a hydrophobic/hydrophilic contrast, which promotes metal binding, particularly in the presence of the sulfur carrying methionine (Yamashita et al., 1990). A conformational movement of residue 2545 upon allosteric binding could easily transfer to the two amino acid distant copper binding His2543 and affect oxygen binding, as minor shifts of only 0.7 Å between the coordinated copper ions suffice to change oxygenation (Gatsogiannis et al., 2007).

The remaining buried positively selected residues 2575 and 2442 are less likely to be involved in functional regulation. Despite the proximity of site 2575 to the copper binding His2571, neither alanine, valine nor threonine had the possibility to interact directly with the active site. Alanine and valine are very non-reactive (Betts and Russell, 2003) and were too distant to affect the active site. Direct polar interaction of threonine was also unlikely, as the only nearby polar group, the terminal amino group of His2571, was involved in a covalent peptide bond. Moreover, inward facing residues involved at site 2442 were exclusively hydrophobic (methionine, isoleucine, leucine or valine), non-reactive and due to their structural similarity and large distance to the active site unlikely to be involved in functional regulation.

Although variation and positive selection was most significant at site 2503 (Figure 4), functional relevance is rather unlikely. Site 2503 is located at the beginning of the linker region connecting FU f and FU g1/g2 that, like all inter-FU linkers, comprise a long

(34-57 Å), drawn-out sequence between 12-20 amino acids (Gatsogiannis et al., 2007). Given this high length and the capacity to extend further, as linkers are unlikely to extend to their maximum length (Gatsogiannis et al., 2007), there is little chance that the identified substitutions among alanine, valine, threonine, or serine (Supplementary Figure S3) affect the positioning or conformation of the ca. 51 Å distant FU g1/g2.

Correlates of temperature adaptation

Temperature affects oxygen supply (Pörtner, 2002), a challenge that octopods have been required to overcome in order to colonize oceans from the tropics to the poles, where they now thrive at high diversity and abundance (Collins and Rodhouse, 2006). Low temperatures increase the affinity of haemocyanin for oxygen, thus hampering oxygen release to the tissue, to an extent that it limits oxygen supply in cephalopods (Melzner et al., 2007; Oellermann et al., 2015). Antarctic octopods rely on oxygen transported by haemocyanin and evolved functional modifications that sustain oxygen supply at temperatures below zero (Zielinski et al., 2001; Oellermann et al., 2015). So far, our data has highlighted positive selection acting on surface charges and a potential allosteric site. We thus assessed whether this explains differences among octopods from polar, temperate, subtropical or tropical climates and in particular the functional adaptations observed in cold adapted, Antarctic octopods.

The analysis of polar surface residues revealed a clear distinction between cold and warm adapted octopods dominated by a decrease of glutamic acid and an increase of positively charged amino acids towards colder climates, causing a more positive net surface charge in polar octopods. This finding helps to explain how cold adapted octopods attenuate the detrimental effect of increased oxygen affinity. Perutz (1970), provided the first structural explanation for altered oxygen affinity in haemoglobin, based on a His-Asp salt bridge linking two haemoglobin subunits. High ambient pH deprotonate the histidine and disrupt this salt bridge, which destabilizes or dilates the haemoglobin quaternary structure and thus increases oxygen affinity by adjacent subunits. High haemolymph pH prevails in octopods living in polar waters due to the temperature dependency of equilibrium constants (pK) of ionisable groups, particularly the imidazole groups of proteins (Reeves, 1972; Burton, 2002). Haemolymph pH of octopods follows such an imidazole like alpha-stat pattern of -0.0153 pH units / °C [Figure 7A, (Oellermann et al., 2015)]. Given the complex cooperative and highly pH dependent interaction among 70 haemocyanin functional units [Bohr coefficients below -1 , (Bridges, 1994)], such high haemolymph pH contributes to increased oxygen affinity

and to the observed impairment of venous oxygen release (Melzner et al., 2007; Oellermann et al., 2015).

This suggests that cold adaptation involves sustained stability of inter-FU salt bridges to maintain a reasonably low oxygen affinity. The disruption of salt bridges upon pH changes, as they occur during temperature changes, depends on the pK values of their ionisable groups, which are not fixed but variable depending on their protein environment (Pace et al., 2009). Charge-charge interactions at the protein surface, are among the most important factors disturbing the pK of ionisable groups, as evidenced by increased numbers of positively charged lysine, which raised the pK value of several surface residues, up to 2.19 units (Pace et al., 2009). Experimental substitutions from glutamic acid to lysine also confirmed increased stability (1.1 kcal mol⁻¹) due to charge-charge interactions at the surface of Ribonuclease T1 (Grimsley et al., 1999). Therefore, considering a more positive net surface charge in polar octopods, due to increased numbers of positively- and decreased numbers of the negatively charged glutamic acid (Figure 6), charge-charge interactions are likely to raise pK of residues linking FU interfaces. Consequently, salt bridges withstand disturbance by high pH occurring at low temperatures and retain the stability of the haemocyanin quaternary structure and accordingly the affinity for oxygen. This is in good agreement with oxygen binding in the Antarctic octopod *Pareledone charcoti*, which showed a lower oxygen affinity than the subtropical octopod *Eledone moschata* at the same pH and temperature [10°C, (Oellermann et al., 2015)]. This compensation of oxygen affinity was particularly due to a shift of the pH dependent oxygen binding range in *Pareledone charcoti* towards higher pH (Figure 7B). Theoretical buffer lines of surface residues of the partial haemocyanin sequence FU f-g depict the more positive net surface charge in *Pareledone charcoti* compared to *Eledone moschata* at a venous pH of 7.27 (Figure 7C). Further, the proposed charge-charge interactions at the protein surface modulate oxygen binding rather via indirect modifications. This is underpinned by the high conservation of the morphological unit interface FU c↔f and the more uniform distribution of positively selected residues at the protein surface.

The presence of two very distinct isoforms in FU g, which does not follow the observed correlation between net surface charge and climatic origin, also supports the view of functionally divergent isoforms that are regulated via differential expression to enable flexible responses to changing environmental or metabolic conditions (Melzner et al., 2007; Kölsch et al., 2013). It remains to be assessed whether the observed

deviations between the Antarctic Enteroctopodidae and the other polar octopods also reflect a differing oxygen binding behaviour.

Moreover, residue 2545 has the potential as allosteric site and interestingly contained mostly methionine in polar octopods and mostly leucine in tropical octopods. The sulfur atom contained in methionine further facilitates local conditions, marked by a hydrophilic/hydrophobic contrast that promotes allosteric metal binding (Yamashita et al., 1990; Long et al., 2010). If this holds true, polar octopods would be more sensitive to allosteric metal binding than tropical octopods, which provides a reasonable mechanism to exploit for example magnesium as oxygen affinity regulator despite the octopods' inability to regulate extracellular magnesium concentrations (Oellermann et al., 2015).

Conclusions

This study provided the first insights into molecular and structural mechanisms that enabled octopods to sustain oxygen supply at sub-zero temperatures. In particular, we revealed natural selection acting on two partial gene regions of the octopods' oxygen transporter haemocyanin. Predominant selection of charge properties at the protein's surface indicated modulation of oxygen binding behaviour via charge-charge interaction. A more positive net surface charge in cold adapted octopods is suggested to stabilize quaternary structure to sustain a lower oxygen affinity under a high pH environment. Selection of a residue linking the surface with the active site further indicates modulation of oxygen affinity via increased sensitivity to allosteric metal binding in cold adapted octopods. Given the high conservation of numerous functional sites being directly involved in oxygen binding or quaternary interactions, modulation of oxygen binding in octopods may prevail on indirect mechanisms such as altered surface charge properties.

Future studies may further assess the mechanisms pinpointed in this study by means of obtaining complete haemocyanin sequences to permit complete modelling of quaternary interactions, ideally complemented by combined functional and mutational experiments on haemocyanin.

Methods

Study design

To assess whether natural selection and adaptation to particular climates acted on the evolution of cephalopod haemocyanin we performed a comparative analysis using benthic octopods, an ideal study group not only because of their accessibility and similar physiological constitution but particularly because of their diverse presence in all major climates, which strongly facilitates analysis of temperature adaptation. We therefore collected samples of 28 octopod species originating from polar, temperate, subtropical and tropical habitats with species represented in each of the five recognised benthic incirrate octopod families [e.g. Eledonidae, Octopodidae, Enteroctopodidae, Megaleledonidae and Bathypolypodidae (Strugnell et al., 2014)]. We did not sequence the full haemocyanin genes for all species to compromise between a high number of species and costs involved in sequencing multiple isoforms, each being more than 13,000 bp long. We therefore constrained our analysis to a partial coding region of the FU f to represent FUs (a-f), which form the wall structure of the cylindrical haemocyanin decamer, and a partial coding region of the FU g, which forms a relatively loosely connected collar structure inside the cylinder (Gatsogiannis et al., 2007). Due to their distinct quaternary arrangement, functional regulation and thus selection may differ.

Sample acquisition

Samples of octopods were provided by collaborators or purchased from traders except for Antarctic octopods, which were collected during Polarstern cruises ANTXV-3, ANTXVII-3 and ANTXIII-8 (see <http://expedition.awi.de> for cruise- and supplementary material S2 for sample details).

Antarctic octopods were caught using bottom and Agassiz trawls and kept in temperature controlled aquaria until sampling. Prior to sampling, animals were anaesthetized in 3% ethanol (Ikeda et al., 2009) until non-responsive, killed by a final cut through the brain and then opened ventrally for organ removal. Excised organs were immediately frozen in liquid nitrogen or preserved in RNAlater (QIAGEN, Germany) and stored at -80°C.

Any handling and sampling of octopods complied to common ethical and experimental procedures for cephalopods (Sykes et al., 2012) and was registered at the veterinary inspection office, Bremen, Germany (reg. no. 522-27-11/02- 370 00(93)). At the time of sampling, German and EU regulations did not require ethical approval for

cephalopods (Smith et al., 2013). Collection of Antarctic octopods complied with the general guidelines under §1 Umweltschutzprotokolls zum Antarktisvertrag (AUG).

PCR, cloning and sequencing

Genomic DNA was extracted from gill glands, mantle tissue or arm tips using the QIAGEN DNeasy Blood and Tissue kit following the manufacturer's instructions. To construct a species phylogeny for the sampled octopods, we amplified partial sequences of cytochrome c oxidase subunit I (COI) and cytochrome c oxidase subunit III (COIII), which are considered selectively neutral, using polymerase chain reaction (PCR) and the primers detailed in (Folmer et al., 1994; Simon et al., 1994; Allcock et al., 2008). COI and COIII were amplified in 25 µl PCR mix containing final concentrations of 0.5 µmol L⁻¹ dNTPs, 0.05 units µl⁻¹ Taq DNA Polymerase, 1 x Taq buffer (5 Prime, Germany) and 1 µmol L⁻¹ of each Primer. The PCR reaction comprised an initial denaturation at 94°C for 4 mins, followed by 35 cycles at 94°C for 40 s, 50°C (COI) or 42°C (COIII) respectively for 40 s, 68°C for 90 s and a final extension step at 68°C for 10 min.

Regions of the haemocyanin gene were amplified using two pairs of degenerate primers, which bind to conserved sites present across all seven functional units [i.e. amino acid sequence PYWDW and WAIWQ, (Lieb et al., 2001)]. Template specificity was enhanced via Touchdown-PCR in 25 µl reaction volume containing final concentrations of 0.2 µmol L⁻¹ dNTPs, 0.05 units µl⁻¹ DreamTaq DNA Polymerase (Thermo Scientific, Germany), 1 x DreamTaq Green buffer (Thermo Scientific, Germany) and 1 µmol L⁻¹ of each primer. The PCR reaction comprised an initial denaturation at 94°C for 4 mins, 12 cycles at 94°C for 45 s, 60→48°C for 60 s (-1°C/cycle), 72°C for 90 s followed by 35 cycles at 94°C for 45 s, 52°C for 60 s, 72°C for 90 s and a final extension at 72°C for 8 min. PCR products were separated on 1.3% agarose gel containing GelRed (Biotium, U.S.A.) and distinct bands excised and purified using the QIAQuick Gel Extraction Kit (QIAGEN, Germany). Purified PCR fragments were then cloned using the pGEM-T Easy vector system (Promega, Germany) due to the potential binding of the primer pairs at each of the seven FUs, the presence of isoforms as well as alleles. Plasmids of positive clones were purified using the QIAprep Spin Miniprep Kit (QIAGEN, Germany) and tested for successful insertion via an EcoRI (Life Technologies, Germany) restriction digest. Sanger sequencing of products was performed by Eurofins MWG Operon or GATC Biotech AG, Germany. Amplicons were most frequent for the regions FU f-g and FU g comprising fragments of 370 bp or 1090

bp length (Figure 2). Amplicons of other regions were not represented across all sampled species and were thus not included in subsequent analysis.

Phylogenetic analysis

Obtained sequences were assembled and verified by means of their chromatograms and primer sequences were trimmed using Geneious 7.1.5 (Biomatters, New Zealand). Published sequences further supplemented the COI (*Enteroctopus dofleini* [GenBank: GU802397], *Nautilus pompilius* [GenBank: AF120628]), the COIII (*Enteroctopus dofleini* [GenBank: X83103]) and the haemocyanin data sets (*Enteroctopus dofleini* [GenBank: AF338426 & AF020548]). COI and COIII were concatenated and multiple sequence alignments obtained using the MUSCLE plugin of Geneious (Edgar, 2004). The two amplified haemocyanin regions FU f-g and FU g were not concatenated as the presence of multiple isoforms as well as allelic variation did not allow reliable sequence matching. Thus, multiple sequence alignments and subsequent analysis were performed separately for each of the two regions. The intron region between the FU g and FU g was identified by means of the *Enteroctopus dofleini* haemocyanin sequence and trimmed from the alignment. For haemocyanin alignments, 3' and 5' ends were trimmed to obtain a consistent reading frame as well as gap free 3' and 5' ends, which would otherwise have produced false results in the selection analysis. Translated sequences containing stop codons were removed. The quality of the COI/COIII and haemocyanin alignments were tested using GBlocks 0.91b (Castresana, 2000; Talavera and Castresana, 2007) tolerating gap positions within final blocks, which retained between 98-100% of the original alignment. Based on the Akaike Information Criteria (Akaike, 1974), JModeltest 2.1.5 (Darriba et al., 2012) identified the GTR+I+G model for the COI-COIII data set and the HKY85 model for the two haemocyanin regions as the best available substitution models.

Based on the COI-COIII and haemocyanin alignments phylogenetic relationships were inferred using Bayesian and maximum likelihood methods. Bayesian trees were constructed using MrBayes (Huelsenbeck and Ronquist, 2001) as implemented in Geneious (v. 2.0.3) running at least two independent Monte Carlo Markov Chain (MCMC) analysis with 10,000,000 generations sampled every 10,000 generation. The appropriate burnin was chosen based on the resulting traces, which showed a stationary distribution before 10% of the MCMC chain. Maximum likelihood trees were constructed using the PhyML (Guindon and Gascuel, 2003) plugin of Geneious and bootstrap values

calculated from 1000 replicates. *Nautilus pompilius* and *Vampyroteuthis infernalis* were used as outgroups for the COI-COIII phylogeny.

Selection analysis

Prior to selection analysis, we screened both partial haemocyanin regions for conserved and variable sites using the Jensen-Shannon Divergence (Capra and Singh, 2007), which identifies conserved sites as deviations of a probability distribution from the overall amino acid distribution of the respective BLOSUM62 alignment as background and also accounts for conservation in neighbouring sites.

To assess whether natural selection affected the evolution of octopods haemocyanin we employed codon-based Bayesian and maximum likelihood approaches to estimate rates of non-synonymous (dN) to synonymous substitutions (dS). Ratios ≤ 1 denote purifying or negative selection and ratios > 1 diversifying or positive selection. The unrooted haemocyanin phylogenies, without outgroup (Figure 3A, B) were uploaded to the Datamonkey webserver [www.datamonkey.org, (Pond and Frost, 2005; Delpont et al., 2010)] and selection inferred via the following methods. Prior to performing selection tests, alignments were tested for recombination using Genetic Algorithms for Recombination Detection analysis (GARD) implemented in Datamonkey. Single sites under selection were identified using Single Likelihood Ancestral Counting (SLAC), Fixed Effects Likelihood (FEL), Mixed Effects Model of Evolution (MEME), Fast Unconstrained Bayesian AppRoximation (FUBAR), Evolutionary Fingerprinting (EF) as well as PProperty Informed Models of Evolution (PRIME). SLAC estimates and compares normalized expected and observed numbers of synonymous and non-synonymous substitutions at each codon position based on a single ancestral sequence reconstruction (Kosakovsky Pond and Frost, 2005). FEL estimates and compares dN and dS independently for each site (Kosakovsky Pond and Frost, 2005). MEME assesses whether single sites undergo positive as well as episodic diversifying selection along particular branches (Murrell et al., 2012). FUBAR enables larger numbers of site classes and efficiently identifies positively selected sites using a hierarchical Bayesian MCMC routine (Murrell et al., 2013). EF compares 'evolutionary fingerprints' between homologous as well as non-homologous sequences obtained from a posterior sample of a bivariate distribution of dN and dS at each site (Kosakovsky Pond et al., 2010). PRIME resembles FEL or MEME but additionally links an amino acid property category (Atchley et al., 2005; Conant et al., 2007) to the non-synonymous substitution rate. Significance thresholds for selection tests were: $P \leq 0.10$ for SLAC, FEL and MEME; P

≤ 0.05 for PRIME; posterior probability ≥ 0.90 for FUBAR and Bayes factor ≥ 0.50 for EF.

We further employed the software TreeSAAP 3.2 [Selection on Amino Acid Properties using phylogenetic trees, (Woolley et al., 2003)] to analyse which out of 31 amino acid properties are under positive selection. TreeSAAP categorizes these physico-chemical properties into eight magnitudes with low magnitudes being more conservative and high magnitudes being more radical and assesses codon by codon whether the distribution of observed changes of amino acid properties differs from an expected uniform distribution. We considered changes of amino acid properties of codons with magnitudes ≥ 6 and z-scores ≤ 0.001 to be positively selected. In this study, sites were considered positively selected if at least three tests yielded significant results.

Amino acid sites under selection were illustrated with PhyMol 1.3 (Schrodinger, 2010) using the crystal structure of the functional unit g based and the protein sequence of *Enteroctopus dofleini* [PDB ID: 1JS8, (Cuff et al., 1998; Miller et al., 1998)]. The homologous partial haemocyanin region of FU f was aligned with the FU g PDB sequence to match and display positively selected FU f residues on the 3D protein structure.

Analysis of polar surface residues

Polar surface residues were assessed for differences between octopods originating from different climates. First, surface residues of the FU g crystal structure were identified via the GETAREA webserver (Fraczkiewicz and Braun, 1998), setting the radius of the water probe to 1.4. This yielded 65 surface residues for the partial haemocyanin fragment FU f-g and 19 surface residues for the partial haemocyanin fragment FU G. Numbers of each type of polar surface residues as well as net charge (at pH 7.27) were determined and analysed via principal component analysis to assess correlation patterns and the impact of climatic origin.

Sequence processing, statistical analysis and graphical display were performed with the 'R' statistical language (Team, 2014) and the packages 'seqinr' (Charif and Lobry, 2007), 'ape' (Paradis et al., 2004) and 'ade4' (Dray and Dufour, 2007) if not mentioned otherwise.

List of abbreviations used

FU	Functional unit
ML	Maximum likelihood
COI	Cytochrome c oxidase subunit I
COIII	Cytochrome c oxidase subunit III
JSD	Jensen-Shannon Divergence
dN	Rate of non-synonymous codon substitutions
dS	Rate of synonymous codon substitutions
PCR	Polymerase chain reaction
GARD	Genetic algorithm for recombination detection
SLAC	Single Likelihood Ancestral Counting
FEL	Fixed Effects Likelihood
MEME	Mixed Effects Model of Evolution
FUBAR	Fast Unconstrained Bayesian AppRoximation
EF	Evolutionary Fingerprinting
PRIME	PRoperty Informed Models of Evolution

Acknowledgements

We wish to thank all colleagues and technical staff of the Alfred Wegener Institute including Timo Hirse, Nils Koschnick, Fredy Véliz Moraleda and Guido Krieten for cephalopod care and technical assistance. We would like to express our special thanks to the crew of FS Polarstern and all colleagues on board, who helped collecting octopods under harshest conditions. This study was supported by a Journal of Experimental Biology travelling fellowship, a PhD scholarship by the German Academic Exchange Service (DAAD, D/11/43882) to MO, the Deutsche Forschungsgemeinschaft DFG (MA4271/1-2 to FCM) and the Alfred Wegener Institute for Polar and Marine Research.

References

- Aguilera, F., McDougall, C. and Degnan, B.** (2013). Origin, evolution and classification of type-3 copper proteins: lineage-specific gene expansions and losses across the Metazoa. *BMC Evol. Biol.* **13**, 96.
- Akaike, H.** (1974). A new look at the statistical model identification. *Automatic Control, IEEE Transactions on* **19**, 716-723.
- Allcock, A. L., Strugnell, J. M. and Johnson, M. P.** (2008). How useful are the recommended counts and indices in the systematics of the Octopodidae (Mollusca: Cephalopoda). *Biol. J. Linn. Soc.* **95**, 205-218.
- Allcock, A. L., Lindgren, A. and Strugnell, J. M.** (2014). The contribution of molecular data to our understanding of cephalopod evolution and systematics: a review. *J. Nat. Hist.*, 1-49.
- Atchley, W. R., Zhao, J., Fernandes, A. D. and Drüke, T.** (2005). Solving the protein sequence metric problem. *Proc. Natl. Acad. Sci. USA* **102**, 6395-6400.
- Bergmann, S., Lieb, B., Ruth, P. and Markl, J.** (2006). The Hemocyanin from a Living Fossil, the Cephalopod *Nautilus pompilius*: Protein Structure, Gene Organization, and Evolution. *J. Mol. Evol.* **62**, 362-374.
- Betts, M. J. and Russell, R. B.** (2003). Amino acid properties and consequences of substitutions. *Bioinformatics for geneticists* **317**, 289.
- Bonnaud, L., Boucher-Rodoni, R. and Monnerot, M.** (1997). Phylogeny of Cephalopods Inferred from Mitochondrial DNA Sequences. *Mol. Phylogenet. Evol.* **7**, 44-54.
- Boyle, P. and Rodhouse, P.** (2008). Cephalopods: ecology and fisheries: John Wiley & Sons.
- Bridges, C. R.** (1994). Bohr and root effects in cephalopod haemocyanins - paradox or pressure in *Sepia officinalis*? *Mar. Freshw. Behav. Physiol.* **25**, 121-130.
- Brix, O., Colosimo, A. and Giardina, B.** (1994). Temperature dependence of oxygen binding to cephalopod haemocyanins: ecological implications. *Mar. Freshw. Behav. Physiol.* **25**, 149-162.
- Burton, R. F.** (2002). Temperature and acid—base balance in ectothermic vertebrates: the imidazole alaphastat hypotheses and beyond. *J. Exp. Biol.* **205**, 3587-3600.
- Capra, J. A. and Singh, M.** (2007). Predicting functionally important residues from sequence conservation. *Bioinformatics* **23**, 1875-1882.
- Castresana, J.** (2000). Selection of Conserved Blocks from Multiple Alignments for Their Use in Phylogenetic Analysis. *Mol. Biol. Evol.* **17**, 540-552.
- Charif, D. and Lobry, J. R.** (2007). SeqinR 1.0-2: a contributed package to the R project for statistical computing devoted to biological sequences retrieval and analysis. In *Structural approaches to sequence evolution*, pp. 207-232: Springer.
- Collins, M. A. and Rodhouse, P. G. K.** (2006). Southern Ocean Cephalopods. In *Adv. Mar. Biol.*, vol. Volume 50 eds. C. M. Y. Alan J. Southward and A. F. Lee), pp. 191-265: Academic Press.
- Conant, G. C., Wagner, G. P. and Stadler, P. F.** (2007). Modeling amino acid substitution patterns in orthologous and paralogous genes. *Mol. Phylogenet. Evol.* **42**, 298-307.

- Cuff, M. E., Miller, K. I., van Holde, K. E. and Hendrickson, W. A.** (1998). Crystal structure of a functional unit from Octopus hemocyanin. *J. Mol. Biol.* **278**, 855-870.
- Darriba, D., Taboada, G. L., Doallo, R. and Posada, D.** (2012). jModelTest 2: more models, new heuristics and parallel computing. *Nat. Meth.* **9**, 772-772.
- Delport, W., Poon, A. F. Y., Frost, S. D. W. and Kosakovsky Pond, S. L.** (2010). Datamonkey 2010: a suite of phylogenetic analysis tools for evolutionary biology. *Bioinformatics* **26**, 2455-2457.
- Dray, S. and Dufour, A.-B.** (2007). The ade4 package: implementing the duality diagram for ecologists. *J. Stat. Softw.* **22**, 1-20.
- Edgar, R. C.** (2004). MUSCLE: multiple sequence alignment with high accuracy and high throughput. *Nucleic Acids Res.* **32**, 1792-1797.
- Folmer, O., Black, M., Hoeh, W., Lutz, R. and Vrijenhoek, R.** (1994). DNA primers for amplification of mitochondrial cytochrome c oxidase subunit I from diverse metazoan invertebrates. *Mol. Mar. Biol. Biotechnol.* **3**, 294-299.
- Fraczkiewicz, R. and Braun, W.** (1998). Exact and efficient analytical calculation of the accessible surface areas and their gradients for macromolecules. *J. Comput. Chem.* **19**, 319-333.
- Gatsogiannis, C., Moeller, A., Depoix, F., Meissner, U. and Markl, J.** (2007). *Nautilus pompilius* Hemocyanin: 9 Å Cryo-EM Structure and Molecular Model Reveal the Subunit Pathway and the Interfaces between the 70 Functional Units. *J. Mol. Biol.* **374**, 465-486.
- Giordano, D., Russo, R., Coppola, D., Di Prisco, G. and Verde, C.** (2010). Molecular adaptations in haemoglobins of notothenioid fishes. *J. Fish Biol.* **76**, 301-318.
- Grimsley, G. R., Shaw, K. L., Fee, L. R., Alston, R. W., Huyghues-Despointes, B. M., Thurlkill, R. L., Scholtz, J. and Pace, C.** (1999). Increasing protein stability by altering long-range coulombic interactions. *Protein Sci.* **8**, 1843-1849.
- Guindon, S. and Gascuel, O.** (2003). A Simple, Fast, and Accurate Algorithm to Estimate Large Phylogenies by Maximum Likelihood. *Syst. Biol.* **52**, 696-704.
- Huelsenbeck, J. P. and Ronquist, F.** (2001). MRBAYES: Bayesian inference of phylogenetic trees. *Bioinformatics* **17**, 754-755.
- Ikeda, Y., Sugimoto, C., Yonamine, H. and Oshima, Y.** (2009). Method of ethanol anaesthesia and individual marking for oval squid (*Sepioteuthis lessoniana* Férussac, 1831 in Lesson 1830–1831). *Aquac. Res.* **41**, 157-160.
- Jeffrey, G. A. and Jeffrey, G. A.** (1997). An introduction to hydrogen bonding: Oxford university press New York.
- Jereb, P., Roper, C. F. E., Norman, M. D. and Finn, J. K.** (2014). Cephalopods of the world: An annotated and illustrated catalogue of cephalopod species known to date. In *Octopods and Vampire Squids*, vol. 3 (ed. F. a. A. O. o. t. U. Nations), pp. 382. Rome.
- Kölsch, A., Hörnemann, J., Wengenroth, C. and Hellmann, N.** (2013). Differential regulation of hexameric and dodecameric hemocyanin from *A. leptodactylus*. *BBA-Proteins Proteom.* **1834**, 1853-1859.
- Kosakovsky Pond, S. L. and Frost, S. D. W.** (2005). Not So Different After All: A Comparison of Methods for Detecting Amino Acid Sites Under Selection. *Mol. Biol. Evol.* **22**, 1208-1222.

- Kosakovsky Pond, S. L., Scheffler, K., Gravenor, M. B., Poon, A. F. Y. and Frost, S. D. W.** (2010). Evolutionary Fingerprinting of Genes. *Mol. Biol. Evol.* **27**, 520-536.
- Kumar, S. and Nussinov, R.** (2002). Close-range electrostatic interactions in proteins. *Chembiochem : a European journal of chemical biology* **3**, 604-617.
- Kusche, K., Hembach, A., Milke, C. and Burmester, T.** (2003). Molecular characterisation and evolution of the hemocyanin from the European spiny lobster, *Palinurus elephas*. *J. Comp. Physiol. B* **173**, 319-325.
- Lieb, B. and Markl, J.** (2004). Evolution of molluscan hemocyanins as deduced from DNA sequencing. *Micron* **35**, 117-119.
- Lieb, B., Altenhein, B. and Markl, J.** (2000). The sequence of a gastropod hemocyanin (HtH1 from *Haliotis tuberculata*). *J. Biol. Chem.* **275**, 5675-5681.
- Lieb, B., Altenhein, B., Markl, J., Vincent, A., van Olden, E., van Holde, K. E. and Miller, K. I.** (2001). Structures of two molluscan hemocyanin genes: Significance for gene evolution. *Proc. Natl. Acad. Sci. USA* **98**, 4546-4551.
- Long, F., Su, C.-C., Zimmermann, M. T., Boyken, S. E., Rajashankar, K. R., Jernigan, R. L. and Yu, E. W.** (2010). Crystal structures of the CusA efflux pump suggest methionine-mediated metal transport. *Nature* **467**, 484-488.
- Markl, J.** (2013). Evolution of molluscan hemocyanin structures. *Biochim. Biophys. Acta* **1834**, 1840-1852.
- Melzner, F., Mark, F. C. and Pörtner, H. O.** (2007). Role of blood-oxygen transport in thermal tolerance of the cuttlefish, *Sepia officinalis*. *Integr. Comp. Biol.* **47**, 645-655.
- Miller, K., Cuff, M., Lang, W., Varga-Weisz, P., Field, K. and van Holde, K.** (1998). Sequence of the *Octopus dofleini* hemocyanin subunit: structural and evolutionary implications¹. *J. Mol. Biol.* **278**, 827-842.
- Miller, K. I.** (1995). Cephalopod haemocyanins. A review of structure and function. *Mar. Freshw. Behav. Physiol.* **25**, 101-120.
- Murrell, B., Wertheim, J. O., Moola, S., Weighill, T., Scheffler, K. and Pond, S. L. K.** (2012). Detecting individual sites subject to episodic diversifying selection. *PLoS genetics* **8**, e1002764.
- Murrell, B., Moola, S., Mabona, A., Weighill, T., Sheward, D., Kosakovsky Pond, S. L. and Scheffler, K.** (2013). FUBAR : A Fast, Unconstrained Bayesian AppRoximation for inferring selection. *Mol. Biol. Evol.*
- O'Dor, R. K. and Webber, D. M.** (1986). The constraints on cephalopods: why squid aren't fish. *Can. J. Zool.* **64**, 1591-1605.
- O'Dor, R. K. and Webber, D. M.** (1991). Invertebrate athletes: trade-offs between transport efficiency and power density in cephalopod evolution. *J. Exp. Biol.* **160**, 93-112.
- Oellermann, M., Pörtner, H. O., Semmens, J. M. and Mark, F. C.** (2015). Blue blood on ice: modulated blood oxygen transport facilitates cold compensation and eurythermy in an Antarctic octopod. *Frontiers in Zoology* 2015, 12:6.
- Pace, C. N., Grimsley, G. R. and Scholtz, J. M.** (2009). Protein Ionizable Groups: pK Values and Their Contribution to Protein Stability and Solubility. *J. Biol. Chem.* **284**, 13285-13289.

- Packard, A.** (1972). Cephalopods and fish: the limits of convergence. *Biological Reviews* **47**, 241-307.
- Padhi, A., Verghese, B., Vaid, A. and Otta, S. K.** (2007). Pattern of nucleotide substitution and divergence of prophenoloxidase in decapods. *Fish Shellfish Immunol.* **22**, 628-640.
- Paradis, E., Claude, J. and Strimmer, K.** (2004). APE: analyses of phylogenetics and evolution in R language. *Bioinformatics* **20**, 289-290.
- Perutz, M. F.** (1970). Stereochemistry of Cooperative Effects in Haemoglobin: Haem-Haem Interaction and the Problem of Allostery. *Nature* **228**, 726-734.
- Pond, S. L. K. and Frost, S. D. W.** (2005). Datamonkey: rapid detection of selective pressure on individual sites of codon alignments. *Bioinformatics* **21**, 2531-2533.
- Pörtner, H. O.** (2002). Climate variations and the physiological basis of temperature dependent biogeography: systemic to molecular hierarchy of thermal tolerance in animals. *Comp. Biochem. Physiol. Part A Mol. Integr. Physiol.* **132**, 739-761.
- Pörtner, H. O. and Zielinski, S.** (1998). Environmental constraints and the physiology of performance in squids. *S. Afr. J. Mar. Sci.* **20**, 207-221.
- Pörtner, H. O. and Knust, R.** (2007). Climate Change Affects Marine Fishes Through the Oxygen Limitation of Thermal Tolerance. *Science* **315**, 95-97.
- Reeves, R. B.** (1972). An imidazole alaphastat hypothesis for vertebrate acid-base regulation: Tissue carbon dioxide content and body temperature in bullfrogs. *Resp. Physiol.* **14**, 219-236.
- Schrodinger, LLC.** (2010). The PyMOL Molecular Graphics System, Version 1.3r1.
- Simon, C., Frati, F., Beckenbach, A., Crespi, B., Liu, H. and Flook, P.** (1994). Evolution, Weighting, and Phylogenetic Utility of Mitochondrial Gene Sequences and a Compilation of Conserved Polymerase Chain Reaction Primers. *Ann. Entomol. Soc. Am.* **87**, 651-701.
- Smith, J. A., Andrews, P. L. R., Hawkins, P., Louhimies, S., Ponte, G. and Dickel, L.** (2013). Cephalopod research and EU Directive 2010/63/EU: Requirements, impacts and ethical review. *J. Exp. Mar. Biol. Ecol.* **447**, 31-45.
- Strugnell, J. and Nishiguchi, M. K.** (2007). Molecular phylogeny of coleoid cephalopods (Mollusca: Cephalopoda) inferred from three mitochondrial and six nuclear loci: a comparison of alignment, implied alignment and analysis methods. *J. Molluscan Stud.* **73**, 399-410.
- Strugnell, J., Jackson, J., Drummond, A. J. and Cooper, A.** (2006). Divergence time estimates for major cephalopod groups: evidence from multiple genes. *Cladistics* **22**, 89-96.
- Strugnell, J., Norman, M., Vecchione, M., Guzik, M. and Allcock, A. L.** (2014). The ink sac clouds octopod evolutionary history. *Hydrobiologia* **725**, 215-235.
- Sykes, A. V., Baptista, F. D., Gonçalves, R. A. and Andrade, J. P.** (2012). Directive 2010/63/EU on animal welfare: a review on the existing scientific knowledge and implications in cephalopod aquaculture research. *Reviews in Aquaculture* **4**, 142-162.
- Talavera, G. and Castresana, J.** (2007). Improvement of Phylogenies after Removing Divergent and Ambiguously Aligned Blocks from Protein Sequence Alignments. *Syst. Biol.* **56**, 564-577.

- Team, R. C.** (2014). R: A language and environment for statistical computing. Vienna, Austria: R Foundation for Statistical Computing.
- Thonig, A., Oellermann, M., Lieb, B. and Mark, F. C.** (2014). A new haemocyanin in cuttlefish (*Sepia officinalis*) eggs: sequence analysis and relevance during ontogeny. *EvoDevo* **5**, 6.
- van Holde, K. E., Miller, K. I. and Decker, H.** (2001). Hemocyanins and Invertebrate Evolution. *J. Biol. Chem.* **276**, 15563-15566.
- Verde, C., Giordano, D., Russo, R., Riccio, A., Coppola, D. and Di Prisco, G.** (2011). Evolutionary Adaptations in Antarctic Fish: The Oxygen-Transport System. *Oecologia Australis* **15**, 40-50.
- Warnke, K. M., Meyer, A., Ebner, B. and Lieb, B.** (2011). Assessing divergence time of Spirulida and Sepiida (Cephalopoda) based on hemocyanin sequences. *Mol. Phylogenet. Evol.* **58**, 390-394.
- Wells, M. and Smith, P.** (1987). The performance of the octopus circulatory system: a triumph of engineering over design. *Cell. Mol. Life Sci.* **43**, 487-499.
- Woolley, S., Johnson, J., Smith, M. J., Crandall, K. A. and McClellan, D. A.** (2003). TreeSAAP: Selection on Amino Acid Properties using phylogenetic trees. *Bioinformatics* **19**, 671-672.
- Yamashita, M. M., Wesson, L., Eisenman, G. and Eisenberg, D.** (1990). Where metal ions bind in proteins. *Proc. Natl. Acad. Sci. USA* **87**, 5648-5652.
- Zielinski, S., Sartoris, F. J. and Pörtner, H. O.** (2001). Temperature effects on hemocyanin oxygen binding in an Antarctic cephalopod. *Biol. Bull. (Woods Hole)* **200**, 67-76.

Figures

Figure 1

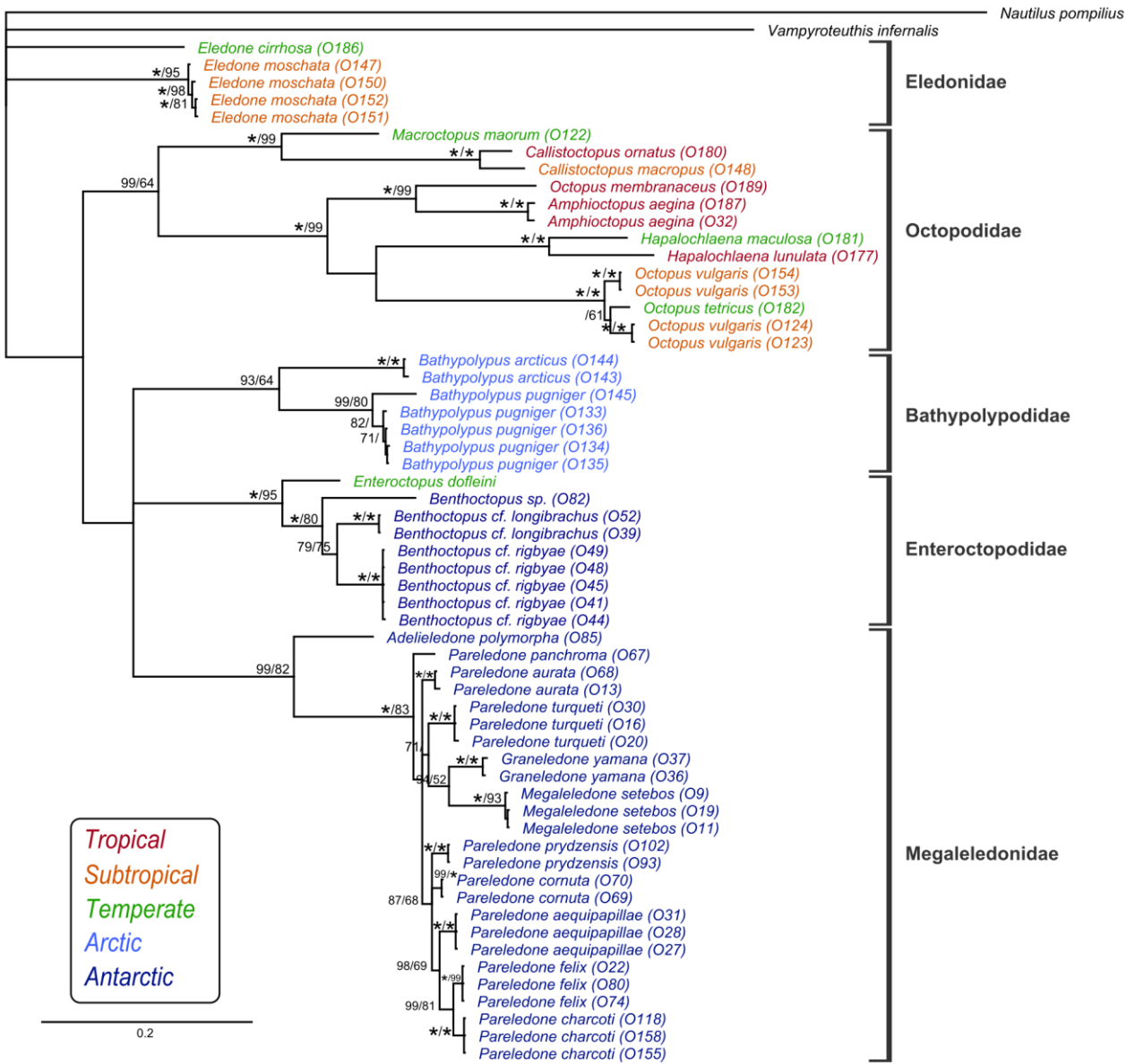


Figure 2

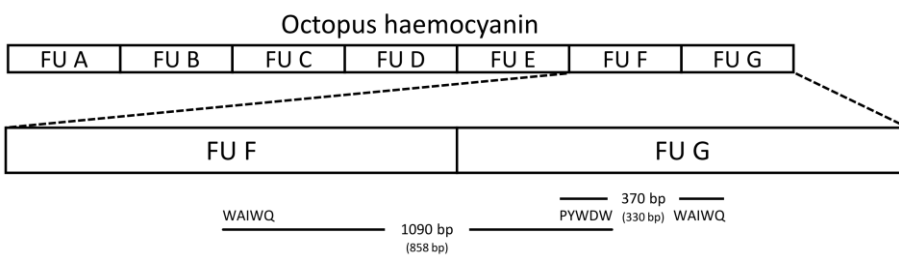
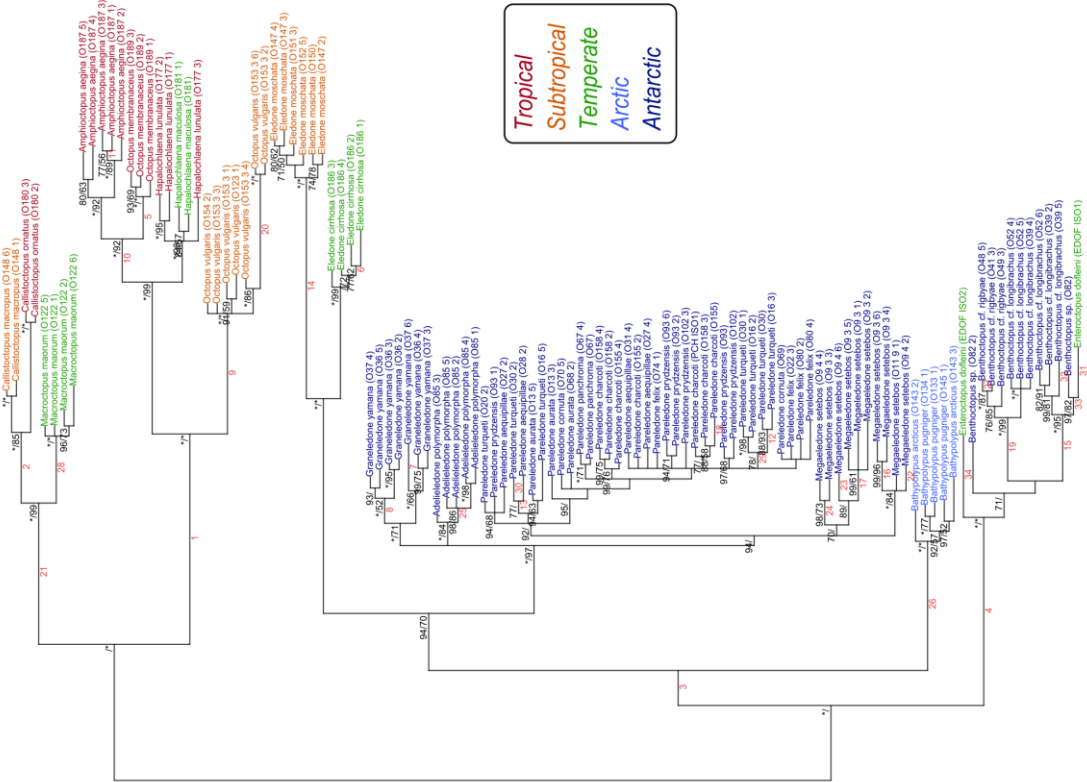


Figure 3

Figure 4

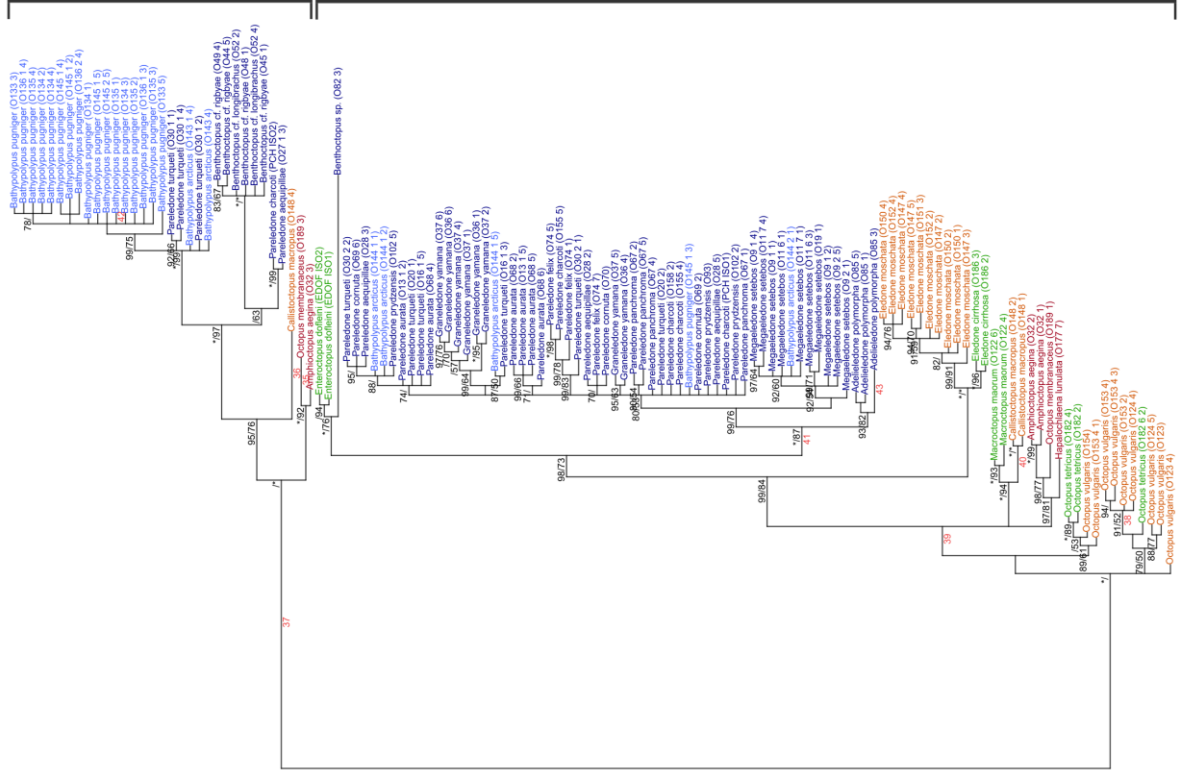
A)

FU f-9



B)

FU 9



Publications

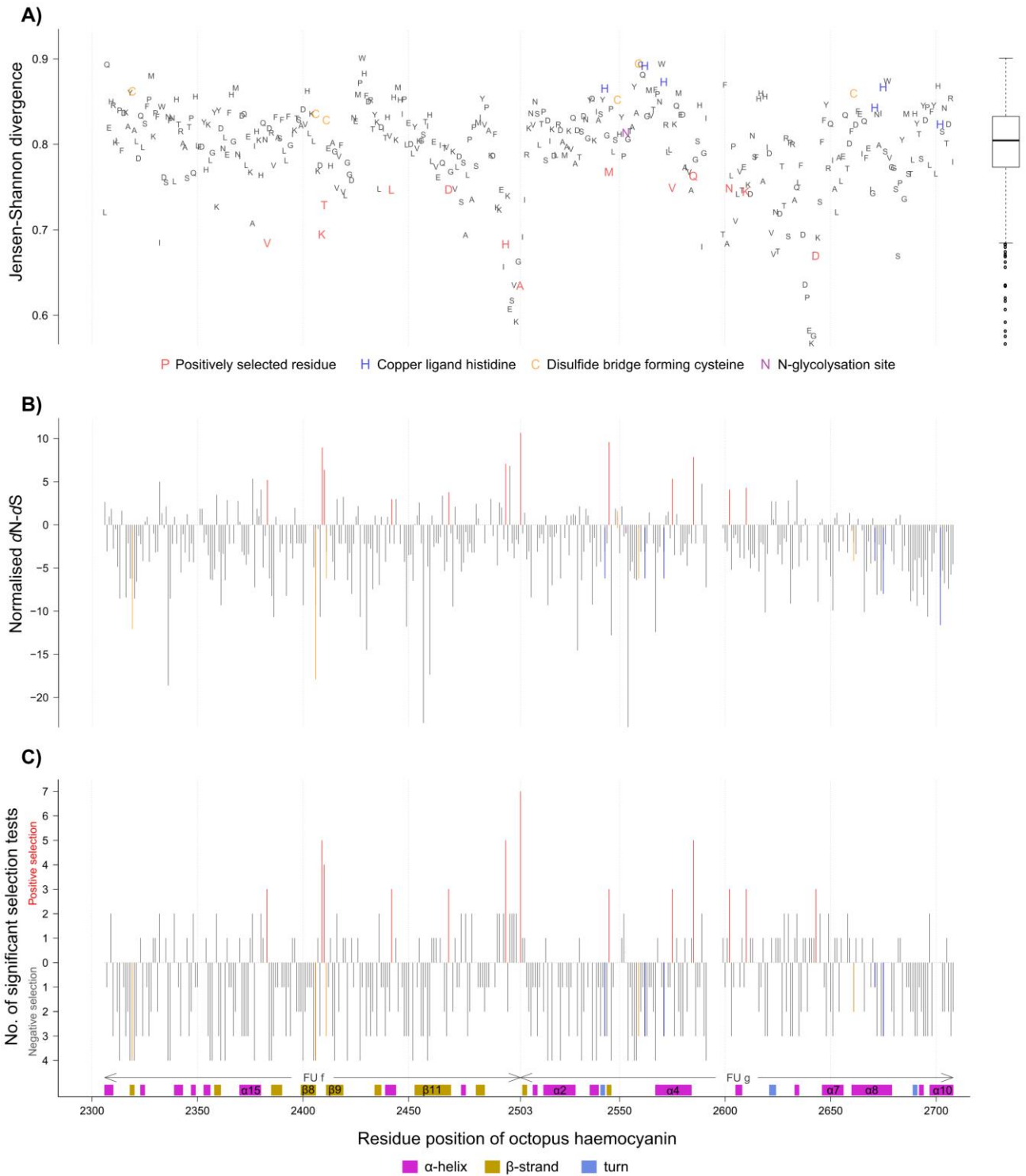
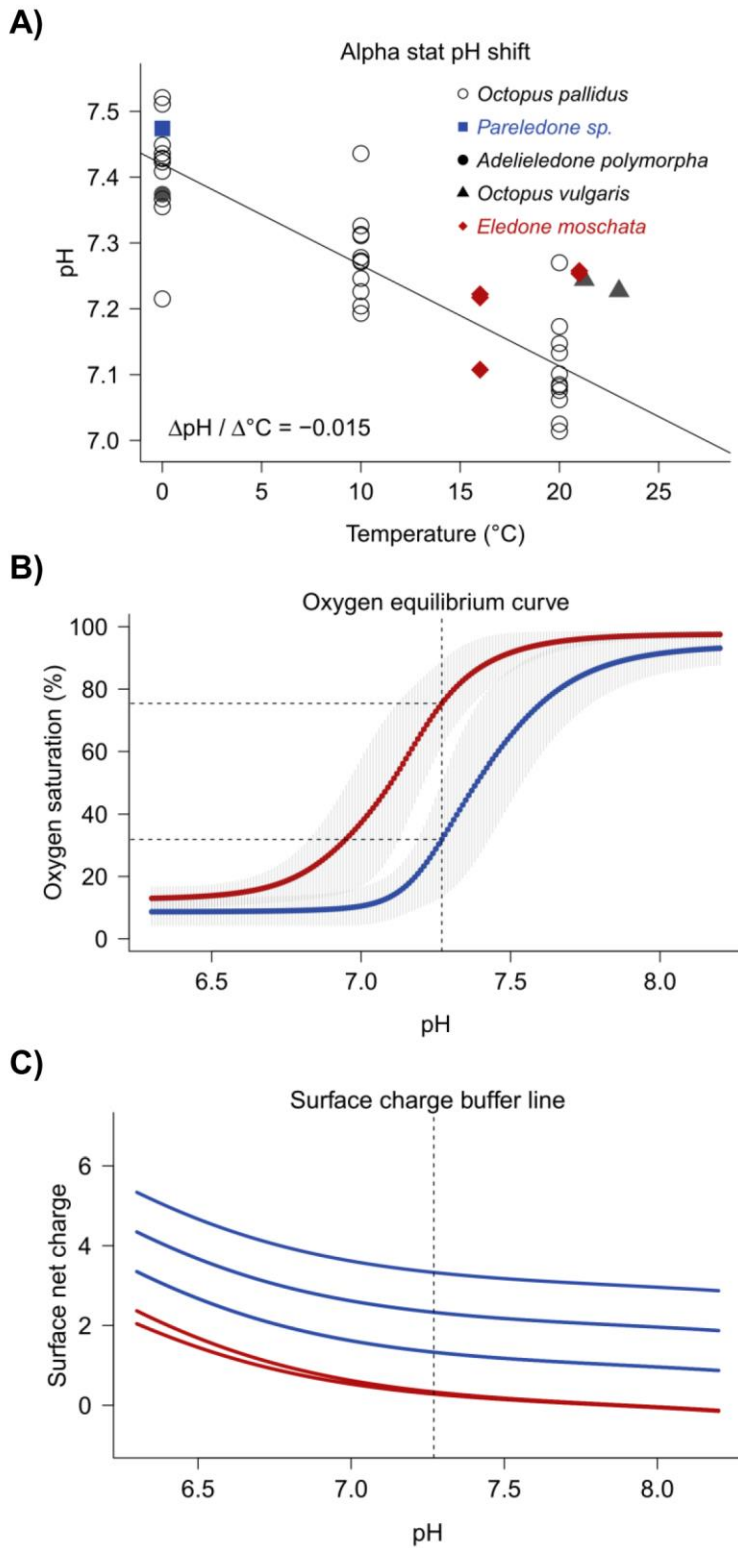


Figure 7



Tables

Residue	SLAC	FEL	MEME	FUBAR	EF	PRIME ^a				TreeSAAP ^c			
						pHi (8)	pK' (8)	pa (6)	PCT (6)				
2383											↓(1) ↑(2-4)		
2409													
2410											↓(5-8)		
2442						(CC)					↓(10) ↑(5,9,11)		
2469						CC						↓(12,13)	
2496										↓(14,15)			
2503						(P)						↓(14,15,22-27) ↑(20)	
2545											↓(4, 20, 28-30) ↑(9,19,31,32)		
2575												↓(33,34)	
2585						pHi	CC	(P)	(V)				
2602										↓(35,36)			↑(35,36)
2610						pHi				↓(37-39) ↑(40,41)			↓(40-42) ↑(37-39)
2643						CC							↓(38)

Significant test result CC Selection for this property (CC) Conservation of this property

^aCC, Chemical Composition; P, Polarity; V, Volume; pHi, Iso-electric point; H, Hydrophathy

^cpHi isoelectric point; pK' equilibrium constant (ionization of COOH); pa alpha helical tendencies; PCT Power to be at the C-terminal (Magnitude of amino acid change)

Figure legends

Figure 1 – Bayesian phylogenetic tree illustrating species and family relationships among the analysed octopods.

Bayesian analysis was performed on concatenated data sets of the mitochondrial genes cytochrome oxidase subunit I (COI) and cytochrome oxidase subunit III (COIII). Colours represent the climatic origin. Nodes were labelled with posterior probabilities and maximum likelihood bootstrap support values following a backslash, above a threshold of 0.7 or 0.5 respectively. Asterisks mark values of 100. Identical colours mark octopods of the same climatic origin.

Figure 2 – Schematic illustration of the functional units of the octopus haemocyanin gene and the partial regions analysed in this study.

Conserved binding sites of the degenerate forward and reverse primers are marked with the corresponding amino acid sequence WAIWQ or PYWDW. Resulting amplicons spanned a region between the functional units F and G and a region within the functional unit g. Fragment lengths are indicated before (in line) and after sequence trimming (in parentheses). Amplicons from other functional units were not considered (see study design).

Figure 3 – Haemocyanin based phylogenetic relationships among the analysed octopods.

Bayesian phylogenetic trees based on the nucleotide alignments of **A)** a partial haemocyanin region between FU f and FU g **B)** a partial haemocyanin region between within FU g (see Figure 2). Note that within FU g two distinct isoforms were present causing a split in the phylogeny. Nodes were labelled with posterior probabilities and maximum likelihood bootstrap support values following a backslash, above a threshold of 0.7 or 0.5 respectively. Asterisks mark values of 100. Red italic numbers below branches indicate positive selection of a particular site at this branch inferred from TreeSAAP analysis (refer to Table 1). Identical colours mark octopods of the same climatic origin.

Figure 4 – A) Protein sequence conservation B) differences between non-synonymous and synonymous substitutions ($dN-dS$) and C) natural selection in octopus haemocyanin.

A) Sequence conservation was estimated using the Jensen-Shannon divergence (Capra and Singh, 2007), which identifies conserved sites as deviations of a probability distribution from the overall amino acid distribution of the respective BLOSUM62 alignment as background and also accounts for conservation in neighbouring sites. Greater scores indicate higher sequence conservation. **B)** Nucleotide substitution pattern analysis was based on estimated differences of non-synonymous and synonymous changes ($dN-dS$) at each site of the haemocyanin nucleotide sequence inferred from Single Likelihood Ancestral Counting (SLAC) normalised to the total length of the underlying maximum likelihood tree. **C)** The y-axis indicates the cumulative number of selection tests that yielded significant results for positive or negative selection at an individual site. Positively selected sites confirmed by two or more tests were marked red. All analysis was performed for two separate alignments, containing 113 or 126 sequences respectively, and covering in total a 396 amino acid long coding region of the haemocyanin's functional units F and G. Residue positions refer to the published full haemocyanin sequence of *Enteroctopus dofleini* (UniProt accession no. O61363) (Cuff et al., 1998; Miller et al., 1998). Significance thresholds were: p-values ≤ 0.10 for SLAC, ≤ 0.10 for FEL, MEME and PRIME; Posterior Probability ≥ 0.90 for FUBAR; Bayes Factor ≥ 0.50 for EF.

Figure 5 – Steric arrangement of positively selected sites in octopus haemocyanin.

The 3D model represents the haemocyanin molecule of the functional unit g of *Enteroctopus dofleini* [PDB ID: 1JS8, (Cuff et al., 1998)]. Positively selected sites were marked red and labelled with its residue number. Copper ligand histidines were marked blue. Due to strong homology, positions of positively selected sites from functional unit F could be mapped onto the FU g 3D structure. 3D structures below illustrate positively selected sites located at the protein surface.

Figure 6 – Principal component analysis for polar surface residues of octopus haemocyanin.

The analysis was performed separately **A)** for 65 surface residues of the partial haemocyanin fragment FU f-g and **B)** for 19 surface residues of the partial haemocyanin fragment FU g. Surface residues were identified for the haemocyanin structural model (PDB ID: 1JS8) using GETAREA (Fraczkiewicz and Braun, 1998). PCA variables comprised the total number of each type of polar surface residue as well as their total net charge. Identical colours mark octopods of the same climatic origin. Rectangles mark the centroid of the respective climatic group. PCA scores were abbreviated with species names as followed: Apo *Adelieledone polymorpha*, Bar *Bathypolypus arcticus*, Blo *Benthooctopus longibrachus*, Bpu *Bathypolypus pugniger*, Bri *Benthooctopus rigbyae*, Bsp *Benthooctopus sp.*, Cma *Callistoctopus macropus*, Cor *Callistoctopus ornatus*, Eci *Eledone cirrhosa*, Edo *Enteroctopus dofleini*, Emo *Eledone moschata*, Gya *Graneledone yamana*, Hlu *Hapalochlaena lunulata*, Hma *Hapalochlaena maculosa*, Mma *Macroctopus maorum*, Mse *Megaeledone setebos*, Ome *Octopus membranaceus*, Ovu *Octopus vulgaris*, Pae *Pareledone aequipillae*, Pau *Pareledone aurata*, Pch *Pareledone charcoti*, Pco *Pareledone cornuta*, Pfe *Pareledone felix*, Ppa *Pareledone panchroma*, Ppr *Pareledone prydzensis*, Ptu *Pareledone turqueti*.

Figure 7: Functional and structural pH dependence.

A) *Alpha-stat* pH change of octopod haemolymph. **B)** Differences between the Antarctic *Pareledone charcoti* (blue) and the Mediterranean *Eledone moschata* (red) regarding pH dependent oxygen binding at 10°C and 1kPa PO₂ (shaded area denotes 95% C.I., n = 5) and **C)** net surface charge of the partial haemocyanin region FU f-g at pH 7.27 based on six partial haemocyanin sequences for each species, whose buffer lines partly overlap. The dashed vertical line indicates the venous pH at 10°C interpolated from A).

Table 1 – Positively selected sites in octopus haemocyanin.

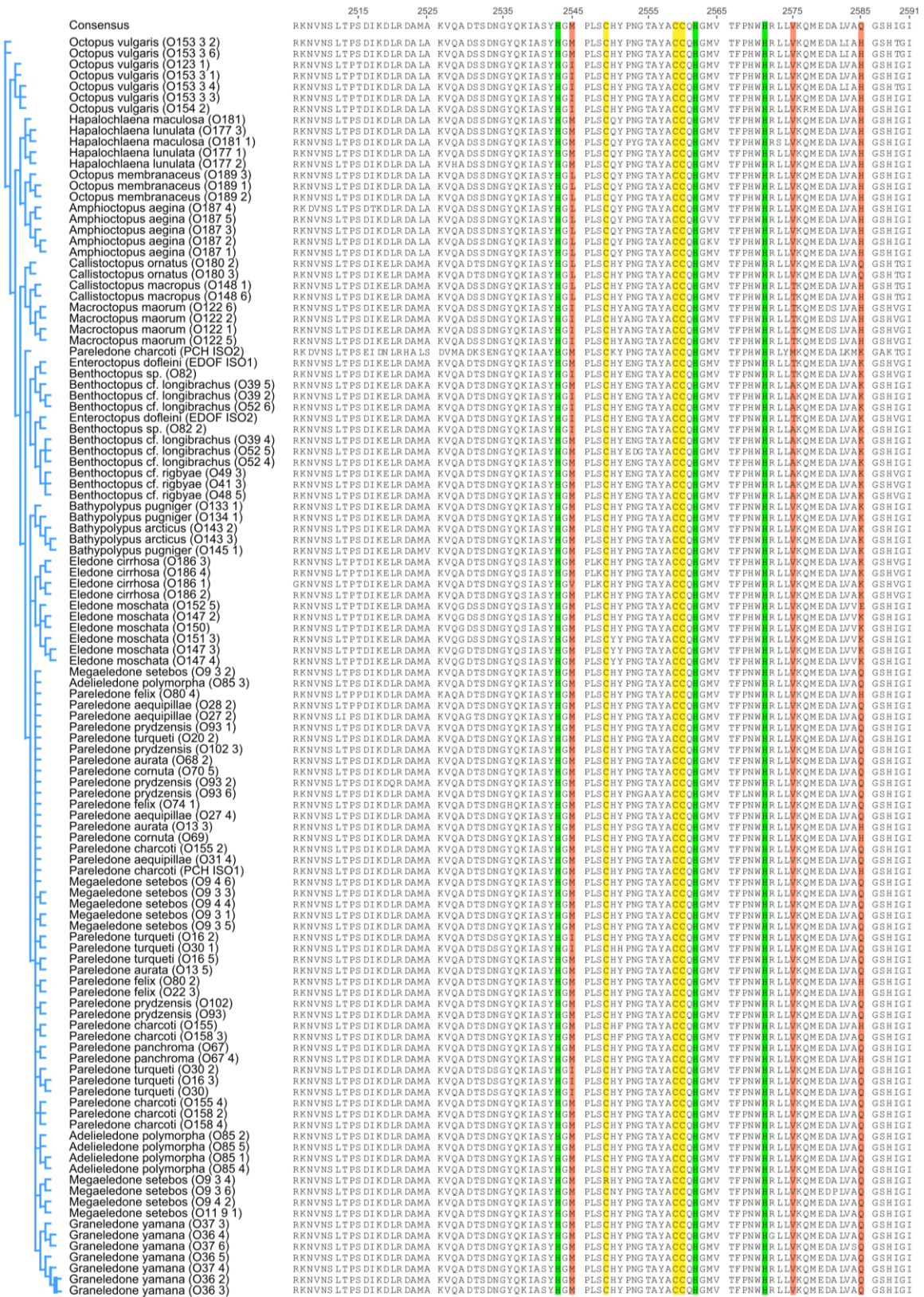
Sites at which at least three or more selection tests identified significant positive selection. Analysis was performed for two separate alignments, containing 113 or 126 sequences respectively, and covering in total a 396 amino acid long region of the haemocyanin's functional units f and g. Numbering of positions refers to the published full haemocyanin sequence of *Enteroctopus dofleini* (UniProt accession no. O61363) (Cuff et al., 1998; Miller et al., 1998). Significance thresholds were: $P \leq 0.10$ for SLAC, ≤ 0.10 for FEL, MEME and PRIME; Posterior Probability ≥ 0.90 for FUBAR; Bayes Factor ≥ 0.50 for EF. See Supplementary Table S4 for detailed results.

Supplementary Material

Supplementary Figure S1 – Location and sampling details of octopods used in this study. Note that for samples obtained from collaborators and commercial traders details are incomplete and that locations marked in red provide only an approximate location of origin.

Animal identifier	Species	Cruise	Station	Fishing gear	Date of capture	Latitude (degrees_north)	Longitude (degrees_east)	Bot. Depth (m)	Location	Temperature at depth (°C)	Salinity (psu)	Total weight (g)	Gutted weight (g)	Mantle Length (cm)	Sex	Comment
O85	<i>Adelieledone polymorpha</i>	ANTXXVII-3	PS 77260-6	Agassiz Trawl	20.03.2011	-70.51	-10.36	253	Antarctic Ocean, Eastern Weddel Sea	-	-	83.3	-	6.1	female	-
O87	<i>Amphioctopus aegina</i>	-	-	-	-	5.48	89.47	-	Indian Ocean	-	-	-	-	-	-	Asia market
O32	<i>Bathypolypus aegina</i>	-	2123	-	24.09.2007	79.13	26.10	256	Barents Sea	-	-	-	-	-	-	-
O143	<i>Bathypolypus arcticus</i>	-	2022	-	12.09.2007	78.97	11.57	315	Barents Sea	-	-	-	-	-	-	-
O133	<i>Bathypolypus puginger</i>	-	2035	-	12.09.2007	79.62	8.00	688	Barents Sea	-	-	-	-	-	-	-
O134	<i>Bathypolypus puginger</i>	-	2035	-	13.09.2007	79.62	8.00	688	Barents Sea	-	-	-	-	-	-	-
O135	<i>Bathypolypus puginger</i>	-	2035	-	13.09.2007	79.62	8.00	688	Barents Sea	-	-	-	-	-	-	-
O136	<i>Bathypolypus puginger</i>	-	2334	-	0.08.2007	73.17	18.07	443	Barents Sea	-	-	-	-	-	-	-
O145	<i>Bathypolypus puginger</i>	-	2666	-	17.08.2007	71.27	28.62	409	Barents Sea	-	-	-	-	-	-	-
O39	<i>Benthinotopus cf. longibrachus</i>	ANTXXVII-3	PS 77208-5	Agassiz Trawl	11.02.2011	-54.32	-56.10	292	Antarctic Ocean, Burwood Bank	4.9	34.1	5.1	2.4	-	-	
O52	<i>Benthinotopus cf. longibrachus</i>	ANTXXVII-3	PS 77211-5	Agassiz Trawl	14.02.2011	-54.32	-42.41	320	Antarctic Ocean, Shag Rocks	2.1	34.4	-	2.7	-	-	
O41	<i>Benthinotopus cf. rigolyae</i>	ANTXXVII-3	PS 77208-5	Agassiz Trawl	11.02.2011	-54.32	-56.10	292	Antarctic Ocean, Burwood Bank	4.9	34.1	-	-	-	-	
O44	<i>Benthinotopus cf. rigolyae</i>	ANTXXVII-3	PS 77208-5	Agassiz Trawl	11.02.2011	-54.32	-56.10	292	Antarctic Ocean, Burwood Bank	4.9	34.1	-	-	-	-	
O45	<i>Benthinotopus cf. rigolyae</i>	ANTXXVII-3	PS 77208-5	Agassiz Trawl	11.02.2011	-54.32	-56.10	292	Antarctic Ocean, Burwood Bank	4.9	34.1	-	-	-	-	
O46	<i>Benthinotopus cf. rigolyae</i>	ANTXXVII-3	PS 77208-5	Agassiz Trawl	11.02.2011	-54.32	-56.10	292	Antarctic Ocean, Burwood Bank	4.9	34.1	-	-	-	-	
O48	<i>Benthinotopus cf. rigolyae</i>	ANTXXVII-3	PS 77208-3	Agassiz Trawl	11.02.2011	-54.32	-56.10	292	Antarctic Ocean, Burwood Bank	4.9	34.1	-	-	-	-	
O148	<i>Benthinotopus sp.</i>	ANTXXVII-3	PS 77208-3	Bottom Trawl	11.02.2011	-54.32	-56.10	286	Antarctic Ocean, Burwood Bank	4.9	34.1	11.3	-	2.1	male	-
O149	<i>Callinectes macropus</i>	-	-	-	Summer 2010	35.2	38.63	-	Mediterranean Sea, Cyprus	-	-	-	-	-	-	-
O180	<i>Callinectes ornatus</i>	-	-	-	-	18.20	146.90	-	Pacific Ocean, Western Australia	-	-	-	-	-	-	-
O186	<i>Eledone cirrata</i>	-	-	-	-	68.60	-4.29	-	North Atlantic Ocean, Western Australia	-	-	-	-	-	-	-
O147	<i>Eledone moschata</i>	-	-	-	Summer 2010	35.13	33.43	-	Mediterranean Sea, Cyprus	-	-	460.2	-	-	-	-
O150	<i>Eledone moschata</i>	-	-	-	2008	45.22	12.28	-	Mediterranean Sea, Italy, Chioggia	-	-	-	-	-	-	male
O151	<i>Eledone moschata</i>	-	-	-	2008	45.22	12.28	-	Mediterranean Sea, Italy, Chioggia	-	-	-	-	-	-	-
O152	<i>Eledone moschata</i>	-	-	-	2008	45.22	12.28	-	Mediterranean Sea, Italy, Chioggia	-	-	-	-	-	-	-
O36	<i>Granelledone yamana</i>	ANTXXVII-3	PS 77208-5	Agassiz Trawl	11.02.2011	-54.32	-56.10	292	Antarctic Ocean, Burwood Bank	4.9	34.1	363.6	-	8	male?	-
O37	<i>Granelledone yamana</i>	ANTXXVII-3	PS 77208-5	Agassiz Trawl	11.02.2011	-54.32	-56.10	292	Antarctic Ocean, Burwood Bank	4.9	34.1	746	-	13	male?	-
O177	<i>Haplochlathra lunulata</i>	ANTXXVII-3	PS 77208-5	Agassiz Trawl	-	-11.35	137.62	-	Pacific Ocean, Eastern Australia	-	-	-	-	-	-	-
O181	<i>Haplochlathra maculosa</i>	ANTXXVII-3	PS 77208-5	Agassiz Trawl	-	-38.72	144.81	-	Pacific Ocean, South-Eastern Australia	-	-	-	-	-	-	-
O122	<i>Macroctopus maorum</i>	ANTXXVII-3	PS 69650	Bottom Trawl	December 2012	-44.83	169.63	-	New Zealand, Otago	-	-	-	-	-	-	-
O11	<i>Megaleledone setebos</i>	ANTXXIII-8	PS 69676	Bottom Trawl	28.12.06	-61.29	-56.20	330	Antarctic Ocean, Elephant Island	-	-	-	-	4.52	female	-
O19	<i>Megaleledone setebos</i>	ANTXXIII-8	PS 69676	Bottom Trawl	02.01.07	-62.18	-60.79	418	Antarctic Ocean, Antarctic Peninsula	-	-	-	-	8	male	-
O9	<i>Megaleledone setebos</i>	ANTXXIII-8	PS 69638	Bottom Trawl	26.12.06	-61.16	-56.00	149	Antarctic Ocean, Elephant Island	-	-	-	-	16	male	-
O189	<i>Octopus membranaceus</i>	-	-	-	-	-2.00	87.00	-	Indian Ocean	-	-	-	-	-	-	-
O182	<i>Octopus tetricus</i>	-	-	-	-	-31.99	115.72	-	Indian Ocean, Western Australia	-	-	-	-	-	-	-
O123	<i>Octopus vulgaris</i>	-	-	-	05.01.2012	22.13	114.17	-	Indian Ocean, China, Hongkong	-	-	-	-	-	-	-
O124	<i>Octopus vulgaris</i>	-	-	-	2011	23.67	128.86	-	Pacific Ocean, Taiwan	-	-	-	-	-	-	-
O153	<i>Octopus vulgaris</i>	-	-	-	September 2008	42.49	3.14	-	Mediterranean Sea, France, Banuyls	-	-	-	-	-	-	-
O154	<i>Octopus vulgaris</i>	-	-	-	September 2008	42.49	3.14	-	Mediterranean Sea, France, Banuyls	-	-	-	-	-	-	-
O27	<i>Pareledone aequilliae</i>	ANTXXIII-8	PS 69687	Bottom Trawl	04.01.07	-62.59	-54.77	263	Antarctic Ocean, Antarctic Peninsula	-	-	-	-	6.16	male	-
O28	<i>Pareledone aequilliae</i>	ANTXXIII-8	PS 69687	Bottom Trawl	04.01.07	-62.59	-54.77	263	Antarctic Ocean, Antarctic Peninsula	-	-	-	-	4.79	female	-
O31	<i>Pareledone aequilliae</i>	ANTXXIII-8	PS 69689	Bottom Trawl	04.01.07	-62.45	-55.30	224	Antarctic Ocean, Antarctic Peninsula	-	-	-	-	3.23	female	-
O13	<i>Pareledone aurata</i>	ANTXXIII-8	PS 69657	Bottom Trawl	28.12.06	-61.24	-55.62	133	Antarctic Ocean, Antarctic Peninsula	-	-	-	-	5.37	male	-
O68	<i>Pareledone aurata</i>	ANTXXVII-3	PS 77217-5	Agassiz Trawl	19.02.2011	-61.90	-43.59	408	Antarctic Ocean, South Orkney Islands	0.1	34.7	55.5	-	4.9	male	-
O118	<i>Pareledone charcoti</i>	-	-	-	31.03.2009	-62.18	-58.41	-	Antarctic Ocean, King George Island	-	-	22.58	-	-	-	-
O155	<i>Pareledone charcoti</i>	-	-	-	-	-62.18	-58.41	-	Antarctic Ocean, King George Island	-	-	-	-	-	-	-
O156	<i>Pareledone charcoti</i>	-	-	-	-	-62.18	-58.41	-	Antarctic Ocean, King George Island	-	-	-	-	-	-	-
O69	<i>Pareledone comata</i>	ANTXXVII-3	PS 77217-5	Agassiz Trawl	19.02.2011	-61.90	-43.59	408	Antarctic Ocean, King George Island	0.1	34.7	52.7	-	4.4	female	-
O70	<i>Pareledone comata</i>	ANTXXVII-3	PS 77217-5	Bottom Trawl	19.02.2011	-62.00	-44.20	354	Antarctic Ocean, South Orkney Islands	0.1	34.7	91.5	-	5.6	female	-
O22	<i>Pareledone felix</i>	ANTXXIII-8	PS 69680	Bottom Trawl	02.01.07	-62.40	-61.40	341	Antarctic Ocean, Antarctic Peninsula	-	-	-	-	5.74	male	-
O74	<i>Pareledone felix</i>	ANTXXVII-3	PS 77222-6	Bottom Trawl	23.02.2011	-62.18	-58.41	459	Antarctic Ocean, King George Island	0.6	34.6	70.2	-	4.8	male	-
O80	<i>Pareledone felix</i>	ANTXXVII-3	PS 77222-6	Bottom Trawl	23.02.2011	-62.18	-58.41	459	Antarctic Ocean, King George Island	0.6	34.6	10.9	-	2.2	male	-
O87	<i>Pareledone panchroma</i>	ANTXXVII-3	PS 77217-5	Agassiz Trawl	19.02.2011	-61.90	-43.59	408	Antarctic Ocean, South Orkney Islands	0.1	34.7	48.1	-	4	male	-
O102	<i>Pareledone phyzzenalis</i>	ANTXXVII-3	PS 77308-1	Bottom Trawl	January 1998	-70.51	-10.36	224	Antarctic Ocean, Eastern Weddel Sea	-	-	10.3	-	2.5	male	-
O63	<i>Pareledone turqueti</i>	ANTXXIII-8	PS 69677	Bottom Trawl	02.01.07	-62.18	-60.55	205	Antarctic Ocean, Antarctic Peninsula	-	-	-	-	5.94	female	-
O20	<i>Pareledone turqueti</i>	ANTXXIII-8	PS 69669	Bottom Trawl	04.01.07	-62.45	-55.30	224	Antarctic Ocean, Antarctic Peninsula	-	-	-	-	12	female	-
O30	<i>Pareledone turqueti</i>	ANTXXIII-8	PS 69661	Bottom Trawl	30.12.06	-61.65	-57	467	Antarctic Ocean, King George Island	-	-	-	-	6.58	female	-

Publications



Legend

-  α -helix
-  β -strand
-  Turn
-  Copper ligand histidine
-  Disulfide bridge
-  Thioether bridge
-  Positively selected site

Supplementary Figure S3 – Detailed results of selection tests.

Residue	SLAC		FEL		MEME		FUBAR		EF		PRIME		TreesAAP					
	dN-dS ^a	p-value (≤ 0.15)	dN-dS ^a	p-value (≤ 0.10)	ω ⁺	p-value (≤ 0.10)	dN-dS ^a	Posterior Probability (≥ 0.90)	dN-dS ^a	Bayes Factor (≥ 50)	Property ^b	Weight	p-value (≤ 0.10)	pHi (8)	pK' (8)	pa (6)	PCT (6)	
2383	5.182	0.161	1.359	0.075	>100	0.084	0.824	0.047	13.3					↓(1)	↑(2-4)			
2409	8.936	0.084	2.424	0.050	>100	0.018	0.960	0.202	7736.5					↓(5-8)				
2410	6.364	0.090	1.397	0.046	>100	0.064	0.873	0.128	35.0				↓(10)					
2442	2.962	0.352	0.641	0.559	6.915	0.409	0.639	0.189	226.1	CC	20.000	0.017		↑(5,9,11)				
2469	3.775	0.320	0.962	0.162	>100	0.006	0.727	-0.203	1.4	CC	-2.722	0.011			↓(12,13)			
2496	7.058	0.230	2.940	0.037	>100	0.000	0.978	0.202	4100140.0									
2503	10.650	0.059	2.543	0.072	3.381	0.094	0.962	0.202	37451500.0	P	3.700	0.032			↓(14,15)			
2545	9.574	0.250	2.144	0.195	>100	0.225	0.913	0.202	93917.8					↓(4, 20, 28-30)				
2575	5.324	0.195	1.249	0.230	13.9	0.080	0.822	0.195	405.9					↑(9,19,31,32)				
2585	7.842	0.173	3.007	0.053	33.4	0.022	0.975	0.202	76683.3	P	8.158	0.017			↓(33,34)			
										V	8.795	0.001						
										pHi	-1.389	0.018						
2602	3.997	0.177	0.666	0.047	>100	0.003	0.827	-0.428	1.000	CC	-7.601	0.006					↑(35,36)	
2610	4.204	0.184	0.604	0.055	>100	0.075	0.879	-0.426	1.000	pHi	-1.474	0.047					↓(40-42)	
2643	-	-	0.371	0.250	>100	0.003	0.576	-0.495	1.000	CC	-5.966	0.049					↑(37-39)	
																		↓(43)

^aDifference of estimated non-synonymous and synonymous changes normalised to total tree length

^bCC, Chemical Composition; P, Polarity; V, Volume; pHi, Iso-electric point; H, Hydrophobicity; Negative weights indicate positive selection and positive weights negative selection

^cpHi: isoelectric point; pK' equilibrium constant (ionization of COOH); pa: alpha helical tendencies; PCT: Power to be at the C-terminal

4 Discussion

This thesis evaluates cold-adaptive traits of the octopods' oxygen transport protein haemocyanin at functional and molecular levels. Three major sections address methodological advancements (Publication I & Patent) and assess functional (Publication II) as well as molecular (Publication III) properties of octopod haemocyanin. This chapter will discuss advantages and shortcomings of the methodological innovations and continues with an integrative discussion of functional and molecular findings and further supportive data. The discussion concludes with a comparative analysis of specific cold-adaptation strategies and the consequences for warm-tolerance of Antarctic octopods and fishes.

4.1. High resolution measurements in blood from non-model organisms

The functional analysis of haemocyanin from shallow water Antarctic octopods of the genus *Pareledone* constituted a major challenge, due to the very limited amount of haemolymph (153 μ l on average) one could withdraw from specimens with an average mantle length of only 5.5 cm. The additional requirement to simultaneously monitor oxygen dependent pigment absorbance and pH in the same sample and a study design requiring replicated data for statistical analysis under multiple settings of PO_2 , pH and temperature, complicated measurements to an extent that technological developments were inevitable. I therefore equipped a diffusion chamber (Niesel and Thews, 1961; Sick and Gersonde, 1969, 1972) with a broad range miniature spectrophotometer and a fibre optic pH microsensor and successfully measured absorbance and pH simultaneously in only 15 μ l haemolymph (Publication I & Patent). This paved the way for detailed functional analyses of haemocyanin and enabled more than 40 measurements of oxygen binding in only 600 μ l haemolymph from five specimens of *Pareledone charcoti* and 160 measurements in haemolymph from *Octopus pallidus* and *Eledone moschata*, at temperatures between 0°C-20°C (Publication II). This technique was also successfully applied to amphipod haemolymph and fish haemolysate (Publication I). In this chapter, I will critically discuss the features advancing blood gas analysis and the instrumental limitations of the modified diffusion chamber followed by a brief perspective on future improvements.

4.1.1. Advances in blood gas analysis

The modified diffusion chamber comprises several combined features that benefit blood gas analysis. Foremost, it allows free variation of pH in response to oxygenation changes (Haldane effect), and thus reflects *in vivo* oxygen binding behaviour more accurately than experiments that fix pH by use of buffers (Brix et al., 1994). Although pH fixation may enable assessments of isolated effects of e.g. allosteric effectors such as lactate or ATP (Sanders et al., 1992; Rasmussen et al., 2009), the buffers applied (e.g. Tris, HEPES) generally confound oxygen binding characteristics such as responses to temperature (Brix et al., 1994). Setups that avoid pH fixation by measuring pH in separately conditioned sub-samples increase sample consumption [e.g. by 60 or 110 μl per measurement (Morris and Bridges, 1985; Weber et al., 2008)] and come with the risk that the gas equilibration state of the sub-sample does not correspond exactly to that of the sample in which oxygenation is measured. Besides, sub-sample based setups are not suitable for continuous measurements. The first setups that were developed to monitor pH and oxygenation in the same sample require 27 – 200 times more sample volume than the modified diffusion chamber discussed here (Pörtner, 1990; Zielinski et al., 2001).

Second, the minute volume of only 15 μl enables analysis in blood from small organisms and extends the spectrum of species where such analysis becomes possible. It further enables experiments that rely on repeated sampling of blood from living animals e.g. during an extended incubation period. Small sample volumes reduce distress and confounding effects by excessive blood loss or invasive sampling procedures (Fluttert et al., 2000). Collection of minute samples promotes replicated measurements and reduces the need to pool blood from various specimens, thereby reducing the number of sacrificed animals. Moreover, a sample droplet spread out to ca. 1 cm in diameter and a few millimetres in height equilibrates far more rapidly with the gas environment than larger sample volumes contained in a cuvette or a tonometer (400-3000 μl , see supplementary material in Publication I). This, decreases measurement time and thus the risk of sample degradation.

Third, broad-range spectra covering a range from 200 to 1100 nm at a resolution of 2048 data points provide highly resolved details of the respective spectrum (Publication I). This is important if non-standard bloods are measured such as haemolymph. Devices using one or a few single wavelength filters (e.g. Morris et al., 1985; Guarnone et al., 1995; Rasmussen et al., 2009) do not monitor complex spectral

changes such as the vertical movement of the haemoglobin peak in the Soret band region at ca. 412 nm (Publication I). Even within similar blood types oxygenation dependent absorbance peaks may differ as illustrated by the haemocyanins of *Octopus vulgaris* and *Eulimnogammarus verrucosus* that were 11 nm apart (Publication I). Aside from oxygen binding, further spectral properties of the sample may enable detection of additional blood components and functional properties, such as the high absorbance seen in the visible range in green coloured blood of a Lake Baikal amphipod (Publication I) or the binding of nitric oxide to haemoglobin [at 418 nm (Gow and Stamler, 1998)].

Fourth, oxygen equilibrium curves can be recorded continuously at very high data resolution (e.g. ~500 data points, Publication I), currently only limited by the data recording interval of the pH meter (min. 1 sec). However, care has to be taken to avoid too rapid changes of pH as this may incur a dynamic error and thus a left shift of the oxygen equilibrium curve (Publication I). Such high data resolution enables direct readings of relevant parameters such as pH₅₀ or facilitates fitting and testing of allosteric models, particularly if oxygen equilibrium curves do not follow a classical sigmoidal shape (Wells and Weber, 1989).

Additional benefits include stable and rapid recordings of fibre optic microsensors at cold temperatures (<5°C) at which increased membrane resistance of pH electrodes causes slow and noisy signals (Barron et al., 2006) as well as high flexibility regarding the gas composition or experimental temperature (so far tested but not limited to -5°C-30°C, Publication I+II).

4.1.2. Instrumental shortcomings

Despite numerous benefits, dye based microsensors and thin blood films also have their own specific problems that require care during experimentation. Potential solutions will be proposed if possible.

First, fluorescent dyes bleach if unprotected from light, which is particularly problematic for the close positioning of the pH microsensor to the light beam penetrating the sample, which caused a higher signal drift than expected from the manufacturer (this study: -0.016 pH units per 100 recordings, manufacturer: -0.0035 pH units per 100 recordings, Publication I). This could be solved by a correction of the apparent linear signal drift (Publication I) and may eventually be overcome by means of commercially available, coated sensors (PreSens GmbH, Germany) that are optically isolated from ambient light. The latter also prevents disturbance of the pH raw signal by fluorescence

light emitted in the range between 530 and 660 nm by coloured samples like whole blood (PreSens, C. Krause, personal communication). However, such coating also reduces the sensor's response time by 5-10 seconds (Huber, 2004).

Second, accurate pH recording with PreSens microsensors are currently restricted to pH values between 5.5 and 8.5, due to their non-linear dynamic range (Weidgans et al., 2004; PreSens, 2005). Yet, pH of most physiological systems, specifically blood lie within this range. Alternative fluorescent dyes covering marginal pH or a broader pH range have already been developed (Safavi and Bagheri, 2003; Ma et al., 2012; Nguyen et al., 2014).

Moreover, by nature, fibre optic sensor tips measuring only 150 microns in diameter break easily, which raises costs and time investments. pH sensor spots (PreSens GmbH, Germany) may be applied instead but require further technical modifications. Although not observed in this study using octopod and amphipod haemolymph and fish haemolysate, clogging of blood on the sensor tip may occur and disturb the signal, which can be prevented by storing the sensor tip in a heparin solution (1000 units ml⁻¹) prior to its use.

Finally, thin blood films are more sensitive to desiccation than larger sample volumes (Reeves, 1980). It is thus crucial to assure full humidification of the inflowing gas mixture via a reduced gas flow or the connection of an additional gas washing bottle. Alternatively, a gas permeable Teflon membrane placed on the sample droplet may reduce desiccation as well (Reeves, 1980; Lapennas and Lutz, 1982; Clark et al., 2008) but inevitably will increase response time.

4.1.3. Future improvements

In its current state the modified diffusion chamber requires skilled users to prevent problems incurred by the outlined disadvantages. Future improvements target an easy to use system with software integrating both pH and spectral recordings including data analysis routines, the optional integration of an automated gas flow system including feedback control to facilitate programmable and un-attended experiments as well as the employment of optically isolated pH microsensors or pH sensor spots.

Overall, the strength of the modified diffusion chamber does not lie in a single feature but in the combination of several technological advantages that particularly

benefits analysis of blood from non-model organisms or novel experimental approaches that require both experimental flexibility and detailed insight. As such, it was most suitable to analyse haemolymph from Antarctic, temperate and subtropical octopods to unravel adaptive traits that facilitated oxygen transport at temperatures close to freezing.

4.2. Functional cold-adaptation of octopod haemocyanin

Given the speciose abundance and ecological importance of incirrate benthic octopods in the Southern Ocean (Collins and Rodhouse, 2006) but a surprising deficit of understanding how this group adapted to and persisted at temperatures near freezing, it is most intriguing to identify and unravel key mechanisms that supported the radiation of octopods but also to improve forecast of their future role in regions subjected to rapid climate change. Physiological capacities and their adjustments to environmental forces are one of the pivotal targets of evolution (Pörtner and Farrell, 2008; Somero, 2010). In particular, oxygen supply has been shown to be the first level limiting species tolerance to high and low temperatures (Pörtner, 2002c; Pörtner and Farrell, 2008; Storch et al., 2014), also in cephalopods (Melzner et al., 2007a). Efficient oxygen supply is crucial in the oxygen dependent octopods and supported by an advanced oxygen supply system and the highly sophisticated respiratory pigment haemocyanin (Wells and Smith, 1987; Wells, 1995). Yet, in the oxygen rich Antarctic waters, it remains unclear whether octopods could afford to relax oxygen supply, similar to Antarctic fishes (Ruud, 1954; Sidell and O'Brien, 2006), or if blood oxygen transport via haemocyanin required adjustments to cold temperatures. This study addressed this question by comparing haemolymph oxygen transport properties between the Antarctic octopod *Pareledone charcoti* and two octopods from warmer climates. This chapter will discuss observed adjustment of blood oxygen transport with regard to cold-adaptation in an oxygen rich environment in comparison to Antarctic fishes, their prime contestants.

4.2.1. Reliance on haemocyanin functioning in an oxygen rich ocean.

High levels of dissolved oxygen in Antarctic waters combined with low oxygen demand have been the major explanation for relaxed blood oxygen transport in Antarctic notothenioid fishes, characterized by reduced levels and multiplicity of oxygen

transporting globins and even their complete loss (Ruud, 1954; Sidell and O'Brien, 2006; Pörtner et al., 2013). The results of this study showed that Antarctic octopods similarly benefit from abundant oxygen and low oxygen demand, however without reducing the content and multiplicity of haemocyanin (Publication II & III). All haemolymph samples from nine species of benthic Antarctic and Sub-Antarctic octopods and two species of Antarctic squids contained haemocyanin indicated by both clearly visible blue coloration of freshly sampled blood (M.O. pers. observation) as well as by native page gel electrophoresis of haemolymph samples showing protein bands close to haemocyanin protein bands of *Sepia officinalis* (Figure 4). Furthermore, all of the 14 Antarctic and two Arctic octopod species analysed in publication III contained functional partial copies of the haemocyanin gene. Fully functional haemocyanin, showing proton and PO_2 dependent cooperative oxygen binding in the Antarctic octopods *Pareledone charcoti* (Publication II) and *Megaleledone setebos* (Zielinski et al., 2001) further underlines its continued role as oxygen transporter in the cold. Most surprisingly, concentrations of haemocyanin in Antarctic octopods were among the highest reported so far for octopods (Publication II), supporting oxygen carrying capacities of 1.86 mmol L^{-1} in *Megaleledone setebos* (Zielinski et al., 2001) and 1.58 mmol L^{-1} in *Pareledone charcoti* (max. 2.20 mmol L^{-1} , Publication II), similar or even higher than those of haemoglobin carrying Antarctic fishes [1.77 mmol L^{-1} , publication II, (Wells et al., 1980)]. Accordingly, unlike Antarctic fishes, cephalopods and particular octopods continue to rely on their respiratory pigment haemocyanin.

This finding is surprising as Antarctic octopods indeed profit from high dissolved oxygen levels in polar waters. In *Pareledone charcoti*, physically dissolved oxygen contributed 18.5% to the total *in vitro* haemolymph oxygen content and up to 42% of the oxygen potentially released to the tissue (i.e. from 13-1 kPa PO_2 , Publication II) and may be further enhanced by oxygen uptake via their thin skin (Madan, J. J. and Wells, J., 1996; Pörtner, 2002b). Is this dependency on blood oxygen transport due to enhanced and compensated oxygen consumption rates? Daly and Peck (2000) demonstrated that this not the case for *Pareledone charcoti*, whose oxygen consumption rates were similar to those of the temperate *Eledone cirrhosa* extrapolated to 0°C and below that of Antarctic fishes [*Pareledone charcoti* $0.319 \text{ mmol O}_2 \text{ kg}^{-1}$ (wet mass) h^{-1} weight corrected to a 1 kg animal (Daly and Peck, 2000) vs. *Trematomus bernacchii* $0.856 \text{ mmol O}_2 \text{ kg}^{-1}$ (wet mass) h^{-1} weight corrected to a 100 g animal (Steffensen, 2002)].

Then why do Antarctic octopods rely so much on haemocyanin (i.e. haemolymph of *Pareledone charcoti* contains 1.46 or 1.39 times more haemocyanin than of the subtropical *Eledone moschata* or the temperate *Octopus pallidus* respectively, Publication II) despite low rates of oxygen consumption and enhanced dissolved oxygen levels? The major reason probably lies within haemocyanin itself, due to a progressive loss of its function towards cold temperatures [Publication II, (Melzner et al., 2007a)]. The affinity of haemocyanin for oxygen is highly temperature dependent in octopods as well as in squids and *Sepiids* [Publication II, (Brix et al., 1994; Zielinski et al., 2001; Seibel, 2012)]. Consequently, oxygen affinities increase when temperatures fall, which reduces the capacity of haemocyanin to release oxygen to the tissues [Publication II, (Melzner et al., 2007a)]. If oxygen affinities increase faster than oxygen consumption decreases, a mismatch between oxygen demand and supply may set in, a pattern supported by the concept of oxygen limited thermal tolerance (Pörtner, 2001; Pörtner and Knust, 2007; Pörtner, 2010), confirmed in *Sepia officinalis* (Melzner et al., 2006a). In case of *Pareledone charcoti*, oxygen affinities decrease with a Q_{10} of 5.7 from 10°C to 0°C (Publication II) and thus much faster than its oxygen consumption rates [$Q_{10} = 3$ (Daly and Peck, 2000)]. This causes venous oxygen release to shrink by more than 60% (at an assumed venous PO_2 of 1kPa, Publication II) leaving little capacity for venous oxygen release at 0°C (16.3%, for a hypothetical arterial-venous transition from 13 to 1 kPa PO_2 , Publication II). Dissolved oxygen levels increase only by a factor of 1.27 between 0 and 10°C [0.282 mmol L⁻¹ at 10°C to 0.358 mmol L⁻¹ at 0°C, (Ramsing and Gundersen)] and thus cannot fully compensate for this sharp increase of oxygen affinity. Consequently, the functional impairment of haemocyanin in the cold compromised oxygen supply to an extent that Antarctic octopods were unable to tolerate low concentrations of their respiratory pigment, unlike Antarctic fishes, but rather continued to rely on even higher haemocyanin contents than warm water octopods to supply oxygen (Publication II).

Discussion

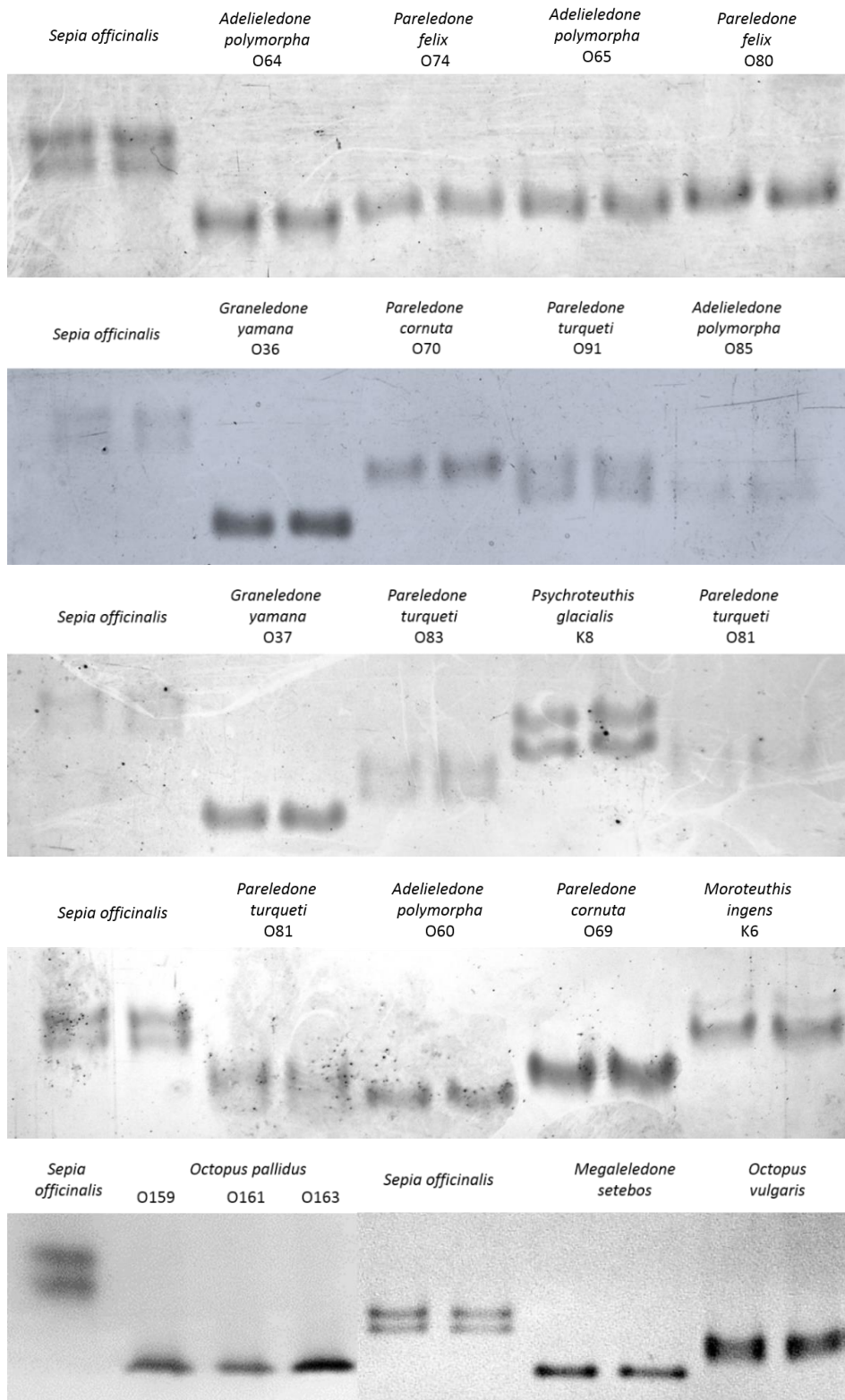


Figure 4: Native page gel electrophoresis of purified cephalopod haemocyanins.

Haemocyanin of *Sepia officinalis* served as protein standard. Data for *Megaleledone setebos* and *Octopus vulgaris* taken from Mark, FC (unpublished).

4.2.2. Cold compensation of haemocyanin function

Comparative functional analysis of Southern Ocean octopods and octopods from warmer climates showed that functional capacity of haemocyanin is low at 0°C, such that blood oxygen transport underwent significant adjustments in the Antarctic octopod *Pareledone charcoti* (Publication II). These adjustments comprised a lowered affinity of haemocyanin for oxygen, increased rates of pH dependent oxygen release as well as a shift of the pH sensitive range of oxygen binding towards higher pH values, which altogether improved venous oxygen release at low temperatures (Publication II+III). However, these improvements were not sufficient to exploit the full capacity of haemocyanin at 0°C as ~77% of oxygen bound to haemocyanin were not released to tissues under the assumed venous conditions (Publication II). Yet, largely increased haemocyanin concentrations (>40%) in *Pareledone charcoti* compared to *Octopus pallidus* or *Eledone moschata* compensate for this incomplete functional adaptation (Publication II). Therefore a combination of (incomplete) functional modification and enhanced expression of haemocyanin as well as high levels of dissolved oxygen sustain oxygen supply in the Antarctic octopod *Pareledone charcoti*.

Red-blooded Antarctic fishes similarly benefit from high dissolved oxygen levels and from reduced oxygen affinities of their haemoglobin to improve venous oxygen unloading, as is the case for *Dissostichus mawsoni* (P_{50} of 1.93 kPa at pH 8.16 and -1.9°C, (Qvist et al., 1977)) or *Pagothenia borchgrevinki* (2.8 kPa at pH 8.1 and -1.5°C), whose oxygen affinities are below that of temperate fish (Tetens et al., 1984). The major difference however is that Antarctic fishes are able to utilise a large fraction of oxygen bound to haemoglobin (Tetens et al., 1984). For example at -1.5°C and a venous pH of 7.5 and a PO_2 of 1kPa, utilisation of bound oxygen ranges from ~95% in the active pelagic *Pagothenia borchgrevinki*, to ~85% in the sedentary benthic *Trematomus bernacchii* or at minimum ~75% in the sluggish benthic *Rhigophila dearborni* (Tetens et al., 1984), in contrast to only ~16.3% in *Pareledone charcoti* (at 0°C, pH 7.4 and PO_2 1kPa, Publication II). Therefore, red-blooded Antarctic fishes seem far more efficient in exploiting the oxygen transport capacity of their respiratory pigment than Antarctic octopods at temperatures near freezing. This also explains why red-blooded fishes are able to tolerate reduced erythrocytes and haemoglobin levels (Ruud, 1954; Sidell and O'Brien, 2006) and why Antarctic octopods are required to increase haemocyanin concentrations instead (Publication II).

Enhanced expression of haemocyanin seems to be a simple solution to overcome such limited adaptive capacity, but may burden the circulation system by increasing haemolymph viscosity. Cephalopods already suffer from the drawback of an extracellular blood pigment which raises colloid osmotic pressures and viscosity to a larger extent than haemoglobin contained in cells (O'Dor and Webber, 1986; Mangum, 1990). Cold temperatures increase blood viscosity even further (Egginton, 1996). The lack or low concentrations of haemoglobins in Antarctic fishes was thus argued to alleviate viscosity stress at cold temperatures (Egginton, 1996). Therefore, as a trade-off do Antarctic octopods suffer from enhanced haemolymph viscosity? In this case one would expect enlarged hearts to overcome the increased flow resistance by more power (Egginton, 1996). However, heart masses of *Pareledone charcoti* resemble those of other octopods from warmer climates (Figure 5). In fact, total haemolymph protein levels and hence viscosity did not seem to be higher in *Pareledone charcoti* than in octopods from warmer climates, despite higher haemocyanin concentrations, due to an apparent parallel reduction of other haemolymph proteins (Publication II). In addition, the isosmotic haemolymph of octopods does not require freeze protection and thus may spare anti-freeze proteins that can largely contribute to blood protein levels and blood viscosity in Antarctic fishes [e.g. 32 mg ml⁻¹ or ~35% of total blood protein concentration in *Dissostichus mawsoni*, (Wells et al., 1980; Ahlgren et al., 1988; Eto and Rubinsky, 1993)]. It is therefore unlikely that Antarctic octopods suffer from enhanced viscosity as a trade-off from increased haemocyanin concentrations.

A further disadvantage of enhanced haemocyanin levels in Antarctic octopods are increased costs of protein synthesis, which may raise the energy consumption of the whole animal. Yet, overall energetic demands do not seem enhanced due to low and uncompensated metabolic rates in *Pareledone charcoti* (Daly and Peck, 2000), indicating compensatory cost-saving mechanisms elsewhere. Most apparently, enhanced haemocyanin levels reduce the workload for the circulation system. This was demonstrated by similar (i.e. uncompensated) systemic heart masses between *Pareledone charcoti* and warm water octopods (Figure 5), unlike in Antarctic icefishes where enlarged ventricles compensate for the lack of haemoglobin (Johnston et al., 1983; Tota et al., 1991). This may also apply to masses of branchial hearts or the pulse frequency of contractile veins and suggests that costs for increasing haemocyanin levels are lower or at least equal to increasing the power output of the blood circulation system. Second, energy metabolism may shift from protein to lipid or carbohydrate fuels

to save amino acid stores required for protein (haemocyanin) synthesis. In fact, *Pareledone charcoti* exhibited O:N ratios of 21.7 [S.D. \pm 6.03, $n = 3$, (Daly and Peck, 2000)] indicating greater lipid or carbohydrate catabolism compared to subtropical *Octopus vulgaris* [O:N ratio of 7.19 and 14.15, (Boucher-Rodoni and Mangold, 1985)] or tropical *Octopus maya* [O:N ratio of 2.3, (Rosas et al., 2007)]. Third, growth may be reduced in favour of haemocyanin synthesis as indicated by a minimal conversion of 4% of the ingested energy into biomass production in *Pareledone charcoti* (Daly and Peck, 2000) compared to 23% in *Octopus vulgaris* (Petza et al., 2006), 68% in *Octopus maya* (Rosas et al., 2007) or 71% in *Enteroctopus megalocyathus* (Pérez et al., 2006). Finally, costs of protein synthesis itself may be reduced similar to embryos of the Antarctic sea urchin *Sterechinus neumayeri*, that consumed up to 25 times less energy to synthesise protein [0.45 J mg protein synthesized⁻¹, (Marsh et al., 2001)] than other temperate animals such as *Gadus morhua* [8.7 J mg⁻¹, (Lyndon et al., 1989)] or *Mytilus edulis* [11.4 J mg⁻¹, (Hawkins et al., 1989)]. Unfortunately, such data are missing for Antarctic octopods. Overall, increased costs for haemocyanin synthesis in Antarctic octopods may be compensated by e.g. reduced need to adapt other circulatory components, shift of metabolic fuels and energy balance or improved energy efficiency of protein synthesis. Future studies need to address these issues to resolve in detail whether increased haemocyanin levels can be considered 'expensive' or cost effective for the whole organism.

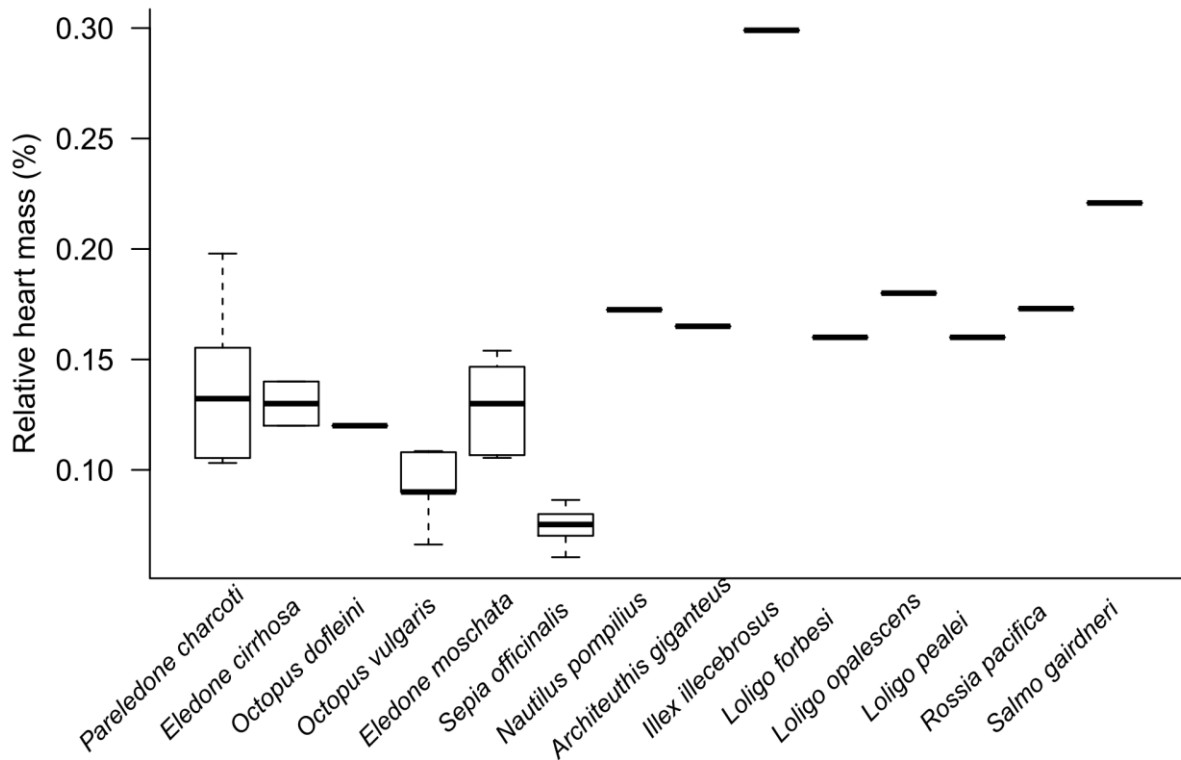


Figure 5: Relative heart masses of cephalopods.

Note that heart mass relative to body mass of the Antarctic octopod *Pareledone charcoti* group within those of other non-polar octopods. See Appendix for raw data and data sources. *Salmo gairdneri* was included for reference to fishes.

Although it appears disadvantageous that large amounts of bound oxygen remain untapped in Antarctic octopods at 0°C, this becomes beneficial once temperatures increase. Due to the high temperature sensitivity of haemocyanin from *Pareledone charcoti*, much of this oxygen is released at 10°C (>80% at pH 7.27 and 1kPa O₂, Publication II). This largely supports systemic oxygen supply when warming increases metabolic demands for oxygen. Haemocyanin reduces the workload for other circulatory components, particularly the hearts (Giomi and Pörtner, 2013), which often limit ectotherm performance at high temperatures (Fiedler, 1992; Farrell, 2002; Pörtner, 2002c; Iftikar and Hickey, 2013). *Pareledone charcoti* may indeed exploit this haemocyanin borne oxygen buffer at higher temperatures, since it prefers shallow water habitats around the Northern Antarctic Peninsula less than 120 m (Allcock, 2005) to very shallow waters (intertidal < 3 m, F. C. Mark, pers. obs.) and even visits rock pools (Joubin, 1905) where water temperatures can vary from -0.5°C to 10.7°C and even exceed 12°C during summer (Rakusa-Suszczewski, 1993; Barnes et al., 1996; Barnes et al., 2006). Fully maintained aerobic metabolism up to 8-10°C in un-acclimatised *Pareledone charcoti* further supports this view (Pörtner and Zielinski, 1998). Likewise,

utilises the eurythermal intertidal crab *Carcinus maenas* haemocyanin as oxygen buffer to delay cardiac exhaustion at higher temperatures, which extends its warm tolerance (Giomi and Pörtner, 2013). The Antarctic *Megaleledone setebos* lacks such buffering capacity (Zielinski et al., 2001) and accordingly resides in deeper waters below 100 m (Allcock et al., 2003) where temperatures remain stable close to freezing all year round (Barnes et al., 2006). Such a 'warm' oxygen buffer may pose a major competitive advantage of *Pareledone charcoti* to benthic Antarctic fishes, which exhibit reduced warm-tolerance due to low levels of haemoglobin or its complete lack (Beers and Sidell, 2011) and their inability to tap a large venous oxygen reserve at warmer temperatures (Tetens et al., 1984). This is intriguing as some red-blooded Antarctic fishes die at temperatures close to 6°C [*Trematomus bernacchii* and *Pagothenia borchgrevinki* (Clark and Peck, 2009)], far before *Pareledone charcoti* becomes anaerobic [8-10°C (Pörtner and Zielinski, 1998)], particularly in the light of anthropogenic warming of ocean waters, which occurs at dramatic rates around the Antarctic peninsula (Meredith and King, 2005). It remains open if such physiological key traits may decide about 'winners and losers' in a region where marine food webs already respond to rapid warming (Schofield et al., 2010; Somero, 2010).

In summary, cold adaptation of Antarctic octopods is characterised by significant but incomplete adjustments of haemocyanin mediated oxygen transport that is further enhanced by increased haemocyanin levels. Therefore, in contrast to Antarctic fishes, dependency on their respiratory pigment is rather increased than relaxed. However, buffering of oxygen by haemocyanin at higher temperatures supports warm-tolerance and eurythermy in *Pareledone charcoti*, which may pose a key competitive advantage over at least some benthic Antarctic fishes in a warming ocean.

4.3. Molecular basis of functional cold-adaptation

A deeper understanding of evolutionary processes requires an integrated analysis of functional and molecular mechanisms. While it is important to unravel physiological traits that explain and determine an animal's responses to its surrounding environment, it is key to grasp the underlying molecular mechanisms to trace adaptive evolutionary history and identify genetic capacities for adaptation or to decipher details (e.g. isoform multiplicity) that cannot be easily distinguished at the functional level. On the other hand, the study of molecules alone is not very informative without knowing

their functional relevance and connected phenotypes. Therefore, this study aimed to identify the molecular basis of functional cold-adaptation in octopod haemocyanin by comparing 239 partial haemocyanin sequences of the functional unit f and g of 28 octopod species of polar, temperate, subtropical and tropical origin, using phylogenetic analysis as well as analysis based on non-synonymous codon substitutions. Following a brief summary of key findings from publication III, this chapter will elaborate the link between ambient pH and protein adaptation, discuss genetic and regulative capacities of octopod haemocyanin and will conclude by proposing the concept of successive cold-adaptation.

The comparative study of partial haemocyanin sequences of 14 Antarctic and two Arctic octopods in comparison to 12 octopods originating from warmer climates revealed that despite high sequence conservation, natural selection has acted on particular sites of the haemocyanin gene, mainly located at the protein's surface (Publication III). Selection involved changes of surface charge properties that differed most between octopods from polar and tropical climates (Publication III). Further analysis indicated the presence of a potential allosteric site involved in cold-adaptation (Publication III).

4.3.1. High pH and surface charge

The functional and molecular analysis of octopods haemocyanin provided first insight how modified molecular traits may facilitate oxygen binding at temperatures near freezing. Significantly reduced oxygen affinity of haemocyanin from the Antarctic octopod *Pareledone charcoti* was marked by a shift of the pH range, within which oxygen binding is most responsive, towards higher pH (Publication II+III). At the molecular level, net surface charge of the haemocyanin functional units (FU) f-g was more positive in most of the polar octopods compared to octopods from warmer climates, marked by decreased numbers of glutamic acid and higher numbers of basic amino acids (Publication III). Additional comparisons of amino acid distributions between *Pareledone charcoti* and the temperate *Enteroctopus dofleini* confirm this pattern to persist for the entire haemocyanin gene (Figure 6).

Discussion

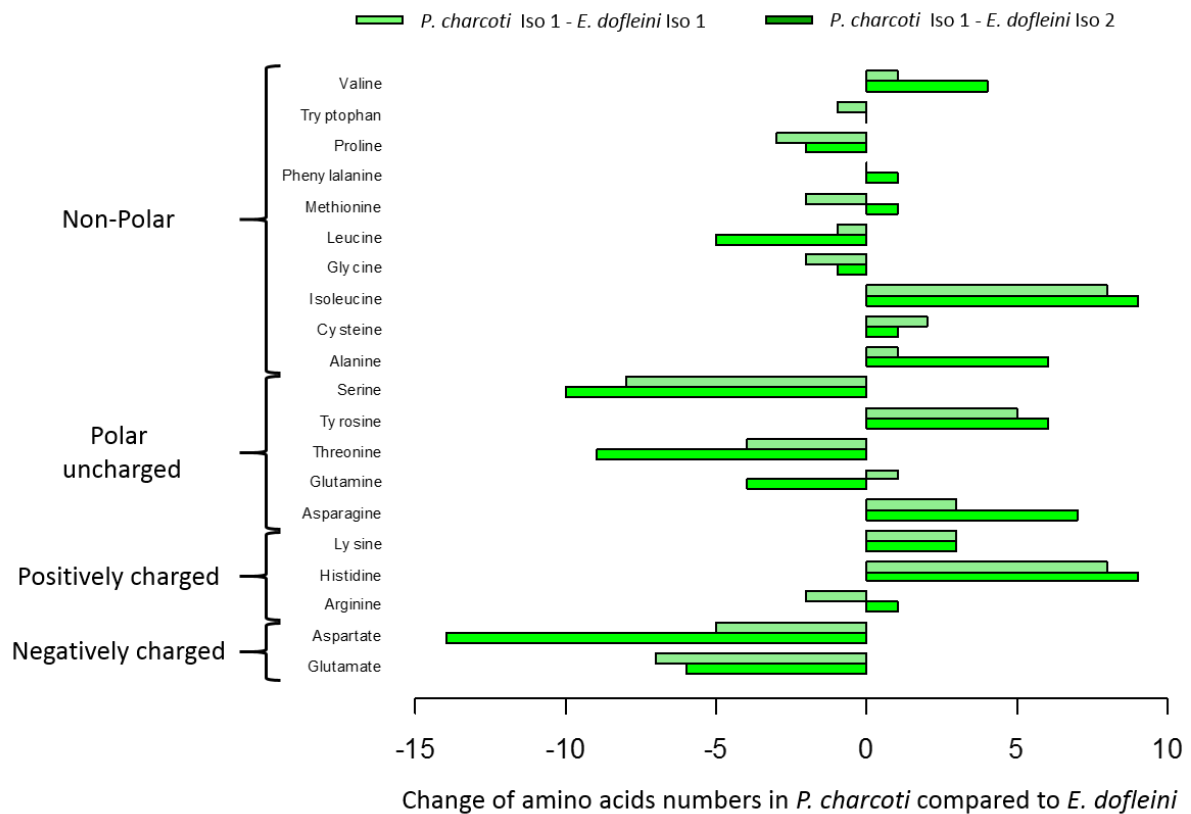


Figure 6: Amino acid differences between Antarctic and temperate haemocyanins.

Amino acid differences were calculated by subtraction of amino acid frequencies of the two haemocyanin isoforms of the temperate *Enteroctopus dofleini* from one fully sequenced haemocyanin isoform of *Pareledone charcoti*

The question arises if and how a more positive net surface charge and the observed shift of the pH sensitive range of oxygen binding towards higher pH link to each other? Most intriguing is that both traits respond to changes of ambient pH (Figure 7B-C in Publication III). First of all, pH increases when temperature falls due to the temperature dependency of equilibrium constants (pK) of ionisable groups, particularly the imidazole groups of proteins (Reeves, 1972; Burton, 2002). Such a pH-temperature dependence has been observed to change the pH of intracellular milieus [e.g. intracellular muscle pH of *Pachycara brachycephalum* (Bock et al., 2002) or of the polychaete worm *Arenicola marina* (Sommer et al., 1997)] where it affects biochemical functioning [of e.g. lactate dehydrogenase (Somero, 2004)]. It also changes the pH of extracellular milieus like the blood of the brown trout *Salmo trutta* (Butler and Day, 1993) or the haemolymph of squids (Howell and Gilbert, 1976) and octopods (Publication II), which follows an approximate alpha-stat pattern (-0.0153 pH units / °C, Publication II). Melzner et al. (2007a) highlighted that such a pH increase towards colder temperatures further impairs oxygen release in *Sepia officinalis* and the Antarctic octopod

Megaleledone setebos towards colder temperatures, an effect also observed for *Pareledone charcoti*, *Octopus pallidus* and *Eledone moschata* in this study (Publication II). The reported shift of the pH dependent oxygen binding range in *Pareledone charcoti* towards higher pH (Publication II, Figure 7B in Publication III)), thus poses a significant adaptation to compensate for impaired oxygen release in response to a cold-induced increase of pH. On the other hand, high pH values decrease the stability of proteins, particularly multimeric proteins like respiratory pigments, by disturbing salt bridges between charged amino acids, linking subunits (Perutz, 1970). This dilates the quaternary structure of haemoglobin and thus facilitates the uptake and affinity for oxygen (Perutz, 1970; Perutz et al., 1998). Haemocyanin may respond similarly. It not only dissociates into its subunits at higher pH (Van Holde and Cohen, 1964; Miller and van Holde, 1982) but is also highly pH sensitive with Bohr coefficients well below -1 (Bridges, 1994; Zielinski et al., 2001). Further, unlike intracellular haemoglobin (Primmitt et al., 1986), haemocyanin is not protected from changes of haemolymph pH. Consequently, one would expect even larger effects of pH disturbances on haemocyanin structure than on haemoglobin.

As a result, an increase of oxygen affinity in response to a cold-induced pH increase may be reduced or prevented if haemocyanin quaternary structure remains stable despite higher pH. The net surface charge, which denotes the total electric charge formed by all positively and negatively charged amino acid residues at the protein surface, may play a role in this regard. A more positive net surface charge of the haemocyanin protein as observed for polar octopods (Publication III) may indeed increase the stability of salt bridges linking functional unit interfaces by increasing the pK values of their ionisable groups (Pace et al., 2009). Salt bridges with higher pK values are more stable at alkaline pH and thus withstand disturbance by high ambient pH better. Therefore, a more positive protein surface charge in the cold may prevent structural disturbance by high haemolymph pH, which explains reduced and partly compensated haemocyanin oxygen affinity in *Pareledone charcoti*.

Protein net surface charge and charge-charge interactions were also found to modulate oxygen binding and temperature stability elsewhere. In mammals for instance, elevated net surface charge enhanced oxygen storage capacities of muscle myoglobin in deep diving species (Mirceta et al., 2013). Charge-charge interactions and additional salt bridges most frequently improve protein stability (Pace and Shaw, 2000; Petsko, 2001) in thermophiles or vice versa relax stability in psychrophiles (Gianese et al.,

2002). In Antarctic fishes however it is still unclear, which molecular mechanisms exactly cause decreased oxygen affinity as no single sites could so far be identified that relate to thermal adaptation (Di Prisco et al., 2007). Conformation and electrostatic environment around the oxygen binding active site of notothenioid haemoglobins remain essentially unmodified (Ito et al., 1995; Verde et al., 2004). Di Prisco et al. (2007) suggested that temperature dependent modifications in Antarctic fish haemoglobin may rather operate at the level of the tetramer structure, haemoglobin synthesis or allosteric regulation instead. Yet, similar to our findings numbers of positively charged residues, histidines in case of notothenioid fishes, were increased in the haemoglobin primary structure (Verde et al., 2008; Verde et al., 2011). Although this was ascribed to increasing buffer capacity (Verde et al., 2011) it may likewise affect protein stability via local or distant surface charge-charge interaction (Loewenthal et al., 1993). Unfortunately, alpha-stat effects of pH on haemoglobin function and structure have not been identified in Antarctic fishes so far to my knowledge. The results of this study thus propose a new hypothesis of changes in blood pigment primary structure that may be likewise tested for notothenioid haemoglobins.

4.3.2. Alternative modulators of haemocyanin function

Apart from the proposed linkage between molecular and functional responses to pH changes, oxygen affinity may be further regulated via allosteric sites, differential isoform expression or post translational modification. The presence of allosteric regulation gained support in publication III by positive selection at site 2545, located in the α -core domain of the functional unit g, where methionine prevails in polar octopods and leucine in tropical octopods. The hydrophobic-hydrophilic contrast of residues surrounding site 2545 promotes metal binding particularly in the presence of the sulfur containing methionine [Publication III, (Yamashita et al., 1990)]. Due to its additional proximity to the molecule's surface and the two amino acid distant copper binding His2543, conformational movements upon metal binding may easily affect oxygenation as minute movements of 0.7 Å between the coordinated copper ions suffice to change oxygenation (Gatsogiannis et al., 2007). Therefore, since cold-adaptation does not seem to occur via the direct regulation of cationic effector concentrations such as magnesium (Publication II), Antarctic octopods may rather increase their intrinsic sensitivity to effectors by switching to methionine at site 2545. Unfortunately, sensitivity of haemocyanin oxygen binding to magnesium was not tested in this study and remains

to be assessed. In the Dungeness crab *Cancer magister* oxygen affinity was similarly regulated via altered intrinsic sensitivity of haemocyanin to magnesium but also via direct control of haemolymph magnesium concentrations during ontogeny (Terwilliger and Brown, 1993). Similar to Antarctic octopods, haemolymph magnesium concentrations often remain unregulated in response to environmental factors as is the case for *Haliotis iris* (Behrens et al., 2002) or Antarctic reptant decapods (Frederich et al., 2000; Frederich et al., 2001). In Antarctic fishes, allosteric ligands seem to be involved in reducing oxygen affinity, e.g. ATP (Qvist et al., 1977). Interestingly, in the Antarctic notothenioid *Trematomus newnesi*, effector regulation seems to be controlled via intrinsic haemoglobin properties as well, since only one of two major haemoglobin isoforms responds to changes of pH or organophosphates (Verde et al., 2006).

This leads to the question if Antarctic octopods contain and employ functionally differing isoforms to regulate oxygen supply? Publication III provided clear evidence for at least two isoforms and extensive allelic variation among polar octopods but also among octopods from warmer climates. Extended sequencing of the entire haemocyanin gene confirmed the presence of two distinct isoforms in *Pareledone charcoti* (Oellermann, unpublished). Native page protein analysis also revealed the presence of electrophoretically distinct haemocyanins in the Antarctic octopod *Pareledone turqueti* as well as in the Antarctic squids *Moroteuthis ingens* and *Psychroteuthis glacialis* (Figure 4). This is consistent with former molecular studies reporting two isoforms in the temperate octopod *Enteroctopus dofleini* (Miller et al., 1998), the tropical bobtail squid *Euprymna scolopes* (Kremer et al., 2014) or *Sepia officinalis* (de Geest, Genbank accession DQ388569, DQ388570), with the latter expressing even a third embryonic haemocyanin isoform (Thonig et al., 2014). Melzner et al. (2007a) proposed differential expression of haemocyanin isoforms in cephalopods to form a regulative mechanisms in response to a given thermal environment, as a functional analogue to differential hemoglobin gene expression in fish (Brix et al., 2004; Andersen et al., 2009). They suggested that differences in isoelectric points between haemocyanin isoforms of *Sepia officinalis* cause different pH optima and thus differential oxygen binding behaviour. This is in line with the observed temperature induced pH effects in this study and also confirmed for the two isoforms of *Pareledone charcoti*, whose calculated isoelectric points differ by 0.14 units (Figure 7). So far there has been only evidence for differential isoform expression during ontogenesis in *Sepia officinalis* (Thonig et al., 2014) but not temperature or PCO_2 (Strobel et al., 2012). However, native

page analysis indicated that grown up specimens of the Antarctic squid *Moroteuthis ingens* express two distinct isoforms at very different levels (*Moroteuthis ingens*, Figure 4), which may be a response to environmental cues or other factors rather than ontogeny. This is likely because in *Sepia officinalis* parallel and differential expression of embryonic and ‘mature’ isoforms only occurs before hatching but not in adult specimens where embryonic haemocyanin virtually disappears [share of 0.267% in gills and 0.027% branchial glands, (Thonig et al., 2014)]. In sum, this study demonstrated the continued presence of at least two haemocyanin isoforms in Antarctic octopods and further indicated regulation of oxygen binding via differential isoforms expression in at least one Antarctic cephalopod species.

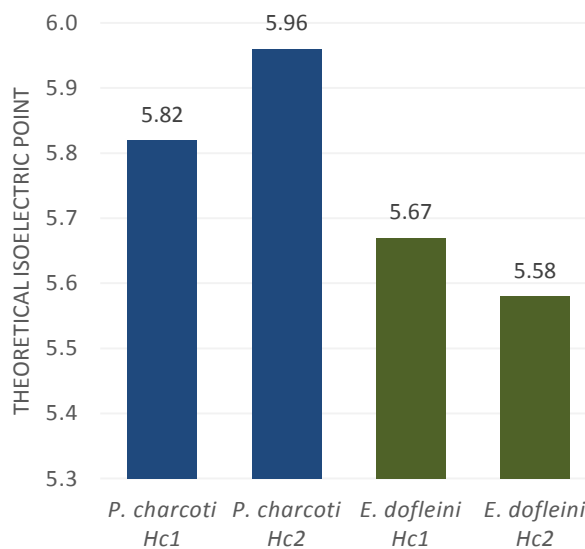


Figure 7: Isoelectric points of octopod haemocyanins.

Calculated theoretic isoelectric points of the two haemocyanin isoforms (Hc1, Hc2) of the Antarctic octopod *Pareledone charcoti* and the temperate *Enteroctopus dofleini*.

In comparison, Antarctic fishes show largely reduced isoform multiplicity and mostly contain only a single major haemoglobin type (Verde et al., 2006; Di Prisco et al., 2007). In contrast, temperate fishes show higher haemoglobin polymorphism (Fago et al., 2001; Verde et al., 2006) and in case of the Atlantic cod, express a high affinity haemoglobin type in cold waters and a temperature insensitive type in warmer waters (Andersen et al., 2009) as well as regulate isoform expression upon temperature acclimatization (Brix et al., 2004). Reduced haemoglobin multiplicity in Antarctic fishes has been attributed to the stable low temperatures in the Southern Ocean reducing the need for functional diversity of oxygen binding (Verde et al., 2006), which however,

impairs Antarctic fishes' ability to cope with rising temperatures (Pörtner et al., 2007). It remains to be assessed whether the continued presence of at least two isoforms in Antarctic octopods implies functional diversity as well as the ability to acclimatize or rapidly adapt to changing environmental conditions.

4.4. Concluding evolutionary perspective

By means of a significant methodological advancement, enabling simultaneous recordings of pigment absorbance and pH in small haemolymph volumes, this thesis investigated functional cold-adaptation of haemocyanin and its putative underlying molecular mechanisms by comparing Antarctic octopods with warm adapted octopods. Building on the above highlighted findings this chapter will conclude the thesis by introducing the mechanistic concept of 'successive cold-adaptation' of protein function and by discussing how diverging cold-adaptation strategies may affect responses of Antarctic octopods and fishes to future environmental change.

The analysis of metabolic enzymes such as lactate dehydrogenase and their role in cold-adaptation in fishes or mussels (Fields and Somero, 1998; Johns and Somero, 2004; Lockwood and Somero, 2012), has formed the notion that adaptive events may be driven by few sequence variations to adjust protein function. For example a single substitution from threonine to alanine at a flexible hinge region in lactate dehydrogenase accounted for the entire difference of enzyme activity between temperate and tropical damselfish (Johns and Somero, 2004). Variation of only few sites were identified within similar flexible regions for lactate dehydrogenase of Antarctic notothenioids as well (Fields and Somero, 1998). Further, radiation of notothenioid fishes in the Southern Ocean has been attributed to the invention of anti-freeze proteins, marked by few events of deletion, insertion and amplification (Chen et al., 1997; Matschiner et al., 2011). The loss of myoglobin expression in Antarctic icefishes was marked by single insertion or mutation events causing reading frame shifts, disruption of transcription or possibly inefficient polyadenylation (Small et al., 1998; Small et al., 2003; Grove et al., 2004). Such single or few genetic events, causing comparatively radical changes of function, require a rather instant exposure to cold conditions to gain selective significance. This may have been true for Antarctic fishes with large dispersal capacities mainly due to drifting pelagic larval stages transported by currents (e.g. circumpolar current) for many months [e.g. 11.5 months for *Champsocephalus gunnari* (Damerou et al., 2012), or ca. four months for *Gobionotothen gibberifrons* (Matschiner et al., 2009)].

Benthic Southern Ocean octopods in contrast, show very limited dispersal abilities due to their bottom dwelling crawling life style, directly developing exclusively benthic larvae [as indicated by egg sizes > 10 mm, (Boletzky, 1974; Barratt et al., 2008; Laptikhovsky et al., 2014)] and their poor ability to cross deep sea barriers leading to geographically isolated populations (Allcock, 1997; Collins and Rodhouse, 2006).

Accordingly, adaptation to the cooling of the Southern Ocean by octopods some 25-28 million years ago (Collins and Rodhouse, 2006), when surface water temperatures peaked at $\sim 6^{\circ}\text{C}$ (Clarke et al., 1992), may have been rather slow and gradual. Ever since water temperatures did not consistently fall to below zero but also increased again up to 10°C in the mid Miocene ca. 17 million years ago (Clarke et al., 1992). Cold adapted proteins, adjusted or invented by not easily reversible single or few mutational events would have been maladaptive under such variable cold-warm conditions. Antarctic icefishes for instance are unable to reverse haemoglobin expression and would severely suffer during recurrent warming periods (Sidell and O'Brien, 2006; Beers and Sidell, 2011) if they are unable to retreat to colder waters during such times. Consequently, molecular mechanisms that advance and reverse protein function gradually, without disturbing basic function, in response to environmental variation, were required.

The reported modification of protein surface charge (Publication III), which may account for the pH dependent regulation of oxygen affinity (Publication II), indicates the presence of such a flexible evolutionary mechanism in Antarctic octopods, here designated as 'successive cold adaption of protein function'. In contrast to cold-adaptation caused by single or few genetic events, successive cold adaption denotes manifold genetic reversible events of which each contributes to small but significant changes of protein function. To obtain the proposed effect of charge-charge interaction on ion pairs stabilising the quaternary structure (see section 4.3.1), single site specific mutation are less essential, but numerous close and even distant changes of surface residues either by substituting, adding or removing one of the five possible negatively or positively charged amino acids. This was the case for octopod haemocyanin that showed seven sites being under selection for their charge properties within a relatively short 396 amino acid long region ranging from FU f to g. Extrapolated to the ~ 2900 amino acid long haemocyanin subunit molecule, more than 50 sites may be involved in changing pH dependent oxygen binding behaviour (or even more if the significance threshold for defining positive selection was decreased to two tests being significant at a site, Publication II). Such successive changes, of structurally and functionally more subtle impact at each step, have much greater chances to occur and to persist than mutations at sites directly involved in protein function or stability (e.g. active site or FU interfaces). For this reason, most residues around oxygen binding active sites are highly conserved in both Antarctic fish haemoglobin (Ito et al., 1995; Verde et al., 2004) and

octopod haemocyanin (Publication III). Each mutation contributing to a change of surface charge could modify oxygen affinity in a conservative successive manner and thus would successively align oxygen supply along with incremental temperature changes. Analogous to cephalopod haemocyanin, myoglobin underwent similar changes of net surface charge to increase oxygen storage capacity in diving mammals via increased electrostatic repulsion, which reduces self-association of myoglobin (Mirceta et al., 2013). These changes were likewise accompanied by multiple amino acid substitutions at the protein's surface [e.g. six substitutions in Muskrat or five in Eurasian beaver, (Mirceta et al., 2013)], which relative to the size of rodent myoglobin (only 154 amino acids for Muskrat, UniProt ID: P32428), exhibits an even higher substitution rate than octopod haemocyanin. The evolution of oxygen secretion of haemoglobin (i.e. Bohr and Root effect) has been suggested to relate to decreased pH buffering via a decrease of non-conserved histidine residues at the surface of haemoglobin (Berenbrink et al., 2005). Here up to eight such histidines accounted for the difference of pH buffering between teleosts and non-teleosts (Berenbrink et al., 2005). This process was reversible in e.g. the swamp eel *Monopterus sp.* or catfish *Silurus sp.* (Berenbrink et al., 2005), similar to e.g. temperate octopod species from three distinct families, which resemble each other in type and number of charged amino acids at the surface of the haemocyanin molecule (Publication III). Such reversibility underlines the value of successive cold adaptation in responding flexibly to changing environmental conditions in contrast to genetic 'one off' inventions or losses (cf. lactate dehydrogenase or icefish globins). It remains to be assessed whether the concept of successive cold adaptation of protein function applies to oxygen binding proteins only or more general to proteins sensitive to ambient parameters such as pH.

Temperature has been the major environmental force driving species evolution and distribution and has gained momentum by anthropogenic warming (Pörtner, 2001; Somero, 2012). Sustenance of oxygen supply forms the first threshold for temperature tolerance in most ectotherms and thus requires adjustments upon exposure to temperature 'extremes' (e.g. Pörtner, 2001; Pörtner and Knust, 2007; Pörtner et al., 2007; Pörtner, 2010). Respiratory pigments like haemoglobin or haemocyanin largely sustain oxygen transport in ectotherms and consequently were frequent evolutionary targets in response to temperature (Whiteley et al., 1997; Di Prisco et al., 2007;

Andersen et al., 2009). Adaptations to near freezing temperatures invoked different changes of oxygen transport function between Antarctic fishes (Verde et al., 2011) and octopods (Publication II + III). It is thus intriguing to know whether the employed cold-adaptive strategies of Antarctic fishes and octopods define 'winners' or 'losers', in face of rapidly warming waters particularly west of the Antarctic Peninsula (Meredith and King, 2005; Somero, 2010).

At least in terms of blood oxygen transport and life style octopods are better equipped to tolerate warming waters than Antarctic fishes. In this regard, *Pareledone charcoti* benefits from several traits. With respect to blood oxygen transport, benefits include i) a large temperature sensitive venous oxygen reserve being largely tapped at 10°C (Publication II), ii) a high oxygen carrying capacity (Publication II), iii) allelic diversity and the continued existence of at least two distinct isoforms (Publication III), iv) and a putative molecular mechanism that enables successive adjustments of oxygen affinity at a relatively high mutational chance (Publication III). With respect to life style, benefits comprise i) little overlap between the parent and the offspring generation as Antarctic octopods only mate and spawn once in life and die thereafter (Laptikhovsky, 2013), and ii) relatively short generation times of cold-adapted octopods, despite reduced growth rates and breeding periods between 1-4.4 years (Nesis, 1999; Robison et al., 2014), which both accelerates the fixation of mutations in a population and thus the speed of adaptation (Patwa and Wahl, 2008). Antarctic fishes, in contrast, experienced the loss of haemoglobin diversity, essential to adjust oxygen transport to new thermal environments as in temperate fish (Andersen et al., 2009) and in case of icefishes lost the genetic basis to express functional globins (Ruud, 1954; Sidell and O'Brien, 2006). It is highly unlikely that Antarctic fishes will ever recover from these genetic losses, especially as the rate warming proceeds. Further, multiple spawning, long lives (e.g. ~25-30 years, *Dissostichus eleginoides*) and late maturity estimated to be e.g. 8-10 years for *Dissostichus eleginoides* or at best 2.8-3 years for *Champsocephalus gunnari* (Kock and Kellermann, 1991; Mesa and Vacchi, 2001), hamper beneficial mutational fixation in a population within shorter time periods. Already, current temperature tolerance of un-acclimated *Pareledone charcoti* seems to be higher [8-10°C, pejus temperature, (Pörtner and Zielinski, 1998)] than in many Antarctic fishes [lethal temperature of 6°C for *Trematomus bernacchii* and *Pagothenia borchgrevinki* (Clark and Peck, 2009) or pejus temperature of 6°C for *Pachycara brachycephalum* (Mark et al., 2002)].

Overall, findings of this and other studies indicate a larger capacity for the Antarctic octopod *Pareledone charcoti* to cope with warmer temperatures compared to various Antarctic fishes, its prime contestants. If this holds true, ectotherms, physiologically advantaged to tackle warming, such as *Pareledone charcoti* or new crustacean invaders (Aronson et al., 2007; Aronson et al., 2014) may quickly restructure the Antarctic benthic community if Antarctic fishes fail to persist or retreat to scarce refugia in times of climate change.

4.5. Research perspectives

While this study unravelled functional cold-adaptive traits of haemocyanin in *Pareledone charcoti*, more physiological parameters are required for a comprehensive picture of cold adaptation but also warm tolerance in this species. Future studies may thus attempt to analyse arterial and venous blood pH and PO_2 *in vivo*, blood volume and cardiac and circulatory performance or skin respiration at both rest and exercise. Whole animal respiration and growth rates at short and long term exposure to temperatures predicted by current climate models will help to assess whether the oxygen buffer function of haemocyanin at higher temperatures indeed supports whole animal performance as well as to assess whole animal capacities to cope with warming waters. Further, the proposed intrinsic mechanisms to facilitate metal binding at a putative allosteric site may be tested for *Pareledone charcoti* by means of oxygen binding experiments under varying magnesium levels. At the molecular level, full haemocyanin sequences of more species are desirable to test whether the observed pattern of selection of surface charge properties holds true for the whole haemocyanin gene. It would then be further possible to test remaining quaternary interfaces not covered in this study for sites involved in temperature adaptation and whether functional units differ among each other in their evolutionary and adaptive response. Rigorous structural modelling may reveal further quaternary interactions, ideally complemented by functional experiments on mutated haemocyanin.

5 References

- Agnisola, C., Venzi, R., Mustafa, T. and Tota, B.** (1994). The systemic heart of *Octopus vulgaris*: effects of exogenous arachidonic acid and capability for arachidonate metabolism. *Mar. Biol.* **120**, 47-53.
- Aguilera, F., McDougall, C. and Degnan, B.** (2013). Origin, evolution and classification of type-3 copper proteins: lineage-specific gene expansions and losses across the Metazoa. *BMC Evol. Biol.* **13**, 96.
- Ahlgren, J. A., Cheng, C. C., Schrag, J. D. and DeVries, A. L.** (1988). Freezing avoidance and the distribution of antifreeze glycopeptides in body fluids and tissues of Antarctic fish. *J. Exp. Biol.* **137**, 549-563.
- Ahn, I.-Y. and Shim, J. H.** (1998). Summer metabolism of the Antarctic clam, *Laternula elliptica* (King and Broderip) in Maxwell Bay, King George Island and its implications. *J. Exp. Mar. Biol. Ecol.* **224**, 253-264.
- Akaike, H.** (1974). A new look at the statistical model identification. *Automatic Control, IEEE Transactions on* **19**, 716-723.
- Allcock, A. and Piertney, S.** (2002). Evolutionary relationships of Southern Ocean Octopodidae (Cephalopoda: Octopoda) and a new diagnosis of *Pareledone*. *Mar. Biol.* **140**, 129-135.
- Allcock, A. L.** (1997). Restricted gene flow and evolutionary divergence between geographically separated populations of the Antarctic octopus *Pareledone turqueti*. *Mar. Biol.* **129**, 97-102.
- Allcock, A. L.** (2005). On the confusion surrounding *Pareledone charcoti* (Joubin, 1905) (Cephalopoda : Octopodidae): endemic radiation in the Southern Ocean. *Zool. J. Linn. Soc.* **143**, 75-108.
- Allcock, A. L., Hochberg, F. G. and Stranks, T. N.** (2003). Re-evaluation of *Graneledone setebos* (Cephalopoda : Octopodidae) and allocation to the genus *Megaleledone*. *J. Mar. Biol. Assoc. U. K.* **83**, 319-328.
- Allcock, A. L., Strugnell, J. M. and Johnson, M. P.** (2008). How useful are the recommended counts and indices in the systematics of the Octopodidae (Mollusca: Cephalopoda). *Biol. J. Linn. Soc.* **95**, 205-218.
- Allcock, A. L., Piatkowski, U., Rodhouse, P. G. K. and Thorpe, J. P.** (2001). A study on octopodids from the eastern Weddell Sea, Antarctica. *Polar Biol.* **24**, 832-838.
- Allcock, A. L., Strugnell, J. M., Prödohl, P., Piatkowski, U. and Vecchione, M.** (2007). A new species of *Pareledone* (Cephalopoda : Octopodidae) from Antarctic Peninsula Waters. *Polar Biol.* **30**, 883-893.
- Allcock, A. L., Barratt, I., Eléaume, M., Linse, K., Norman, M. D., Smith, P. J., Steinke, D., Stevens, D. W. and Strugnell, J. M.** (2011). Cryptic speciation and the circumpolarity debate: A case study on endemic Southern Ocean octopuses using the COI barcode of life. *Deep-Sea Res. Pt. II* **58**, 242-249.
- Andersen, O., Wetten, O. F., De Rosa, M. C., Andre, C., Carelli Alinovi, C., Colafranceschi, M., Brix, O. and Colosimo, A.** (2009). Haemoglobin polymorphisms affect the oxygen-binding properties in Atlantic cod populations. *Proceedings. Biological sciences / The Royal Society* **276**, 833-841.
- André, J., Pecl, G. T., Grist, E. P. M., Semmens, J. M., Haddon, M. and Leporati, S. C.** (2009). Modelling size-at-age in wild immature female octopus: a bioenergetics approach. *Mar. Ecol. Prog. Ser.* **384**, 159-174.
- Andrews, P. L. R., Darmaillacq, A.-S., Dennison, N., Gleadall, I. G., Hawkins, P., Messenger, J. B., Osorio, D., Smith, V. J. and Smith, J. A.** (2013). The identification and management of pain, suffering and distress in cephalopods,

- including anaesthesia, analgesia and humane killing. *J. Exp. Mar. Biol. Ecol.* **447**, 46-64.
- Arntz, W. E., Gutt, J. and Klages, M.** (1997). Antarctic marine biodiversity: an overview. *Antarctic communities: species, structure and survival*. Cambridge University Press, Cambridge, 3-14.
- Aronson, R. B., Frederich, M., Price, R., Thatje, S. and Alistair Crame, J.** (2014). Prospects for the return of shell-crushing crabs to Antarctica. *J. Biogeogr.*, 1-7.
- Aronson, R. B., Thatje, S., Clarke, A., Peck, L. S., Blake, D. B., Wilga, C. D. and Seibel, B. A.** (2007). Climate Change and Invasibility of the Antarctic Benthos. *Annu. Rev. Ecol. Evol. Syst.* **38**, 129-154.
- Artegiani, A., Paschini, E., Russo, A., Bregant, D., Raicich, F. and Pinardi, N.** (1997). The Adriatic Sea general circulation. Part I: Air-sea interactions and water mass structure. *J. Phys. Oceanogr.* **27**, 1492-1514.
- Atchley, W. R., Zhao, J., Fernandes, A. D. and Drüke, T.** (2005). Solving the protein sequence metric problem. *Proc. Natl. Acad. Sci. USA* **102**, 6395-6400.
- Barker, P. F. and Burrell, J.** (1977). The opening of Drake Passage. *Marine Geology* **25**, 15-34.
- Barnes, D. K. A., Rothery, P. and Clarke, A.** (1996). Colonisation and development in encrusting communities from the Antarctic intertidal and sublittoral. *J. Exp. Mar. Biol. Ecol.* **196**, 251-265.
- Barnes, D. K. A., Fuentes, V., Clarke, A., Schloss, I. R. and Wallace, M. I.** (2006). Spatial and temporal variation in shallow seawater temperatures around Antarctica. *Deep-Sea Res. Pt. II* **53**, 853-865.
- Barratt, I. M., Johnson, M. P., Collins, M. A. and Allcock, A. L.** (2008). Female reproductive biology of two sympatric incirrate octopod species, *Adelieledone polymorpha* (Robson 1930) and *Pareledone turqueti* (Joubin 1905) (Cephalopoda: Octopodidae), from South Georgia. *Polar Biol.* **31**, 583-594.
- Barron, J., Ashton, C. and Geary, L.** (2006). Effects of Temperature on pH. In *Annual Meeting of the International Society of Electrochemistry*, vol. 57, pp. 7. Edinburgh Reagecon Diagnostics Ltd.
- Beers, J. M. and Sidell, B. D.** (2011). Thermal tolerance of Antarctic notothenioid fishes correlates with level of circulating hemoglobin. *Physiol. Biochem. Zool.* **84**, 353-362.
- Behrens, J. W., Elias, J. P., Taylor, H. H. and Weber, R. E.** (2002). The archaeogastropod mollusc *Haliothis iris*: tissue and blood metabolites and allosteric regulation of haemocyanin function. *J. Exp. Biol.* **205**, 253-263.
- Berenbrink, M., Koldkjaer, P., Kepp, O. and Cossins, A. R.** (2005). Evolution of oxygen secretion in fishes and the emergence of a complex physiological system. *Science* **307**, 1752-1757.
- Bock, C., Sartoris, F., Wittig, R.-M. and Pörtner, H.-O.** (2002). Temperature-dependent pH regulation in stenothermal Antarctic and eurythermal temperate eelpout (Zoaridae): an in-vivo NMR study. In *Ecological Studies in the Antarctic Sea Ice Zone*, eds. W. Arntz and A. Clarke), pp. 266-271: Springer Berlin Heidelberg.
- Boletzky, S.** (1974). The 'larvae' of cephalopods: a review: Thalassia Jugosl.
- Boucher-Rodoni, R. and Mangold, K.** (1985). Ammonia excretion during feeding and starvation in *Octopus vulgaris*. *Mar. Biol.* **86**, 193-197.
- Bradford, M.** (1976). A rapid and sensitive method for the quantitation of microgram quantities of protein utilizing the principle of protein-dye binding. *Anal. Biochem.* **72**, 248-254.

- Bridges, C., Bicudo, J. and Lykkeboe, G.** (1979). Oxygen content measurement in blood containing haemocyanin. *Comp. Biochem. Physiol. A Physiol.* **62**, 457-461.
- Bridges, C. R.** (1994). Bohr and root effects in cephalopod haemocyanins - paradox or pressure in *Sepia officinalis*? *Mar. Freshw. Behav. Physiol.* **25**, 121-130.
- Brix, O., Colosimo, A. and Giardina, B.** (1994). Temperature dependence of oxygen binding to cephalopod haemocyanins: ecological implications. *Mar. Freshw. Behav. Physiol.* **25**, 149-162.
- Brix, O., Thorkildsen, S. and Colosimo, A.** (2004). Temperature acclimation modulates the oxygen binding properties of the Atlantic cod (*Gadus morhua* L.) genotypes—HbI*1/1, HbI*1/2, and HbI*2/2—by changing the concentrations of their major hemoglobin components (results from growth studies at different temperatures). *Comp. Biochem. Physiol. Part A Mol. Integr. Physiol.* **138**, 241-251.
- Brix, O., Bårdgard, A., Cau, A., Colosimo, A., Condo, S. and Giardina, B.** (1989). Oxygen-binding properties of cephalopod blood with special reference to environmental temperatures and ecological distribution. *J. Exp. Zool.* **252**, 34-42.
- Buckley, B. A., Hedrick, M. S. and Hillman, S. S.** (2014). Cardiovascular oxygen transport limitations to thermal niche expansion and the role of environmental PO₂ in Antarctic notothenioid fishes. *Physiol. Biochem. Zool.* **87**, 499-506.
- Burmester, T.** (2002). Origin and evolution of arthropod hemocyanins and related proteins. *J. Comp. Physiol. B* **172**, 95-107.
- Burton, R. F.** (2002). Temperature and acid—base balance in ectothermic vertebrates: the imidazole alaphastat hypotheses and beyond. *J. Exp. Biol.* **205**, 3587-3600.
- Bustamante, P., Cherel, Y., Caurant, F. and Miramand, P.** (1998). Cadmium, copper and zinc in octopuses from Kerguelen Islands, Southern Indian Ocean. *Polar Biol.* **19**, 264-271.
- Butler, P. J. and Day, N.** (1993). The relationship between intracellular pH and seasonal temperature in the brown trout *Salmo trutta*. *J. Exp. Biol.* **177**, 293-297.
- Capra, J. A. and Singh, M.** (2007). Predicting functionally important residues from sequence conservation. *Bioinformatics* **23**, 1875-1882.
- Castresana, J.** (2000). Selection of conserved blocks from multiple alignments for their use in phylogenetic analysis. *Mol. Biol. Evol.* **17**, 540-552.
- Charif, D. and Lobry, J. R.** (2007). SeqinR 1.0-2: a contributed package to the R project for statistical computing devoted to biological sequences retrieval and analysis. In *Structural approaches to sequence evolution*, pp. 207-232: Springer.
- Chen, L., DeVries, A. L. and Cheng, C.-H. C.** (1997). Evolution of antifreeze glycoprotein gene from a trypsinogen gene in Antarctic notothenioid fish. *Proc. Natl. Acad. Sci. USA* **94**, 3811-3816.
- Cheng, C.-H. C.** (1998). Evolution of the diverse antifreeze proteins. *Curr. Opin. Genet. Dev.* **8**, 715-720.
- Chown, S. L., Hoffmann, A. A., Kristensen, T. N., Angilletta Jr, M. J., Stenseth, N. C. and Pertoldi, C.** (2010). Adapting to climate change: a perspective from evolutionary physiology. *Climate research (Open Access for articles 4 years old and older)* **43**, 3.
- Clark, M. S. and Peck, L. S.** (2009). HSP70 heat shock proteins and environmental stress in Antarctic marine organisms: A mini-review. *Mar Genom* **2**, 11-18.
- Clark, T. D., Seymour, R. S., Wells, R. M. G. and Frappell, P. B.** (2008). Thermal effects on the blood respiratory properties of southern bluefin tuna, *Thunnus maccoyii*. *Comp. Biochem. Physiol. Part A Mol. Integr. Physiol.* **150**, 239-246.
- Clarke, A.** (1991). What Is Cold Adaptation and How Should We Measure It? *Am. Zool.* **31**, 81-92.

- Clarke, A. and Johnston, N. M.** (1999). Scaling of metabolic rate with body mass and temperature in teleost fish. *J. Anim. Ecol.* **68**, 893-905.
- Clarke, A. and Johnston, N. M.** (2003). Antarctic marine benthic diversity. *Oceanography and marine biology* **41**, 47-114.
- Clarke, A., Crame, J. A., Stromberg, J.-O. and Barker, P. F.** (1992). The Southern Ocean benthic fauna and climate change: A historical perspective. *Philos. Trans. R. Soc. Lond. B Biol. Sci.* **338**, 299-309.
- Clarke, A., Aronson, R. B., Crame, J. A., Gili, J.-M. and Blake, D. B.** (2004). Evolution and diversity of the benthic fauna of the Southern Ocean continental shelf. *Antarct. Sci.* **16**, 559-568.
- Collins, M. A. and Rodhouse, P. G. K.** (2006). Southern Ocean Cephalopods. In *Adv. Mar. Biol.*, vol. 50 eds. C. M. Y. Alan J. Southward and A. F. Lee), pp. 191-265. London: Academic Press Ltd.
- Collins, M. A., Allcock, A. L. and Belchier, M.** (2004). Cephalopods of the South Georgia slope. *J. Mar. Biol. Assoc. U. K.* **84**, 415-419.
- Conant, G. C., Wagner, G. P. and Stadler, P. F.** (2007). Modeling amino acid substitution patterns in orthologous and paralogous genes. *Mol. Phylogenet. Evol.* **42**, 298-307.
- Connelly, P. R., Gill, S. J., Miller, K. I., Zhou, G. and Van Holde, K.** (1989). Identical linkage and cooperativity of oxygen and carbon monoxide binding to *Octopus dofleini* hemocyanin. *Biochemistry* **28**, 1835-1843.
- Cuff, M. E., Miller, K. I., van Holde, K. E. and Hendrickson, W. A.** (1998). Crystal structure of a functional unit from *Octopus* hemocyanin. *J. Mol. Biol.* **278**, 855-870.
- D'Avino, R. and Di Prisco, G.** (1989). Hemoglobin from the Antarctic fish *Notothenia coriiceps neglecta*. *Eur. J. Biochem.* **179**, 699-705.
- Daly, H. and Peck, L.** (2000). Energy balance and cold adaptation in the octopus *Pareledone charcoti*. *J. Exp. Mar. Biol. Ecol.* **245**, 197-214.
- Daly, H. I.** (1996). Ecology of the Antarctic octopus *Pareledone* from the Scotia Sea, pp. 162. Aberdeen: University of Aberdeen.
- Damerau, M., Matschiner, M., Salzburger, W. and Hanel, R.** (2012). Comparative population genetics of seven notothenioid fish species reveals high levels of gene flow along ocean currents in the southern Scotia Arc, Antarctica. *Polar Biol.* **35**, 1073-1086.
- Darriba, D., Taboada, G. L., Doallo, R. and Posada, D.** (2012). jModelTest 2: more models, new heuristics and parallel computing. *Nat. Meth.* **9**, 772-772.
- Decker, H. and Jaenicke, E.** (2004). Recent findings on phenoloxidase activity and antimicrobial activity of hemocyanins. *Dev. Comp. Immunol.* **28**, 673-687.
- Decker, H., Hellmann, N., Jaenicke, E., Lieb, B., Meissner, U. and Markl, J.** (2007). Minireview: Recent progress in hemocyanin research. *Integr. Comp. Biol.* **47**, 631-644.
- Delport, W., Poon, A. F. Y., Frost, S. D. W. and Kosakovsky Pond, S. L.** (2010). Datamonkey 2010: a suite of phylogenetic analysis tools for evolutionary biology. *Bioinformatics* **26**, 2455-2457.
- DeVries, A. L.** (1988). The role of antifreeze glycopeptides and peptides in the freezing avoidance of antarctic fishes. *Comp. Biochem. Physiol., B: Comp. Biochem.* **90**, 611-621.
- Di Prisco, G., Eastman, J. T., Giordano, D., Parisi, E. and Verde, C.** (2007). Biogeography and adaptation of Notothenioid fish: Hemoglobin function and globin-gene evolution. *Gene* **398**, 143-155.

- Dickson, A.** (2010). The carbon dioxide system in seawater: equilibrium chemistry and measurements. In *Guide to best practices for ocean acidification research and data reporting*, eds. U. Riebesell V. J. Fabry L. Hansson and J.-P. Gattuso). Luxembourg: Publications Office of the European Union.
- Dickson, A. G.** (1984). pH scales and proton-transfer reactions in saline media such as sea water. *Geochimica et Cosmochimica Acta* **48**, 2299-2308.
- Dray, S. and Dufour, A.-B.** (2007). The ade4 package: implementing the duality diagram for ecologists. *J. Stat. Softw.* **22**, 1-20.
- Driedzic, W., Sidell, B., Stewart, J. and Johnston, I.** (1990). Maximal activities of enzymes of energy metabolism in cephalopod systemic and branchial hearts. *Physiol. Zool.* **63**, 615-629.
- Edgar, R. C.** (2004). MUSCLE: multiple sequence alignment with high accuracy and high throughput. *Nucleic Acids Res.* **32**, 1792-1797.
- Egginton, S.** (1996). Blood rheology of Antarctic fishes: viscosity adaptations at very low temperatures. *J. Fish Biol.* **48**, 513-521.
- Eto, T. K. and Rubinsky, B.** (1993). Antifreeze glycoproteins increase solution viscosity. *Biochem. Biophys. Res. Commun.* **197**, 927-931.
- EXPEDITION.** (2012). An information portal for research platforms of the Alfred Wegener Institute Helmholtz Centre for Polar and Marine Research Bremerhaven, Germany: Alfred Wegener Institute Helmholtz Centre for Polar and Marine Research (AWI).
- Fago, A., Forest, E. and Weber, R. E.** (2001). Hemoglobin and subunit multiplicity in the rainbow trout (*Oncorhynchus mykiss*) hemoglobin system. *Fish Physiol. Biochem.* **24**, 335-342.
- Farrell, A. P.** (2002). Cardiorespiratory performance in salmonids during exercise at high temperature: insights into cardiovascular design limitations in fishes. *Comp. Biochem. Physiol. Part A Mol. Integr. Physiol.* **132**, 797-810.
- Fiedler, A.** (1992). Die Rolle des venösen Füllungsdrucks bei der Autoregulation der Kiemenherzen von *Sepia officinalis* L.(Cephalopoda). *Zoologische Jahrbücher. Abteilung für allgemeine Zoologie und Physiologie der Tiere* **96**, 265-278.
- Fields, P. A. and Somero, G. N.** (1998). Hot spots in cold adaptation: Localized increases in conformational flexibility in lactate dehydrogenase A4 orthologs of Antarctic notothenioid fishes. *Proc. Natl. Acad. Sci. USA* **95**, 11476-11481.
- Fluttert, M., Dalm, S. and Oitzl, M. S.** (2000). A refined method for sequential blood sampling by tail incision in rats. *Laboratory Animals* **34**, 372-378.
- Folmer, O., Black, M., Hoeh, W., Lutz, R. and Vrijenhoek, R.** (1994). DNA primers for amplification of mitochondrial cytochrome c oxidase subunit I from diverse metazoan invertebrates. *Mol. Mar. Biol. Biotechnol.* **3**, 294-299.
- Fraczkiewicz, R. and Braun, W.** (1998). Exact and efficient analytical calculation of the accessible surface areas and their gradients for macromolecules. *J. Comput. Chem.* **19**, 319-333.
- Frederich, M., Sartoris, F. and Pörtner, H.-O.** (2001). Distribution patterns of decapod crustaceans in polar areas: a result of magnesium regulation? *Polar Biol.* **24**, 719-723.
- Frederich, M., Sartoris, F. J., Arntz, W. E. and Portner, H.** (2000). Haemolymph Mg⁽²⁺⁾ regulation in decapod crustaceans: physiological correlates and ecological consequences in polar areas. *J. Exp. Biol.* **203**, 1383-1393.
- Galarza-Muñoz, G., Soto-Morales, S. I., Holmgren, M. and Rosenthal, J. J. C.** (2011). Physiological adaptation of an Antarctic Na⁺/K⁺-ATPase to the cold. *J. Exp. Biol.* **214**, 2164-2174.

- Garofalo, F., Pellegrino, D., Amelio, D. and Tota, B.** (2009). The Antarctic hemoglobinless icefish, fifty five years later: a unique cardiocirculatory interplay of disaptation and phenotypic plasticity. *Comp. Biochem. Physiol. Part A Mol. Integr. Physiol.* **154**, 10-28.
- Garrett, S. and Rosenthal, J. J.** (2012). RNA editing underlies temperature adaptation in K⁺ channels from polar octopuses. *Science* **335**, 848-851.
- Gatsogiannis, C., Moeller, A., Depoix, F., Meissner, U. and Markl, J.** (2007). *Nautilus pompilius* hemocyanin: 9 Å cryo-EM structure and molecular model reveal the subunit pathway and the interfaces between the 70 functional units. *J. Mol. Biol.* **374**, 465-486.
- Gianese, G., Bossa, F. and Pascarella, S.** (2002). Comparative structural analysis of psychrophilic and meso- and thermophilic enzymes. *Proteins: Structure, Function, and Bioinformatics* **47**, 236-249.
- Giomi, F. and Pörtner, H.-O.** (2013). A role for haemolymph oxygen capacity in heat tolerance of eurythermal crabs. *Front. Physiol.* **4**, 110.
- Gow, A. J. and Stamler, J. S.** (1998). Reactions between nitric oxide and haemoglobin under physiological conditions. *Nature* **391**, 169-173.
- Griffiths, H. J.** (2010). Antarctic marine biodiversity—what do we know about the distribution of life in the Southern Ocean? *Plos One* **5**, e11683.
- Grove, T., Hendrickson, J. and Sidell, B.** (2004). Two species of antarctic icefishes (genus *Champscephalus*) share a common genetic lesion leading to the loss of myoglobin expression. *Polar Biol.* **27**, 579-585.
- Guarnone, R., Centenara, E. and Barosi, G.** (1995). Performance characteristics of Hemox-Analyzer for assessment of the hemoglobin dissociation curve. *Haematologica* **80**, 426-430.
- Guindon, S. and Gascuel, O.** (2003). A simple, fast, and accurate algorithm to estimate large phylogenies by maximum likelihood. *Syst. Biol.* **52**, 696-704.
- Gutowska, M. A., Melzner, F., Langenbuch, M., Bock, C., Claireaux, G. and Portner, H. O.** (2010). Acid-base regulatory ability of the cephalopod (*Sepia officinalis*) in response to environmental hypercapnia. *J Comp Physiol B* **180**, 323-335.
- Haldane, J. S. and Priestley, J. G.** (1935). Respiration. London: Oxford University Press.
- Hawkins, A. J. S., Widdows, J. and Bayne, B. L.** (1989). The relevance of whole-body protein metabolism to measured costs of maintenance and growth in *Mytilus edulis*. *Physiol. Zool.* **62**, 745-763.
- Helmuth, B.** (2009). From cells to coastlines: how can we use physiology to forecast the impacts of climate change? *J. Exp. Biol.* **212**, 753-760.
- Houlihan, D., Agnisola, C., Hamilton, N. and GENOINO, I.** (1987). Oxygen consumption of the isolated heart of *Octopus*: effects of power output and hypoxia. *J. Exp. Biol.* **131**, 137.
- Howell, B. J. and Gilbert, D. L.** (1976). pH-temperature dependence of the hemolymph of the squid, *Loligo pealei*. *Comp. Biochem. Physiol. A Physiol.* **55**, 287-289.
- Huber.** (2004). PreSens product sheet for Microx TX3-trace-trace, pp. 4. Regensburg, Germany: Precision Sensing GmbH
- Huelsenbeck, J. P. and Ronquist, F.** (2001). MRBAYES: Bayesian inference of phylogenetic trees. *Bioinformatics* **17**, 754-755.
- Iftikar, F. I. and Hickey, A. J. R.** (2013). Do mitochondria limit hot fish hearts? Understanding the role of mitochondrial function with heat stress in *Notolabrus celidotus*. *Plos One* **8**, e64120.

- Ikeda, Y., Sugimoto, C., Yonamine, H. and Oshima, Y.** (2009). Method of ethanol anaesthesia and individual marking for oval squid (*Sepioteuthis lessoniana* Férussac, 1831 in Lesson 1830–1831). *Aquac. Res.* **41**, 157-160.
- Ito, N., Komiyama, N. H. and Fermi, G.** (1995). Structure of deoxyhaemoglobin of the antarctic fish *Pagothenia bernacchii* with an analysis of the structural basis of the root effect by comparison of the liganded and unliganded haemoglobin structures. *J. Mol. Biol.* **250**, 648-658.
- Jacobs, S. S., Amos, A. F. and Bruchhausen, P. M.** (1970). Ross sea oceanography and antarctic bottom water formation. *Deep-Sea Res Oceanogr Abstr* **17**, 935-962.
- Jiang, N., Tan, N. S., Ho, B. and Ding, J. L.** (2007). Respiratory protein-generated reactive oxygen species as an antimicrobial strategy. *Nat. Immunol.* **8**, 1114-1122.
- Johns, G. C. and Somero, G. N.** (2004). Evolutionary convergence in adaptation of proteins to temperature: A4-lactate dehydrogenases of pacific damselfishes (*Chromis spp.*). *Mol. Biol. Evol.* **21**, 314-320.
- Johnston, I., Calvo, J., Guderley, H., Fernandez, D. and Palmer, L.** (1998). Latitudinal variation in the abundance and oxidative capacities of muscle mitochondria in perciform fishes. *J. Exp. Biol.* **201**, 1.
- Johnston, I. A., Fitch, N., Zummo, G., Wood, R. E., Harrison, P. and Tota, B.** (1983). Morphometric and ultrastructural features of the ventricular myocardium of the haemoglobin-less icefish *Chaenocephalus aceratus*. *Comp. Biochem. Physiol. A Physiol.* **76**, 475-480.
- Joubin, L.** (1905). Description de deux Élédones provenant de l'Expédition du Dr Charcot dans l'Antarctique. *Mémoires de la Société Zoologique de France* **18**, 22-31.
- Kawall, H., Torres, J., Sidell, B. and Somero, G. N.** (2002). Metabolic cold adaptation in Antarctic fishes: evidence from enzymatic activities of brain. *Mar. Biol.* **140**, 279-286.
- Klinck, J. M., Hofmann, E. E., Beardsley, R. C., Salihoglu, B. and Howard, S.** (2004). Water-mass properties and circulation on the west Antarctic Peninsula Continental Shelf in Austral Fall and Winter 2001. *Deep-Sea Res. Pt. II* **51**, 1925-1946.
- Knox, G. and Lowry, J.** (1977). A comparison between the benthos of the Southern Ocean and the North Polar Ocean with special reference to the Amphipoda and the Polychaeta. *Polar oceans. Arctic Institute of North America, Calgary*, 423-462.
- Kock, K.-H. and Kellermann, A.** (1991). Reproduction in Antarctic notothenioid fish. *Antarct. Sci.* **3**, 125-150.
- Kosakovsky Pond, S. L. and Frost, S. D. W.** (2005). Not so different after all: A comparison of methods for detecting amino acid sites under selection. *Mol. Biol. Evol.* **22**, 1208-1222.
- Kosakovsky Pond, S. L., Scheffler, K., Gravenor, M. B., Poon, A. F. Y. and Frost, S. D. W.** (2010). Evolutionary fingerprinting of genes. *Mol. Biol. Evol.* **27**, 520-536.
- Kremer, N., Schwartzman, J., Augustin, R., Zhou, L., Ruby, E. G., Hourdez, S. and McFall-Ngai, M. J.** (2014). The dual nature of haemocyanin in the establishment and persistence of the squid–vibrio symbiosis. *Proc. R. Soc. Biol. Sci. Ser. B* **281**.
- Lapennas, G. N. and Lutz, P. L.** (1982). Oxygen affinity of sea turtle blood. *Resp. Physiol.* **48**, 59-74.

- Laptikhovsky, V.** (2013). Reproductive strategy of deep-sea and Antarctic octopods of the genera *Graneledone*, *Adelieledone* and *Muusoctopus* (Mollusca: Cephalopoda). *Aquat Biol* **18**, 21-29.
- Laptikhovsky, V., Salman, A., Önsoy, B., Akalin, M. and Ceylan, B.** (2014). Reproduction in rare bathyal octopods *Pteroctopus tetracirrhus* and *Scaeurigus unicolor* (Cephalopoda: Octopoda) in the east Mediterranean as an apparent response to extremely oligotrophic deep seas. *Deep Sea Research Part I: Oceanographic Research Papers* **92**, 85-92.
- Leporati, S. C., Pecl, G. T. and Semmens, J. M.** (2006). Cephalopod hatchling growth: the effects of initial size and seasonal temperatures. *Mar. Biol.* **151**, 1375-1383.
- Lieb, B. and Markl, J.** (2004). Evolution of molluscan hemocyanins as deduced from DNA sequencing. *Micron* **35**, 117-119.
- Lieb, B., Altenhein, B. and Markl, J.** (2000). The sequence of a gastropod hemocyanin (HtH1 from *Haliotis tuberculata*). *J. Biol. Chem.* **275**, 5675-5681.
- Lieb, B., Altenhein, B., Markl, J., Vincent, A., van Olden, E., van Holde, K. E. and Miller, K. I.** (2001). Structures of two molluscan hemocyanin genes: Significance for gene evolution. *Proc. Natl. Acad. Sci. USA* **98**, 4546-4551.
- Lieb, B., Gebauer, W., Gatsogiannis, C., Depoix, F., Hellmann, N., Harasewych, M., Strong, E. and Markl, J.** (2010). Molluscan mega-hemocyanin: an ancient oxygen carrier tuned by a ~550 kDa polypeptide. *Frontiers in Zoology* **7**, 14.
- Livermore, R., Nankivell, A., Eagles, G. and Morris, P.** (2005). Paleogene opening of Drake Passage. *Earth Planet Sc. Lett.* **236**, 459-470.
- Locarnini, R., Mishonov, A., Antonov, J., Boyer, T., Garcia, H., Baranova, O., Zweng, M. and Johnson, D.** (2009). World Ocean Atlas 2009: Temperature. In *NOAA Atlas NESDIS*, vol. 1 (ed. S. Levitus), pp. 184. Washington, D.C.: U.S. Government Printing Office.
- Lockwood, B. L. and Somero, G. N.** (2012). Functional determinants of temperature adaptation in enzymes of cold- versus warm-adapted mussels (genus *Mytilus*). *Mol. Biol. Evol.* **29**, 3061-3070.
- Loewenthal, R., Sancho, J., Reinikainen, T. and Fersht, A. R.** (1993). Long-range surface charge-charge interactions in proteins: Comparison of experimental results with calculations from a theoretical method. *J. Mol. Biol.* **232**, 574-583.
- Logue, J. A., de Vries, A. L., Fodor, E. and Cossins, A. R.** (2000). Lipid compositional correlates of temperature-adaptive interspecific differences in membrane physical structure. *J. Exp. Biol.* **203**, 2105-2115.
- Lyndon, A., Houlihan, D. and Hall, S.** (1989). The apparent contribution of protein synthesis to specific dynamic action in cod. *Arch. Int. Physiol. Biochem* **97**, C31.
- Ma, Q.-J., Li, H.-P., Yang, F., Zhang, J., Wu, X.-F., Bai, Y. and Li, X.-F.** (2012). A fluorescent sensor for low pH values based on a covalently immobilized rhodamine-naphthalimide conjugate. *Sensor Actuat. B-Chem.* **166-167**, 68-74.
- Madan, J. J. and Wells, M. J.** (1996). Why squid can breathe easy. *Nature* **380**, 590-590.
- Madan, J. J. and Wells, J.** (1996). Cutaneous respiration in *Octopus vulgaris*. *J. Exp. Biol.* **199**, 2477.
- Mangum, C.** (1980). Respiratory function of the hemocyanins. *Integr. Comp. Biol.* **20**, 19.
- Mangum, C. P.** (1990). Gas transport in the blood. In *Squid as experimental animals*, eds. D. L. Gilbert W. J. Adelman Jr and J. M. Arnold), pp. 443-468. New York: Plenum Publishing Corporation.

- Mark, F. C., Bock, C. and Pörtner, H. O.** (2002). Oxygen-limited thermal tolerance in Antarctic fish investigated by MRI and ³¹P-MRS. *Am J Physiol-Reg I* **283**, R1254-R1262.
- Markl, J.** (2013). Evolution of molluscan hemocyanin structures. *Biochim. Biophys. Acta* **1834**, 1840-1852.
- Marsh, A. G., Maxson, R. E. and Manahan, D. T.** (2001). High macromolecular synthesis with low metabolic cost in Antarctic sea urchin embryos. *Science* **291**, 1950-1952.
- Martín-Durán, J. M., de Mendoza, A., Sebé-Pedrós, A., Ruiz-Trillo, I. and Hejnol, A.** (2013). A broad genomic survey reveals multiple origins and frequent losses in the evolution of respiratory hemerythrins and hemocyanins. *Genome biology and evolution* **5**, 1435-1442.
- Mäthger, L. M., Bell, G. R. R., Kuzirian, A. M., Allen, J. J. and Hanlon, R. T.** (2012). How does the blue-ringed octopus (*Hapalochlaena lunulata*) flash its blue rings? *J. Exp. Biol.* **215**, 3752-3757.
- Matschiner, M., Hanel, R. and Salzburger, W.** (2009). Gene flow by larval dispersal in the Antarctic notothenioid fish *Gobionotothen gibberifrons*. *Mol. Ecol.* **18**, 2574-2587.
- Matschiner, M., Hanel, R. and Salzburger, W.** (2011). On the origin and trigger of the notothenioid adaptive radiation. *Plos One* **6**, e18911.
- Melzner, F., Bock, C. and Pörtner, H. O.** (2006a). Critical temperatures in the cephalopod *Sepia officinalis* investigated using in vivo ³¹P NMR spectroscopy. *J. Exp. Biol.* **209**, 891.
- Melzner, F., Bock, C. and Pörtner, H. O.** (2006b). Temperature-dependent oxygen extraction from the ventilatory current and the costs of ventilation in the cephalopod *Sepia officinalis*. *J. Comp. Physiol. B Biochem. Syst. Environ. Physiol.* **176**, 607-621.
- Melzner, F., Mark, F. C. and Pörtner, H. O.** (2007a). Role of blood-oxygen transport in thermal tolerance of the cuttlefish, *Sepia officinalis*. *Integr. Comp. Biol.* **47**, 645-655.
- Melzner, F., Bock, C. and Pörtner, H. O.** (2007b). Coordination between ventilatory pressure oscillations and venous return in the cephalopod *Sepia officinalis* under control conditions, spontaneous exercise and recovery. *J. Comp. Physiol. B Biochem. Syst. Environ. Physiol.* **177**, 1-17.
- Meredith, M. P. and King, J. C.** (2005). Rapid climate change in the ocean west of the Antarctic Peninsula during the second half of the 20th century. *Geophys Res Lett* **32**, L19604.
- Mesa, M. L. and Vacchi, M.** (2001). Age and growth of high Antarctic notothenioid fish. *Antarct. Sci.* **13**, 227-235.
- Miller, K., Cuff, M., Lang, W., Varga-Weisz, P., Field, K. and van Holde, K.** (1998). Sequence of the *Octopus dofleini* hemocyanin subunit: structural and evolutionary implications1. *J. Mol. Biol.* **278**, 827-842.
- Miller, K. I.** (1985). Oxygen equilibria of *Octopus dofleini* hemocyanin. *Biochemistry* **24**, 4582-4586.
- Miller, K. I.** (1995). Cephalopod haemocyanins. A review of structure and function. *Mar. Freshw. Behav. Physiol.* **25**, 101-120.
- Miller, K. I. and van Holde, K. E.** (1982). The structure of *Octopus dofleini* hemocyanin. *Comp. Biochem. Physiol., B: Comp. Biochem.* **73**, 1013-1018.
- Miller, K. I., Van Holde, K. E., Toumadje, A., Johnson Jr, W. and Lamy, J.** (1988). Structure and function of the carboxyl-terminal oxygen-binding domain from the subunit of *Octopus dofleini* hemocyanin. *Biochemistry* **27**, 7282-7288.

- Mirceta, S., Signore, A. V., Burns, J. M., Cossins, A. R., Campbell, K. L. and Berenbrink, M. (2013). Evolution of mammalian diving capacity traced by myoglobin net surface charge. *Science* **340**.
- Morris, S. and Bridges, C. R. (1985). An investigation of haemocyanin oxygen affinity in the semi-terrestrial crab *Ocypode saratan* forsk. *J. Exp. Biol.* **117**, 119-132.
- Morris, S., Taylor, A. C., Bridges, C. R. and Grieshaber, M. K. (1985). Respiratory properties of the haemolymph of the intertidal prawn *Palaemon elegans* (Rathke). *J. Exp. Zool.* **233**, 175-186.
- Murrell, B., Wertheim, J. O., Moola, S., Weighill, T., Scheffler, K. and Pond, S. L. K. (2012). Detecting individual sites subject to episodic diversifying selection. *PLoS genetics* **8**, e1002764.
- Murrell, B., Moola, S., Mabona, A., Weighill, T., Sheward, D., Kosakovsky Pond, S. L. and Scheffler, K. (2013). FUBAR : A Fast, Unconstrained Bayesian AppRoximation for inferring selection. *Mol. Biol. Evol.*
- Nesis, K. (1999). The duration of egg incubation in high-latitude and deep-sea cephalopods. *Russian Journal of Marine Biology* **25**, 499-506.
- Nguyen, T. H., Venugopala, T., Chen, S., Sun, T., Grattan, K. T. V., Taylor, S. E., Basheer, P. A. M. and Long, A. E. (2014). Fluorescence based fibre optic pH sensor for the pH 10–13 range suitable for corrosion monitoring in concrete structures. *Sensor Actuat. B-Chem.* **191**, 498-507.
- Niesel, W. and Thews, G. (1961). Ein neues Verfahren zur schnellen und genauen Aufnahme der Sauerstoffbindungskurve des Blutes und konzentrierter Hämoproteidlösungen. *Pflügers Archiv* **273**, 380-395.
- O'dor, R. K. and Wells, M. J. (1984). Circulation time, blood reserves and extracellular space in a cephalopod. *J. Exp. Biol.* **113**, 461-464.
- O'Dor, R. K. and Webber, D. M. (1986). The constraints on cephalopods: why squid aren't fish. *Can. J. Zool.* **64**, 1591-1605.
- O'Dor, R. K. and Webber, D. M. (1991). Invertebrate athletes: trade-offs between transport efficiency and power density in cephalopod evolution. *J. Exp. Biol.* **160**, 93-112.
- Oellermann, M., Pörtner, H.-O. and Mark, F. C. (2014). Simultaneous high-resolution pH and spectrophotometric recordings of oxygen binding in blood microvolumes. *J. Exp. Biol.* **217**, 1430-1436.
- Oellermann, M., Lieb, B., Portner, H.-O., Semmens, J. and Mark, F. (2015). Blue blood on ice: modulated blood oxygen transport facilitates cold compensation and eurythermy in an Antarctic octopod. *Frontiers in Zoology* **12**, 6.
- Oosthuizen, A. and Smale, M. J. (2003). Population biology of *Octopus vulgaris* on the temperate south-eastern coast of South Africa.
- Pace, C. N. and Shaw, K. L. (2000). Linear extrapolation method of analyzing solvent denaturation curves. *Proteins: Structure, Function, and Bioinformatics* **41**, 1-7.
- Pace, C. N., Grimsley, G. R. and Scholtz, J. M. (2009). Protein ionizable groups: pk values and their contribution to protein stability and solubility. *J. Biol. Chem.* **284**, 13285-13289.
- Packard, A. (1972). Cephalopods and fish: the limits of convergence. *Biological Reviews* **47**, 241-307.
- Paradis, E., Claude, J. and Strimmer, K. (2004). APE: analyses of phylogenetics and evolution in R language. *Bioinformatics* **20**, 289-290.
- Patwa, Z. and Wahl, L. M. (2008). The fixation probability of beneficial mutations. *J. Royal Soc. Interface* **5**, 1279-1289.

- Peck, L. S., Pörtner, H. O. and Hardewig, I.** (2002). Metabolic demand, oxygen supply, and critical temperatures in the Antarctic bivalve *Laternula elliptica*. *Physiol. Biochem. Zool.* **75**, 123-133.
- Pérez, M. C., López, D. A., Aguila, K. and González, M. L.** (2006). Feeding and growth in captivity of the octopus *Enteroctopus megalocyathus* Gould, 1852. *Aquac. Res.* **37**, 550-555.
- Perutz, M. F.** (1970). Stereochemistry of cooperative effects in haemoglobin: Haem-haem interaction and the problem of allostery. *Nature* **228**, 726-734.
- Perutz, M. F., Wilkinson, A. J., Paoli, M. and Dodson, G. G.** (1998). The stereochemical mechanism of the cooperative effects in hemoglobin revisited. *Annu. Rev. Biophys. Biomol. Struct.* **27**, 1-34.
- Petsko, G. A.** (2001). Structural basis of thermostability in hyperthermophilic proteins, or "There's more than one way to skin a cat". *Methods Enzymol.* **334**, 469-478.
- Petza, D., Katsanevakis, S. and Verriopoulos, G.** (2006). Experimental evaluation of the energy balance in *Octopus vulgaris*, fed ad libitum on a high-lipid diet. *Mar. Biol.* **148**, 827-832.
- Piatkowski, U., Allcock, L. and Vecchione, M.** (2003). Cephalopod diversity and ecology. *Ber. Polarforsch* **470**, 32-38.
- Pond, S. L. K. and Frost, S. D. W.** (2005). Datamonkey: rapid detection of selective pressure on individual sites of codon alignments. *Bioinformatics* **21**, 2531-2533.
- Pörtner, H. O.** (1990). An analysis of the effects of pH on oxygen binding by squid (*Illex illecebrosus*, *Loligo pealei*) haemocyanin. *J. Exp. Biol.* **150**, 407.
- Pörtner, H. O.** (1994). Coordination of metabolism, acid-base regulation and haemocyanin function in cephalopods. *Mar. Behav. Physiol.* **25**, 131-148.
- Pörtner, H. O.** (2001). Climate change and temperature-dependent biogeography: oxygen limitation of thermal tolerance in animals. *Naturwissenschaften* **88**, 137-146.
- Pörtner, H. O.** (2002a). Physiological basis of temperature-dependent biogeography: trade-offs in muscle design and performance in polar ectotherms. *J. Exp. Biol.* **205**, 2217-2230.
- Pörtner, H. O.** (2002b). Environmental and functional limits to muscular exercise and body size in marine invertebrate athletes. *Comp. Biochem. Physiol. Part A Mol. Integr. Physiol.* **133**, 303-321.
- Pörtner, H. O.** (2002c). Climate variations and the physiological basis of temperature dependent biogeography: systemic to molecular hierarchy of thermal tolerance in animals. *Comp. Biochem. Physiol. Part A Mol. Integr. Physiol.* **132**, 739-761.
- Pörtner, H. O.** (2004). Biological impact of elevated ocean CO₂ concentrations: Lessons from animal physiology and earth history.
- Pörtner, H. O.** (2006). Climate-dependent evolution of Antarctic ectotherms: An integrative analysis. *Deep-Sea Res. Pt. II* **53**, 1071-1104.
- Pörtner, H. O.** (2010). Oxygen-and capacity-limitation of thermal tolerance: a matrix for integrating climate-related stressor effects in marine ecosystems. *J. Exp. Biol.* **213**, 881.
- Pörtner, H. O. and Zielinski, S.** (1998). Environmental constraints and the physiology of performance in squids. *S. Afr. J. Mar. Sci.* **20**, 207-221.
- Pörtner, H. O. and Knust, R.** (2007). Climate change affects marine fishes through the oxygen limitation of thermal tolerance. *Science* **315**, 95-97.
- Pörtner, H. O. and Farrell, A. P.** (2008). Ecology. Physiology and climate change. *Science* **322**, 690-692.
- Pörtner, H. O., O'Dor, R. K. and Macmillan, D. L.** (1994). Physiology of cephalopod molluscs - Lifestyle and performance adaptations. Basel: Gordon and Breach.

- Pörtner, H. O., Peck, L. and Somero, G.** (2007). Thermal limits and adaptation in marine Antarctic ectotherms: an integrative view. *Philos. Trans. R. Soc. Lond. B Biol. Sci.* **362**, 2233-2258.
- Pörtner, H. O., Walther, K. and Wittmann, A.** (2013). Excess oxygen in polar evolution: A whole organism perspective. In *Adaptation and Evolution in Marine Environments*, vol. 2 eds. C. Verde and G. di Prisco), pp. 67-87. Berlin Heidelberg: Springer-Verlag
- PreSens.** (2005). Instruction manual pH-4 micro, pp. 51. Regensburg, Germany: Precision Sensing GmbH
- Primmitt, D. R., Randall, D. J., Mazeaud, M. and Boutilier, R. G.** (1986). The role of catecholamines in erythrocyte pH regulation and oxygen transport in rainbow trout (*Salmo gairdneri*) during exercise. *J. Exp. Biol.* **122**, 139-148.
- Qvist, J., Weber, R. E., DeVries, A. L. and Zapol, W. M.** (1977). pH and haemoglobin oxygen affinity in blood from the Antarctic cod *Dissostichus mawsoni*. *J. Exp. Biol.* **67**, 77-88.
- Rakusa-Suszczewski, S.** (1993). Hydrography and hydrochemistry. In *The Maritime Antarctic Coastal Ecosystem of Admiralty Bay*, vol. 32, pp. 32-34. Warsaw: Department of Antarctic Biology, Polish Academy of Sciences.
- Ramsing, N. and Gundersen, J.** Seawater and Gases: Tabulated physical parameters of interest to people working with microsensors in marine systems. .
- Rasmussen, J. R., Wells, R. M. G., Henty, K., Clark, T. D. and Brittain, T.** (2009). Characterization of the hemoglobins of the Australian lungfish *Neoceratodus forsteri* (Kreffft). *Comp. Biochem. Physiol., A: Comp. Physiol.* **152**, 162-167.
- Redfield, A., Coolidge, T. and Hurd, A.** (1926). The transport of oxygen and carbon dioxide by some bloods containing hemocyanin. *J. Biol. Chem.* **69**, 475.
- Reeves, R. B.** (1972). An imidazole alphasat hypothesis for vertebrate acid-base regulation: Tissue carbon dioxide content and body temperature in bullfrogs. *Resp. Physiol.* **14**, 219-236.
- Reeves, R. B.** (1980). A rapid micro method for obtaining oxygen equilibrium curves on whole blood. *Resp. Physiol.* **42**, 299-315.
- Reiber, C. L. and McGaw, I. J.** (2009). A review of the “open” and “closed” circulatory systems: New terminology for complex invertebrate circulatory systems in light of current findings. *International Journal of Zoology* **2009**, 1-8.
- Ritz, C. and Streibig, J. C.** (2005). Bioassay analysis using R. *J. Stat. Softw.* **12**, 1-22.
- Robertson, J. D.** (1953). Further studies on ionic regulation in marine invertebrates. *J. Exp. Biol.* **30**, 277-296.
- Robison, B., Seibel, B. and Drazen, J.** (2014). Deep-sea octopus (*Graneledone boreopacifica*) conducts the longest-known egg-brooding period of any animal. *Plos One* **9**, e103437.
- Rosas, C., Cuzon, G., Pascual, C., Gaxiola, G., Chay, D., López, N., Maldonado, T. and Domingues, P.** (2007). Energy balance of *Octopus maya* fed crab or an artificial diet. *Mar. Biol.* **152**, 371-381.
- Ruud, J. T.** (1954). Vertebrates without erythrocytes and blood pigment. *Nature* **173**, 848-850.
- Safavi, A. and Bagheri, M.** (2003). Novel optical pH sensor for high and low pH values. *Sensor Actuat. B-Chem.* **90**, 143-150.
- Sanders, N. K., Morris, S., Childress, J. J. and McMahon, B. R.** (1992). Effects of ammonia, trimethylamine, l-lactate and CO₂ on some decapod crustacean haemocyanins. *Comp. Biochem. Physiol. A Physiol.* **101**, 511-516.
- Schipp, R.** (1987). General morphological and functional characteristics of the cephalopod circulatory system. An introduction. *Cell. Mol. Life Sci.* **43**, 474-477.

- Schlitzer, R.** (2002). Interactive analysis and visualization of geoscience data with Ocean Data View. *Computers & geosciences* **28**, 1211-1218.
- Schofield, O., Ducklow, H. W., Martinson, D. G., Meredith, M. P., Moline, M. A. and Fraser, W. R.** (2010). How do polar marine ecosystems respond to rapid climate change? *Science* **328**, 1520-1523.
- Scholander, P., Hock, R., Walters, V. and Irving, L.** (1950). Adaptation to cold in arctic and tropical mammals and birds in relation to body temperature, insulation, and basal metabolic rate. *The Biological Bulletin* **99**, 259-271.
- Schrodinger, LLC.** (2010). The PyMOL Molecular Graphics System, Version 1.3r1.
- Seibel, B. A.** (2007). On the depth and scale of metabolic rate variation: scaling of oxygen consumption rates and enzymatic activity in the Class Cephalopoda (Mollusca). *J. Exp. Biol.* **210**, 1-11.
- Seibel, B. A.** (2012). The jumbo squid, *Dosidicus gigas* (Ommastrephidae), living in oxygen minimum zones II: Blood-oxygen binding. *Deep-Sea Res. Pt. II* **95**, 139-144.
- Seibel, B. A. and Childress, J. J.** (2000). Metabolism of benthic octopods (Cephalopoda) as a function of habitat depth and oxygen concentration. *Deep-Sea Res. Part I Oceanogr. Res. Pap.* **47**, 1247-1260.
- Senozan, N., Avinc, A. and Unver, Z.** (1988). Hemocyanin levels in *Octopus vulgaris* and the cuttlefish *Sepia officinalis* from the Aegean sea. *Comp. Biochem. Physiol. A Physiol.* **91**, 581-585.
- Sick, H. and Gersonde, K.** (1969). Method of continuous registration of oxygen binding curves of hemoproteins by means of a diffusion chamber. *Anal. Biochem.* **32**, 362-376.
- Sick, H. and Gersonde, K.** (1972). Theory and application of the diffusion technique for measurement and analysis of O₂-binding properties of very autoxidizable hemoproteins. *Anal. Biochem.* **47**, 46-56.
- Sidell, B. D.** (1998). Intracellular oxygen diffusion: the roles of myoglobin and lipid at cold body temperature. *J. Exp. Biol.* **201**, 1119-1128.
- Sidell, B. D. and O'Brien, K. M.** (2006). When bad things happen to good fish: the loss of hemoglobin and myoglobin expression in Antarctic icefishes. *J. Exp. Biol.* **209**, 1791-1802.
- Simon, C., Frati, F., Beckenbach, A., Crespi, B., Liu, H. and Flook, P.** (1994). Evolution, weighting, and phylogenetic utility of mitochondrial gene sequences and a compilation of conserved polymerase chain reaction primers. *Ann. Entomol. Soc. Am.* **87**, 651-701.
- Small, D. J., Vayda, M. E. and Sidell, B. D.** (1998). A novel vertebrate myoglobin gene containing three A+T-rich introns is conserved among antarctic teleost species which differ in myoglobin expression. *J. Mol. Evol.* **47**, 156-166.
- Small, D. J., Moylan, T., Vayda, M. E. and Sidell, B. D.** (2003). The myoglobin gene of the Antarctic icefish, *Chaenocephalus aceratus*, contains a duplicated TATAAAA sequence that interferes with transcription. *J. Exp. Biol.* **206**, 131-139.
- Smith, J. A., Andrews, P. L. R., Hawkins, P., Louhimies, S., Ponte, G. and Dickel, L.** (2013). Cephalopod research and EU Directive 2010/63/EU: Requirements, impacts and ethical review. *J. Exp. Mar. Biol. Ecol.* **447**, 31-45.
- Somero, G. N.** (2004). Adaptation of enzymes to temperature: searching for basic "strategies". *Comparative biochemistry and physiology. Part B, Biochemistry & molecular biology* **139**, 321-333.
- Somero, G. N.** (2010). The physiology of climate change: how potentials for acclimatization and genetic adaptation will determine 'winners' and 'losers'. *J. Exp. Biol.* **213**, 912-920.

- Somero, G. N.** (2012). The physiology of global change: Linking patterns to mechanisms. *Annual Review of Marine Science* **4**, 39-61.
- Sommer, A., Klein, B. and Pörtner, H. O.** (1997). Temperature induced anaerobiosis in two populations of the polychaete worm *Arenicola marina* (L.). *J. Comp. Physiol. B* **167**, 25-35.
- Steffensen, J. F.** (2002). Metabolic cold adaptation of polar fish based on measurements of aerobic oxygen consumption: fact or artefact? Artefact! *Comp. Biochem. Physiol. Part A Mol. Integr. Physiol.* **132**, 789-795.
- Storch, D., Menzel, L., Frickenhaus, S. and Pörtner, H.-O.** (2014). Climate sensitivity across marine domains of life: limits to evolutionary adaptation shape species interactions. *Global Change Biol*, 1-9.
- Strobel, A., Hu, M. Y., Gutowska, M. A., Lieb, B., Lucassen, M., Melzner, F., Pörtner, H. O. and Mark, F. C.** (2012). Influence of temperature, hypercapnia, and development on the relative expression of different hemocyanin isoforms in the common cuttlefish *Sepia officinalis*. *J. Exp. Zool. A Ecol. Genet. Physiol.* **9999**, 1-13.
- Strugnell, J., Norman, M., Vecchione, M., Guzik, M. and Allcock, A. L.** (2014). The ink sac clouds octopod evolutionary history. *Hydrobiologia* **725**, 215-235.
- Strugnell, J., Cherel, Y., Cooke, I., Gleadall, I., Hochberg, F., Ibanez, C., Jorgensen, E. and Laptikhovskiy, V.** (2011). The Southern Ocean: Source and sink? *Deep-Sea Res. Pt. II* **58**, 196-204.
- Strugnell, J. M., Rogers, A. D., Prodöhl, P. A., Collins, M. A. and Allcock, A. L.** (2008). The thermohaline expressway: the Southern Ocean as a centre of origin for deep-sea octopuses. *Cladistics* **24**, 853-860.
- Sykes, A. V., Baptista, F. D., Gonçalves, R. A. and Andrade, J. P.** (2012). Directive 2010/63/EU on animal welfare: a review on the existing scientific knowledge and implications in cephalopod aquaculture research. *Reviews in Aquaculture* **4**, 142-162.
- Talavera, G. and Castresana, J.** (2007). Improvement of phylogenies after removing divergent and ambiguously aligned blocks from protein sequence alignments. *Syst. Biol.* **56**, 564-577.
- Tamburrini, M., Brancaccio, A., Ippoliti, R. and Di Prisco, G.** (1992). The amino acid sequence and oxygen-binding properties of the single hemoglobin of the cold-adapted Antarctic teleost *Gymnodraco acuticeps*. *Arch. Biochem. Biophys.* **292**, 295-302.
- Team, R. C.** (2014). R: A language and environment for statistical computing. Vienna, Austria: R Foundation for Statistical Computing.
- Terwilliger, N. B.** (1998). Functional adaptations of oxygen-transport proteins. *J. Exp. Biol.* **201**, 1085-1098.
- Terwilliger, N. B. and Brown, A. C.** (1993). Ontogeny of hemocyanin function in the dungeness crab cancer magister: The interactive effects of developmental stage and divalent cations on hemocyanin oxygenation properties. *J. Exp. Biol.* **183**, 1-13.
- Tetens, V., Wells, R. M. G. and DeVries, A. L.** (1984). Antarctic fish blood: respiratory properties and the effects of thermal acclimation. *J. Exp. Biol.* **109**, 265.
- Thonig, A., Oellermann, M., Lieb, B. and Mark, F.** (2014). A new haemocyanin in cuttlefish (*Sepia officinalis*) eggs: sequence analysis and relevance during ontogeny. *EvoDevo* **5**, 6.
- Tota, B., Acierno, R. and Agnisola, C.** (1991). Mechanical performance of the isolated and perfused heart of the haemoglobinless antarctic icefish *Chionodraco*

- hamatus* (Lonnberg): Effects of loading conditions and temperature. *Philos. Trans. R. Soc. Lond. B Biol. Sci.* **332**, 191-198.
- Undheim, E. A., Georgieva, D. N., Thoen, H. H., Norman, J. A., Mork, J., Betzel, C. and Fry, B. G.** (2010). Venom on ice: first insights into Antarctic octopus venoms. *Toxicon* **56**, 897-913.
- Van Holde, K. E. and Cohen, L. B.** (1964). Physical studies of hemocyanins. I. Characterization and subunit structure of *Loligo pealei* hemocyanin. *Biochemistry* **3**, 1803-1808.
- van Holde, K. E. and Miller, K. I.** (1995). Hemocyanins. In *Adv. Protein Chem.*, vol. Volume 47 eds. F. M. R. J. T. E. C.B. Anfinsen and S. E. David), pp. 1-81: Academic Press.
- van Holde, K. E., Miller, K. I. and Decker, H.** (2001). Hemocyanins and Invertebrate Evolution. *J. Biol. Chem.* **276**, 15563-15566.
- Verde, C., Parisi, E. and Di Prisco, G.** (2006). The evolution of thermal adaptation in polar fish. *Gene* **385**, 137-145.
- Verde, C., Berenbrink, M. and di Prisco, G.** (2008). Evolutionary physiology of oxygen secretion in the eye of fishes of the suborder Notothenioidei. In *Dioxygen Binding and Sensing Proteins*, pp. 49-65: Springer.
- Verde, C., Giordano, D., Russo, R., Riccio, A., Coppola, D. and Di Prisco, G.** (2011). Evolutionary adaptations in antarctic fish: The oxygen-transport system. *Oecologia Australis* **15**, 40-50.
- Verde, C., Howes, B. D., De Rosa, M. C., Raiola, L., Smulevich, G., Williams, R., Giardina, B., Parisi, E. and Di Prisco, G.** (2004). Structure and function of the Gondwanian hemoglobin of *Pseudaphritis urvillii*, a primitive nototheniid fish of temperate latitudes. *Protein Sci.* **13**, 2766-2781.
- Walther, K., Sartoris, F. J., Bock, C. and Pörtner, H. O.** (2009). Impact of anthropogenic ocean acidification on thermal tolerance of the spider crab *Hyas araneus*. *Biogeosciences* **6**, 2207-2215.
- Weber, R. E. and Campbell, K. L.** (2011). Temperature dependence of haemoglobin-oxygen affinity in heterothermic vertebrates: mechanisms and biological significance. *Acta Physiol (Oxf)* **202**, 549-562.
- Weber, R. E., Behrens, J. W., Malte, H. and Fago, A.** (2008). Thermodynamics of oxygenation-linked proton and lactate binding govern the temperature sensitivity of O₂ binding in crustacean (*Carcinus maenas*) hemocyanin. *J. Exp. Biol.* **211**, 1057-1062.
- Weidgans, B. M., Krause, C., Klimant, I. and Wolfbeis, O. S.** (2004). Fluorescent pH sensors with negligible sensitivity to ionic strength. *Analyst* **129**, 645-650.
- Wells, M.** (1992). The cephalopod heart: The evolution of a high-performance invertebrate pump. *Cell. Mol. Life Sci.* **48**, 800-808.
- Wells, M.** (1995). The evolution of a racing snail. *Marine Behaviour and Physiology-Sections A and B* **25**, 1-12.
- Wells, M. and Smith, P.** (1987). The performance of the octopus circulatory system: a triumph of engineering over design. *Cell. Mol. Life Sci.* **43**, 487-499.
- Wells, M. J., O'Dor, R. K., Mangold, K. and Wells, J.** (1983). Feeding and metabolic rate in octopus. *Mar. Behav. Physiol.* **9**, 305-317.
- Wells, R. M. G. and Weber, R. E.** (1989). The measurement of oxygen affinity in blood and haemoglobin solutions. *Techniques in comparative respiratory physiology: an experimental approach.* Cambridge University Press, Cambridge, 279-303.
- Wells, R. M. G., Ashby, M. D., Duncan, S. J. and Macdonald, J. A.** (1980). Comparative study of the erythrocytes and haemoglobins in nototheniid fishes from Antarctica. *J. Fish Biol.* **17**, 517-527.

- Whiteley, N. M., Taylor, E. W. and El Haj, A. J.** (1997). Seasonal and latitudinal adaptation to temperature in crustaceans. *J. Therm. Biol.* **22**, 419-427.
- Wittmann, A. C., Pörtner, H. O. and Sartoris, F. J.** (2012). A role for oxygen delivery and extracellular magnesium in limiting cold tolerance of the sub-antarctic stone crab *Paralomis granulosa*? *Physiol. Biochem. Zool.* **85**, 285-298.
- Woolley, S., Johnson, J., Smith, M. J., Crandall, K. A. and McClellan, D. A.** (2003). TreeSAAP: Selection on Amino Acid Properties using phylogenetic trees. *Bioinformatics* **19**, 671-672.
- Yamashita, M. M., Wesson, L., Eisenman, G. and Eisenberg, D.** (1990). Where metal ions bind in proteins. *Proc. Natl. Acad. Sci. USA* **87**, 5648-5652.
- Zachos, J., Pagani, M., Sloan, L., Thomas, E. and Billups, K.** (2001). Trends, rhythms, and aberrations in global climate 65 ma to present. *Science* **292**, 686-693.
- Zielinski, S., Sartoris, F. J. and Pörtner, H. O.** (2001). Temperature effects on hemocyanin oxygen binding in an Antarctic cephalopod. *Biol. Bull. (Woods Hole)* **200**, 67-76.
- Zolla, L., Brunori, M., Richey, B. and Gill, S. J.** (1985). Heterogeneous binding of oxygen and carbon monoxide to dissociated molluscan hemocyanin. *Biophys. Chem.* **22**, 271-280.

6 Appendix

6.1. Patent

Diffusionskammer zur Ermittlung unterschiedlicher Parameter einer
wässrigen Substanz

M Oellermann, FC Mark. E Dunker

Issued on July 7th 2014

Deutsches Patent- und Markenamt

No. DE 10 2013 011 343

BUNDESREPUBLIK DEUTSCHLAND

URKUNDE

über die Erteilung des

Patents

Nr. 10 2013 011 343

IPC

G01N 21/05

Bezeichnung

Diffusionskammer zur Ermittlung unterschiedlicher Parameter einer wässrigen Substanz

Patentinhaber

Alfred-Wegener-Institut Helmholtz-Zentrum für Polar- und Meeresforschung, 27570 Bremerhaven, DE

Erfinder

Dunker, Erich, 27619 Schiffdorf, DE; Mark, Felix Christopher, 27574 Bremerhaven, DE; Oellermann, Michael, 28201 Bremen, DE

Tag der Anmeldung

01.07.2013

München, den 10.07.2014



Die Präsidentin des Deutschen Patent- und Markenamts

Rudloff-Schäffer

Rudloff-Schäffer

(19)  Deutsches Patent- und Markenamt



(10) **DE 10 2013 011 343 B3** 2014.07.10

(12) **Patentschrift**

(21) Aktenzeichen: **10 2013 011 343.1**
 (22) Anmeldetag: **01.07.2013**
 (43) Offenlegungstag: –
 (45) Veröffentlichungstag der Patenterteilung: **10.07.2014**

(51) Int Cl.: **G01N 21/05 (2006.01)**
G01N 33/49 (2006.01)

Innerhalb von neun Monaten nach Veröffentlichung der Patenterteilung kann nach § 59 Patentgesetz gegen das Patent Einspruch erhoben werden. Der Einspruch ist schriftlich zu erklären und zu begründen. Innerhalb der Einspruchsfrist ist eine Einspruchsgebühr in Höhe von 200 Euro zu entrichten (§ 6 Patentkostengesetz in Verbindung mit der Anlage zu § 2 Abs. 1 Patentkostengesetz).

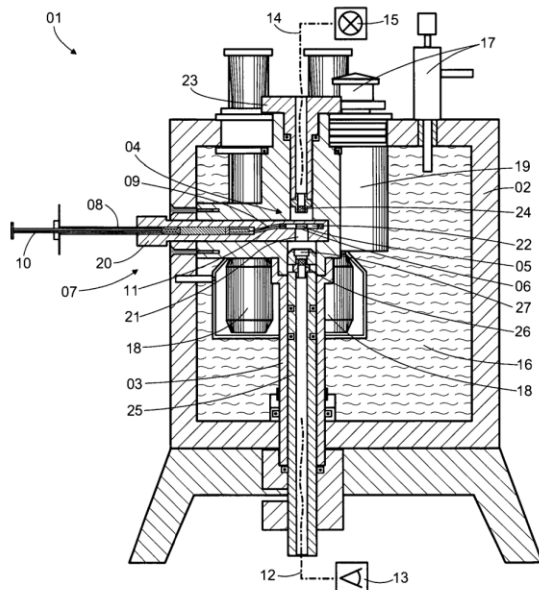
(73) Patentinhaber:
Alfred-Wegener-Institut Helmholtz-Zentrum für Polar- und Meeresforschung, 27570, Bremerhaven, DE

(72) Erfinder:
Oellermann, Michael, 28201, Bremen, DE; Mark, Felix Christopher, 27574, Bremerhaven, DE; Dunker, Erich, 27619, Schiffdorf, DE

(56) Ermittelte Stand der Technik:
siehe Folgeseiten

(54) Bezeichnung: **Diffusionskammer zur Ermittlung unterschiedlicher Parameter einer wässrigen Substanz**

(57) Zusammenfassung: Bekannte Diffusionskammern zur pH-Wert- und Absorptionsmessung an wässrigen Substanzproben messen mit relativ geringer Auflösung, großen Substanzprobenmengen oder nicht zeitgleich in derselben Probe. Bei der erfindungsgemäßen Diffusionskammer (01) sind eine hochauflösende pH-Optode (07) und ein kompaktes Spektrophotometer (13) vorgesehen, deren jeweilige Glasfaseroptik über spezielle konstruktive Maßnahmen in den Zentralzylinder (03) der Diffusionskammer (01) integriert sind. Dabei ist die pH-Optode (07) spritzenförmig ausgebildet und in einen Probenschlitten (20) eingelegt, wobei die Kanüle (11) in eine schräge Nut (32) eingelegt und gasdicht durch einen Dichtring (22) auf dem Probenschlitten (20) geführt ist. Dadurch können kleinste Substanzproben (05) (< 20 µl) gemessen und trotzdem sichergestellt werden, dass die Messspitze (28) in den Randbereich (29) der Substanzprobe (05) eintaucht und nicht den Strahlengang (30) für die Absorptionsmessung stört. Die lichtzu- und ableitende Faseroptik des Spektrophotometers ist in einen oberen und unteren zylindrischen Optikhalter (23, 25) integriert, wobei durch den eingeschobenen unteren Optikhalter (25) über einen Abstandsring (27) die Probenkammer (04) abgedichtet ist und ein Minimalabstand zwischen Kollimatorlinse (26) und Probe (05) gewährleistet wird. Anwendung findet die Diffusionskammer (01) beispielsweise bei der Ermittlung von Sauerstoffbindungskurven geringster Blutmengen kleinster Organismen.





(10) **DE 10 2013 011 343 B3** 2014.07.10

(56) Ermittelter Stand der Technik:

DE	20 2011 051 637	U1
US	2008 / 0 285 011	A1
US	5 056 520	A
US	5 564 419	A
EP	2 110 430	B1

Fa. OceanOptics: USB2000+ Plug-and-Play Spectrometer; URL-Stand 23.06.2013: <http://www.oceanoptics.com/products/usb2000+.asp>.

Fa. PreSens: pH Microsensors, "Measuring with high spatial resolution"; URL-Stand 23.06.2013: <http://www.presens.de/products/brochures/category/sensor-probes/brochure/ph-microsensors.html>.

PÖRTNER, H.-O.; "Coordination of metabolism, acid-base regulation and haemocyanin function in cephalopods", Mar. Fresh. Behav. Physiol. 25, 131-148, 1994.

PÖRTNER, H.-O.; „An analysis of the effects of pH on oxygen binding by squid (*Illex illecebrosus*, *Loligo pealei*) haemocyanin", J. Exp. Biol. 150, 407-424, 1990.

SICK, H. et al: Method for Continuous Registration of O₂-Binding Curves of Hemoproteins by Means of a Diffusion Chamber; ANALYTICAL BIOCHEMISTRY 32, 362-376 (1969).

Universität Rostock, Angewandte Ökologie & Phykologie, Sauerstoff-Mikrooptode, URL Stand 20.06.2013: <http://www.angewandteoekologie.uni-rostock.de/en/forschung3/analytik0/mikroopt/>

WOELFEL, J. et al: Oxygen evolution in a hypersaline crust: in situ photosynthesis quantification by microelectrode profiling and use of planar optode spots in incubation chambers; AQUATIC MICROBIAL ECOLOGY, Vol. 56: 263-273, 2009, doi: 10.3354/arne01326.

ZIELINSKI, S. et al: Temperature Effects on Hemocyanin Oxygen Binding in an Antarctic Cephalopod; Biol. Bull. 200: 67-76 (February 2001).

DE 10 2013 011 343 B3 2014.07.10

Beschreibung

[0001] Die Erfindung bezieht sich auf eine Diffusionskammer zur Ermittlung unterschiedlicher Parameter einer wässrigen Substanz mit einem vertikalen Zentralzylinder mit zumindest einer Probenkammer zur Aufnahme einer Substanzprobe, einem nadelförmigen pH-Messsensor mit einer die Substanzprobe kontaktierenden Messspitze, einem Spektrophotometer mit einer die Substanzprobe durchstrahlenden Glasfaseroptik und einer Gaszuführung in die Probenkammer zur veränderlichen Begasung der Substanzprobe während der Parameterermittlung.

[0002] Der pH-Wert ist ein Maß für den sauren oder basischen Charakter einer wässrigen Substanz. Diese kann in Abhängigkeit von ihrem aktuellen pH-Wert stark variierende Eigenschaften zeigen. Beispielsweise wirkt sich bei Blut der pH-Wert auf die Sauerstoffbindungseigenschaften von Blutpigmenten, wie Hämoglobin oder Hämocyanin, aus. Je geringer der pH-Wert ist, desto weniger Sauerstoff kann das Blutpigment über seine prosthetische Gruppe (d. h. Eisen oder Kupfer) binden. Diese Eigenschaft führt zu einer erleichterten Abgabe von Sauerstoff im Gewebe, wenn dort der Blut-pH-Wert durch stoffwechselbedingte Kohlendioxidabgabe sinkt (Bohr-Effekt). Wird umgekehrt in der Lunge Kohlendioxid abgeatmet, so steigt dort der pH-Wert des Blutes und somit die Aufnahmefähigkeit des Blutpigmentes für Sauerstoff. pH-Wert-Änderungen fließen in die Sauerstoff-Bindungskurven ein, die die Beziehung zwischen dem herrschenden Sauerstoff-Partialdruck und dem prozentualen Anteil des an das Blutpigment gebundenen Sauerstoffs (Blutpigmentsättigung) darstellen. Das Sauerstoffgefälle als Abnahme der Sauerstoff-Partialdrücke zwischen der Außenluft und den Körperzellen bestimmt die Aufnahme des Sauerstoffs. Eine optimale Sauerstoffaufnahme und -abgabe ermöglicht einen effizienten Sauerstofftransport und damit eine hohe Leistungsfähigkeit des Organismus. Mit Sauerstoff angereichertes Blut verändert seinen Farbton durch Konformationsänderungen der jeweiligen prosthetischen Gruppe bei Bindung von Sauerstoff. Beispielsweise zeigt oxygeniertes Hämoglobin einen helleren und kräftigeren Farbton als de-oxygeniertes Hämoglobin, oxygeniertes Hämocyanin hingegen färbt sich blau. Dies hat eine Veränderung des Absorptionsverhaltens der Substanzprobe bei Bestrahlung mit ultraviolettem oder sichtbarem Licht zur Folge. Durch simultane Messungen des pH-Werts und des Absorptionsverhaltens zur Ermittlung der Sauerstoffbindungseigenschaften von Blut bei in-vivo- oder quasi-in-vivo-Untersuchungen können somit wichtige Aussagen über den aktuellen Zustand der Substanz bzw. ihres Trägers gewonnen werden. Dabei ist es aber insbesondere auch wichtig, mit nur geringen Probenvolumen der zu untersuchenden Substanz auskommen zu können, da die Menge des Pro-

benmaterials oft stark limitiert ist (beispielsweise bei Kleinstorganismen).

Stand der Technik

[0003] Aus der US 5 564 419 A ist eine Vorrichtung zur photometrischen in-vitro-Bestimmung des Sauerstoffgehalts in einer Blutprobe bekannt. Mit einer spritzenähnlichen Vorrichtung kann das Blut direkt aus dem Organismus gesogen und über einen Kanal geleitet werden. Dieser wird von Öffnungen in einem Träger gekreuzt, durch die Licht zur Absorptionsmessung eingestrahlt wird. Die Öffnungen sind mit einem Dichtring abgedichtet. Eine pH-Wert-Messung erfolgt jedoch nicht. Aus der EP 2 110 430 B1 ist eine Messzelle zur Messung des biochemischen Sauerstoffbedarfs bekannt, bei der das Ende eines Lichtwellenleiters von einem Spektrophotometer über ein Dichtelement mit der zu untersuchenden Substanz in Verbindung gebracht wird. Aus der US 5 056 520 ist ein nadelförmiger optischer Messsensor mit einem Lichtwellenleiter aus Silizium bekannt, mit dem der pH-Wert einer Blutprobe festgestellt werden kann. Der Lichtwellenleiter wird von einer Hülse geführt und endet mit der Messspitze in einem Tropfen der zu untersuchenden Substanz.

[0004] Aus der Veröffentlichung „Method for Continuous Registration of O₂-Binding Curves of hemoproteins by Means of a Diffusion Chamber“ von H. Sick und K. Gersonde (in *Analytical Biochemistry* 32, 362–376 (1969)) ist eine Diffusionskammer zur photometrischen Messung des Absorptionsverhaltens von Blut unter verschiedenen Begasungen bekannt. In einem Zentralzylinder wird die zu untersuchende Blutprobe auf einem Plexiglasschlitten gelagert und mit Licht einer Quecksilberdampfampe durchstrahlt, das in einem Photodetektor detektiert wird. Der Plexiglasschlitten ist mit einem Dichtring gegenüber dem Zentralzylinder abgedichtet. Die Gasmischungen werden über eine Gaszufuhr in den Zentralzylinder eingeleitet. Eine pH-Wert-Messung erfolgt nicht.

[0005] Aus der Veröffentlichung „Oxygen evolution in a hypersaline crust: in situ photosynthesis quantification by microelectrode profiling and use of planar optode spots in incubation chambers“ von J. Woelfel et al. (in *Aquat Microb Ecol* Vol. 56: 263–273, 2009) ist es bekannt, eine Sauerstoff-Mikrooptode mit Sensor-Spots und einer Faseroptik zur optischen Messung der Primärproduktion von Sauerstoff in der Arktis einzusetzen. Dabei wird die Sauerstoffentwicklung von bodenlebenden Diatomeen im Freiland in einer benthischen Kammer online über optische Fasern erfasst. Das Grundprinzip der optischen Sauerstoffmessung beruht auf Anregung eines spezifischen Fluoreszenzfarbstoffes (Indikatormolekül) durch Licht einer definierten Wellenlänge sowie dessen Fluoreszenzlöschung in Abhängigkeit von der Sauerstoffkonzentration, vergleiche URL Stand

DE 10 2013 011 343 B3 2014.07.10

20.06.2013 <http://www.angewandteoekologie.uni-rostock.de/en/forschung3/analytik0/mikroopt/>.

[0006] Der der Erfindung nächstliegende Stand der Technik wird in der Veröffentlichung „Temperature Effects an Hemocyanin Oxygen Binding in an Antarctic Cephalopod“ von S. Zielinski et al. (in Biol. Bull. 200: 67–76 (February 2001) offenbart. Beschrieben wird eine Diffusionskammer mit einer modifizierten Quarzglasküvette zur simultanen Ermittlung von pH- und Absorptionsveränderungen von Blut eines Kopffüßers unter in-vitro-Bedingungen. Bei Zugabe in die Küvette verteilt sich das zu untersuchende Blut (400 µl) auf ein oberes und unteres Reservoir, das kontinuierlich mit Hilfe von Magnetrührern gemischt wird. Das Blut verläuft zudem in einem Bereich zwischen den beiden Reservoirs zu einer dünnen Schicht (0, 45 mm), in der die Absorptionsmessung stattfindet. Die Messspitze einer Mikro-pH-Elektrode wird über einen oberen abdichtenden Deckel in die Blutprobe zur pH-Wert-Messung eingeführt. Eine zweite Öffnung im Deckel ermöglicht die Begasung mit einem während der Messung veränderbaren Gasgemisch (Sauerstoff, Kohlendioxid, Stickstoff). Die auftretende Absorptionsveränderung wird mit einem Spektrophotometer mit Glasfaseroptik gemessen. Der genaue konstruktive Aufbau wird in der Veröffentlichung nicht weiter dargestellt, vergleiche **Fig. 1** und Absatz „Analysis of Oxygen binding“.

[0007] Die Messprozedur wird jedoch ausführlich beschrieben. Die Analyse der Sauerstoffsättigung und Bindungseigenschaften von Blutpigmenten durch Messung der Lichtabsorption wird zum überwiegenden Teil mit Blutproben vorgenommen, die gepuffert wurden, um den pH-Wert zu stabilisieren. Puffer sind wässrige Lösungen einer schwachen Säure und ihrer konjugierten Base. Bei Zugabe von sauren (mit H_3O^+ -Ionen) und alkalischen Lösungen (OH^-) werden die Hydroniumionen von der Pufferbase und die Hydroxidionen von der Puffersäure abgefangen (abgepuffert), sodass sich der pH-Wert bei dieser Zugabe nur sehr wenig ändert. Ein Puffer ist jedoch nur wirksam, wenn größere Mengen von Puffersäure und Pufferbase vorhanden sind. Die Pufferung beeinflusst jedoch nachweislich die Bindungseigenschaften des Blutpigments und gibt somit die tatsächlichen physiologischen Eigenschaften nicht immer wahrheitsgemäß wieder. Dieses Problem wird bei Pörtner (1990 („An analysis of the effects of pH on oxygen binding by squid (*Illex illecebrosus*, *Loligo pealei*) haemocyanin“, J. Exp. Biol. 150, 407), 1994 („Coordination of metabolism, acid-base regulation and haemocyanin function in cephalopods“, Mar. Fresh. Behav. Physiol. 25, 131–148)) und Zielinski et al. (2001, „Temperature effects an hemocyanin Oxygen binding in an Antarctic cephalopod“, Biol. Bull. (Woods Hole) 200, 67–76) dadurch gelöst, dass natives, ungepuffertes Blut bei konstantem Sauerstoffpartialdruck, aber variiertem pH-Wert untersucht

wurde. Durch die Messung weiterer Bindungskurven bei verschiedenen Sauerstoffpartialdrücken konnten dann dieselben Parameter bestimmt werden wie bei der konventionellen Methodik mit den o. g. Nachteilen. Nachteilig bei der Methode von Pörtner und Zielinski et al. ist jedoch wiederum, dass ein hoher Probenverbrauch auftritt und die pH-Wert-Messungen an gepoolten Blutproben durchgeführt werden, sodass die Messwerte nicht eindeutig einzelnen Organismen zugeordnet werden können als auch statistisch nicht ausgewertet werden können.

Aufgabenstellung

[0008] Ausgehend von dem zuletzt genannten Stand der Technik ist die Aufgabe für die vorliegende Erfindung darin zu sehen, die gattungsgemäße Diffusionskammer so weiterzuentwickeln, dass sowohl pH-Wert- als auch Absorptionsmessungen gleichzeitig auch an sehr kleinen Substanzproben durchgeführt werden können. Dabei sollen die Messungen möglichst schnell verlaufen bei gleichzeitig hoher Auflösung der Messergebnisse. Die erfindungsgemäße Lösung für diese Aufgabe ist dem Anspruch 1 zu entnehmen. Vorteilhafte Weiterbildungen der Erfindung werden in den Unteransprüchen aufgezeigt und im Folgenden im Zusammenhang mit der Erfindung näher erläutert.

[0009] Die erfindungsgemäße Diffusionskammer ist dadurch gekennzeichnet, dass radial in den Zentralzylinder gasdicht ein Probenschlitten eingeschoben ist, der eine zylindrische Öffnung und eine schräg verlaufende Nut aufweist. Oberhalb der zylindrischen Öffnung ist ein zylindrischer, die Probenkammer umschließender Dichtring auf dem Probenschlitten angeordnet. In die schräg verlaufende Nut im Probenschlitten ist erfindungsgemäß eine Kanüle eines spritzenartigen optischen Mikrosensors eingelegt. Dieser bildet den pH-Messsensor. Dabei ist in der Kanüle eine die Messspitze tragende Glasfaser verschiebbar gelagert. Außerdem ist die Kanüle durch den Dichtring gasdicht hindurchgeführt. Weiterhin ist die erfindungsgemäße Diffusionskammer dadurch gekennzeichnet, dass axial in den Zentralzylinder oberhalb der Probenkammer ein oberer zylindrischer Optikkhalter mit einer lichtzuleitenden Glasfaser und einer oberen Kollimatorlinse und unterhalb der Probenkammer ein unterer zylindrischer Optikkhalter mit einer lichtleitenden Glasfaser, einer unteren Kollimatorlinse und einem Abstandsring gasdicht eingeschoben sind. Dabei wird erfindungsgemäß durch den eingeschobenen Abstandsring sowohl der minimale Lichtweg von der Kollimatorlinse zur Probe eingehalten als auch der Dichtring auf dem Probenschlitten gegen den Zentralzylinder gedrückt und die Probenkammer dicht gegenüber Gasen aus der Umgebung der Diffusionskammer verschlossen.

DE 10 2013 011 343 B3 2014.07.10

[0010] Bei der erfindungsgemäßen Diffusionskammer wird erstmals bei einer Diffusionskammer ein optischer Mikrosensor – eine sogenannte „pH-Optode“ – zur Messung des pH-Werts eingesetzt, durch die die Messwerte mit einer guten Messfrequenz und hohen Messgenauigkeit auf optischem Wege ermittelt werden. Alle bekannten Diffusionskammern messen den pH-Wert bislang extern in einer parallel begasteten Blutprobe, auf elektrischem Wege mit pH-Elektroden, die einen größeren Platzbedarf haben und durch die größeren Sensordurchmesser auch ein größeres Probenvolumen benötigen. Ein weiterer Vorteil der pH-Optode besteht darin, dass über einen breiten Temperaturbereich (auch 0°C und kälter) stabil, genau und schnell gemessen werden kann. Herkömmliche pH-Elektroden messen im Gegensatz dazu bei kalter Umgebung nur äußerst träge und instabil. Die bei der Erfindung eingesetzte pH-Optode ist spritzenartig aufgebaut und verfügt über eine Kanüle, in der eine Glasfaser verschiebbar gelagert ist. Das freie Ende der Glasfaser trägt die Messspitze und kann einen Durchmesser 150 µm oder weniger haben. Entsprechend klein kann das Messvolumen der Substanzprobe sein, es kann 20 µl oder weniger betragen. Beispielsweise genügen 10–15 µl für die Substanzprobe – im Vergleich dazu werden bislang im Stand der Technik 400 µl bis 3 ml benötigt.

[0011] Eine besondere Herausforderung bei der erfindungsgemäßen Diffusionskammer ist die Integration einer solchen pH-Optode in den Messaufbau. Dazu ist bei der Erfindung ein spezieller Probenschlitten vorgesehen, der eine schräge Nut aufweist. Die Nut verläuft vom Körper der Kanüle schräg ansteigend zum Ende der Kanüle. Dadurch ist gewährleistet, dass die aus der Kanüle herausgeschobene Glasfaser mit der Messspitze in die Substanzprobe eintaucht und nicht darüber hinweg verläuft. Die Substanzprobe wird während der Messungen gezielt mit Gasmischungen bekannter Zusammensetzung (Partialdruck) begast. Dabei muss ausgeschlossen werden, dass versehentlich Umgebungsluft in den Gastrom oder direkt in Kontakt mit der Substanzprobe gerät. Dafür ist bei der Diffusionskammer erfindungsgemäß vorgesehen, dass auf dem Probenschlitten ein Dichtring angeordnet ist, durch den die Kanüle gasdicht hindurchgeführt ist. Der Dichtring umschließt die Probenkammer, die oberhalb einer Öffnung im Probenschlitten gebildet ist. Die zu untersuchende Substanzprobe wird auf ein Glasplättchen aufgetragen, das über der Öffnung unterhalb des Dichtrings positioniert ist. Dadurch kann der Lichtstrahl des Spektrophotometers die Substanzprobe durchstrahlen und deren Absorption messen.

[0012] Eine weitere Herausforderung bei der erfindungsgemäßen Diffusionskammer stellt die Integration der Faseroptik des Spektrophotometers in den Messaufbau dar. Dieses wurde erfindungsgemäß durch zwei zylindrische Optikhalter gelöst, die

ober- und unterhalb der Probenkammer angeordnet sind. Die beiden Optikhalter fixieren die Glasfasern von der Lichtquelle (oben) und zum Spektrophotometer (unten) und tragen die Sammellinsen sowie mehrere Dichtringe. Sie lassen sich einfach in den Zentralzylinder einschieben oder einschrauben und damit abdichten. Auf dem unteren Optikhalter ist noch zusätzlich ein Abstandsring angeordnet. Dieser drückt im eingeschobenen Zustand von unten gegen den eingeschobenen Probenschlitten und gewährleistet einen Mindestabstand von der Sammellinse zur Substanzprobe. Der Probenschlitten wiederum drückt den auf ihm angeordneten Dichtring gegen das Innere des Zentralzylinders und bewirkt so eine Abdichtung des Dichtrings im Zentralzylinder. Dadurch wird das Einströmen von die Messungen verfälschender Umgebungsluft in die Probenkammer während des Messvorgangs verhindert.

[0013] Durch die Verwendbarkeit einer kompakten hochauflösenden pH-Optode und eines kompakten hochauflösenden Spektrophotometers aufgrund der speziellen Integration der jeweiligen Faseroptik kann mit der Diffusionskammer nach der Erfindung eine sehr kompakte, transportable und leistungsfähige Messapparatur zur Verfügung gestellt werden, mit der zuverlässig und genau auch kleinste Substanzprobenvolumina, beispielsweise geringe Mengen Blut von sehr kleinen Organismen, hochaufgelöst gemessen werden können. Dabei können die Messwerte synchron an identischen Substanzproben ermittelt werden, sodass durch diese Konkordanz die Aussagekräftigkeit der Messergebnisse noch erhöht und die Anwendungspalette erweitert werden kann.

[0014] Weiter oben wurde bereits ausgeführt, dass es essenziell ist, dass die Messspitze in die Substanzprobe gelangt. Dazu wird die Kanüle der pH-Optode schräg in den Probenschlitten eingelegt. Dieser weist dazu eine schräge Nut auf. Um das Eintauchen der Messspitze am Ende der Glasfaser in die Substanzprobe noch zu verbessern, ist es vorteilhaft und bevorzugt, wenn die Kanüle zweifach winklig gebogen ist, sodass das zum Herausschieben der Glasfaser offene Ende der Kanüle parallel verschoben ist. Die Kanüle wird dadurch auf ein Niveau in der Mitte der zu untersuchenden Substanz angehoben. Die Glasfaser braucht dadurch nur noch ein kleines Stück aus der Kanüle herausgeschoben werden und kann sich nicht mehr absenken. Die Substanzprobe wird zur Absorptionsmessung von Licht durchstrahlt. Dabei ist sicherzustellen, dass keine Fremdkörper in den Lichtstrahl gelangen, die Licht absorbieren und zu Messfehlern führen würden. Solche Fehler bei der Absorptionsmessung können bei der Diffusionskammer nach der Erfindung bevorzugt und vorteilhaft dadurch verhindert werden, dass das zum Herausschieben der Glasfaser offene Ende der Kanüle bündig mit der Innenkontur des Dichtrings abschließt und das die aus der Kanüle herausgeschobene

DE 10 2013 011 343 B3 2014.07.10

bene Glasfaser mit ihrer Messspitze in einen Randbereich der zu untersuchenden Substanzprobe eingetaucht ist. Weder die Kanüle noch die herausgeschobene Glasfaser beeinträchtigen so den einfallenden Lichtstrahl. Damit dies während der Messungen auch sicher gewährleistet bleibt, ist es bevorzugt und vorteilhaft, wenn der optische Mikrosensor durch eine schräge Verschraubung in einer geraden Nut im Probenschlitten fixiert ist. Nach dem Einlegen kann die leicht zugängliche Verschraubung betätigt und der optische Mikrosensor bzw. sein Spritzenkörper fixiert werden. Weiterhin ist es zur Sicherung von zuverlässigen Messergebnissen bevorzugt und vorteilhaft, wenn die Messspitze einen Durchmesser von unter 150 µm aufweist. Dadurch können zum einen sehr kleine Substanzprobenvolumina eingesetzt werden. Das zuverlässige Eintauchen der besonders kleinen Messspitze ist trotzdem sicher gewährleistet. Zum anderen absorbieren weder die kleine Messspitze noch die diese tragende Glasfaser Licht in einem solchen Anteil, dass die Messergebnisse verfälscht werden könnten.

[0015] Durch den möglichen Einsatz von sehr kleinen Substanzprobenvolumina bei der Diffusionskammer nach der Erfindung kann bevorzugt und vorteilhaft in der Probenkammer ein Messvolumen von unter 20 µl für die zu untersuchende Substanzprobe eingesetzt werden. Damit können beispielsweise mehr Messungen pro Blutprobe durchgeführt oder auch Blutproben von kleinsten Organismen mit limitierten Blutmengen untersucht werden. Weiterhin können dabei auch Messprofile, beispielsweise die Ermittlung von pH-Wert-Gradienten, über die Veränderung der anderen Messparametern, beispielsweise Variationen in der Gaszusammensetzung, Temperatur, Anregungs- und Detektionswellenlänge, erstellt werden, wenn bevorzugt und vorteilhaft der optische Mikrosensor eine Messsteuerung zur Ermittlung von zumindest einem Messwert pro Sekunde aufweist. Ebenfalls besonders vorteilhaft und bevorzugt bei der Erstellung von genauen Messprofilen ist es, wenn das Spektrophotometer eine Messsteuerung zur Ermittlung von zumindest 1000 Spektren pro Sekunde in einem kontinuierlichen Wellenlängenbereich zwischen 200 nm und 1100 nm aufweist. Dabei kann jedes Spektrum in beispielsweise 2048 Datenpunkte aufgelöst sein. Diese hohe Datendichte bietet sehr viele Details über das gesamte Spektrum, was beispielsweise bei Nicht-Modellorganismen oder abnormen Blutproben von Vorteil ist. Derartige Spektrophotometer und auch pH-Optoden sind kommerziell erhältlich, vergleiche Ausführungsbeispiele. Durch solche leistungsfähigen Messgeräte, die flexibel und kompakt sind und daher auch Feldversuche ermöglichen, wird die Datendichte beispielsweise pro ermittelter Bindungskurve deutlich erhöht. Beispielsweise können bei einer zweistündigen Messdauer 7.200 Datenpunkte bei einer nur geringen Integrationszeit ermittelt werden. In bekannten Verfahren können im

Vergleich dazu in der Regel nur 6 bis 20 Datenpunkte ermittelt werden. Eine derart hohe Aufzeichnungsrate kann einerseits dazu genutzt werden, durch Mittelung das instrumentelle Rauschen deutlich zu verringern. Andererseits können nahezu kontinuierliche Bindungskurven ermittelt werden, wodurch neue, teilweise parametrisch sehr eng begrenzte Bindungseigenschaften aufgedeckt werden können. Als Beispiel sei die Kurvenasymmetrie der Bindungskurven in Abhängigkeit vom Sauerstoffpartialdruck genannt.

[0016] Weiter oben wurde bereits ausgeführt, dass bei der Diffusionskammer nach der Erfindung die Flexibilität bezüglich der Messparameter von Vorteil ist. Die Erfindung ermöglicht durch ihren besonderen konstruktiven Aufbau den Einsatz spezieller hochauflösender, fasergebundener pH-Optoden und Spektrophotometer. Insbesondere ist es auch vorteilhaft und bevorzugt, wenn das Spektrophotometer eine Halogen- oder Lumineszenz-Lichtquelle zur Bestrahlung der zu untersuchenden Substanzprobe aufweist. Dadurch können mit der Diffusionskammer nach der Erfindung auch kolorimetrische Assays oder Fluoreszenz- oder Lumineszenzassay erstellt werden. Dies gilt beispielsweise für Zellsuspensionen, bei denen beispielsweise die NADH-, Kalzium- und ATP-, Sauerstoff-Radikal- oder Caspase-Aktivität bei gleichzeitiger Messung des pH-Werts und zellulär bzw. physiologisch relevanter Gaszusammensetzung gemessen werden soll. Für Fluoreszenzmessungen muss dann lediglich eine LED-Lichtquelle, die bei einer einzelnen definierten Wellenlänge Licht emittiert, über einen Y-Wellenleiter an das optische Fasersystem des Spektrophotometers angeschlossen werden. Ein Austausch des Spektrophotometers ist nicht erforderlich. Weiterhin kann vorteilhaft und bevorzugt der Probenkammer über die Gaszufuhr eine einstellbare Gasmischung, beispielsweise aus Stickstoff, Sauerstoff und Kohlendioxid, zugeführt sein, um die oben genannte Parametervariation der Umgebung der zu untersuchenden Substanzprobe zu ermöglichen.

[0017] Die Flexibilität der Diffusionskammer nach der Erfindung bezüglich ihrer Anwendbarkeit auf unterschiedliche Messprobleme kann noch weiter verbessert werden, wenn bevorzugt und vorteilhaft in die Probenkammer weitere Messspitzen von weiteren optischen Mikrosensoren, beispielsweise zur Messung des O₂-, CO₂- oder NO-Gehalts, oder von chemischen Mikrosensoren, beispielsweise zur Detektion von farbsensitiven Verbindungen, der zu untersuchenden Substanzprobe eingeführt sind. Durch die Verfügbarkeit von O₂-, CO₂- oder NO-Optoden, die am Markt erhältlich sind und ohne Weiteres in den konstruktiven Aufbau der Diffusionskammer nach der Erfindung integriert werden können, können neben dem pH-Wert noch weitere Parameter ermittelt werden (O₂-, CO₂- oder NO-Gehalt). Dadurch kann die Bandbreite der Einsatzmöglichkeiten der Diffusionskammer nach der Erfindung noch weiter vergrößert

DE 10 2013 011 343 B3 2014.07.10

werden. Zudem ist es möglich, beispielsweise chemische Messungen, bei denen beispielsweise farbsensitive Verbindungen gemessen werden, mit der gleichzeitigen pH-Wert-Messung mit der Diffusionskammer nach der Erfindung zu verbinden. Für die zu untersuchende Substanzprobe, bevorzugt und vorteilhaft eine Substanz biologischen Ursprungs, beispielsweise Blut oder eine Zellsuspension, ist es dabei von Vorteil und bevorzugt, wenn die Probenkammer bzw. das Gehäuse, das die Probenkammer umgibt, mit destilliertem oder mit Glykol angereichertem Wasser temperiert wird. Weitere vorteilhafte Modifikationen und Erläuterungen zu den genannten Ausführungsformen der Diffusionskammer nach der Erfindung sind den nachfolgend beschriebenen Ausführungsbeispielen zu entnehmen.

Ausführungsbeispiele

[0018] Die Diffusionskammer nach der Erfindung wird im Folgenden anhand der schematischen, nicht maßstäblichen Figuren zum besseren Verständnis noch weitergehend erläutert. Im Einzelnen zeigt die

[0019] Fig. 1 eine Ausführungsform der Diffusionskammer im schematischen Querschnitt,

[0020] Fig. 2 ein Detail der Ausführungsform der Diffusionskammer,

[0021] Fig. 3 eine Ausführungsform des Probenschlittens im Detail,

[0022] Fig. 4 eine Ausführungsform des oberen Linsenhalters im Detail,

[0023] Fig. 5 eine Ausführungsform des unteren Linsenhalters im Detail,

[0024] Fig. 6A verschiedene Sauerstoffbindungskurven, die mit der Diffusionskammer nach der Erfindung erstellt wurden und

[0025] Fig. 6B den zeitlichen Verlauf der Veränderung des Blut-pH-Werts und der Absorption bei 294 nm und 348 nm einer Hämocyanin-haltigen Blutprobe.

[0026] In der Fig. 1 ist die Diffusionskammer **01** nach der Erfindung schematisch im Querschnitt dargestellt. In einem Gehäuse **02** befindet ein vertikaler Zentralzylinder **03**, in dessen Mittenbereich eine Probenkammer **04** zur Aufnahme einer wässrigen Substanzprobe **05** angeordnet ist. Die Substanzprobe **05** ist auf einer Glasplatte **06** (rechteckiges Hämatokritgläschen, dickeres Deckgläschen) in dünner Verteilung aufgetragen. An der linken Seite des Gehäuses **02** ist ein optischer Mikrosensor **07** (pH-Optode) mit einem Spritzenkörper **08**, einem Stößel **10** und einer Kanüle **11** angeordnet, in der eine Glasfaser **09** ge-

führt ist. Im unteren Bereich des Gehäuses **02** verläuft mittig im Zentralzylinder **03** eine Glasfaser **12**, die zu einem Spektrophotometer **13** führt. Im oberen Bereich des Gehäuses **02** verläuft mittig im Zentralzylinder **03** eine weitere Glasfaser **14**, die zu einer Lichtquelle **15** führt.

[0027] Das Gehäuse **02** ist mit einem Wasserreservoir **16** gefüllt, dessen Temperatur über ein Thermostat (nicht gezeigt) konstant gehalten wird. Ein Gas-einlassverteiler **17** (zum Anschluss mehrerer Leitungen für unterschiedliche Gasgemische) ist oben auf dem Gehäuse **02** angeordnet. Von dort wird das jeweilig aktuell zugeführte Gasgemisch, das über eine Gasmischpumpe (nicht gezeigt) auf die gewünschten Gasverhältnisse vorgemischt wird, dauerhaft und in einem gleichmäßigen Gasstrom während des gesamten Messzyklus eingeleitet wird, über das temperierte Wasserreservoir **16** zu Gasbefeuchtern **18** geleitet. Hierbei handelt es sich um Glaszylinder, in denen das zugeführte trockene Gasgemisch mit Wasser gesättigt und auf die Messtemperatur equilibriert wird. Dadurch wird die Substanzprobe beim Begasen nicht ausgetrocknet und ändert auch nicht ihre Messtemperatur. In den Gasbefeuchtern **18** wird das Gasgemisch durch eine poröse Membran, über der eine kleine Wassersäule ruht, getrieben. Dadurch entstehen feine Gasbläschen, die sich schnell mit Wasserdampf sättigen. Von den Gasbefeuchtern **18** strömt das feuchte Gasgemisch in einen Gasverteiler **19**, der das Gasgemisch dann kontinuierlich in die Probenkammer **04** und über die Substanzprobe **05** leitet.

[0028] Radial in den Zentralzylinder **03** ist gasdicht ein Probenschlitten **20** eingeschoben, der eine zylindrische Öffnung **21** aufweist. Oberhalb dieser ist ein zylindrischer Dichtring **22** angeordnet, der die Probenkammer **04** gasdicht umschließt. Weitere Details sind den Fig. 2, Fig. 3 zu entnehmen. Axial ist in den Zentralzylinder **03** oberhalb der Probenkammer **04** ein oberer zylindrischer Optikkhalter **23** mit der lichtzuleitenden Glasfaser **14** und einer oberen Kollimatorlinse **24** und unterhalb der Probenkammer **04** ein unterer zylindrischer Optikkhalter **25** mit der lichtableitenden Glasfaser **12**, einer unteren Kollimatorlinse **26** und einem Abstandsring **27** gasdicht eingeschoben. Zu erkennen ist, dass der eingeschobene Abstandsring **27** den Probenschlitten **20** und den darauf angeordneten Dichtring **22** gegen die Innenkontur des Zentralzylinders **03** drückt und dadurch die Probenkammer **04** während der Messungen gegen Eindringen von messverfälschender Umgebungsluft schützt.

[0029] Weitere Details sind den Fig. 4, Fig. 5 zu entnehmen.

[0030] Ein möglicher Messzyklus mit der Diffusionskammer **01** sieht folgendermaßen aus:

DE 10 2013 011 343 B3 2014.07.10

- 15 µl Substanzprobe **05** (beispielsweise Blut) werden auf die Glasplatte **06** des Probenschlittens **20** aufgetragen und dann in die Probenkammer **04** geschoben
- anschließend wird die Substanzprobe **05** mit einem 100% O₂-Gasstrom begast, bis sich die Absorption der Substanzprobe **05** nicht mehr verändert (= 100% Kalibrierung)
- anschließend wird der O₂-Gasstrom konstant auf z. B. 21 kPa (Partialdruck PO₂ während des Messzyklus) eingestellt und gewartet, bis die Absorption der Substanzprobe **05** wieder stabil ist und sich nicht mehr verändert.
- anschließend wird ein CO₂-Gasstrom schrittweise (oder kontinuierlich) erhöht, um den pH-Wert der Substanzprobe **05** soweit zu senken, bis sich die Absorption der Substanzprobe **05** nicht weiter erniedrigt (CO₂ löst sich in der Substanzprobe **05** und erzeugt über die Bildung von Kohlensäure die pH-Wert-Erniedrigung),
- abschließend wird mit einem 100% N₂-Gasstrom begast, um den 0% Kalibrierungswert (der Absorption der Substanzprobe **05**) zu bestimmen
- während des gesamten Messzyklus werden der pH-Wert mit der pH-Optode **07** und die Absorption der Substanzprobe **05** (mit dem Spektrophotometer **13**) mit einer größtmöglichen Messfrequenz gemessen, um aus den gewonnenen Datensätzen möglichst hochaufgelöste und damit besonders aussagekräftige Sauerstoff-Bindungskurven ermitteln zu können.

[0031] In der **Fig. 2** ist im Detail der Probenschlitten **20** mit der pH-Optode **07** dargestellt. Zu erkennen sind der Spritzenkörper **08**, der Stößel **10** und die Kanüle **11**. In der Kanüle **11** ist die optische Glasfaser **09** geführt. Sie trägt eine Messspitze **28**, die beispielsweise mit einem Indikatormolekül beschichtet ist (vergleiche Beschreibungseinleitung). Über eine Bewegung (Doppelpfeil) des Stößels **10** wird die Glasfaser **09** und damit die Messspitze **28** radial verschoben und aus dem offenen Ende **52** der Kanüle **11** herausgeschoben. Dadurch gelangt die Messspitze **28** in einen Randbereich **29** der Substanzprobe **05** und stört den Strahlengang **30** zur Absorptionsmessung nicht. Die Kanüle **11** ist gasdicht durch den Dichtring **22** hindurchgeschoben und endet an dessen Innenkontur **31** bündig mit dem Dichtring **22**. Somit wird auch durch die Kanüle **11** der Strahlengang **29** nicht gestört. In der **Fig. 2** ist noch zu erkennen, dass der Probenschlitten **20** eine Nut **32** aufweist, die schräg ansteigend zur Probenkammer **04** verläuft. Dadurch und durch eine zweifach winklige Biegung **33**, **34** der Kanüle **11** wird erreicht, dass die Messspitze **28** auch zuverlässig in den Randbereich **29** der Substanzprobe **05** eintaucht und nicht darüber hinwegragt.

[0032] Als pH-Optode **07** mit einer sehr kleinen Messspitze **28** (150 µm) ist beispielsweise der kommerziell erhältliche glas-

fasergebundene pH-Microsensor der Firma PreSens einsetzbar, vergleiche PreSens GmbH, www.presens.de/products/brochures/category/sensor-probes/brochure/ph-microsensors.html, Stand 23.06.2013. diese pH-Optode ist temperaturstabil und mit einer Messung pro Sekunde auch sehr schnell. Als Spektrophotometer **13** ist beispielsweise das kommerziell erhältliche glasfasergebundene Spektrophotometer der Firma OceanOptics einsetzbar, vergleiche OceanOptics, <http://www.oceanoptics.com/products/usb2000+.asp>, Stand 23.06.2013. Dieses Spektrophotometer in Kombination mit einer Deuterium- und Halogen-Lichtquelle **15** (DT-Mini-2-GS, OceanOptics) zeichnet ein breites kontinuierliches Spektrum auf (200–1100 nm) mit einer Auflösung von 2048 Datenpunkten pro Spektrum auf. Diese hohe Datendichte bietet sehr viele Details über das gesamte Spektrum. Weiterhin kann das Spektrophotometer bis zu 1000 Spektren pro Sekunde aufzeichnen. Zusammen mit der ebenfalls hohen Datenmenge durch die pH-Optode wird die Datenmenge deutlich erhöht gegenüber bekannten Diffusionskammern.

[0033] Die **Fig. 3** zeigt den Probenschlitten **22** im Detail. Zu erkennen ist ein Schlittenkörper **35**, in den die schräge Nut **32** eingefräst ist. Eine gerade Nut **36** ist zum Einlegen des Spritzenkörpers **08** vorgesehen. Weiterhin ist eine schräge Bohrung **37** für eine schräge Verschraubung **38** des Spritzenkörpers **08** im eingelegten Zustand vorgesehen. Im vorderen Bereich trägt der Schlittenkörper **35** eine rechteckige Auflagefläche **39** zum Auflegen der Glasplatte **06** mit der Substanzprobe **05**. In der rechteckigen Auflagefläche **39** ist die zylindrische Öffnung **21** angeordnet, durch die während des Messens der Strahlengang **30** fällt. Weiterhin weist der Schlittenkörper **35** einen Knebelgriff **40** zum einfachen Ein- und Ausschieben des Probenschlittens **22** in den Zentralzylinder **03** auf.

[0034] Die **Fig. 4** zeigt im Detail den oberen Optikhalter **23** mit der lichtzuleitenden Glasfaser **14**. Zu erkennen ist ein oberer Halterkörper **41** mit einem Handrad **42** und einem in eine Nut eingelegten Dichtungsring **43**. Am unteren Ende ist eine Fassung **44** mit der oberen Kollimatorlinse **24** eingeschraubt und mit einer Abdeckkappe **45** gesichert. Der obere Optikhalter **23** wird mittels eines Gewindes **46** in den Zentralzylinder **03** eingeschraubt.

[0035] Die **Fig. 5** zeigt im Detail den unteren Optikhalter **25** mit der lichtableitenden Glasfaser **12**. Zu erkennen ist ein unterer Halterkörper **47** mit einem in einer Nut eingelegten Dichtungsring **48**. Am oberen Ende ist eine Fassung **49** mit der unteren Kollimatorlinse **26** eingeschraubt und mit dem Abstandsring **27** über ein Gewinde fixiert. Der untere Optikhalter **25** wird einfach in den Zentralzylinder **03** eingeschoben und hält durch die Dichtungsringe **48**. Weiterhin weist er noch ein Justiergewinde **50** auf, das

DE 10 2013 011 343 B3 2014.07.10

mit einem Knebel **51** betätigbar ist und der Fokussierung der unteren Kollimatorlinse **26** dient. Im eingeschobenen Zustand wird über den Abstandsring **27** der Probenschlitten **20** bzw. der Dichtring **22** gegen den Zentralzylinder **03** nach oben gedrückt und dadurch die Probenkammer **04** abgedichtet. Außerdem wird durch den Abstandsring **27** ein Minimalabstand zwischen der unteren Kollimatorlinse **26** und der Substanzprobe **05** eingehalten, der den Strahlengang **30** optimal auf die Substanzprobe **05** fokussiert.

[0036] In der Fig. 6A sind abschließend zur Unterstützung der guten erreichbaren Auflösung der Diffusionskammer **01** nach der Erfindung verschiedene ermittelte Sauerstoffbindungskurven vom Hämocyanin-haltigem Blut des antarktischen Kraken *Pareledone charcoti* dargestellt, gemessen bei einer Temperatur von 0°C. Dabei zeigt sich, dass zunächst mit nur insgesamt 60 µl Probenvolumen (4 × 15 µl) Messungen bei vier verschiedenen Sauerstoffpartialdrücken durchgeführt werden konnten vom Blut eines einzigen Kraken, von dem allgemein nur maximal 200 µl Blut gewonnen werden können. Die hohe Auflösung der Bindungskurven offenbarte dabei eine Asymmetrie der Bindungskurven in Abhängigkeit vom Sauerstoffpartialdruck. Dieses Phänomen wurde in vorangegangenen Studien aufgrund von nur wenigen Datenpunkten und Kurveninterpolation unter Annahme eines symmetrischen Kurvenverlaufes bislang nicht detektiert und weist auf komplexere Sauerstoffbindungseigenschaften hin als bisher angenommen.

[0037] Die Messungen belegen zudem deutlich in Fig. 6B, dass die Oxygenierung bzw. De-Oxygenierung von Hämocyanin einhergeht mit einer Abgabe bzw. Aufnahme von Kohlendioxid, reflektiert durch den Abfall bzw. Anstieg des pH-Wertes der analysierten Blutprobe. Die breite spektrale Aufzeichnung offenbarte außerdem, dass die maximale Proteinabsorption von Kopffüßer-Hämocyanin nicht – wie bisher angenommen – bei 280 nm, sondern bei 294 nm liegt und zudem eine Abhängigkeit zwischen der Proteinabsorption und dem Oxygenierungsgrad des Blutpigmentes besteht. Diese neuen Erkenntnisse müssen bei zukünftigen Messungen zur Proteinbestimmung von Blutproben beachtet werden.

Bezugszeichenliste

01	Diffusionskammer
02	Gehäuse
03	Zentralzylinder
04	Probenkammer
05	Substanzprobe
06	Glasplatte
07	optischer Mikrosensor (pH-Optode)
08	Spritzenkörper
09	Glasfaser
10	Stößel
11	Kanüle

12	lichtleitende Glasfaser
13	Spektrophotometer
14	lichtzuleitende Glasfaser
15	Lichtquelle
16	Wasserreservoir
17	Gaseinlassverteiler
18	Gasbefeuchter
19	Gasverteiler
20	Probenschlitten
21	zylindrische Öffnung
22	Dichtring
23	oberer zylindrischer Optikhalter
24	obere Kollimatorlinse
25	unterer zylindrischer Optikhalter
26	untere Kollimatorlinse
27	Abstandsring
28	Messspitze
29	Randbereich
30	Strahlengang
31	Innenkontur
32	schräge Nut
33	winklige Biegung
34	winklige Biegung
35	Schlittenkörper
36	gerade Nut
37	schräge Bohrung
38	Verschraubung
39	Auflagefläche
40	Knebelgriff
41	oberer Halterkörper
42	Handrad
43	Dichtungsring
44	Fassung
45	Abdeckkappe
46	Gewinde
47	unterer Halterkörper
48	Dichtungsring
49	Fassung
50	Justiergewinde
51	Knebel
52	offenes Ende von 11

Patentansprüche

1. Diffusionskammer zur Ermittlung unterschiedlicher Parameter einer wässrigen Substanz mit einem vertikalen Zentralzylinder mit zumindest einer Probenkammer zur Aufnahme einer Substanzprobe, einem nadelförmigen pH-Messsensor mit einer die Substanzprobe kontaktierenden Messspitze, einem Spektrophotometer mit einer die Substanzprobe durchstrahlenden Glasfaseroptik und einer Gaszuführung in die Probenkammer zur veränderlichen Begasung der Substanzprobe während der Parametermittlung, **dadurch gekennzeichnet**, dass

- radial in den Zentralzylinder (**03**) gasdicht ein Probenschlitten (**20**) eingeschoben ist, der eine zylindrische Öffnung (**21**), oberhalb der ein zylindrischer, die Probenkammer (**04**) umschließender Dichtring (**22**)

DE 10 2013 011 343 B3 2014.07.10

auf dem Probenschlitten (20) angeordnet ist, und eine schräg verlaufende Nut (32) aufweist, in die eine Kanüle (11) des als spritzenartiger optischer Mikrosensor (07) ausgebildeten pH-Messensors eingelegt ist, wobei in der Kanüle (11) eine die Messspitze (28) tragende Glasfaser (09) verschiebbar gelagert ist und die Kanüle (11) durch den Dichtring (22) gasdicht hindurchgeführt ist, und dass

- axial in den Zentralzylinder (03) oberhalb der Probenkammer (04) ein oberer zylindrischer Optikhalter (23) mit einer lichtzuleitenden Glasfaser (14) und einer oberen Kollimatorlinse (24) und unterhalb der Probenkammer (04) ein unterer zylindrischer Optikhalter (25) mit einer lightableitenden Glasfaser (12), einer unteren Kollimatorlinse (26) und einem Abstandsring (27) gasdicht eingeschoben sind, wobei durch den eingeschobenen Abstandsring (27) der Dichtring (22) auf dem Probenschlitten (20) gegen den Zentralzylinder (03) gedrückt und die Probenkammer (04) dicht gegenüber Gasen aus der Umgebung der Diffusionskammer (01) verschlossen sowie ein Minimalabstand zwischen der unteren Kollimatorlinse (26) und Substanzprobe (05) eingehalten ist.

2. Diffusionskammer nach Anspruch 1, **dadurch gekennzeichnet**, dass die Kanüle (11) zweifach winklig (33, 34) gebogen ist, sodass das zum Herausschieben der Glasfaser (09) offene Ende (52) der Kanüle (11) parallel verschoben ist.

3. Diffusionskammer nach Anspruch 1 oder 2, **dadurch gekennzeichnet**, dass das zum Herausschieben der Glasfaser (09) offene Ende (52) der Kanüle (11) bündig mit der Innenkontur (31) des Dichtrings (22) abschließt und die aus der Kanüle (11) herausgeschobene Glasfaser (09) mit ihrer Messspitze (28) in einen Randbereich (29) der zu untersuchenden Substanzprobe (05) eingetaucht ist.

4. Diffusionskammer nach einem oder mehreren der vorangehenden Ansprüche, **dadurch gekennzeichnet**, dass der optische Mikrosensor (07) durch eine schräge Verschraubung (38) in einer geraden Nut (36) im Probenschlitten (20) fixiert ist.

5. Diffusionskammer nach einem oder mehreren der vorangehenden Ansprüche, **dadurch gekennzeichnet**, dass die Messspitze (28) einen Durchmesser von 150 µm oder weniger aufweist.

6. Diffusionskammer nach Anspruch 5, **dadurch gekennzeichnet**, dass in der Probenkammer (04) ein Messvolumen von 20 µl oder weniger für die zu untersuchende Substanzprobe (05) eingesetzt ist.

7. Diffusionskammer nach einem oder mehreren der vorangehenden Ansprüche, **dadurch gekennzeichnet**, dass der optische Mikrosensor (07) eine Messsteuerung zur Ermittlung von zumindest einem Messwert pro Sekunde aufweist.

8. Diffusionskammer nach einem oder mehreren der vorangehenden Ansprüche, **dadurch gekennzeichnet**, dass das Spektrophotometer (13) eine Messsteuerung zur Ermittlung von zumindest 1000 Spektren pro Sekunde in einem kontinuierlichen Wellenlängenbereich zwischen 200 nm und 1100 nm aufweist.

9. Diffusionskammer nach einem oder mehreren der vorangehenden Ansprüche, **dadurch gekennzeichnet**, dass das Spektrophotometer (13) eine Halogen- oder Lumineszenz-Lichtquelle (15) zur Bestrahlung der zu untersuchenden Substanzprobe (05) aufweist.

10. Diffusionskammer nach einem oder mehreren der vorangehenden Ansprüche, **dadurch gekennzeichnet**, dass die Probenkammer (04) mit destilliertem oder mit Glykol angereichertem Wasser temperiert ist.

11. Diffusionskammer nach einem oder mehreren der vorangehenden Ansprüche, **dadurch gekennzeichnet**, dass der Probenkammer (04) über die Gaszufuhr (17) eine einstellbare Gasmischung, beispielsweise aus Stickstoff, Sauerstoff und Kohlendioxid, zugeführt ist.

12. Diffusionskammer nach einem oder mehreren der vorangehenden Ansprüche, **dadurch gekennzeichnet**, dass in die Probenkammer (04) weitere Messspitzen von weiteren optischen Mikrosensoren, beispielsweise zur Messung des O₂-, CO₂- oder NO-Gehalts, oder von chemischen Mikrosensoren, beispielsweise zur Detektion von farbsensitiven Verbindungen, der zu untersuchenden Substanzprobe (05) eingeführt sind.

13. Diffusionskammer nach einem oder mehreren der vorangehenden Ansprüche, **dadurch gekennzeichnet**, dass für die Substanzprobe (05) eine Substanz biologischen Ursprungs, beispielsweise Blut oder eine Zellsuspension, ausgewählt ist.

Es folgen 6 Seiten Zeichnungen

DE 10 2013 011 343 B3 2014.07.10

Anhängende Zeichnungen

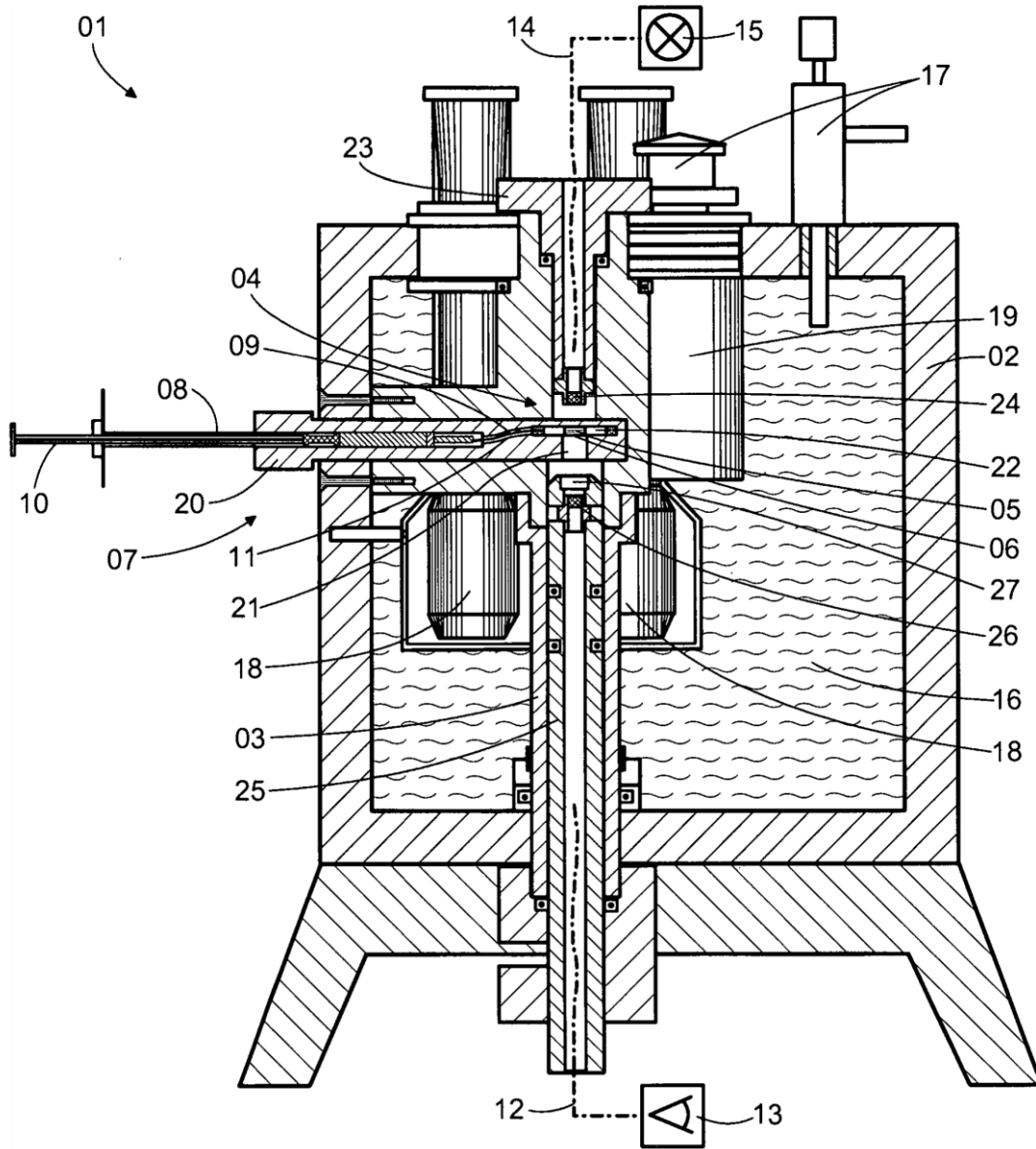
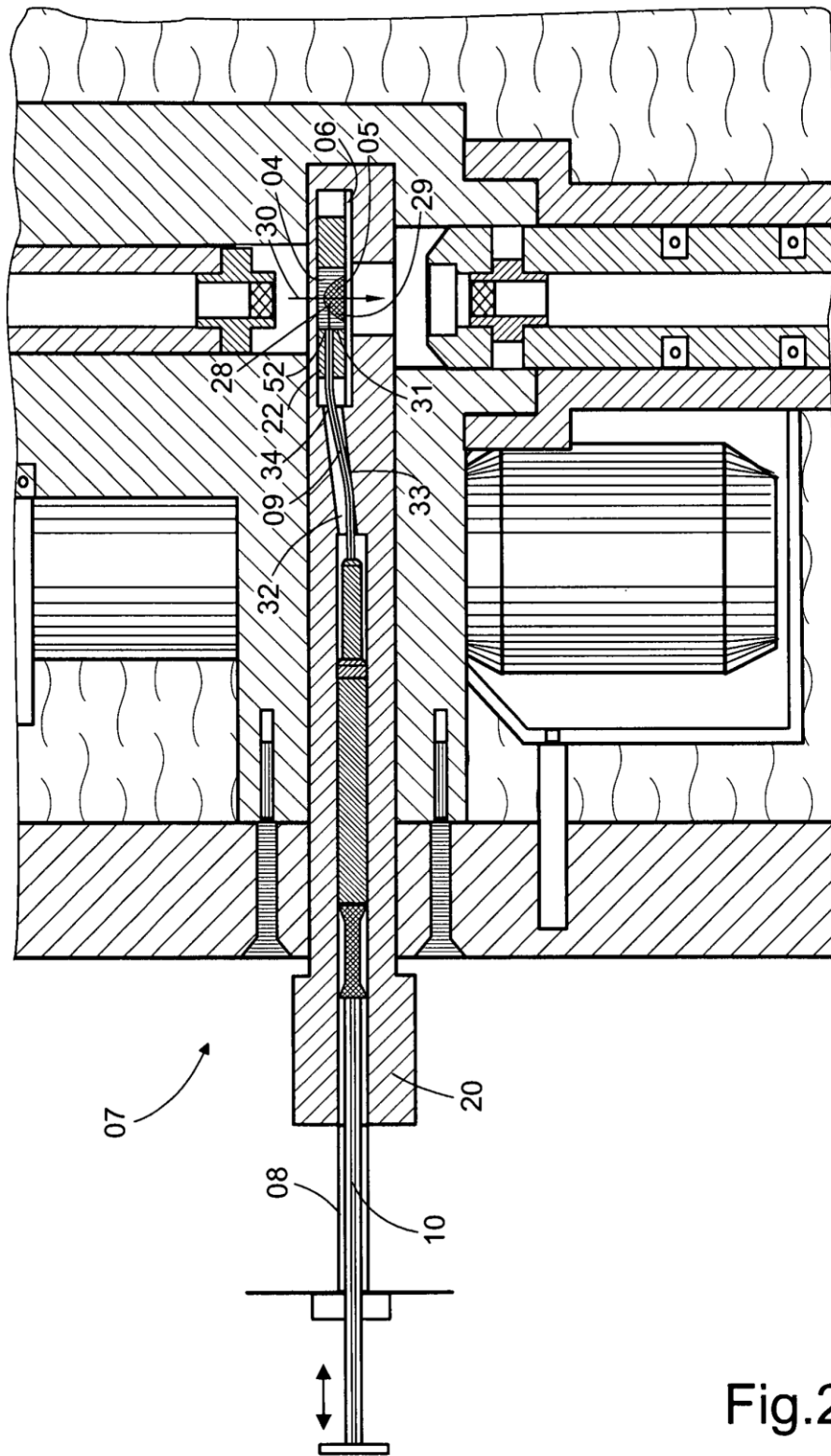


Fig. 1



DE 10 2013 011 343 B3 2014.07.10

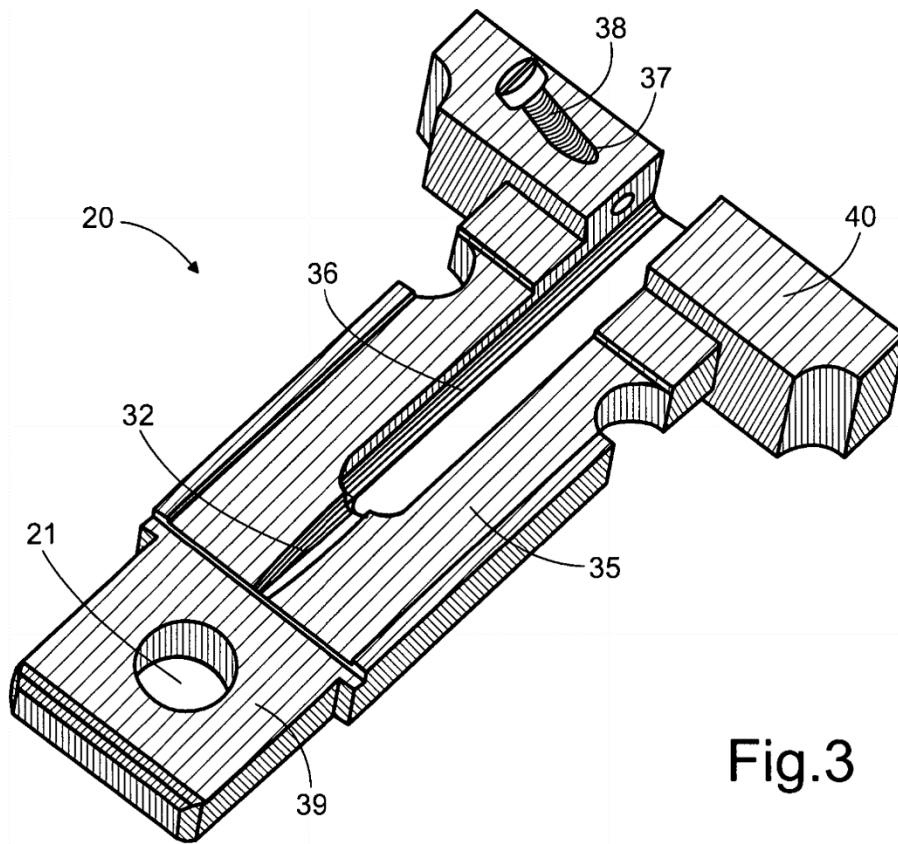


Fig.3

DE 10 2013 011 343 B3 2014.07.10

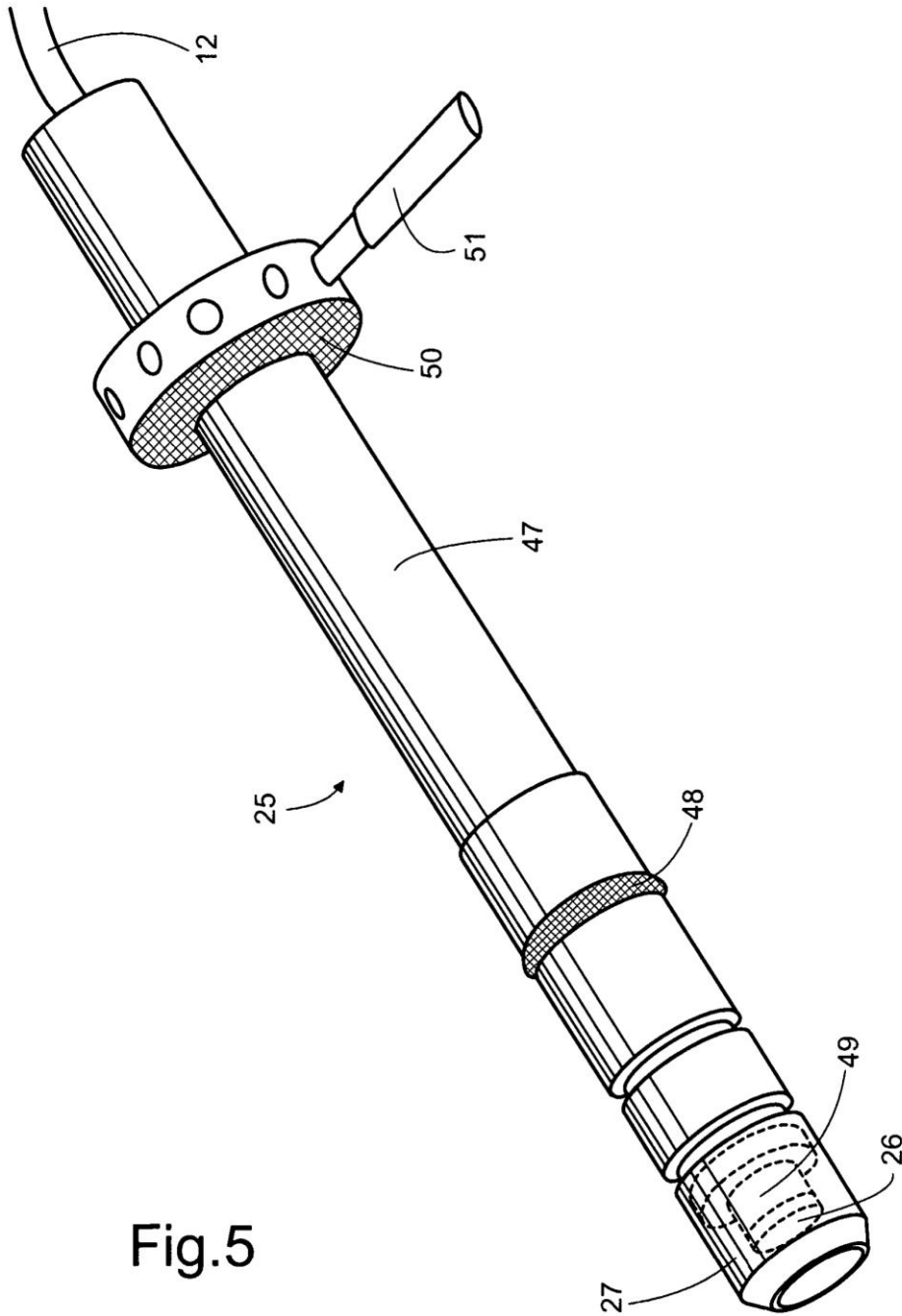


Fig.5

DE 10 2013 011 343 B3 2014.07.10

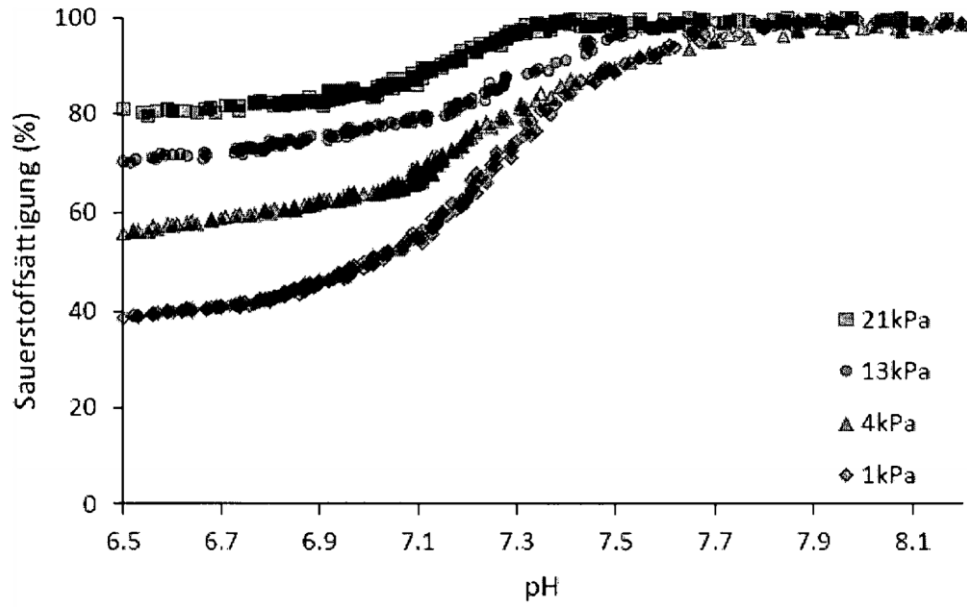


Fig.6A

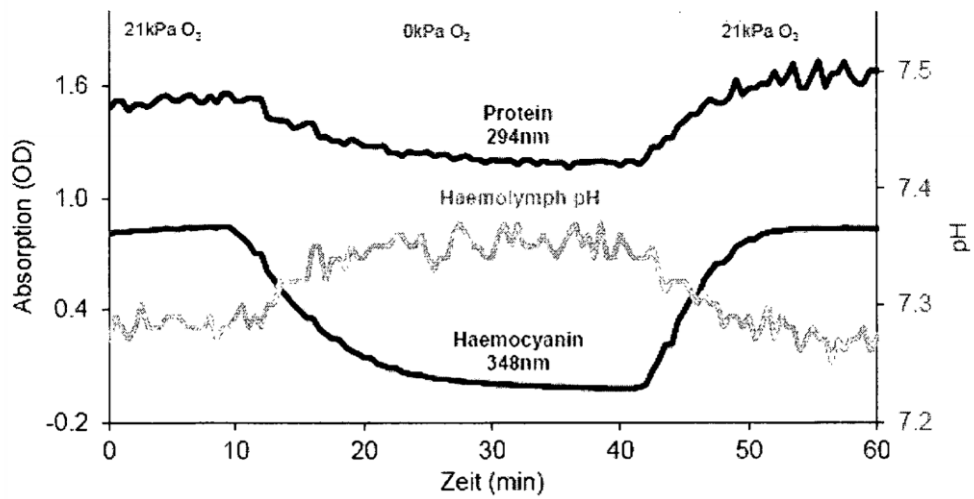


Fig.6B

6.2. Relative heart masses of cephalopods

Species	Relative mass of systemic heart (%)	Source
<i>Pareledone charcoti</i>	0.103	This study
<i>Pareledone charcoti</i>	0.105	This study
<i>Pareledone charcoti</i>	0.152	This study
<i>Pareledone charcoti</i>	0.198	This study
<i>Pareledone charcoti</i>	0.155	This study
<i>Pareledone charcoti</i>	0.112	This study
<i>Eledone cirrhosa</i>	0.140	Wells and Smith, 1987
<i>Eledone cirrhosa</i>	0.120	Driedzi,c 1990
<i>Octopus dofleini</i>	0.120	Wells and Smith, 1987
<i>Octopus vulgaris</i>	0.108	Wells, 1992
<i>Octopus vulgaris</i>	0.090	Wells and Smith, 1987
<i>Octopus vulgaris</i>	0.108	Houlihan <i>et al.</i> , 1987
<i>Octopus vulgaris</i>	0.090	Driedzic, 1990
<i>Octopus vulgaris</i>	0.066	Agnisola <i>et al.</i> , 1994
<i>Eledone moschata</i>	0.138	Strobel, A (unpublished)
<i>Eledone moschata</i>	0.147	Strobel, A (unpublished)
<i>Eledone moschata</i>	0.154	Strobel, A (unpublished)
<i>Eledone moschata</i>	0.122	Strobel, A (unpublished)
<i>Eledone moschata</i>	0.107	Strobel, A (unpublished)
<i>Eledone moschata</i>	0.105	Strobel, A (unpublished)
<i>Sepia officinalis</i>	0.080	Driedzic 1990
<i>Sepia officinalis</i>	0.060	Strobel, A (unpublished)
<i>Sepia officinalis</i>	0.070	Strobel, A (unpublished)
<i>Sepia officinalis</i>	0.063	Strobel, A (unpublished)
<i>Sepia officinalis</i>	0.086	Strobel, A (unpublished)
<i>Sepia officinalis</i>	0.082	Strobel, A (unpublished)
<i>Sepia officinalis</i>	0.078	Strobel, A (unpublished)
<i>Sepia officinalis</i>	0.075	Strobel, A (unpublished)
<i>Sepia officinalis</i>	0.074	Strobel, A (unpublished)
<i>Nautilus pompilius</i>	0.173	Wells, 1992
<i>Architeuthis giganteus</i>	0.165	Wells and Smith, 1987
<i>Illex illecebrosus</i>	0.299	Wells and Smith, 1987
<i>Loligo forbesi</i>	0.160	Driedzi,c 1990
<i>Loligo opalescens</i>	0.180	Wells, 1992
<i>Loligo pealei</i>	0.160	Wells, 1992
<i>Rossia pacifica</i>	0.173	Wells and Smith, 1987
<i>Salmo gairdneri</i>	0.221	Wells 1992

6.3. Sponsoring and supporting organisations

Financial support

This study was supported by the Deutsche Forschungsgemeinschaft DFG (MA4271/1-2), a PhD scholarship by the German Academic Exchange Service (DAAD, D/11/43882), a Journal of Experimental Biology travelling fellowship, travel grants by the Company of Biologists and the Society of Experimental Biology and the Alfred Wegener Institute for Polar and Marine Research.



6.4. Media releases

Most of the selected media feedback was an unexpected response to my talk at the SEB conference 2013 in Barcelona, Spain, followed by a perfectly marketed press release by the SEB Press Officer Clara Ferreira. An instructive experience and illustration of global media connectivity.

<u>New York Times</u>	(www.nytimes.com/2013/07/09/science/genetic-differences-that-let-octopods-flourish.html?_r=0)
<u>National geographic online</u>	(http://voices.nationalgeographic.com/2013/07/10/blue-blood-helps-octopus-survive-brutally-cold-temperatures/)
<u>Scientific American</u>	(http://blogs.scientificamerican.com/octopus-chronicles/2013/07/13/octopuses-survive-sub-zero-temps-thanks-to-specialized-blue-blood/)
<u>French Tribune</u>	(www.frenchtribune.com/teneur/1318947-blue-colored-pigment-blood-enables-octopods-survive-extreme-temperatures)
<u>Berliner Zeitung</u>	(www.berliner-zeitung.de/wissen/meeresbiologie-kraken-koennen-ueberall-leben,10808894,23636782.html)
<u>Bild der Wissenschaft</u>	(www.wissenschaft.de/archiv/-/journal_content/56/12054/1721874/Erfolg-liegt-ihnen-im-Blut/)
<u>Times of India</u>	(http://timesofindia.indiatimes.com/home/environment/flora-fauna/Blue-blood-allows-octopus-to-survive-extreme-temperatures/articleshow/20931925.cms)
<u>EfeFuturo</u>	(www.efefuturo.com/blog/la-sangre-azul-de-los-pulpos-les-permite-conquistar-todos-los-mares/)
<u>Pogoda</u>	(http://pogoda.wp.pl/kat,1034985,title,Niskie-temperatury-niestraszne-osmiornicom-dzieki-niebieskiej-krwi,wid,15813639,wiadomosc.html?ticaid=113adb)
<u>Bagnet</u>	(www.bagnet.org/news/world/222312)
<u>The Syria Times</u>	(http://syriatimes.sy/index.php/science/6674-octopus-blue-blood-allows-them-to-rule-the-waves)
<u>NerdAlert on Youtube</u>	(www.youtube.com/watch?v=YMTbyChzBS4)
<u>Application note PreSens</u>	(www.presens.de/uploads/tx_presensapplicationnotes/140512_APP_Blood_pH__Oxygenation_w_02.pdf)

7 Acknowledgements

First of all I would like to thank **Prof. Dr Hans-Otto Pörtner** for his continuous support, his dedication to my 'non-mainstream' research even at very busy times and his enriching and insightful contributions.

My dear supervisor **Dr Felix C. Mark**, for his patient and endless practical, theoretical, logistical, financial, bureaucratic, mental, motivational, sweetish or coffeish support always spiced with a pinch of wisdom. This thesis would have not been possible without him! Tons of thanks!

My second supervisor **Prof. Dr Bernhard Lieb** for his ongoing insightful advice and numerous visits to us physiologists to the rainy Bremerhaven at AWI.

Prof. Dr Juliane Filser for joining the examining board of my doctor's thesis defence.

I would further like to thank all colleagues, technical staff and the logistics department of the Alfred Wegener Institute particularly **Timo Hirse, Nils Koschnick, Fredy Véliz Moraleda** and **Guido Krieten** for cephalopod acquisition, care and technical assistance and the **crew of FS Polarstern** and all colleagues on board, who helped collecting octopods under harshest conditions.

I would like to express my special thanks to **Maria Morris** and **Dr Elizabeth Morgan** (University of Southampton) who saved and donated the diffusion chamber to our department.

Many thanks to **Dr Jan Strugnell** (La Trobe University, Bundoora) for providing lab space and her extensive ongoing support as well as **Michael Imsic** and all other staff and technicians of the La Trobe University for their kind support during the initial tests of the modified diffusion chamber.

Dr Jayson Semmens (University of Tasmania) for his support in attaining and sampling *Octopus pallidus* as well as the **fishermen of T.O.P. Fish Pty Ltd** for catching *Octopus pallidus*.

Erich Dunker, Matthias Littmann and **Dirk Wethje**, (scientific workshop, Alfred Wegener Institute, Bremerhaven) for the technical modifications and drawings of the diffusion chamber as well as **Dr Eberhard Sauter** (Technology Transfer Office, Alfred Wegener Institute, Bremerhaven) and **Nicola Cochu** (Technology Transfer Transactions, Berlin) for their support in the patenting process

Acknowledgements

Lena Jakob, for providing haemolymph samples from *Eulimnogammarus verrucosus* and **Dr Marian Y Hu** for his help to catch *Octopus vulgaris*.

Dr Anneli Strobel for providing haemolymph pH and heart mass data of *Eledone moschata* and *Sepia officinalis* and her company during the endless measurements at the lab bench on board of FS Polarstern.

Dr Uwe John for his support in sequencing the full haemocyanin gene and **Dr Christoph Held** for his dedicated blood sampling down in Antarctica and subsequent sample provision.

Dr Heidi Windisch for her ongoing advice and support.

Laura Stapp for not being angry answering my phone calls, checking my mail and doing so many other annoying things on my behalf during my home office days.

Anyone else who contributed to the completion of my thesis but who I simply forgot to mention by name.

My family for their believe in my abilities and the recovering rural outings, where stressed PhD students can chill with chickens, rabbits and cat fleas.

Maa, who provided unconditional logistical and culinary support and deep wisdom at all stages of our young family life, particularly at the end of this project. धन्यवाद!

Lastly and most importantly **my wife Saumya** who spiced up my life und always stood by my side at times of frustration, stress and grumpiness. You and our **two sons** are the essence in my life. You gave me the energy, dedication and motivation to complete the (second) biggest project of my life so far. Endless thanks!

Michael Oellermann
Meyerstr 191
28201 Bremen

Bremen, den 18.11.2014

Erklärung gemäß § 6 (5) der PromO der Universität Bremen
(Stand 14 März 2007)

Hiermit erkläre ich, dass ich die Doktorarbeit mit dem Titel

„Blue Blood on Ice: Cephalopod haemocyanin function and evolution in a latitudinal cline”

- ohne unerlaubte fremde Hilfe angefertigt habe,
- keine anderen als die angegebenen Quellen und Hilfsmittel benutzt habe
- die den benutzten Werken wörtlich oder inhaltlich entnommenen Stellen als solche kenntlich gemacht habe.

Des Weiteren erkläre ich, dass es sich bei den von mir abgegebenen Arbeiten um drei identische Exemplare handelt.

Michael Oellermann